

Impact of Seasonal Environmental Variations on 2,4-D Fate and Metabolism in Urban
Landscapes

By

Amarilys Enid González Vázquez

A dissertation submitted in partial fulfillment
of the requirements for the degree of

Doctor of Philosophy

(Molecular and Environmental Toxicology)

at the

UNIVERSITY OF WISCONSIN-MADISON

2021

Date of final oral examination: November 9, 2021

The dissertation is approved by the following members of the Final Oral Committee:

Paul L. Koch, Associate Professor, Plant Pathology

Christina R. Remucal, Associate Professor, Civil and Environmental Engineering

Katherine McMahon, Professor, Bacteriology

Russell Groves, Professor, Entomology

Acknowledgments

There are so many people who helped pave the way to the completion of my graduate degree. First and foremost, I would like to thank my advisor, Dr. Paul L. Koch. I will always remember the first time I stepped into the Koch lab, I felt right at home. Thank you, Paul, for accepting and welcoming me since the very beginning and for believing in me even when, at times, I struggled believing in myself. The phrase “Keep chugging along!” became a mantra I instilled in both my professional and personal life, and I owe that to you. I also want to thank my committee members: Drs. Christy Remucal, Trina McMahon, Russell Groves, and Joel Pedersen for their invaluable feedback, help, and collaboration. Your insights helped me become a better scientist, critical thinker, and writer.

To all the lab members and colleagues (both past and current), I am extremely grateful for your guidance and suggestions and for teaching me all things science, thank you! Graduate school would not have been the same without your guidance and support! I want to especially thank Dr. Brijesh Karakkat and Ron Townsend for welcoming me into the office my first years in the lab, Dr. Ming-Yi Chou for introducing me to the world of microbial ecology and next-generation sequencing, and Kurt Hockemeyer for his help on the experimental design and collecting soil cores when I did not have the muscle strength to do it myself! Thank you to both Brian Schaefer and Daowen Huo for your friendship and for being there through all the ups and downs. Thank you to James Lazarcik for his training and help troubleshooting methods at the Water Science and Engineering Laboratory. Thank you to Russell Labs members, Sue Lueloff, Brooke Babler, Andy Witherell, and Carol Groves for always being open to answer my questions and providing a lot of helpful insight. A huge thanks to Tom Dettinger and Tim Lorenz for their tremendous work in

helping upkeep and maintain lab equipment and for being there when I needed help installing Nitrogen tanks. I also want to thank Amber White and Angela Mae Buch for their collaboration running experiments and making graduate school a fun time! Lastly, I want to acknowledge Dr. Claudia Solís Lemus and the CALS Statistical Consulting Group for their assistance and taking time of their day to meet with me and discuss statistical analysis.

I also want to give special thanks to the undergraduate and research assistants I had the opportunity to mentor as well as learn from. Each and every one brought a unique skill to the table and I am very proud to have seen you all grow as a scientist. This work would have not been completed without them.

To my family and friends, I feel extremely lucky to have your support in and outside of my graduate career. My friends Dr. Anne Turco, Maisie Dantuma, Dr. Joni Sedillo, and Dr. Morgan Walcheck, I am so happy we were part of the same cohort! Anne, you are an amazing human being, I will forever miss our windsurfing, kite snowing, tech boat sailing, hiking, and tattooing endeavors, but most of all, our fun conversations about all science and life! Maisie, you are the sweetest and most caring person, thank you for always believing in me, for being my crafting and farmer's market buddy, and for being there through the highs and lows! Morgan, your positive attitude is infectious! You taught me that there's always something to look forward to each day. Thank you for being the optimistic, happy, wonderful person you are! Joni, you are truly one of the most special people I have ever met. Thank you so much for your support and being there. I could not have done it without any of you! Thanks to my friends Brenda Rojas and Dr. Emmanuel Vázquez Rivera, for always making me feel like family and at home, love you guys! Thanks to my dear friend and neighbor, Vickie Rod, your spirit and love for life was exactly what I needed in my times of stress. Thank you for reminding me that YOLO! Jenyne Loarca, I wish we could have

met from the very beginning of our graduate careers. Thank you for kindness, empathy, and for being my accountability buddy on this journey! Mark Marohl, thank you so much for your constant support and cheering me on. I am forever grateful to have met you. The best program coordinator EVER!

To my significant other, Joshua Lee Kornowske, what an adventure! Thank you for joining me on this journey, standing by my side, and encouraging me every step of the way, for being with me 24/7, supporting and listening to me talk about science, putting up with my grad school stress, and coming to lab with me at crazy hours. I also want to thank my cutie pie, Alice, my best friend. I don't know what I would have done without my wonderful puppy. Although Alice may not understand much (since she's a dog), she does understand love. Joshua and Alice, my home away from home, I am so fortunate to have you both in my life. Thank you for always making sure I have a smile on my face at the end of the day.

Finally, my parents, Gloria E. Vázquez Villanueva and Julio C. González Rodríguez, my biggest cheerleaders, I would not be where I am today without you. Words can't describe how thankful and lucky I am to have you as my parents. Mami y Papi los amo. Mami, gracias por estar a mi lado cuando más lo necesitaba, por tolerar mis loqueras, por levantarme cuando necesitaba ayuda y por todos tus sacrificios y deseos de verme feliz. Papi, tus palabras de apoyo y amor nunca fallaron. Gracias por apoyarme junto a mami y por ser el mejor padre del mundo. My sister Gisselle and baby niece, Zhamira, ustedes son mi felicidad y lo mejor de mi vida. Los amo.

Dedication

This accomplishment is dedicated to my angels in heaven, Rufina Villanueva Rivera and Arnaldo

R. Vázquez Acevedo. Los extraño todos los días.

Abstract

The herbicide 2,4-dichlorophenoxyacetic acid (2,4-D) is one of the most commonly used herbicides on urban landscapes in the U.S. Although 2,4-D fate and breakdown have been well documented, interactions with the entire soil microbiome and simultaneous assessments of its transformation products (TPs) in urban soils remain poorly understood. Microorganisms, namely bacteria, are the primary drivers of pesticide transformation in the soil. Seasonal environmental variations are key factors that directly influence soil bacterial community structure and function, which may alter pesticide degradation networks resulting in the formation of TPs. This dissertation aimed to assess how varying seasonal conditions influenced the soil bacterial community, ultimately resulting in the degradation of 2,4-D and potential formation of its major TP, 2,4-dichlorophenol (2,4-DCP). Chapter 2 showed that 2,4-D was actively being degraded in urban soils at varying seasonal conditions, resulting in the formation of 2,4-DCP. Chapter 3 assessed shifts in the soil bacterial community at spring and summer conditions and how this influenced 2,4-D degradation. Overall, results from Chapter 3 tied with Chapter 2 suggest that bacteria shifted at varying seasonal conditions and were mainly involved in the degradation of 2,4-D in urban soils. In Chapter 4, the results suggest that 2,4-D breakdown activity in soil changes at different seasonal conditions, potentially resulting in TP formation in urban landscapes. However, a major finding in this study was that previously published PCR primers targeting the different gene classes resulted in non-specific amplification, leading to false-positive detection in soil samples. Chapter 5, a side study conducted in 2016, showed that translocation of the fungicide, propiconazole, was primarily limited to the lowest segment of the plant regardless of temperature or time following application. Together, results from this dissertation found that, indeed, negative impacts of pesticides do not end at the point of application. Seasonal environmental variations can shift the soil bacterial

community, thus leading to the formation of 2,4-D's main TP, 2,4-DCP, in urban landscapes. which can behave differently in the environment. Altogether, all four chapters provide important information on the application of pesticides in turfgrass landscapes at varying seasonal conditions and their effect on non-target organisms. Ultimately, these findings will ensure better intensive plant and pest management strategies that provide landscapes of high quality with fewer non-target impacts on environmental and human health and enhance our overall understanding of pesticide fate and behavior.

List of Tables

Table 1. 1 Most used pesticide active ingredients in the Home and Garden Market Sector. H= Herbicide, I = Insecticide. *2,4-D: 2,4-Dichlorophenoxyacetic acid; **MCPP: Methylchlorophenoxypropionic acid; ***MCPA: 2-methyl-4-chlorophenoxyacetic acid. Table recreated from “Pesticides Industry Sales and Usage, 2008-2012 Market Estimates”.....	3
Table 1. 2 Physico-chemical properties and structure of 2,4-D acid and its primary soil TPs.	9
Table 1. 3 Types of 2,4-D-degrading bacteria classified into three groups.	12
 Table 2. 1 Soil analysis for O.J. Noer and Pleasant View field sites in 2018 and 2019. OJ= O.J. Noer; PV = Pleasant View; ppm = parts per million; [P] = Phosphorous; [K] = Potassium; OM = Organic Matter.....	31
Table 2. 2 Temperature and photoperiods simulating spring and summer conditions.	32
Table 2. 3 Mass spectrometry optimization parameters of 2,4-D, 2,4-DCP and their internal standards.	35
Table 2. 4 Average recoveries, standard deviations, limit of detection (LOD) and limit of quantitation (LOQ) for 2,4-D and 2,4-DCP in soil and leaf extraction methods. ND = Not Detected	37
Table 2. 5 Average residual amount found for 2,4-D in leaf tissue samples at spring and summer-simulated conditions and different timepoints.	46
 Table 3. 1 Comparison of soil bacterial community structure dissimilarity in 2018 and 2019 field trials using paired-PERMANOVA with Bonferroni correction.	82
Table 3. 2 Comparison of bacterial community structure dissimilarity in OJ and PV soil from 2018 and 2019 using permutational multivariate analysis of variance (PERMANOVA). The p-values of dispersion test were derived from ANOVA.....	84
Table 3. 3 Comparison of bacterial community structure dissimilarity in spring and summer-simulated growth chamber soil samples using permutational multivariate analysis of variance (PERMANOVA). The p-values of the dispersion test were derived from ANOVA.....	89
Table 3. 4 Comparison of bacterial community structure dissimilarity in 2-4-D Treated (Trt) and Non-treated (NT) spring and summer-simulated growth chamber soil samples using paired-PERMANOVA with Bonferroni correction.	90
 Table 4. 1 <i>TfdA</i> gene classes of 2,4-D-degrading bacteria belonging to Group 1 (see Chapter 1, Table 3).	127
Table 4. 2 Temperature and photoperiods simulating spring and summer conditions.	131
Table 4. 3 Primers and probes for qPCR.....	133
Table 4. 4 Comparison of <i>tfdA</i> class I, II, and III quantification in 2018 and 2019 soil field samples using linear regression analysis and analysis of variance (ANOVA). • indicates p-value < 0.1; * indicates p-value< 0.05; ** indicates p-value < 0.01; *** indicates p-value <0.001; NS=Not Significant.	138
Table 4. 5 Comparison of <i>tfdA</i> class I, II, and III quantification in growth chamber samples using linear regression analysis and analysis of variance (ANOVA). • indicates p-value < 0.1; * indicates	

p-value < 0.05; ** indicates p-value < 0.01; *** indicates p-value < 0.001; NS=Not Significant.

..... 139

Table 4. 6 Tukey's HSD pairwise comparison of *tfdA* class I, II, and III quantification in growth chamber samples between season-simulated temperatures (spring and summer) and days. 140

Table 4. 7 Tukey's HSD pairwise comparison of *tfdA* class I, II, and III quantification in growth chamber samples between soil layers (upper and lower) and days. 142

Table 5. 1 Average raw uptake amount of propiconazole ($\mu\text{g g}^{-1}$) from leaf segments at varying time points per temperature per run^a 177

List of Figures

Figure 1. 1 2-EHE formulation	8
Figure 1. 2 2,4-D degradation pathway encoded by <i>tfd</i> genes in <i>R. eutropha</i> JMP134. TCA, tricarboxylic acid cycle. Figure obtained from Kitagawa et al. (2002) ⁵⁰	11
Figure 2. 1 Chromatogram of 2,4-D, 2,4-DCP, and their internal standards, 2,4-D,d3 and 2,4-DCP,d3.....	35
Figure 2. 2 Box-whisker plots of 2,4-D quantification in soil samples collected from 2018 (A and B) and 2019 (C and D) field trials (n=509). Panels show values for A) PV (n = 125), B) OJ (n = 128), C) PV (n = 128), and D) OJ (n = 128) field sites. Boxes start at the 25 th and end at the 75 th percentile. The center line represents the median value. Dots represent outliers that fall outside of the percentile ranges. The red dashed line represents the LOQ in soil, 0.98 µg g ⁻¹ . A Kruskal-Wallis test was performed between groups, and a statistically significant differences was accepted at p < 0.05 by Bonferroni correction.....	38
Figure 2. 3 Box-whisker plots of 2,4-D quantification in treated soil samples collected from 2018 and 2019 field trials. Panels show values for A) PV 2018 (n = 31), B) OJ 2018 (n = 32), C) PV 2019 (n = 32), and D) OJ 2019 (n = 32) field sites and months at the varying days. Boxes start at the 25 th and end at the 75 th percentile. The center line represents the median value. Dots represent outliers that fall outside of the percentile ranges. The red dashed line represents the LOQ in soil, 0.98 µg g ⁻¹ . A Kruskal-Wallis test was performed between groups, and a statistically significant differences was accepted at p < 0.05 by Bonferroni correction. Samples in July 2019 were collected on day 37 post-application.	41
Figure 2. 4 Box-whisker plots of 2,4-D quantified in upper and lower soil depths in treated soil samples. Panels show values for A) PV 2018 (n = 31), B) OJ 2018 (n = 32), C) PV 2019 (n = 32), and D) OJ 2019 (n = 32) field sites and months at the varying days. Boxes start at the 25 th and end at the 75 th percentile. The center line represents the median value. Dots represent outliers that fall outside of the percentile ranges. The red dashed line represents the LOQ in soil, 0.98 µg g ⁻¹ . A Kruskal-Wallis test was performed between groups, and a statistically significant differences was accepted at p < 0.05 by Bonferroni correction. Samples in July 2019 were collected on day 37 post-application.....	42
Figure 2. 5 Box-whisker plots of 2,4-D quantification in soil samples collected from the growth chamber study (n=287). Panels show values for A) Treatments (Treated = 143, NT =144), B) season-simulated temperatures (Spring = 71, Summer = 72), C) Autoclaving method (Autoclaved = 48, Not Autoclaved = 95), and D) soil layers (Upper = 72, Lower = 71). Boxes start at the 25 th and end at the 75 th percentile. The center line represents the median value. Dots represent outliers that fall outside of the percentile ranges. The red dashed line represents the LOQ in soil, 0.98 µg g ⁻¹ . A Kruskal-Wallis test was performed between groups, and a statistically significant differences was accepted at p < 0.05 by Bonferroni correction.	44
Figure 2. 6 Box-whisker plots of 2,4-D residues detected in leachate samples at day 5 post-application from the growth chamber study (n=35). Panels show values for A) Treatments (Treated = 18, NT = 27), B) season-simulated temperatures (Spring = 17, Summer = 18), and C) Autoclaving method at the varying seasonal-simulated temperatures. Boxes start at the 25 th and end at the 75 th percentile. The center line represents the median value. Dots represent outliers that fall outside of the percentile ranges. The red dashed line represents the LOQ in water, 0.49 µg mL ⁻¹	

¹ A Kruskal-Wallis test was performed between groups, and a statistically significant differences was accepted at $p < 0.05$ by Bonferroni correction. 45

Figure 2. 7 Line plot showing 2,4-D residue levels in leaf tissue collected at the different timepoints and season-simulated conditions (spring and summer). Standard deviation is presented by the error bars from each timepoint where $n=3$. The red dashed line represents the LOQ in leaf tissue, $2.45 \mu\text{g g}^{-1}$. A Kruskal-Wallis test was performed between timepoints and season-simulated conditions. Statistically significant differences were accepted at $p < 0.05$ by Bonferroni correction. 46

Figure 2. 8 Mass balance for 2,4-D in experimental systems simulating spring or summer seasonal conditions at 1-, 5-, 7-, and 10 – days post application. Recovery percentage of 2,4-D is shown for each day, bottom to top of bars: Soil (brown), leaf (green), and leachate (blue). Leachate samples were only collected at day 5 post application. Errors bars represent the standard deviation where $n = 6$ for soil samples, $n = 6$ for leaf, and $n = 3$ for leachate. 48

Figure 3. 1 A) Principal coordinates analysis (PCoA) of bacterial communities (16S V4 region) of upper and lower soil layers from OJ and PV field sites collected in 2018 and 2019. The ordination is based on the Bray-Curtis distance metric, with samples clustered by field site and soil layer, and treatments. **B)** Differential relative abundance of bacterial community phyla identified in OJ and PV field sites using Welch's t-test with Storey FDR correction. **C)** Boxplot featuring the differential relative abundance of the phyla Actinobacteria in the different sites and layers using ANOVA with Storey FDR correction. **D)** Boxplot featuring the differential relative abundance of the phyla Proteobacteria in the different sites and layers using ANOVA with Storey FDR correction. 80

Figure 3. 2 Principal coordinate analysis (PCoA) ordinations of bacterial communities (16S V4 region) derived from **A)** 2018 and **B)** 2019 field trials. The PCoA is based on the Bray-Curtis distance metric, with samples clustering by field site (OJ and PV) and month (May and July). OJ July = Yellow; OJ May = Brown; PV July = Light Blue; PV May = Dark Blue. **C)** Differential relative abundance of bacterial community phyla identified in May and July using Welch's t-test with Storey FDR correction. 81

Figure 3. 3 Principal coordinate analysis (PCoA) ordinations of bacterial communities (16S V4 region) of upper and lower soil layers from sterilized (YES) and unsterilized (NO) soil samples. The ordination is based on the Bray-Curtis distance metric, with samples clustered by sterilization and soil layer, and treatments. 86

Figure 3. 4 Differential relative abundance of bacterial community phyla identified in sterilized and unsterilized samples from **A)** upper and **B)** lower soil layers using Welch's t-test with Storey FDR correction. 87

Figure 3. 5 A) Principal coordinate analysis (PCoA) ordinations of bacterial communities (16S V4 region) derived from spring and summer simulated temperatures. The PCoA is based on the Bray-Curtis distance metric, with samples clustering by Season (spring and summer) and Treatment (Trt and NT). **B)** Differential relative abundance of bacterial community phyla identified in spring and summer samples using Welch's t-test with Storey FDR correction. Boxplot featuring the differential relative abundance of the phyla **C)** Actinobacteria, **D)** Proteobacteria, and **E)** Firmicutes in spring and summer-simulated temperatures using ANOVA with Storey FDR correction. 88

Figure 3. 6 Differential relative abundance of treated (Trt) and non-treated (NT) bacterial microbiome belonging to A) Spring and B) Summer-simulated temperatures samples at Order level. Welch's t-test was implemented with no correction.	91
Figure 3. 7. Bar plot of significant differences in predicted xenobiotic degradation pathways of Upper and Lower soil layers from OJ and PV field samples using Tax4Fun2 and Welch's t-test with Storey FDR correction.	92
Figure 3. 8 Bar plot of significant differences in predicted xenobiotic degradation pathways of Upper and Lower soil layers from OJ and PV field samples using Tax4Fun2 and Welch's t-test with Storey FDR correction.	93
Figure 3. 9 Bar plot of significant differences in predicted xenobiotic degradation pathways of treated (Trt) and Non-treated (NT) samples from spring and summer-simulated temperatures using Tax4Fun2 and Welch's t-test with Storey FDR correction.	94
Figure 3. 10 Pathways overviewing the enzymes involved in 2,4-D degradation resulting in benzoate degradation. The enzymes catalyzing the catabolic steps are <i>TfdA</i> , α -ketoglutarate dependent 2,4-D dioxygenase enzyme, <i>TfdB</i> , 2,4-dichlorophenol hydroxylase, <i>TfdC</i> , chlorocatechol 1,2-dioxygenase, <i>TfdD</i> , chloromuconate cycloisomerase, <i>TfdE</i> , carboxymethelenebutenolidase, and <i>TfdF</i> , maleylacetate reductase. Alternative pathways are highlighted in red, grey, green, and blue. Adapted from the chlorocyclohexane and chlorobenzene degradation KEGG pathway.	96
Figure 3. 12 Functional prediction of 8 functions in the KEGG categories involved in bacterial 2,4-D degradation in soil at Spring and Summer-simulated temperatures and treated (Trt) vs non-treated (NT.) applications. Functional prediction was performed with Tax4Fun.....	97
Figure 3. 11 Functional prediction of 9 functions in the KEGG categories involved in bacterial 2,4-D degradation in soil at OJ and PV field sites during the months of May and July in A) 2018 and B) 2019. Functional prediction was performed with Tax4Fun.	97
Figure 4. 1 2,4-D degradation pathway encoded by <i>tfd</i> genes in <i>R. eutropha</i> JMP134. TCA, tricarboxylic acid cycle. Figure obtained from Kitagawa et al. (2002) ⁵⁰	128
Figure 4. 2 Log relative quantity of <i>tfdA</i> classes 1, 2 and 3 at the following field sites and months in 2018: A) PV May, B) PV July, C) OJ May, and D) OJ July overall soil samples. Error bars indicate the standard error of the mean.	136
Figure 4. 3 Relative quantity of <i>tfdA</i> classes 1, 2 and 3 at the following field sites and months in 2019: A) PV May, B) PV July, C) OJ May, and D) OJ July. Error bars indicate the standard error of the mean.	137
Figure 4. 4 Relative quantity of <i>tfdA</i> gene class A) I, B) II, and C) III in urban soil at upper and lower soil layers in the growth chamber study. Error bars represent the standard error of n=3.	141
Figure 4. 5 Relative quantity of <i>tfdA</i> gene class A) I, B) II, and C) III in urban soil at spring and summer-simulated temperatures in the growth chamber study. Error bars represent the standard error of n=3.	141
Figure 4. 6 Bacteria classified by random forest algorithms as most important predictors int A) class I, B) class II, and C) class III <i>tfdA</i> gene in urban soil samples (n=508) collected from 2018 and 2019 field trials.	143
Figure 4. 7 Key bacteria classified by random forest algorithms as most important predictors in A) class I, B) class II, and C) class III <i>tfdA</i> gene in urban soil samples (n=278) collected from the growth chamber study.	144

Figure 4. 8 Electrophoresis gel of a qPCR amplification product of *tfdA* class I in soil sample collected from the growth chamber study. 147

Figure 5. 1 Chemical structure and physicochemical properties of propiconazole. M.W. = Molecular weight; C_w = Water solubility; pK_a = Acid dissociation constant; K_{ow} = n-octanol-water partition coefficient; K_{oc} = organic carbon to water partition coefficient; soil adsorption coefficient. 167

Figure 5. 2 Diagram depicting apoplastic translocation of propiconazole. Acropetal penetrants diffuse through the cuticle, travel to the vasculature tissue, and enter the xylem, where they are transported upward to leaf tips. Red dots represent the propiconazole molecule. Created with BioRender.com 168

Figure 5. 3 Log-transformed propiconazole concentrations detected in 0-1 (green), 1-2 (yellow), and 2-3 cm (red) leaf blade segments ($n=3$) for (a) Run 1 and (b) Run 2. Results are presented as the raw normalized values. An estimated marginal means ± 1 SE was implemented for pairwise comparison and statistical analysis of the significance between each leaf segment, presented by the black dots. Double asterisks (**) indicate $p \leq 0.01$; and triple asterisks (***) indicate $p \leq 0.001$ 178

Figure 5. 4 Log-transformed propiconazole concentrations detected in samples ($n=3$) at 24 (green), 48 (yellow), and 72-hpi (red) for (a) Run 1 and (b) Run 2. Results are presented as the raw normalized values. An estimated marginal means ± 1 SE was implemented for pairwise comparison and statistical analysis of the significance between each timepoint, presented by the black dots. A single asterisk (*) indicates $p \leq 0.05$; and triple asterisks (***) indicate $p \leq 0.001$ 179

Figure 5. 6 Log-transformed propiconazole concentration detected at temperatures 1 (green), 10 (yellow), 14 (red), and 22 °C (dark green) in (a) Run 1 and (b) Run 2. Results are presented as the raw normalized values. An estimated marginal means ± 1 SE was implemented for pairwise comparison and statistical analysis of the significance between each temperature, presented by the black dots. 180

Figure 5. 7 Log-transformed propiconazole concentration detected in 0-1 (green), 1-2 (yellow), and 2-3 cm (red) leaf blade segments at 1, 10, 14, and 22°C for (a) Run 1 and (b) Run 2. Results are presented as the raw normalized values. An estimated marginal means ± 1 SE was implemented for pairwise comparison and statistical analysis of the significance between each leaf segment at each temperature, presented by the black dots. A single asterisk (*) indicates $p \leq 0.05$; and triple asterisks (***) indicate $p \leq 0.001$ 181

Figure 5. 8 Correlation between measured and predicted log transformed propiconazole uptake in (a) Run 1 and (b) Run 2. Predictive power of linear mixed effect models including temperature, time, and leaf segment as the explanatory variables. All panels show dots for predicted versus measured values of propiconazole uptake, with black dots including and open dots excluding random effects. Red solid lines and dotted lines depict the model fits when random effects are included (R^2 value in parentheses) and excluded (upper R^2 value), respectively. 182

Figure 5. 9 Correlation between measured and predicted log transformed propiconazole uptake in Run 1 (a, c, e) and Run 2 (b, d, f). Predictive power of linear mixed effect models of the individual explanatory variables, (a) and (b) leaf segment, (c) and (d) time, and (e) and (f) temperature. All panels show dots for predicted versus measured values of propiconazole uptake, with black dots including and open dots excluding random effects. Red solid lines and dotted lines depict the model

fits when random effects are included (R^2 value in parenthesis) and excluded (upper R^2 value), respectively.	184
--	-----

Table of Contents

Acknowledgments	i
Dedication	iv
Abstract.....	v
List of Tables	vii
List of Figures.....	ix
Table of Contents	xiv
Chapter 1. Introduction	1
Summary	2
1.1 Defining the need for improved pesticide management and usage in urban landscapes .	3
1.2 Biological mechanisms – the primary driving force of pesticide degradation in soil.....	4
1.3 2,4-Dichlorophenoxyacetic acid (2,4-D) – a commonly applied herbicide in urban landscapes.....	7
1.4 Assessing 2,4-D degrading activity in soil.....	11
1.5. Rationale and Summary	13
References	15
Chapter 2. Detection and Quantification of 2,4-D and its Major Transformation Product, 2,4-DCP, in Urban Landscapes.....	25
Abstract	26
Introduction	27
Materials and Methods	29
Results	36
Discussion	49
References	54
Supplementary Materials.....	60
Chapter 3. Compositional Shifts in the Bacterial Community at Varying Environmental Conditions and its Impact on 2,4-D Degradation in Urban Soil Landscapes	68
Abstract	69
Introduction	70
Materials and Methods	73
Results	78
Discussion	98
References	106
Supplementary Materials.....	117

Chapter 4. Quantification of the 2,4-D Degrading Gene, <i>TfdA</i>, in Urban Soil Bacterial Communities Using qPCR	124
Abstract	125
Introduction	127
Materials and Methods	130
Results	135
Discussion	148
References	153
Supplementary Materials.....	160
Chapter 5. Assessment of Temperature and Time Following Application as Predictors of Propiconazole Translocation in <i>Agrostis stolonifera</i>	165
Abstract	166
Introduction	167
Materials and Methods	170
Results	177
Discussion	184
References	190
Supplementary Materials.....	195
Chapter 6. Concluding Remarks and Future Directions	197
References	201

Chapter 1. Introduction

Summary

The United States contains 50 million acres of managed turfgrass, much of which receives inputs of water, fertilizer, and pesticides on a routine basis.¹ Although lawn pest management strategies vary across the country, they typically involve one or more pesticide applications to suppress weed, insect, and disease pests throughout the growing season.² Pesticide applications over an area this large, and in many cases in areas of close contact with human populations and non-target organisms, increase the potential for pesticide exposure.³ Further, adverse impacts of pesticides do not end at the point of application; pesticides undergo environmental degradation and may result in transformation products (TPs) that interact with the environment differently than the parent molecule.⁴ In terms of degradation, microorganisms are considered the primary mechanism of pesticide breakdown in soil. However, interactions with the soil microbiome, specifically bacteria, and simultaneous TPs assessments in urban soil remain poorly understood.^{5,6} This chapter reviews the history of pesticide usage and the need for improving our understanding of pesticide fate and behavior in urban landscapes. The herbicide 2,4-D is introduced as a model compound due to its widespread use in urban landscapes, especially due to the seasonal environmental variations in which it is applied. The major TPs of 2,4-D and analytical techniques used to detect such compounds in plants, soil, and leachate, are outlined. Specific examples of the biological mechanisms and factors involved in pesticide biodegradation are also provided. Methods that aid in assessing 2,4-D degrading activity in soil are discussed in detail, as are the challenges of studying the interaction between 2,4-D and bacteria in the soil.

1.1 Defining the need for improved pesticide management and usage in urban landscapes

Although pesticides in agriculture typically receive more attention than in non-agricultural settings⁷, urban landscapes also represent an important area where pesticides are used on a routine basis. According to a 2012 U.S. Environmental Protection Agency (EPA) survey, approximately 107 million lbs of pesticides were applied to urban sectors – Home and Garden – representing more than 11% of total U.S. pesticide usage.⁷ The USEPA also estimated that 88 million households in the U.S. use pesticides, where six of the top ten active ingredients are herbicides and four are insecticides (**Table 1.1**).⁷

Table 1. 1 Most used pesticide active ingredients in the Home and Garden Market Sector. H= Herbicide, I = Insecticide. *2,4-D: 2,4-Dichlorophenoxyacetic acid; **MCP: Methylchlorophenoxypropionic acid; ***MCPA: 2-methyl-4-chlorophenoxyacetic acid. Table recreated from “Pesticides Industry Sales and Usage, 2008-2012 Market Estimates”

Active Ingredient	Type
*2,4-D	H
Glyphosate	H
**MCP	H
Pendimethalin	H
Carbaryl	I
Acephate	I
Permethrin and other pyrethroids	I
Dicamba	H
***MCPA	H
Malathion	I

While lawn pest management approaches vary across the country, pesticide applications in urban areas have become a widespread concern due to offsite contamination and non-target exposure resulting in negative human and environmental impacts.^{8,9} Pesticide exposure to non-target organisms, such as aquatic organisms, can also result from other processes such as leaching into groundwater, surface runoff through urban waterways, volatilization, and plant uptake.

Adverse impacts of pesticides can result in the formation of transformation products (TPs) that may be more or less persistent and toxic than the parent molecule.⁴ The EPA recommends

pesticide laboratory fate assessments be conducted at $20^{\circ}\text{C} \pm 2^{\circ}\text{C}$ as part of its Good Laboratory Practices Standards (GLPS) Compliance Monitoring Program. However, pesticide field applications in real-life conditions are routinely made in ranges well outside of 20°C to control pests in turfgrass sites around the country.¹⁰ A study conducted by Getzin (1981) found that temperature had a pronounced effect on the breakdown of the insecticide, chlorpyrifos, in soil, at 15° , 25° , and 35°C , especially at the highest temperature studied.¹¹ Another study assessed temperature effects on the fate of the herbicide clomazone in soils and found its degradation to be higher at a temperature of 15°C and lower at 35°C .¹² These studies show that applications conducted at varying temperatures can influence pesticide fate and behavior in soil environments. Furthermore, the formation of pesticide TPs may also occur due to the varying temperatures in which pesticides are applied, which is of concern because TPs may behave differently in the environment due to their physico-chemical properties.¹³ For example, certain TPs can persist in environmental matrices at longer periods, increasing the chance of exposure to non-target organisms; other TPs may have a higher solubility in water and are more mobile than their parent compound, resulting in leaching and groundwater contamination.^{13,14}

The purpose of pesticides in urban landscapes remains mainly of aesthetic value, as opposed to agricultural settings, in which pesticides are meant to reduce or control pests and encourage the growth of edible crops. For this reason, rising concern for human and environmental health in urban areas¹⁵ demands for further investigation on the effects of pesticides when applied at varying environmental conditions and in regions where humans and other non-target organisms are most likely to become exposed.

1.2 Biological mechanisms – the primary driving force of pesticide degradation in soil

Pesticides undergo various biotic and abiotic mechanisms when released into the environment. The two primary abiotic processes through which pesticides are broken down are physical and chemical reactions. Physical reactions include photolysis.¹⁶ Chemical processes are those involving hydrolysis, oxidation, and reduction reactions.^{14,16–18} Biotic transformation is mediated by live organisms such as invertebrates, plants, and microorganisms.¹⁹ Microorganisms, namely bacteria, are considered the primary force of pesticide degradation in the soil.²⁰ Moreover, microbial transformation of pesticides can occur via three mechanisms: 1) Co-metabolism, where microbes cause the incomplete transformation of the pesticide without using it as an energy source thus, requiring another substrate for growth;^{21,22} 2) catabolism, which leads to the complete mineralization of the pesticide;²³ and 3) detoxification, resulting in the conversion of the pesticide to less harmful metabolites.²⁴ However, biotic mechanisms involving microbes are largely dependent on a broad range of environmental factors.

Factors influencing pesticide biodegradation. Pesticide breakdown is most often accomplished by a consortium of microorganisms and influenced by many environmental factors. Parameters such as temperature, moisture, cultural management practices, physicochemical properties and conditions of the soil (structure, texture, pH, among others) can change or alter the microbiome and its ability to transform pesticides.²⁵

Temperature is one of the most important factors influencing microbial community structure and function.^{19,25} For example, changes in the bacterial community structure due to seasonal temperature fluctuations were observed in microbial communities under snow cover in the Rocky Mountains.²⁶ More specifically, the composition changed where *Acidobacterium* was most abundant in the spring, *Verrucomicrobium* and *Betaproteobacteria* were most abundant in the summer, and *Actinobacteria* was more abundant in the winter.²⁶ In another study, soil samples

collected during two different seasons, spring and fall, also showed differences in the structure and composition of the soil bacterial community where *Bacilli* and *Actinobacteria* dominated in the spring while *Betaproteobacteria* were most abundant in the summer.²⁷ These previous findings suggest that soil microbial communities shift in structure and activity in response to various seasonal conditions, which is relevant to this study. Since microbes are the primary degrader of pesticides in the soil, shifts in structure and activity in response to seasonal environmental changes may have important consequences for how pesticides are transformed.

Turfgrass-associated soil microbial communities. Microorganisms are ubiquitous in soil environments and serve as important players in various activities such as sustainable land use, nutrient availability/cycling, water retention, and agricultural practices and management that improve pathogen resistance and the quality of crops.^{28–30} Turfgrass is ranked as the top irrigated agricultural “crop”,¹ and receives higher rates of pesticides than in agriculture.^{31,32} However, since turfgrasses were believed to have reduced soil microbial activity,³³ little research on the turfgrass soil microbial community composition has only been conducted and expanded since early 2000.^{32–37} Concerning nutrient availability and cycling, Elliot et al. (2003) explored the root mass and rhizosphere bacterial population of creeping bentgrass affected by root-zone mix and nitrogen rates and found differences in numbers gram-positive, gram-negative, heat tolerant, and aerobic bacteria.³⁷ In terms of sustainable land use, Shi et al. (2006) observed changes in soil microbial biomass and activity with the chronological development of turfgrass systems.³⁸ In a further study, turfgrass chronosequence of bermudagrass systems established from native pines were characterized by a very diverse soil microbial community.³³ As an example of using microorganisms to improve the management of plant pathogens in turfgrass, a study conducted in our lab at the University of Wisconsin-Madison also investigated the localized variation in the

development of dollar spot, a foliar pathogen caused by the fungus *Clarireedia* spp., common to occur in turfgrass.³⁶ Rhizosphere and soil bacterial communities were examined and found to be important factors in driving variation in dollar spot disease development. Although research in the turfgrass microbiome is gaining importance, there is still more to be understood.

1.3 2,4-Dichlorophenoxyacetic acid (2,4-D) – a commonly applied herbicide in urban landscapes

The herbicide 2,4-D was the most used pesticide active ingredient in the U.S. home and garden sector in 2012, with 3 to 4 million kg used³⁹. Since its introduction in the 1940s, this synthetic auxin plant growth hormone has been used to control broadleaf weeds and woody plants in small grain, fruit, nut, and vegetable crops, pastures and rangeland, residential lawns and turfgrass, rights-of-way, and aquatic forestry sites.³⁹ Here, we discuss the different formulations in which 2,4-D is applied in urban landscapes and its fate and transport in the environment. Foremost, the transformation of 2,4-D to other products in the environment, with more attention to the degradation pathways involved in the soil compartment, is described.

Types of formulations. 2,4-D is a relatively non-volatile acid commonly found in two types of commercial formulations, amine salts and esters.³⁹ The amine salt formulations are mainly non-volatile and have a higher solubility in water relative to the ester formulation.⁴⁰ 2,4-D amine salt formulations can be found as isopropylamine, triisopropanolamine, and dimethylamine, with the latter being the most widely used⁴¹. Due to their higher water solubility, these salt formulations are usually applied in warmer weather. These types of formulations may also include sequestering agents in order to reduce the precipitation of insoluble salts.

On the other hand, ester formulations are less soluble in water, have a higher vapor pressure than amines, and tend to be applied during cooler weather.⁴⁰ A few of the 2,4-D esters are butoxyethyl ester, 2-ethylhexylester, propylene glycol butyl ether ester, methyl ester, isopropyl ester, and butyl ester.⁴¹ 2-Ethylhexyl esters are widely used due to their low

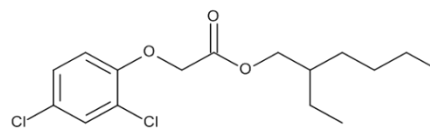


Figure 1. 1 2-EHE formulation

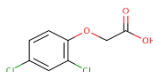
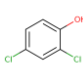
volatility compared to other ester formulations. For this dissertation, we used the 2,4-D-2-ethylhexyl ester (2-EHE) formulation (**Figure 1.1**) to simulate real-life pesticide applications during the spring. In order to maintain consistency throughout the study and better understand how its physico-chemical properties influence its behavior in the environment, 2-EHE was also used during the summer applications.

Major 2,4-D soil transformation products and their toxicity. In soils, 2,4-D esters and salts are first converted to the acid form and are mainly degraded by soil bacteria.⁴¹ The major TP of 2,4-D is 2,4-dichlorophenol (2,4-DCP), which involves the removal of the acetic acid side chain. Compared to 2,4-D, 2,4-DCP is described to contain stronger toxicity in humans and other organisms than its parent compound.⁴² Specifically, 2,4-DCP had a higher effect in erythrocytes hemolysis, i.e., destruction of red blood cells.^{43,44} In addition, exposure to 2,4-DCP has shown endocrine-disrupting effects in zebrafish, resulting in adverse outcomes on reproduction.⁴⁵

Another TP of 2,4-D is 2,4-dichloroanisole (2,4-DCA), which is considered to be formed from 2,4-DCP through a microbial methylation reaction.^{46,47} Other intermediates that form via 2,4-D degradation are 3,5-dichlorocatechol (3,5-DCC) and 4-chlorophenol (4-CP).^{48,49} In the case of 3,5-DCC, this TP can also be formed via photolytic degradation in soils and water, where its toxic effects have been shown to increase in aquatic systems.⁵⁰ Other studies have also shown 3,5-DCC

acute toxicity in bacteria and higher organisms, affecting their membranes, causing narcosis, i.e., mode of toxic action that is non-specific produced by a chemical substance or drug.⁵¹

Table 1. 2 Physico-chemical properties and structure of 2,4-D acid and its primary soil TP.

Properties at 25°C	2,4-D Acid	2,4-Dichlorophenol
Log K _{ow}	2.65	2.96
Vapor pressure (mPa)	2.69	9772.53
Henry's Law Constant (Pa · m ³ /mol)	3.01 x 10 ⁻⁴	0.135
pKa	2.81	7.44
Log K _{oc} (L/kg)	45.70	646
Chemical Structure		

Overall, transformation product toxicity is partially assessed through their mode of action and physico-chemical properties (pKa, log K_{ow}, and log K_{oc}). Previous research showed that from 60 registered pesticides, 485 different transformation products were identified in soil, water, sediment, and air samples. Of these, 30% exhibited more toxicity than the parent molecule, and 4.2% of TPs were more than an order of magnitude more toxic than the parent, including the herbicide 2,4-D.¹³ TPs derived from turfgrass pesticides that exhibited greater toxicity– such as triclopyr, 2,4-D, and acephate– were explained by the presence of a toxicophore (i.e., chemical moiety that is necessary for a specific toxic mechanism), differences in uptake, and their mode of action.¹³ While 2,4-D TPs did not contain a toxicophore, they did show an increase in hydrophobicity and were less dissociated than 2,4-D in non-target organisms.¹³ Generally, compounds with greater hydrophobicity (or K_{ow}) and were less dissociated than the parent compound were considered more likely to bioaccumulate in the environment. Therefore, knowledge of the physico-chemical properties of TPs produced throughout the growing season is of utmost importance for fully understanding pesticides' impacts on the environment. **Table 1.2**

compares the physico-chemical properties of 2,4-D with its main soil TP, 2,4-dichlorophenol (2,4-DCP).⁵²

Previous analytical techniques have been developed to detect and quantify 2,4-D and its major TP, 2,4-DCP, in various matrices.^{6,53–57} These methods include Liquid Chromatography with Diode Array Detector (DAD), Gas Chromatography (GC) with Electron Capture Detector (ECD) and Mass Spectrometric detection (MS). However, limitations arise with these methods since 2,4-D is not a volatile compound, and a derivatization step is required for GC detection.⁵⁸ Using DAD or ultraviolet (UV) detection does not guarantee 2,4-D and TP detection since background compounds may absorb light within the same range resulting in the reduction of compound specificity. Thus, developing a chromatographic method is crucial for the simultaneous detection of 2,4-D and its TP. Using LC-MS/MS provides optimal detection for each compound of interest without derivatization and improves compound specificity from various matrices. In complex environmental matrices, chemical compounds interact differently depending on their physico-chemical properties and the matrix itself.⁵⁹ These matrix effects influence the compound's fate, resulting in adsorption, leaching, or degradation.⁵⁹ Because soil is a complex heterogeneous matrix, the fate and breakdown of compounds vary due to their interference with the soil particles, pH, and other chemical properties.⁵⁹ Since water and leaf tissue are less complex matrices, pollutants can be more easily extracted than those associated with soil. Thus, developing an effective extraction and cleanup method for 2,4-D and its TP from soil is crucial for their effective analysis.

1.4 Assessing 2,4-D degrading activity in soil

Tfd gene cluster and its role in degrading 2,4-D. Genes have recently been identified in soil bacteria that serve as reporter genes for detecting or identifying 2,4-D biodegradation activity.⁶⁰ Specifically, 2,4-D biodegradation has been extensively studied in *Cupriavidus necator* JMP134 (formerly known as *Ralstonia eutropha* and *Alcaligenes eutrophus*).⁶¹ *C. necator* harbors

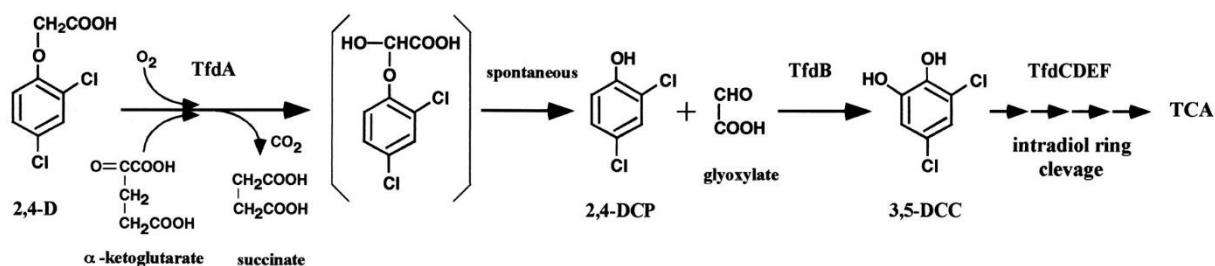


Figure 1. 2 2,4-D degradation pathway encoded by *tfd* genes in *R. eutropha* JMP134. TCA, tricarboxylic acid cycle. Figure obtained from Kitagawa et al. (2002)⁵⁰

the pJP4 plasmid, which contains a gene cluster known as *tfd* (two, four-dichlorophenoxyacetic acid) *ABCDEF*. The proposed catabolic pathway can be described in the following steps: (1) 2,4-D is converted to 2,4-DCP by α-ketoglutarate-dependent 2,4-D dioxygenase encoded by *tfdA*; (2) *tfdB* gene encodes for a phenol hydroxylase that metabolizes 2,4-DCP to 3,5-DCC; (3) 3,5-DCC aromatic ring is further cleaved by a pathway encoded by *tfdCDEF* (**Figure 1.2**).⁶¹ Of special interest within this gene cluster is the *tfdA* gene, which has been considered a good reporter for 2,4-D degradation activity. Due to its high diversity and distribution over different phylogenetic groups, bacterial strains that degrade 2,4-D have been classified into three groups (**Table 1.3**).^{61,62} For the first group, McGowan et al. (1998) sequenced the first gene, *tfdA*, and found that the sequences fell into three unique classes (I, II, and III), depending on their *tfdA* gene sequences, and consisted of *Beta*- and *Gammaproteobacteria*, typically isolated from contaminated environments.⁶³ The class I gene is typically located on self-transmissible plasmids, first isolated from *C. necator*.⁶⁴ It has also been found in other strains such as *Burkholderia*-like strains and the *Comamonas-Rhodospirillum rubrum* group, all in the *Betaproteobacteria* group.⁶⁵ The class II gene, unlike

class I, can be coded in chromosomes such as in *Burkholderia* sp. belonging to *Betaproteobacteria*. Class II has also been shown to share 76% identity to the class I gene.⁶⁶ The class III gene was 77 and 80% identical to the class I and II *tfdA* genes, respectively.⁶⁶ The second group of 2,4-D-degrading genes consists of *Alphaproteobacteria*, mainly isolated from non-contaminated environments.⁶⁷ The third group is comprised of *Alphaproteobacteria*, specifically of the genus *Sphingomonas*.⁶⁷

Table 1. 3 Types of 2,4-D-degrading bacteria classified into three groups.

2,4-D-Degrading Groups	Description
1	<ul style="list-style-type: none"> - (+) fast-growing <i>Beta</i>- and <i>Gammaproteobacteria</i> - Comprised of 3 classes (I, II, and III). - Related to <i>C. necator</i> - Isolated from contaminated environments.
2	<ul style="list-style-type: none"> - (-) fast-growing <i>Alphaproteobacteria</i> - Related to <i>Sphingomonas</i> spp. - Isolated from contaminated environments.
3	<ul style="list-style-type: none"> - (-) slow-growing <i>Alphaproteobacteria</i> - Isolated from <i>Bradyrhizobium</i>. - Isolated from non-contaminated sites.

Other 2,4-D-degrading genes. Another family of 2,4-D-degrading genes is *cadRABKC*, which was initially discovered two decades after the *tfd* gene system from an organism present in a non-2,4-D-contaminated site, and is widely distributed among groups 2 and 3 (**Table 1.3**).^{61,62} Like *tfdA*, the *cadA* gene is responsible for catalyzing the transformation of 2,4-D to 2,4-DCP. This gene system has been widely found in the genera *Bradyrhizobium*, *Sphingomonas*, and possibly others.⁶⁸ Although the *cadA* gene has bolstered our knowledge of 2,4-D biodegradation research, all bacteria that harbor *cad* genes are not necessarily capable of degrading 2,4-D.⁶¹ Thus, the *tfdA* gene (**Group 1, Table 1.3**) continues to be an important model for 2,4-D biodegradation. Previous findings support this statement where it has been shown that organisms harboring *tfdA* are quick to respond and adapt to 2,4-D-contaminated sites, which makes it a good marker for

detecting 2,4-D degradation.^{61,62,68} Further, because pesticides are degraded by a consortium of soil microorganisms in the environment, studying the soil microbiome through in situ high-throughput sequencing is critical to better understand their response to seasonal environmental variation and potential to interact with 2,4-D.

1.5. Rationale and Summary

Evaluating the formation of pesticide TPs by soil microbes and how these TPs may behave differently than the parent compound requires more attention to reduce non-target impacts of pesticide usage. While advances in pesticide assessments and microbial analysis have allowed researchers to identify pesticide biodegradation pathways and mechanisms under standard laboratory conditions, future studies are needed to bolster our understanding of how varying seasonal conditions such as temperature, influence soil bacterial activity and how potential changes in that activity alters pesticide metabolism in urban landscapes, resulting in TPs that may behave differently than the parent compound.

As outlined above, soil bacteria are the primary degraders of 2,4-D in the soil. They can shift in structure and activity in response to seasonal environmental changes, ultimately resulting in important consequences for how 2,4-D is transformed in urban landscapes. With this in mind, I hypothesized that seasonal environmental fluctuations are expected to: 1) shift soil bacterial structure, function, and diversity, and 2) lead to variations in 2,4-D fate and breakdown in urban landscapes, resulting in varying TP detection and concentration. Chapter 2 describes the development of a pesticide extraction method for the effective analysis of 2,4-D and its TP, 2,4-DCP, in urban soil, turfgrass leaf tissue, and leachate samples. I use the extraction method and conduct analytical techniques to detect and quantify 2,4-D and 2,4-DCP residues. Chapter 3 focuses on evaluating the impact of altered turfgrass-associated soil bacterial communities on 2,4-D metabolism. I show how seasonal fluctuations lead to changes in soil bacterial activities, how

potential environment-driven changes in that microbial activity alters 2,4-D metabolism in urban landscapes, and how predicted xenobiotic degradation pathways link the ability of urban soil bacteria to degrade 2,4-D. Chapter 4 assesses 2,4-D-degrading activity using the three *tfdA* gene classes and identifies important bacterial predictors involved with the different classes. While the main objective was to determine if 2,4-D-degrading activity changes in response to different environmental conditions throughout the season, I also assess whether non-specific amplification of the *tfdA* gene occurred by testing previously designed primers. Next, in Chapter 5, I conduct a side study that assesses the duration and distance of upward mobility of the fungicide, propiconazole, into turfgrass leaves in conditions that reflect a late fall and early winter environment and develop a simple plant uptake model specific to these fungicides that take into consideration leaf height, time after application, and temperature. Lastly, Chapter 6 summarizes the dissertation's conclusions and describes possible future directions that will further enhance our understanding of how pesticides interact with the microbial world and may lead to reductions in pesticide exposure for pesticide applicators and citizens that interact with intensively managed turfgrass systems. Overall, this work highlights the knowledge gap regarding the impact of altered turfgrass-associated microbial communities on pesticide metabolism and demonstrates the importance of conducting studies *in situ* to ensure better intensive plant and pest management strategies that provide landscapes of high quality with fewer non-target impacts on environmental and human health.

References

- (1) Milesi, C.; Running, S.; Elvidge, C.; Dietz, J.; Tuttle, B.; Nemani, R. Mapping and Modeling the Biogeochemical Cycling of Turf Grasses in the United States. *Environmental Management* **2005**, *36* (3), 426–438.
- (2) Held, D.; Potter, D. Prospects for Managing Turfgrass Pests with Reduced Chemical Inputs. *Annual Review of Entomology* **2012**, *57*, 329–354. <https://doi.org/10.1146/annurev-ento-120710-100542>.
- (3) Gan, H.; Wickings, K. Soil Ecological Responses to Pest Management in Golf Turf Vary with Management Intensity, Pesticide Identity, and Application Program. *Agriculture, Ecosystems & Environment* **2017**, *246*, 66–77. <https://doi.org/10.1016/j.agee.2017.05.014>.
- (4) Corke, C. T.; Thompson, F. R. Effects of Some Phenylamide Herbicides and Their Degradation Products on Soil Nitrification. *Can. J. Microbiol.* **1970**, *16* (7), 567–571. <https://doi.org/10.1139/m70-095>.
- (5) Reedich, L. M.; Millican, M. D.; Koch, P. L. Temperature Impacts on Soil Microbial Communities and Potential Implications for the Biodegradation of Turfgrass Pesticides. *Journal of Environmental Quality* **2017**, *46* (3), 490–497. <https://doi.org/10.2134/jeq2017.02.0067>.
- (6) McManus, S.-L.; Moloney, M.; Richards, K. G.; Coxon, C. E.; Danaher, M. Determination and Occurrence of Phenoxyacetic Acid Herbicides and Their Transformation Products in Groundwater Using Ultra High Performance Liquid Chromatography Coupled to Tandem Mass Spectrometry. *Molecules* **2014**, *19* (12), 20627–20649. <https://doi.org/10.3390/molecules191220627>.

- (7) Atwood, D.; Paisley-Jones, C. *Pesticides Industry Sales and Usage 2008-2012 Market Estimates*; U.S. Environmental Protection Agency, **2017**.
- (8) Md Meftaul, I.; Venkateswarlu, K.; Dharmarajan, R.; Annamalai, P.; Megharaj, M. Pesticides in the Urban Environment: A Potential Threat That Knocks at the Door. *Science of The Total Environment* **2020**, *711*, 134612.
<https://doi.org/10.1016/j.scitotenv.2019.134612>.
- (9) Hoover, S. National Movement Targets Lawn Care Poisons. **2005**, *25* (1), 4.
- (10) USEPA. Fate, transport, and transformation test guidelines: OPPTS 835.4100 aerobic soil metabolism, OPPTS 835.4200 anaerobic soil metabolism.
<https://nepis.epa.gov/Exe/ZyPURL.cgi?Dockey=P100J6WF.txt> (accessed 2019 -04 -29).
- (11) Getzin, L. W. Degradation of Chlorpyrifos in Soil: Influence of Autoclaving, Soil Moisture, and Temperature¹. *Journal of Economic Entomology* **1981**, *74* (2), 158–162.
<https://doi.org/10.1093/jee/74.2.158>.
- (12) Mervosh, T. L.; Sims, G. K.; Stoller, E. W. Clomazone Fate in Soil as Affected by Microbial Activity, Temperature, and Soil Moisture. *J. Agric. Food Chem.* **1995**, *43* (2), 537–543.
<https://doi.org/10.1021/jf00050a052>.
- (13) Sinclair, C. J.; Boxall, A. B. A. Assessing the Ecotoxicity of Pesticide Transformation Products. *Environ. Sci. Technol.* **2003**, *37* (20), 4617–4625.
<https://doi.org/10.1021/es030038m>.
- (14) Somasundaram, L.; Coats, J. R. Pesticide Transformation Products: Fate and Significance in the Environment. *ACS symposium series (USA)* **1991**, No. 459.

- (15) *National Turfgrass Research Initiative: Enhancing America's Beauty Protecting America's Natural Resources Ensuring the Health and Safety of All Americans*; National Turfgrass Evaluation Program, Beltsville Agricultural Research Center: Beltsville, Md., **2003**.
- (16) Ortiz-Hernández, M. L.; Sánchez-Salinas, E.; Dantán-González, E.; Castrejón-Godínez, M. L. Pesticide Biodegradation: Mechanisms, Genetics and Strategies to Enhance the Process. *Biodegradation - Life of Science* **2013**. <https://doi.org/10.5772/56098>.
- (17) Coats, J. Pesticide Degradation Mechanisms and Environmental Activation. *ACS Symposium Series* **1991**, 459, 10–30.
- (18) Remucal, C. K. The Role of Indirect Photochemical Degradation in the Environmental Fate of Pesticides: A Review. *Environmental Science: Processes & Impacts* **2014**, 16 (4), 628. <https://doi.org/10.1039/c3em00549f>.
- (19) Nedwell, D. B.; Floodgate, G. D. The Seasonal Selection by Temperature of Heterotrophic Bacteria in an Intertidal Sediment. *Marine Biology* **1971**, 11 (4), 306–310. <https://doi.org/10.1007/BF00352448>.
- (20) Bollag, J. M. *Biological Transformation Processes of Pesticides*; Soil Science Society of America: Madison, Wis (USA), **1990**.
- (21) Singh, R. Microbial Biotransformation: A Process for Chemical Alterations. *JBMOA* **2017**, 4 (2). <https://doi.org/10.15406/jbmoa.2017.04.00085>.
- (22) Horvath, R. S. Microbial Co-Metabolism and the Degradation of Organic Compounds in Nature. *Bacteriol Rev* **1972**, 36 (2), 146–155.
- (23) Huang, X.; He, J.; Yan, X.; Hong, Q.; Chen, K.; He, Q.; Zhang, L.; Liu, X.; Chuang, S.; Li, S.; Jiang, J. Microbial Catabolism of Chemical Herbicides: Microbial Resources, Metabolic

- Pathways and Catabolic Genes. *Pesticide Biochemistry and Physiology* **2017**, *143*, 272–297. <https://doi.org/10.1016/j.pestbp.2016.11.010>.
- (24) Lal, R.; Lal, S.; Shivaji, S.; Pemberton, J. M. Use of Microbes for Detoxification of Pesticides. *Critical Reviews in Biotechnology* **1985**, *3* (1), 1–16. <https://doi.org/10.3109/07388558509150778>.
- (25) Fenner, K.; Canonica, S.; Wackett, L.; Elsner, M. Evaluating Pesticide Degradation in the Environment: Blind Spots and Emerging Opportunities. *Science* **2013**, *341* (6147), 752–758.
- (26) Lipson, D. A.; Schmidt, S. K. Seasonal Changes in an Alpine Soil Bacterial Community in the Colorado Rocky Mountains. *Applied and Environmental Microbiology* **2004**, *70* (5).
- (27) Bevivino, A.; Paganin, P.; Bacci, G.; Florio, A.; Pellicer, M. S.; Papaleo, M. C.; Mengoni, A.; Ledda, L.; Fani, R.; Benedetti, A.; Dalmastri, C. Soil Bacterial Community Response to Differences in Agricultural Management along with Seasonal Changes in a Mediterranean Region. *PLoS ONE* **2014**, *9* (8), e105515. <https://doi.org/10.1371/journal.pone.0105515>.
- (28) Mendes, R.; Kruijt, M.; de Bruijn, I.; Dekkers, E.; van der Voort, M.; Schneider, J. H. M.; Piceno, Y. M.; DeSantis, T. Z.; Andersen, G. L.; Bakker, P. A. H. M.; Raaijmakers, J. M. Deciphering the Rhizosphere Microbiome for Disease-Suppressive Bacteria. *Science* **2011**, *332* (6033), 1097–1100. <https://doi.org/10.1126/science.1203980>.
- (29) Singh, J. S.; Pandey, V. C.; Singh, D. P. Efficient Soil Microorganisms: A New Dimension for Sustainable Agriculture and Environmental Development. *Agriculture, Ecosystems & Environment* **2011**, *140* (3), 339–353. <https://doi.org/10.1016/j.agee.2011.01.017>.
- (30) Zheng, W.; Zeng, S.; Bais, H.; LaManna, J. M.; Hussey, D. S.; Jacobson, D. L.; Jin, Y. Plant Growth-Promoting Rhizobacteria (PGPR) Reduce Evaporation and Increase Soil Water

- Retention. *Water Resources Research* **2018**, *54* (5), 3673–3687.
<https://doi.org/10.1029/2018WR022656>.
- (31) Pimentel, D.; McLaughlin, L.; Zepp, A.; Lakitan, B.; Kraus, T.; Kleinman, P.; Vancini, F.; Roach, W. J.; Graap, E.; Keeton, W. S.; Selig, G. Environmental and Economic Impacts of Reducing U.S. Agricultural Pesticide Use. In *The Pesticide Question: Environment, Economics, and Ethics*; Pimentel, D., Lehman, H., Eds.; Springer US: Boston, MA, **1993**; pp 223–278. https://doi.org/10.1007/978-0-585-36973-0_10.
- (32) Xia, Q.; Rufty, T.; Shi, W. Predominant Microbial Colonizers in the Root Endosphere and Rhizosphere of Turfgrass Systems: *Pseudomonas Veronii*, *Janthinobacterium Lividum*, and *Pseudogymnoascus* Spp. *Front Microbiol* **2021**, *12*, 643904.
<https://doi.org/10.3389/fmicb.2021.643904>.
- (33) Yao, H.; Bowman, D.; Shi, W. Soil Microbial Community Structure and Diversity in a Turfgrass Chronosequence: Land-Use Change versus Turfgrass Management. *Applied Soil Ecology* **2006**, *34* (2), 209–218. <https://doi.org/10.1016/j.apsoil.2006.01.009>.
- (34) Yao, H.; Bowman, D.; Shi, W. Seasonal Variations of Soil Microbial Biomass and Activity in Warm- and Cool-Season Turfgrass Systems. *Soil Biology and Biochemistry* **2011**, *43* (7), 1536–1543. <https://doi.org/10.1016/j.soilbio.2011.03.031>.
- (35) Zhang, W.; Zhang, Z.; Wang, Y.; Ai, D.; Wen, P.; Zhu, Y.; Cao, L.; Yao, T. Effect of Turfgrass Establishment on Soil Microbiota Using Illumina Sequencing. *Nature Environment and Pollution Technology* **2017**, *16* (3), 679.
- (36) Chou, M.-Y.; Shrestha, S.; Rioux, R.; Koch, P. Hyperlocal Variation in Soil Iron and the Rhizosphere Bacterial Community Determines Dollar Spot Development in Amenity

- Turfgrass. *Appl. Environ. Microbiol.* **2021**, 87 (10). <https://doi.org/10.1128/AEM.00149-21>.
- (37) Elliott, M. L.; Guertal, E. A.; Des Jardin, E. A.; Skipper, H. D. Effect of Nitrogen Rate and Root-Zone Mix on Rhizosphere Bacterial Populations and Root Mass in Creeping Bentgrass Putting Greens. *Biol Fertil Soils* **2003**, 37 (6), 348–354. <https://doi.org/10.1007/s00374-003-0603-8>.
- (38) Shi, W.; Yao, H.; Bowman, D. Soil Microbial Biomass, Activity and Nitrogen Transformations in a Turfgrass Chronosequence. *Soil Biology* **2006**, 9.
- (39) Islam, F.; Wang, J.; Farooq, M. A.; Khan, M. S. S.; Xu, L.; Zhu, J.; Zhao, M.; Muños, S.; Li, Q. X.; Zhou, W. Potential Impact of the Herbicide 2,4-Dichlorophenoxyacetic Acid on Human and Ecosystems. *Environment International* **2018**, 111, 332–351. <https://doi.org/10.1016/j.envint.2017.10.020>.
- (40) Nice, Glenn. *Amine or Ester, Which Is Better?*; Purdue University, Cooperative Extension Service: West Lafayette, IN, **2004**.
- (41) Peterson, M.; McMaster, S.; Riechers, D.; Skelton, J.; Stahlman, P. 2,4-D Past, Present, and Future: A Review. *Weed Technology* **2016**, 30 (2), 303–345.
- (42) Abate Jote, C. A Review of 2,4-D Environmental Fate, Persistence and Toxicity Effects on Living Organisms. *OMCIJ* **2019**, 9 (1). <https://doi.org/10.19080/OMCIJ.2019.09.555755>.
- (43) Duchnowicz, P.; Koter, M.; Duda, W. Damage of Erythrocyte by Phenoxyacetic Herbicides and Their Metabolites. *Pesticide Biochemistry and Physiology* **2002**, 74 (1), 1–7. [https://doi.org/10.1016/S0048-3575\(02\)00139-6](https://doi.org/10.1016/S0048-3575(02)00139-6).
- (44) Bukowska, B. Effects of 2,4-D and Its Metabolite 2,4-Dichlorophenol on Antioxidant Enzymes and Level of Glutathione in Human Erythrocytes. *Comparative Biochemistry and*

- Physiology Part C: Toxicology & Pharmacology* **2003**, 135 (4), 435–441.
[https://doi.org/10.1016/S1532-0456\(03\)00151-0](https://doi.org/10.1016/S1532-0456(03)00151-0).
- (45) Ma, Y.; Han, J.; Guo, Y.; Lam, P. K. S.; Wu, R. S. S.; Giesy, J. P.; Zhang, X.; Zhou, B. Disruption of Endocrine Function in in Vitro H295R Cell-Based and in in Vivo Assay in Zebrafish by 2,4-Dichlorophenol. *Aquatic Toxicology* **2012**, 106–107, 173–181.
<https://doi.org/10.1016/j.aquatox.2011.11.006>.
- (46) Buerge, I. J.; Pavlova, P.; Hanke, I.; Bächli, A.; Poiger, T. Degradation and Sorption of the Herbicides 2,4-D and Quizalofop-P-Ethyl and Their Metabolites in Soils from Railway Tracks. *Environ Sci Eur* **2020**, 32 (1), 150. <https://doi.org/10.1186/s12302-020-00422-6>.
- (47) Smith, A. E. Identification of 2,4-Dichloroanisole and 2,4-Dichlorophenol as Soil Degradation Products of Ring-Labelled [14C]2,4-D. *Bull. Environ. Contam. Toxicol.* **1985**, 34 (1), 150–157. <https://doi.org/10.1007/BF01609717>.
- (48) Tiedje, J. M.; Duxbury, J. M.; Alexander, M.; Dawson, J. E. 2,4-D Metabolism: Pathway of Degradation of Chlorocatechols by *Arthrobacter* Sp. *J. Agric. Food Chem.* **1969**, 17 (5), 1021–1026. <https://doi.org/10.1021/jf60165a037>.
- (49) Walters, J. *Environmental Fate of 2,4-Dichlorophenoxyacetic Acid*; 2019; p 18.
- (50) Svenson, A.; Hynning, P.-Å. Increased Aquatic Toxicity Following Photolytic Conversion of an Organochlorine Pollutant. *Chemosphere* **1997**, 34 (8), 1685–1692.
[https://doi.org/10.1016/S0045-6535\(97\)00025-8](https://doi.org/10.1016/S0045-6535(97)00025-8).
- (51) Schweigert, N.; Hunziker, R. W.; Escher, B. I.; Eggen, R. I. L. Acute Toxicity of (Chloro-)Catechols and (Chloro-)Catechol-Copper Combinations in *Escherichia Coli* Corresponds to Their Membrane Toxicity in Vitro. *Environmental Toxicology and Chemistry* **2001**, 20 (2), 239–247. <https://doi.org/10.1002/etc.5620200203>.

<https://comptox.epa.gov/dashboard/dsstoxdb/results?search=2,4-D-2-ethylhexyl%20ester>
(accessed 2019 -03 -26).

- (53) Moret, S.; Hidalgo, M.; Sánchez, J. M. Development of an Ion-Pairing Liquid Chromatography Method for the Determination of Phenoxyacetic Herbicides and Their Main Metabolites: Application to the Analysis of Soil Samples. *Chroma* **2006**, *63* (3), 109–115. <https://doi.org/10.1365/s10337-005-0711-8>.
- (54) de Amarante, O. P.; Brito, N. M.; dos Santos, T. C. R.; Nunes, G. S.; Ribeiro, M. L. Determination of 2,4-Dichlorophenoxyacetic Acid and Its Major Transformation Product in Soil Samples by Liquid Chromatographic Analysis. *Talanta* **2003**, *60* (1), 115–121. [https://doi.org/10.1016/S0039-9140\(03\)00113-9](https://doi.org/10.1016/S0039-9140(03)00113-9).
- (55) Gavin, Q. W.; Ramage, R. T.; Waldman, J. M.; She, J. Development of HPLC-MS/MS Method for the Simultaneous Determination of Environmental Phenols in Human Urine. *International Journal of Environmental Analytical Chemistry* **2014**, *94* (2), 168–182. <https://doi.org/10.1080/03067319.2013.814123>.
- (56) Schaner, A.; Konecny, J.; Luckey, L.; Hickes, H. Determination of Chlorinated Acid Herbicides in Vegetation and Soil by Liquid Chromatography/Electrospray-Tandem Mass Spectrometry. *Journal of AOAC International* **2007**, *90* (5), 1402–1410.
- (57) Koesukwiwat, U.; Sanguankaew, K.; Leepipatpiboon, N. Rapid Determination of Phenoxy Acid Residues in Rice by Modified QuEChERS Extraction and Liquid Chromatography–Tandem Mass Spectrometry. *Analytica Chimica Acta* **2008**, *626* (1), 10–20. <https://doi.org/10.1016/j.aca.2008.07.034>.

- (58) Sutherland, D. J.; Stearman, G. K.; Wells, M. J. M. Development of an Analytical Scheme for Simazine and 2,4-D in Soil and Water Runoff from Ornamental Plant Nursery Plots. *J. Agric. Food Chem.* **2003**, *51* (1), 14–20. <https://doi.org/10.1021/jf025661p>.
- (59) Vera, J.; Correia-Sá, L.; Paíga, P.; Bragança, I.; Fernandes, V. C.; Domingues, V. F.; Delerue-Matos, C. QuEChERS and Soil Analysis. An Overview. *Sample Preparation* **2013**, *1*.
- (60) Steenson, T. I.; Walker, N. The Pathway of Breakdown of 2:4-Dichloro- and 4-Chloro-2-Methyl-Phenoxyacetic Acid by Bacteria. *Journal of general microbiology* **1957**, *16* (1).
- (61) Kitagawa, W.; Kamagata, Y. Diversity of 2,4-Dichlorophenoxyacetic Acid (2,4-D)-Degradative Genes and Degrading Bacteria. In *Biodegradative Bacteria: How Bacteria Degrade, Survive, Adapt, and Evolve*; Springer Japan, **2014**; pp 43–57.
- (62) Kitagawa, W.; Takami, S.; Miyauchi, K.; Masai, E.; Kamagata, Y.; Tiedje, J. M.; Fukuda, M. Novel 2,4-Dichlorophenoxyacetic Acid Degradation Genes from Oligotrophic Bradyrhizobium Sp. Strain HW13 Isolated from a Pristine Environment. *Journal of Bacteriology* **2002**, *184* (2), 509–518. <https://doi.org/10.1128/JB.184.2.509-518.2002>.
- (63) McGowan, C.; Fulthorpe, R.; Wright, A.; Tiedje, J. M. Evidence for Interspecies Gene Transfer in the Evolution of 2,4-Dichlorophenoxyacetic Acid Degradation. *Appl Environ Microbiol* **1998**, *64* (10), 4089–4092. <https://doi.org/10.1128/AEM.64.10.4089-4092.1998>.
- (64) Streber, W. R.; Timmis, K. N.; Zenk, M. H. Analysis, Cloning, and High-Level Expression of 2,4-Dichlorophenoxyacetate Monooxygenase Gene TfdA of Alcaligenes Eutrophus JMP134. *J Bacteriol* **1987**, *169* (7), 2950–2955.

- (65) Fulthorpe, R. R.; McGowan, C.; Maltseva, O. V.; Holben, W. E.; Tiedje, J. M. 2,4-Dichlorophenoxyacetic Acid-Degrading Bacteria Contain Mosaics of Catabolic Genes. *APPL. ENVIRON. MICROBIOL.* **1995**, *61*, 8.
- (66) Itoh, K.; Kanda, R.; Sumita, Y.; Kim, H.; Kamagata, Y.; Suyama, K.; Yamamoto, H.; Hausinger, R. P.; Tiedje, J. M. TfdA-Like Genes in 2,4-Dichlorophenoxyacetic Acid-Degrading Bacteria Belonging to the Bradyrhizobium-Agromonas-Nitrobacter-Afipia Cluster in α -Proteobacteria. *Applied and Environmental Microbiology* **2002**, *68* (7), 3449–3454. <https://doi.org/10.1128/AEM.68.7.3449-3454.2002>.
- (67) Bælum, J.; Henriksen, T.; Hansen, H. C. B.; Jacobsen, C. S. Degradation of 4-Chloro-2-Methylphenoxyacetic Acid in Top- and Subsoil Is Quantitatively Linked to the Class III TfdA Gene. *Appl Environ Microbiol* **2006**, *72* (2), 1476–1486. <https://doi.org/10.1128/AEM.72.2.1476-1486.2006>.
- (68) Kumar, A.; Trefault, N.; Olaniran, A. O. Microbial Degradation of 2,4-Dichlorophenoxyacetic Acid: Insight into the Enzymes and Catabolic Genes Involved, Their Regulation and Biotechnological Implications. *Critical Reviews in Microbiology* **2016**, *42* (2), 194–208.

**Chapter 2. Detection and Quantification of 2,4-D and its Major Transformation Product,
2,4-DCP, in Urban Landscapes**

Abstract

The U.S. contains approximately 50 million acres of managed turfgrass, especially in highly populated areas. To maintain these urban areas, pesticides will be applied at varying times and seasonal conditions. 2,4-Dichlorophenoxyacetic acid (2,4-D) is the most commonly used herbicide in home lawns and gardens. Due to its widespread and varied use, 2,4-D can result in the formation of its main transformation product (TPs), 2,4-dichlorophenol (2,4-DCP), among others. The main route of degradation of 2,4-D is via biotic mechanisms, specifically bacteria, which are influenced by a wide range of environmental factors, such as seasonal temperature variations. This study focused on assessing the detection and quantification of the herbicide 2,4-D and its major TP, 2,4-DCP via bacterial degradation in leaf, soil, and leachate matrices derived from urban landscapes using liquid chromatography-tandem mass spectrometry (LC-MS/MS). Field studies in 2018 and 2019, in addition to a growth chamber study, were conducted. To eliminate the impact of soil microbial activity and account for potential abiotic transformation of 2,4-D, a select number of soil samples were autoclaved and included in the study. Results from the growth chamber study show that 2,4-D residues were detected in soil, leaf, and leachate samples. However, the degradation of 2,4-D and subsequent formation of 2,4-DCP was only observed in soil matrices. A mass balance analysis was also conducted and showed 2,4-D losses after time in soil, a stable amount in leaf samples throughout time, and leaching potential at day 5 post-application. With this in mind, the 2,4-D missing in our controlled system suggested that leaching contributed to its disappearance from soil or that abiotic transformation may have played a role in its degradation. Overall, our results suggest that bacterial activity was the main route of 2,4-D degradation in soil, resulting in the transformation of 2,4-DCP.

Introduction

Urban landscapes are ubiquitous in the continental U.S., consisting of approximately 50 million acres of managed turfgrass, especially in areas where recent population growth has occurred.^{1,2} In order to maintain these urban areas, various inputs include water, fertilizer, and pesticides.¹ Among the pesticides that are applied, the herbicide 2,4-dichlorophenoxyacetic acid (2,4-D) is widely used to control broadleaf weeds in urban landscapes.³⁻⁵ 2,4-D acts as a synthetic auxin herbicide to promote uncontrolled cell division and elongation in plants, ultimately resulting in plant death.⁶

According to the U.S. Environmental Protection Agency (EPA), 2,4-D was the most used herbicide in home lawns and gardens in 2009 and 2012.⁷ Due to its extensive and frequent use in urban landscapes, 2,4-D fate and breakdown have been well documented in various matrices including soil, agricultural and non-agricultural crops, and water.^{5,8-10} However, the potential adverse impact of 2,4-D does not end at the point of application.¹¹ 2,4-D can undergo environmental degradation and may result in transformation products (TPs) that interact with the environment differently than the parent molecule.¹² Once applied in the soil, the behavior and fate of 2,4-D will depend on different factors, such as the formulation in which it was applied.¹³ For example, as an amine formulation, 2,4-D can be readily soluble in water.⁸ In contrast, as an ester formulation, 2,4-D is insoluble in water and less volatile.⁸ For this reason, 2,4-D amine and ester formulations are typically applied in warmer and cooler weather, respectively.¹⁴ Although different 2,4-D formulations behave differently according to their physico-chemical properties, they readily convert to the acid form once they are applied. In this case, once 2,4-D converts to its acid form, it becomes more water-soluble, increasing its ability to leach to groundwater.^{5,15} Other scenarios include 2,4-D becoming airborne through volatilization, although little has been found to

occur.^{16,17} Although 2,4-D has a low vapor pressure, EPA studies have found that 2,4-D has a half-life of 6.2 days in aerobic mineral soils.¹⁸ Other field dissipation studies have found that 2,4-D's half-life can range from 1.70 to 13.1 days,⁸ which can also depend on the composition and properties of the soil matrix.¹³

2,4-D can undergo various biotic and abiotic mechanisms when released to the environment. The primary abiotic processes through which 2,4-D can be broken down are photodegradation, hydrolysis, oxidation, and reduction reactions.^{19–21} Biotic interactions are mediated by organisms that include invertebrates, plants, and microorganisms.²² In particular, 2,4-D is mainly broken down by bacteria in soil, which are influenced by a wide range of environmental factors such as temperature, moisture, cultural management practices, and soil type/conditions (structure, texture, pH, among others),²³ thus resulting in the formation of its major TP, 2,4-dichlorophenol (2,4-DCP), as well as other soil TPs such as 3,5-dichlorocatechol (3,5-DCC). Other 2,4-D TPs include 4-chlorophenol (4-CP), typically formed through anaerobic aquatic metabolism, 1,2,4-benzenetriol, through aqueous photolysis, and 2,4-dichloroanisole (2,4-DCA), which is formed from 2,4-DCP through microbial methylation.^{24–28}

TP toxicity is partially assessed through their mode of action and physico-chemical properties (pKa, log K_{ow} , and log K_{oc}).²⁹ In the case of 2,4-D's main TP, 2,4-DCP contains a higher K_{ow} than its parent compound – 2.96 versus 2.65 – which may result in less dissociation and more likely to bioaccumulate in organisms.²⁹ Also, 2,4-DCP contains a higher vapor pressure than 2,4-D – 9772.53 mPa versus 2.69 mPa – and can also result in volatilization and off-site contamination. Another important property of 2,4-DCP is its high K_{oc} value. Compared to 2,4-D, 2,4-DCP's high K_{oc} value describes its ability to bind strongly to soil – 646 L kg⁻¹ versus 45.7 L kg⁻¹ (**See Chapter 1, Table 1.2**).²⁹

Because seasonal fluctuations are one of the most important factors influencing bacterial community structure and function,^{22,23} it is important to evaluate pesticide TP formation, especially in urban areas where 2,4-D is commonly applied. It is, therefore, of rising concern when 2,4-D is applied at varying seasonal conditions since soil bacteria may shift in composition and structure, influencing how 2,4-D breaks down to its TPs. This study assessed the detection and quantification of the herbicide 2,4-D and its major TP, 2,4-DCP, in leaf, soil, and leachate matrices derived from urban landscapes at varying seasonal conditions. Field studies were conducted in two consecutive years – 2018 and 2019 – in addition to a growth chamber study simulating spring and summer conditions. Autoclaved samples were included in this study to eliminate the impact of soil microbial activity on 2,4-D degradation and account for potential abiotic transformation. Therefore, we hypothesized that: i) 2,4-D breakdown mainly occurs via soil bacterial activity degradation pathways, resulting in the formation of 2,4-DCP and ii) higher seasonal temperature conditions increase 2,4-D degradation. The development and optimization of a solid-phase extraction (SPE) method for 2,4-D and 2,4-DCP in soil matrices and a dispersive SPE (d-SPE) technique for leaf tissue is also described in this study. The SPE method for soil samples described here is a variation of the method proposed by Moret et al. (2005).¹³

Materials and Methods

Chemicals and Reagents. 2,4-Dichlorophenoxyacetic acid (97%) (2,4-D) and 2,4-dichlorophenol (2,4-DCP) were obtained from Sigma Aldrich (St. Louis, MO) and EMD Millipore Corp. (Billerica, MA), respectively. Internal standards 2,4-D (Ring-d3, 98%) and 2,4-DCP (Ring-d3, 98%) were purchased from Cambridge Isotopes Laboratories Inc. (Andover, MA). The formulated commercial product containing the 2-EHE form of 2,4-D (Radar LV4) was purchased from Growmark (Bloomington, IL). Methanol (MeOH) and formic acid (FA) were used as high-

performance liquid chromatography (HPLC)-grade solvents and obtained from Fisher Scientific Co. (Fair Lawn, NJ). HPLC-grade acetonitrile (ACN) was purchased from Sigma Aldrich (St. Louis, MO). Sodium hydroxide prepared at 0.01 M concentration. Ultrapure water was also obtained using a Milli-Q water purification system maintained at 18.2 M Ω cm. The sorbents used for solid-phase extraction and preconcentration of soil samples were 5 mL disposable cartridges packed with 500 mg of Bond Elut-ENV (Agilent Technologies, Wilmington, DE). For leaf samples, dispersive solid-phase extraction (d-SPE) 2-mL tubes containing primary secondary amines (PSA), graphitized carbon black (GCB), and magnesium sulfate (MgSO₄) were also obtained from Agilent Technologies, Inc. (Folsom, CA).

Standard Stock Preparation. A 50 $\mu\text{g mL}^{-1}$ stock solution mixture of 2,4-D and 2,4-DCP was prepared in 100% MeOH and stored at -20°C. Standard solutions of the mixture were then prepared from the initial stock at the concentrations of 1, 5, 10, 15, and 25 $\mu\text{g mL}^{-1}$ using Milli-Q H₂O. Similarly, a 1 mg mL⁻¹ stock solution of the internal standard mixture was prepared using MeOH. Another internal standard stock was prepared at 50 $\mu\text{g mL}^{-1}$ using Milli-Q H₂O and stored at -20°C.

Field Study. Field trials were conducted on mature strands of perennial ryegrass (*Lolium perenne*) and Kentucky bluegrass (*Poa pratensis*) at the OJ Noer Turfgrass Research Station (OJ) in Madison, WI, and Pleasant View Golf Course (PV) in Middleton, WI in 2018 and 2019. Soil analysis from each site was performed by the UW Soil and Forage Analysis Lab in Marshfield, WI, before conducting our first application for each field trial (**Table 2.1**). Field plots were maintained by weekly mowing of the grass at approximately 6 cm in height. No supplemental pesticides, fertilizer, or irrigation were applied to the plot over the course of the study. Treatment formulations of 2,4-D and water as a non-treated (NT) control were applied on May 1st and July

1st in 2018 and April 30th and July 3rd in 2019, representing conditions for spring and summer seasons, respectively. 2,4-D was applied to field plots at a nozzle pressure of 40 psi using a CO₂ pressurized boom sprayer equipped with two XR Teejet AI8004 nozzles. The herbicide was agitated by hand and applied at a rate equivalent to 0.35 mL per m² of the commercial 2,4-D product with an initial concentration of 2.62 mg mL⁻¹. The design consisted of a randomized complete block design with four replications per treatment, where each plot contained an area of 1.39 m². Soil temperature was measured once at each sampling date using a digital soil thermometer from Spectrum Technologies (Aurora, IL) (**See Chapter 3, Figure S4 for results**). Soil moisture content from each plot was measured using a soil moisture meter from Spectrum Technologies (**See Chapter 3, Figure S5 for results**). Soil cores 2.5 cm in diameter were collected from each plot at 0, 7, 14, and 21 days after treatment application using a stainless-steel soil probe. Subsamples of leaf, upper soil (top 5 cm) and lower soil (15 to 20 cm depth) were then collected and stored at -80°C until further processing.

Table 2. 1 Soil analysis for O.J. Noer and Pleasant View field sites in 2018 and 2019. OJ= O.J. Noer; PV = Pleasant View; ppm = parts per million; [P] = Phosphorous; [K] = Potassium; OM = Organic Matter

Year	Sites	% Sand	% Silt	% Clay	Texture Name	pH	[P] (ppm)	[K] (ppm)	OM %
2018	<i>OJ</i>	18	59	23	Silt Loam	6.9	70	23	3.4
	<i>PV</i>	36	47	17	Loam	7.2	89	134	5.7
2019	<i>OJ</i>	13	61	26	Silt Loam	7.2	53	115	2.5
	<i>PV</i>	45	37	18	Loam	7.4	110	141	3.0

Growth Chamber Study. The growth chamber study was conducted at the Plant Pathology Department at UW-Madison. 100-mm diameter soil core samples of 50:50 Perennial ryegrass and Kentucky bluegrass with a depth of 200 mm were collected at the OJ Noer Turfgrass Research Station in Madison, WI, close to where 2018 and 2019 field trials were conducted. A total of 36 samples were collected and transferred on July 30th, 2020, to two individual growth

chambers for a total of 18 cores per chamber, each simulating one of the average seasonal temperatures and photoperiods listed in **Table 2.2** and allowed to acclimate for 14 days (**Figure S1**).³⁰ A PVC column with a diameter of 101.6 mm and a depth of 203.3 mm was used to hold the collected core samples. On the bottom of each column were 12 holes with an approximate diameter of 1 mm, serving as drainage systems to allow for leachate collection. 20 mLs of MQ H₂O were applied to each soil core sample each day using a pipette. On day 5 post-application, leachate was allowed to percolate after adding MQ H₂O and collected using a beaker. The study consisted of a randomized sample design with three replications per treatment per temperature (**Figure S1**).

Table 2. 2 Temperature and photoperiods simulating spring and summer conditions.

SEASON	GROWTH CHAMBER
SPRING	14h day:10h night 18°C: 6.5°C
SUMMER	15h day: 9h night 28°C:15.5°C

Treatments of the 2,4-D and NT control were applied after acclimation was achieved after 14 days. 2,4-D was applied to core samples at the same rate as in the field study. Subsamples from each core were collected in the following regions: upper soil (top 5 cm), lower soil (15-20 cm depth), leaf tissue, and leachate. Lysimeters aided in collecting the amount of water flow in the soil. Collection days for 2,4-D and NT samples were at 1-, 5-, 7-, and 10-days post-application and samples were stored at -80°C until further processing.

Testing Autoclaving Effectiveness in Growth Chamber Core Samples. After acclimation, 6 core samples from each chamber were autoclaved twice for 45 min on slow exhaust settings on two consecutive days. Autoclaved soil cores were allowed to cool, and 0.1 g of soil was collected from the center of each core to test for the presence of viable bacteria. The soil was diluted in 1 mL of sterilized H₂O, and serial dilutions were then performed and plated in nutrient

agar. Plates were incubated at 25°C for two days, and colony-forming units (CFU) were counted after incubation (**Figure S2**).

Soil Sample Extraction and Cleanup. 5.0 g of upper and lower soil subsamples were weighed and placed directly into individual 50-mL polypropylene tubes and spiked with 50 μL of the internal standard mixture (1 mg mL^{-1}). Samples were allowed to sit at room temperature for 30 min and were then placed at 4°C overnight to allow the internal standard to adhere to the soil. Then 10 mL of 0.01 M NaOH was added, and samples were rotated at 210 rpm for 30 min ($25^\circ\text{C} \pm 1^\circ\text{C}$). Alkaline extracts were then centrifuged for 20 mins at 6000 rpm to separate the soil supernatants and filtered through 0.20 μm .

A solid-phase extraction method was optimized and developed according to a study conducted by Moret et al. (2005).¹³ First, the sorbent was conditioned with 10 mL of 100% MeOH. Second, a washing step was performed with 5 mL of Milli-Q water. Care was taken to not let sorbent dry. Third, the alkaline extract was loaded and allowed to percolate slowly onto the cartridge. Fourth, interferents were washed off with 5 mL of Milli-Q water and dried under vacuum for 10 s. Fifth, analytes were eluted with 5 mL of 100% MeOH. Lastly, extracts were evaporated under N_2 until dryness at 30°C and were then reconstituted in 500 μL of ACN: H_2O (50:50).

Leaf Sample Extraction and Cleanup. 0.2 g of leaf tissue sample was transferred to an individual lysing matrix D tube. Then 100 μL of the internal standard mixture ($50 \mu\text{g mL}^{-1}$) was applied directly to the leaf material (final concentration of $5 \mu\text{g mL}^{-1}$). The internal standard mixture was left to adhere to the leaf material for 30 min, and 600 μL of ACN containing 1% FA was added for a final volume of 1 mL. Samples were macerated using an MP Biomedicals FastPrep-24 benchtop homogenizer at 6 m s^{-1} for 40 s. Then 50 mg of MgSO_4 and 15 mg of anhydrous sodium acetate were added to remove excess water from the sample. Samples were

macerated once again and centrifuged at 6,000 rpm for 5 min. to separate solid and liquid portions. The entire liquid portion from the top was removed via pipette and transferred to a 2-mL d-SPE tube, shaken vigorously by hand for one min, and centrifuged a second time at 6,000 rpm for 5 min. All leaf extracts were filtered using a 0.22 μm filter and transferred to a 2-mL amber glass sample vial (Fisher Scientific Co.) for liquid chromatography-tandem mass spectrometry (LC-MS/MS) analysis.

Leachate Sample Cleanup. All leachate samples collected from the growth chamber study were filtered using a 0.20 μm filter and transferred to 2-mL amber glass sample vial (Agilent Technologies, Wilmington, DE) for LC-MS/MS analysis.

LC-MS/MS Quantification. According to previous literature, the primary soil metabolite of 2,4-D is 2,4-dichlorophenol (2,4-DCP).^{29,31–33} Analytes were optimized by infusing 20 μM of each compound prepared in HPLC grade 100% methanol (MeOH) through direct injection on an Agilent 1260 HPLC coupled to a 6460 Triple Quad MS using multiple reaction monitoring (MRM) and negative electrospray ionization (ESI-). Optimization results for both the analytes of interest and their internal standards (IS) are shown in **Table 2.3**. The best chromatographic separation and MS signals were achieved on a Poroshell 120 Bonus-RP, 2.7- μm , 3.0 x 100 mm column using the following analysis conditions: flow rate, 0.30 ml min^{-1} ; column temperature, 40°C; mobile phase A, 0.1% formic acid (FA) in H_2O ; and mobile phase B, 0.1% FA in MeOH, filtered through a 0.20 μm filter. Gradient elution was performed as follows: (1) 0.0 min→1.6 min, 70% A; (2) 1.6 min→2.0 min 30% A; (3) 2.0 min→13.0 min 5% A; (4) 13.0 min→13.10 min, 5% A; (5) 13.10→17.0 min, 70% A. The total run time was 17 min. The injection volume was 5 μL for all standards and sample extracts. Mass spectrometry analysis contained the following source parameters: capillary voltage of 3,500 V, nebulizer pressure of 45 psi, gas flow of 5 L min^{-1} , gas

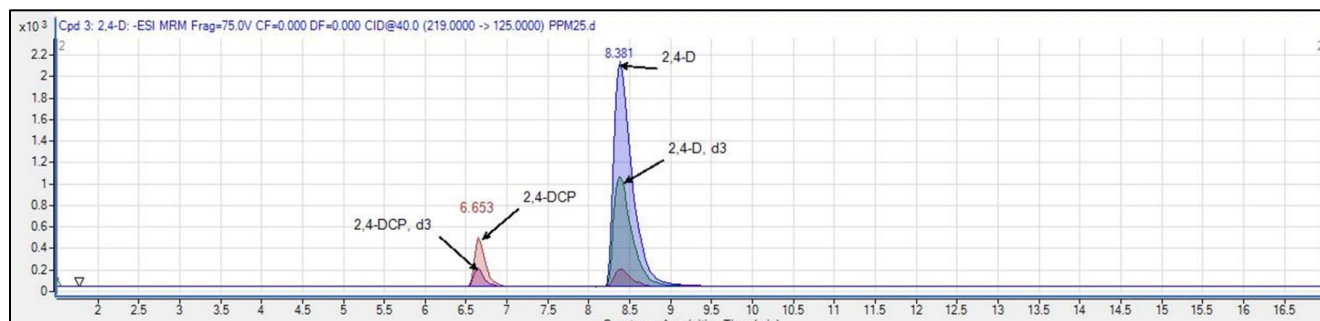


Figure 2. 1 Chromatogram of 2,4-D, 2,4-DCP, and their internal standards, 2,4-D,d3 and 2,4-DCP,d3.

temperature of 300°C, sheath gas flow of 11 L min⁻¹, and sheath gas temperature of 250°C.

Detection was acquired using MRM with a dwell time of 200 ms. Ion transitions were quantified using Agilent's Mass Hunter Workstation software (version B.07.00).

Table 2. 3 Mass spectrometry optimization parameters of 2,4-D, 2,4-DCP and their internal standards.

Target Analyte	Precursor Ion	Product Ion	Fragmentor Voltage (V)	Collision Energy Voltage (V)	Retention Time (min)
2,4-D	219	125.0	75	11	8.40
2,4-D		164.0		22	
(Ring-D3, 98%)	222	127.0	85	32	8.40
2,4-DCP	161.10	124.90		20	
		89	80	30	6.70
2,4-DCP		127.0		20	
(Ring-D3, 98%)	164	89.8	90	25	6.70

Mass Balance Calculations. The surface area of the lysimeter (0.081 m²) was calculated implementing the diameter (101.6 mm) and depth (203.3 mm) values in the following formula:

$$\text{Surface Area of a Cylinder} = 2\pi r(r + h)$$

Where 'r' denotes the radius and 'h' denotes the height (depth) of the lysimeter. After, the rate in which 2,4-D was applied (0.35 mL m²) was multiplied by the area previously calculated to obtain

how much of the herbicide solution was added to each lysimeter (Amount in volume sprayed = 0.028 mL). Lastly, the concentration of 2,4-D in the solution (2.62 mg mL⁻¹) was multiplied by the volume sprayed to determine the total amount of 2,4-D applied to each soil core sample, obtaining a value of 73.36 µg. The amount of 2,4-D recovered in the soil, leaf, and leachate samples at the different time points (except for leachate samples, which were only collected at day 5 post-application) was then compared with the amount that was initially added (73.36 µg) to conduct the mass balance.

Data Processing and Statistical Analysis. The data was processed and analyzed using R software, version 3.6.2. A Shapiro-Wilks test was conducted to evaluate the normality of the dataset using the *shapiro.test()* function in R. Since normality was not met (p-value < 0.05; data not shown), the data was recorded as the median and the 25th to 75th interquartile range. The Kruskal-Wallis test was performed to test the effects of autoclaving methods, treatment, layers, days, and season-simulated temperatures using the *kruskal.test()* function in R. Pairwise comparisons was performed to evaluate intergroup differences using the package *PMCMRplus* and the function *kwAllPairsConoverTest()* in R while implementing a Bonferroni correction. The level of statistical significance was set at $p < 0.05$.

Results

LC-MS/MS Method Validation. Recovery experiments were performed to verify the effectiveness of the soil and leaf extraction method. **Table 2.4** summarizes the recovery data for soil and leaf samples fortified at three different concentration levels – 10, 20, and 30 µg g⁻¹ and 15, 25, and 50 µg g⁻¹ – and extracted using the methods mentioned previously. Standard curves demonstrated optimal linearity ($R^2 > 0.995$) for each compound (data not shown). The limits of detection (LOD) and quantification (LOQ) of 2,4-D were calculated from the signal-to-noise ratio

corresponding to 3 and 10 times the noise level, respectively. The LOD and LOQ were 0.16 and 0.49 $\mu\text{g mL}^{-1}$, respectively, for 2,4-D, and 0.45 and 1.37 $\mu\text{g mL}^{-1}$, respectively, for 2,4-DCP.

Table 2. 4 Average recoveries, standard deviations, limit of detection (LOD) and limit of quantitation (LOQ) for 2,4-D and 2,4-DCP in soil and leaf extraction methods. ND = Not Detected

Compounds	n	Matrix	Fortification Level ($\mu\text{g g}^{-1}$)	Recovery (%)	LOD ($\mu\text{g g}^{-1}$)	LOQ ($\mu\text{g g}^{-1}$)
2,4-D	3	Soil	10	101.27 \pm 0.10	0.32	0.98
	3		20	49.60 \pm 0.04		
	3		30	32.97 \pm 0.11		
	2	Leaf	15	194.40 \pm 5.02	0.8	2.45
	2		25	120.58 \pm 3.24		
	2		50	51.04 \pm 0.42		
2,4-DCP	3	Soil	10	95.34 \pm 0.15	2.25	2.74
	3		20	90.49 \pm 0.11		
	3		30	83.41 \pm 2.39		
	2	Leaf	15	ND	0.45	6.85
	2		25	92.53 \pm 5.52		
	2		50	101.21 \pm 1.80		

Field Study.

Treated versus non-treated samples. To avoid false-positive detection or errors due to potential contamination from the analysis, 2,4-D- treated and non-treated samples were compared by considering the LOQ and blank samples. There were no differences observed between non-treated and treated samples in PV 2018 (p-value = 0.44) (**Figure 2.2A**) and OJ 2019 (p-value = 10.10) (**Figure 2.2D**). On the other hand, treatments were significantly different in OJ 2018 (p-value = 0.01) (**Figure 2.2B**) and PV 2019 (p-value = 1×10^{-5}) soils (**Figures 2.2C**) but were under the LOQ.

2,4-D and 2,4-DCP detection in OJ and PV soils. The concentrations of 2,4-D detected in treated soil ranged from < LOQ (0.98 $\mu\text{g g}^{-1}$) to $5.61 \pm 6.39 \mu\text{g g}^{-1}$ (**Table 2.5**). Overall, 2,4-D

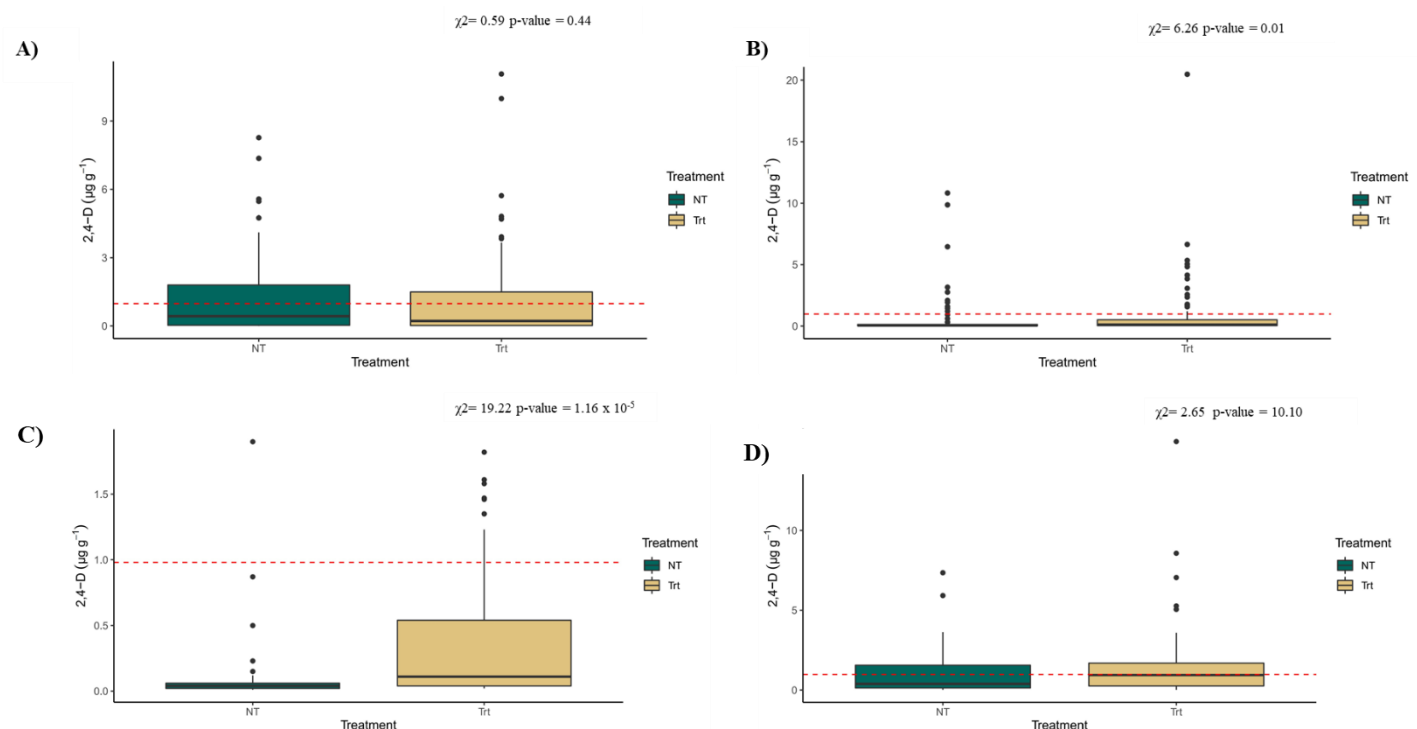


Figure 2. 2 Box-whisker plots of 2,4-D quantification in soil samples collected from 2018 (A and B) and 2019 (C and D) field trials (n=509). Panels show values for **A)** PV (n = 125), **B)** OJ (n = 128), **C)** PV (n = 128), and **D)** OJ (n = 128) field sites. Boxes start at the 25th and end at the 75th percentile. The center line represents the median value. Dots represent outliers that fall outside of the percentile ranges. The red dashed line represents the LOQ in soil, $0.98 \mu\text{g g}^{-1}$. A Kruskal-Wallis test was performed between groups, and a statistically significant differences was accepted at $p < 0.05$ by Bonferroni correction.

residues measured in 2018 soil samples had a higher concentration at day 0 post-application (**Table 2.5**). A gradual decrease of 2,4-D was observed at the varying time points, especially in PV 2018 soil samples (**Figure 2.3A**). A similar trend of a decrease in 2,4-D at the different time points was observed in PV 2019 samples, however, concentrations were under the LOQ at days 7-, 14-, and 21-days post-application (**Figure 2.3C**). In OJ 2018 and 2019 collected soils, 2,4-D residues were also under the LOQ at the varying time points post-application (**Figures 2.3B and 2.3D**). 2,4-DCP residue concentrations ranged from $< \text{LOQ}$ ($2.74 \mu\text{g g}^{-1}$ to $19.72 \pm 17.47 \mu\text{g g}^{-1}$ (**Table 2.5**). 2,4-DCP was not detected in PV samples during the month of May in 2018 (**Table 2.5**). However, higher concentrations were observed in both PV and OJ field sites in soil samples collected in July, specifically after day 0 post-application (**Table 2.5**).

Soil samples collected in 2019 in PV field site exhibited 2,4-D residues under the LOQ in both May and July (**Table 2.6**). In OJ field sites, 2,4-D concentrations ranged from < LOQ to $6.10 \pm 4.52 \mu\text{g g}^{-1}$. Higher concentrations of 2,4-D were observed at day 0 post-application during the month of May in OJ field site (**Table 2.6**). 2,4-DCP residues ranged from < LOQ to $69.43 \pm 138.26 \mu\text{g g}^{-1}$ (**Table 2.6**). High concentrations of 2,4-DCP were primarily observed in PV field sites during the months of May (**Table 2.6**).

Table 2. 5 Average concentrations found for 2,4-D and 2,4-DCP in PV and OJ field soil at May and July season conditions at the varying time points in 2018.

Site	Month	Day	n	Analyte concentration ($\mu\text{g g}^{-1}$ soil)	
				2,4-D	2,4-DCP
PV	May	0	8	3.24 ± 3.31	ND
		7	8	< LOQ	ND
		14	7	< LOQ	ND
		21	8	< LOQ	ND
	July	0	8	2.95 ± 1.87	ND
		7	8	1.51 ± 1.88	9.98 ± 21.25
		14	8	1.68 ± 3.83	3.87 ± 7.53
		21	8	< LOQ	< LOQ
OJ	May	0	8	1.34 ± 2.06	< LOQ
		7	8	< LOQ	< LOQ
		14	8	< LOQ	ND
		21	8	5.61 ± 6.39	ND
	July	0	8	< LOQ	< LOQ
		7	8	< LOQ	< LOQ
		14	8	< LOQ	19.72 ± 17.47
		21	8	< LOQ	15.71 ± 14.71

Experimental conditions consisted of 5 g of soil, followed by the extraction method described in the “soil sample extraction and cleanup” section above. ND = Not Detected; <LOQ = Detected but below the quantification limit.

Table 2. 6 Average concentrations found for 2,4-D and 2,4-DCP in PV and OJ field soil at May and July season conditions at the varying time points in 2019.

Site	Month	Day	n	Analyte concentration ($\mu\text{g g}^{-1}$ soil)	
				2,4-D	2,4-DCP
PV	May	0	8	< LOQ	25.39 ± 29.03
		7	8	< LOQ	69.43 ± 138.26
		14	7	< LOQ	15.11 ± 21.32
		21	8	< LOQ	50.36 ± 103.22
	July	0	8	< LOQ	< LOQ
		7	8	< LOQ	< LOQ
		14	8	< LOQ	< LOQ
		37	8	< LOQ	< LOQ
OJ	May	0	8	6.10 ± 4.52	< LOQ
		7	8	1.50 ± 0.82	< LOQ
		14	8	< LOQ	< LOQ
		21	8	1.26 ± 1.58	< LOQ
	July	0	8	< LOQ	< LOQ
		7	8	< LOQ	< LOQ
		14	8	1.13 ± 0.93	< LOQ
		37	8	< LOQ	< LOQ

Experimental conditions consisted of 5 g of soil, followed by the extraction method described in the “soil sample extraction and cleanup” section above. ND = Not Detected; <LOQ = Detected but below the quantification limit.

Determination of 2,4-D residues at different soil depths. Differences were observed in the detection of 2,4-D at the different soil depths in OJ 2018 soils (p-value = 0.01) (**Figure 2.4B**). No significant differences between the soil depths were observed in PV 2018 (**Figure 2.4A**), PV 2019 (**Figure 2.4C**), and OJ 2019 (**Figure 2.4D**).

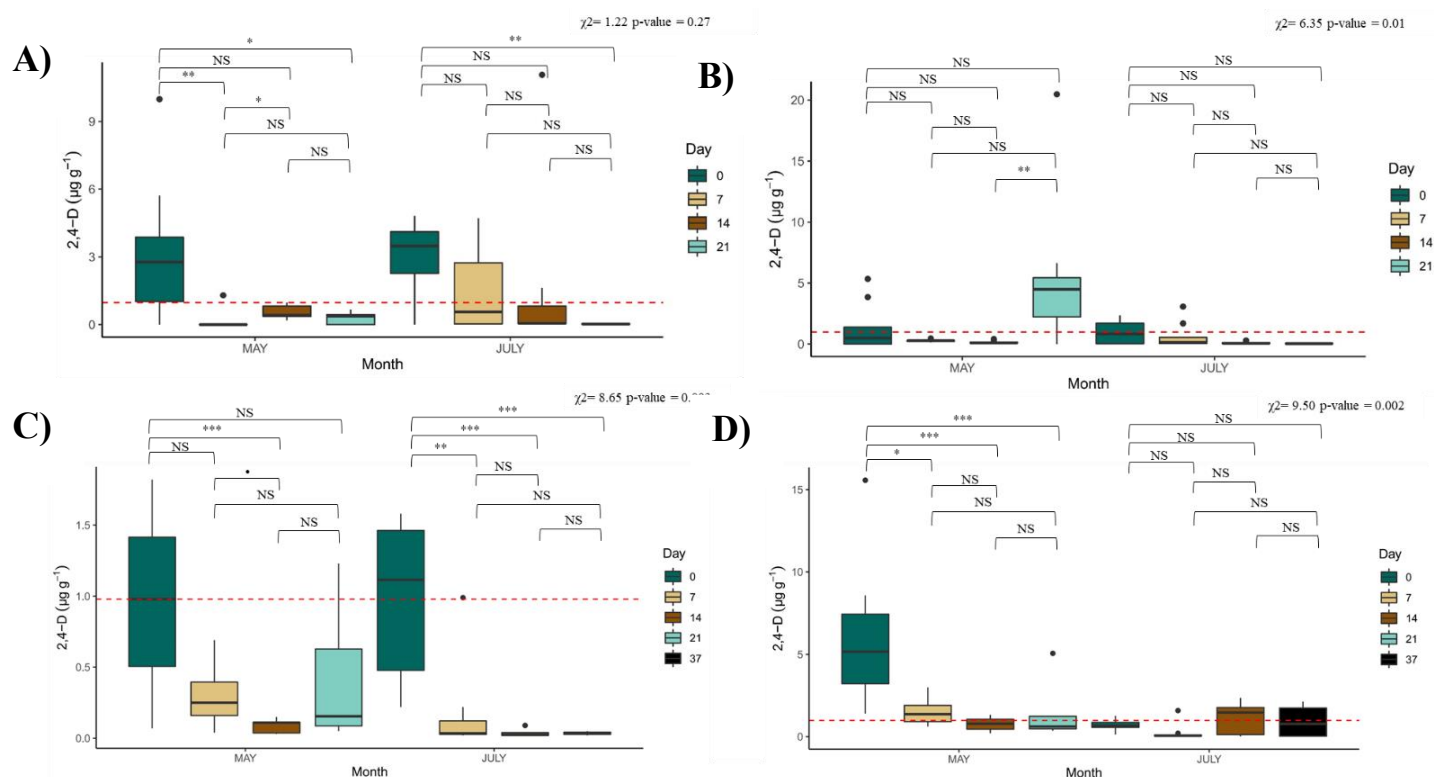


Figure 2.3 Box-whisker plots of 2,4-D quantification in treated soil samples collected from 2018 and 2019 field trials. Panels show values for **A)** PV 2018 ($n = 31$), **B)** OJ 2018 ($n = 32$), **C)** PV 2019 ($n = 32$), and **D)** OJ 2019 ($n = 32$) field sites and months at the varying days. Boxes start at the 25th and end at the 75th percentile. The center line represents the median value. Dots represent outliers that fall outside of the percentile ranges. The red dashed line represents the LOQ in soil, $0.98 \mu\text{g g}^{-1}$. A Kruskal-Wallis test was performed between groups, and a statistically significant differences was accepted at $p < 0.05$ by Bonferroni correction. Samples in July 2019 were collected on day 37 post-application.

Growth Chamber Study

2,4-D and 2,4-DCP residues detected in urban soil. Higher concentrations of 2,4-D were detected compared to 2,4-DCP in all treated soil samples (**Table S1**). The detected concentrations of 2,4-D in urban soils ranged from $< \text{LOQ}$ ($0.98 \mu\text{g g}^{-1}$) to $21.91 \mu\text{g g}^{-1}$ (**Table S1**). 2,4-DCP was either not detected or under the LOQ ($6.85 \mu\text{g g}^{-1}$) (**Table S1**). Similar to the field trial, 2,4-D-treated and non-treated samples were compared by considering the LOQ and blank samples. The non-treated and blank samples were below the LOQ of 2,4-D, and values were considered

insignificant (**Figure 2.5A**). According to the Kruskal-Wallis test, treated samples were significantly higher ($p\text{-value} = 8 \times 10^{-6}$).

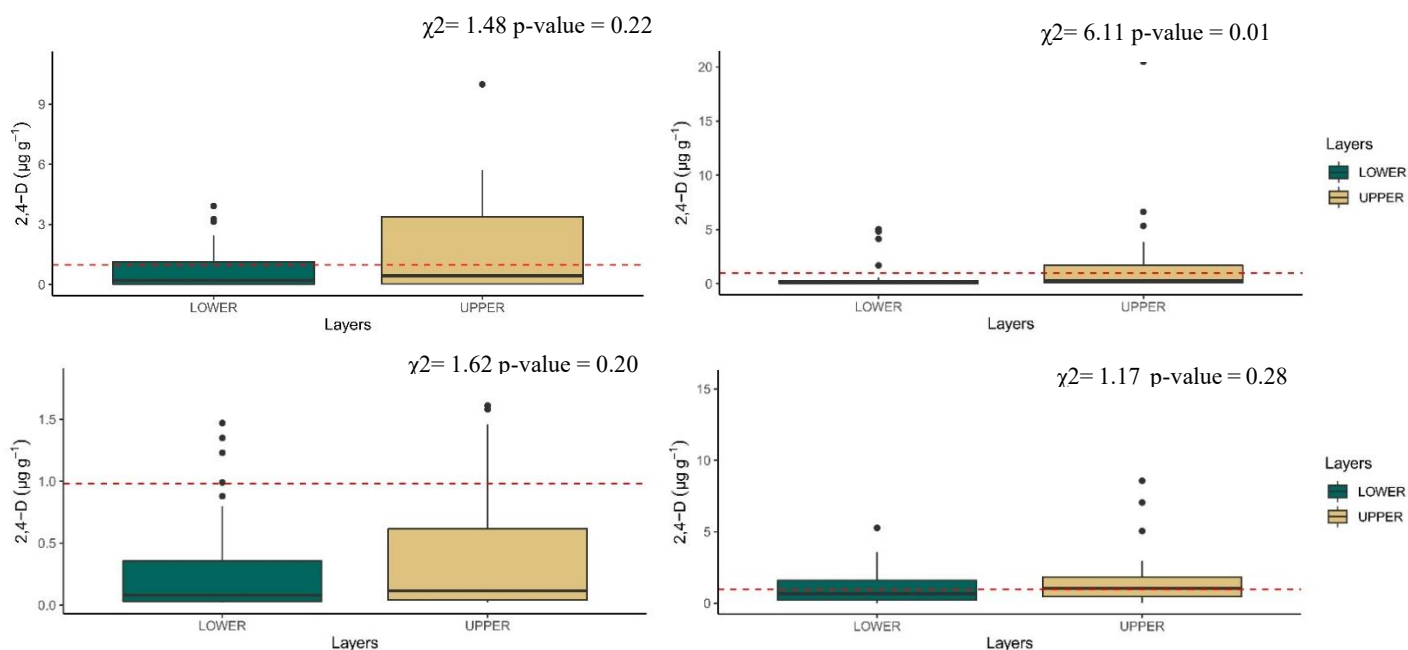


Figure 2. 4 Box-whisker plots of 2,4-D quantified in upper and lower soil depths in treated soil samples. Panels show values for **A**) PV 2018 ($n = 31$), **B**) OJ 2018 ($n = 32$), **C**) PV 2019 ($n = 32$), and **D**) OJ 2019 ($n = 32$) field sites and months at the varying days. Boxes start at the 25th and end at the 75th percentile. The center line represents the median value. Dots represent outliers that fall outside of the percentile ranges. The red dashed line represents the LOQ in soil, $0.98 \mu\text{g g}^{-1}$. A Kruskal-Wallis test was performed between groups, and a statistically significant differences was accepted at $p < 0.05$ by Bonferroni correction. Samples in July 2019 were collected on day 37 post-application.

There were no significant differences in 2,4-D detection between the spring- and summer-simulated conditions ($p\text{-value} = 0.40$) (**Figure 2.5B**). However, differences in 2,4-D concentration at individual sampling dates between the two temperatures were detected. Specifically, for spring-simulated conditions, 2,4-D residues were higher at day 1 post-application in comparison to days 5 and 7. There were no significant differences of 2,4-D residues between day 1 and 10 post-application (**Figure 2.5B**). Although statistical differences were not observed in spring-simulated conditions, the descriptive statistics show that 2,4-D values were $6.03 \pm 7.39 \mu\text{g g}^{-1}$ and $2.69 \pm 1.85 \mu\text{g g}^{-1}$, on days 1 and 10, respectively (**Table 2.5**). For summer-simulated conditions, 2,4-D

residues were significantly detected at day 1 versus day 7 post-application (**Figure 2.5B**). However, differences of 2,4-D concentration between day 1 and days 5 and 10 were not significant (**Figure 2.5B**). **Table S4** shows the raw average concentration of 2,4-D decreased from $7.15 \pm 8.53 \mu\text{g g}^{-1}$ on day 1 to $1.21 \pm 2.50 \mu\text{g g}^{-1}$ on day 10-post application in the summer-simulated conditions.

To assess whether the autoclaving procedure effectively eliminated or reduced the majority of the active soil bacteria, autoclaved and non-autoclaved soil was plated with nutrient agar, and colony-forming units (CFUs) were counted. Non-autoclaved soil samples contained approximately 160 CFUs, while autoclaved samples had less than 20 CFUs (**Figure S2**). 2,4-D degradation was then assessed in autoclaved versus non-autoclaved soil samples. There were no significant differences in 2,4-D residue levels (p-value = 0.18) between autoclaved and non-autoclaved soil (**Figure 2.5C**). Similar to season-simulated conditions effects shown in **Figure 2.5B**, the amount and variation of 2,4-D residue detected was also higher on day 1 post-application, especially in non-autoclaved samples (**Figure 2.5C**). Interestingly, pesticide residue on day 1 exhibited lower levels in autoclaved samples than in non-autoclaved samples ($3.93 \pm 5.78 \mu\text{g g}^{-1}$ versus $7.92 \pm 8.54 \mu\text{g g}^{-1}$) (**Table S5**).

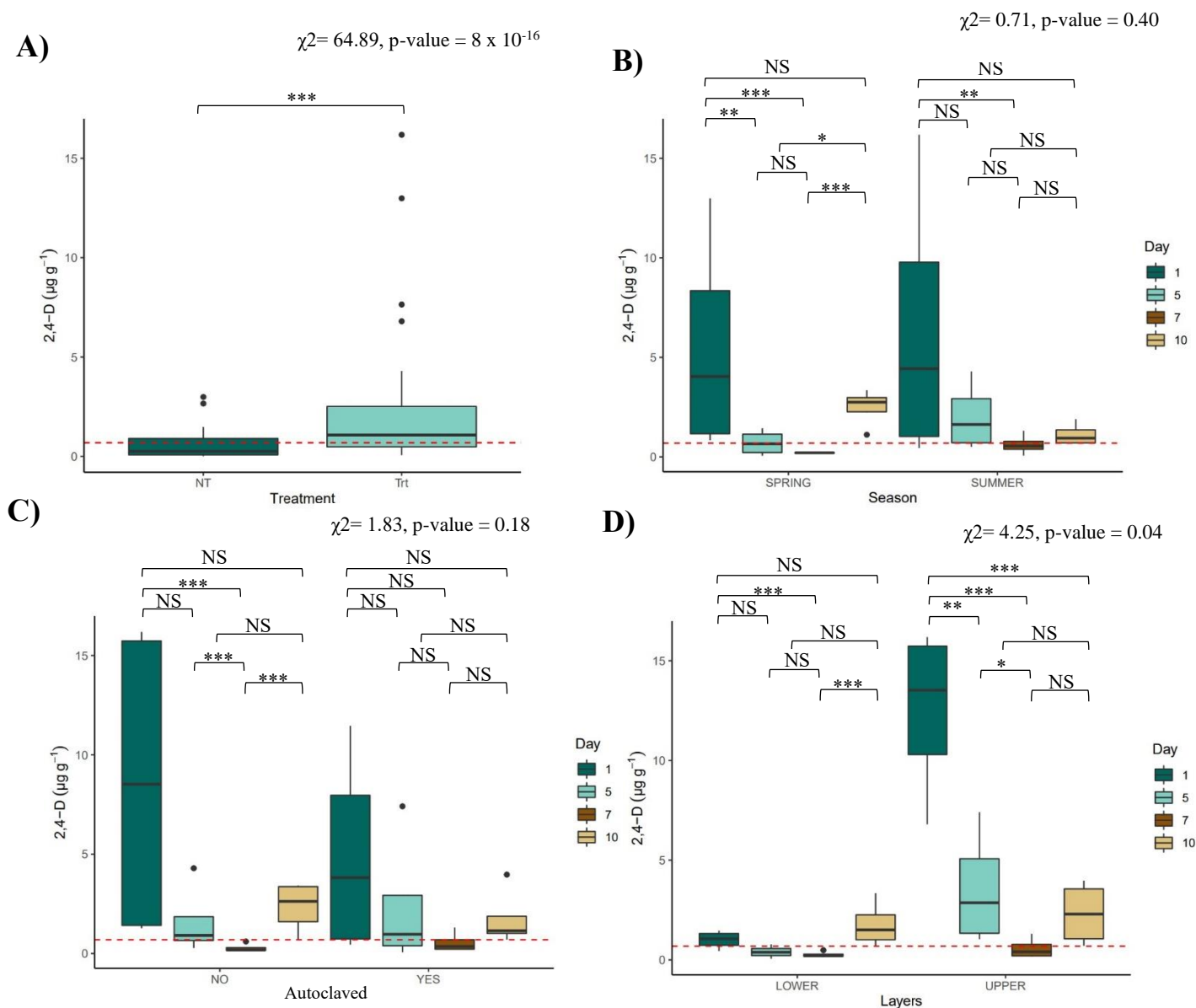


Figure 2. 5 Box-whisker plots of 2,4-D quantification in soil samples collected from the growth chamber study (n=287). Panels show values for **A)** Treatments (Treated = 143, NT =144), **B)** season-simulated temperatures (Spring = 71, Summer = 72), **C)** Autoclaving method (Autoclaved = 48, Not Autoclaved = 95), and **D)** soil layers (Upper = 72, Lower = 71). Boxes start at the 25th and end at the 75th percentile. The center line represents the median value. Dots represent outliers that fall outside of the percentile ranges. The red dashed line represents the LOQ in soil, $0.98 \mu\text{g g}^{-1}$. A Kruskal-Wallis test was performed between groups, and a statistically significant differences was accepted at $p < 0.05$ by Bonferroni correction.

Clear differences were observed in the detection of 2,4-D at the different soil depths (p-value = 0.04) (**Figure 2.5D**). Upper soil layers exhibited a higher detection of 2,4-D on day 1

post-application with an average raw concentration of $12.13 \pm 7.87 \mu\text{g g}^{-1}$ versus $1.04 \pm 0.97 \mu\text{g g}^{-1}$ in the lower soil layer (**Figure 2.5D and Table S6**). Overall, a distinct trend was observed, where 2,4-D disappeared throughout time and 2,4-DCP was detected at 5-, 7-, and 10-days post-application but was not quantifiable (**Figure 2.5, Table S4, Table S5, and Table S6**).

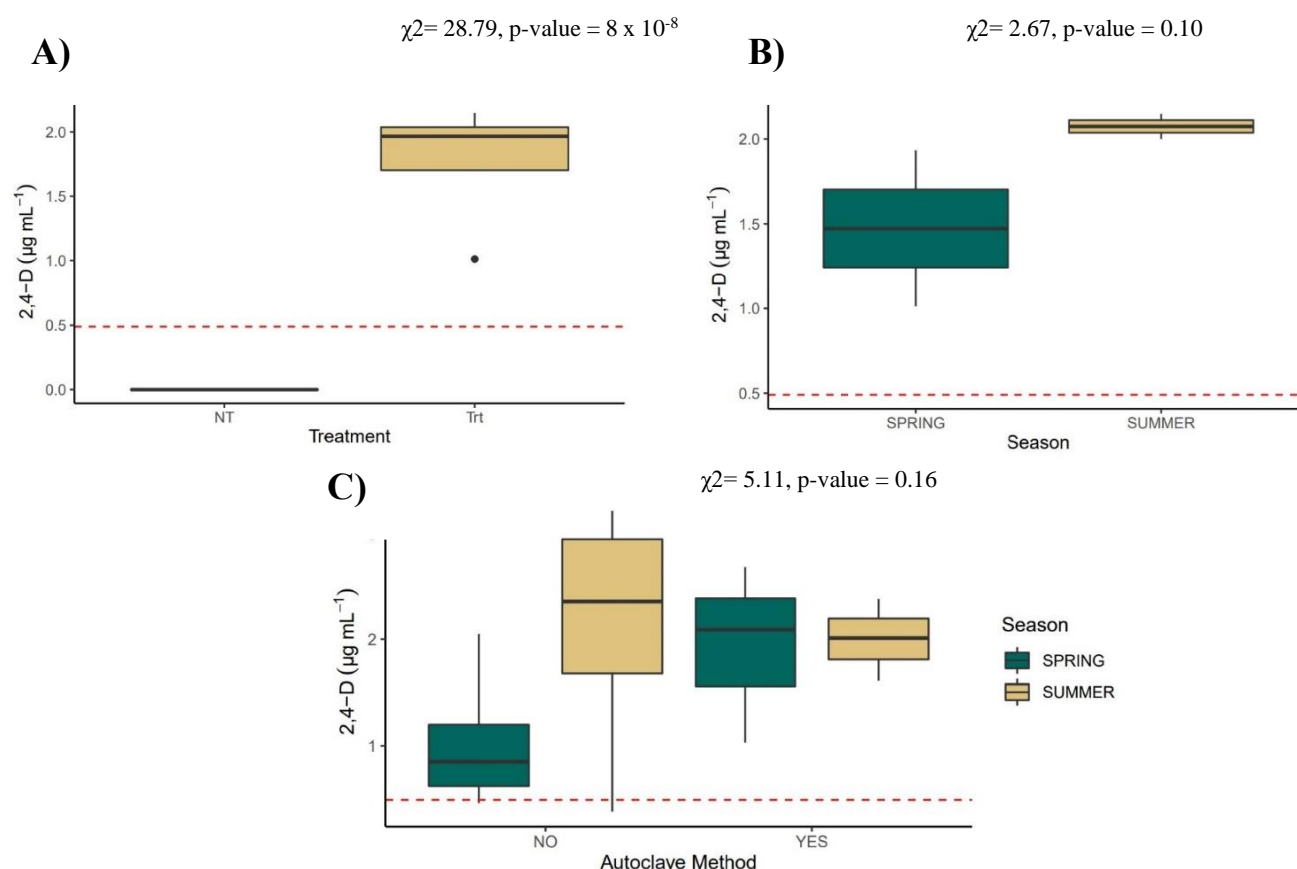


Figure 2. 6 Box-whisker plots of 2,4-D residues detected in leachate samples at day 5 post-application from the growth chamber study (n=35). Panels show values for **A)** Treatments (Treated = 18, NT = 27), **B)** season-simulated temperatures (Spring = 17, Summer = 18), and **C)** Autoclaving method at the varying seasonal-simulated temperatures. Boxes start at the 25th and end at the 75th percentile. The center line represents the median value. Dots represent outliers that fall outside of the percentile ranges. The red dashed line represents the LOQ in water, $0.49 \mu\text{g mL}^{-1}$. A Kruskal-Wallis test was performed between groups, and a statistically significant differences was accepted at $p < 0.05$ by Bonferroni correction.

Leaching potential of 2,4-D herbicide at varying season-simulated temperatures.

Leachate samples at day 5 post-application were collected to assess the potential of the 2,4-D

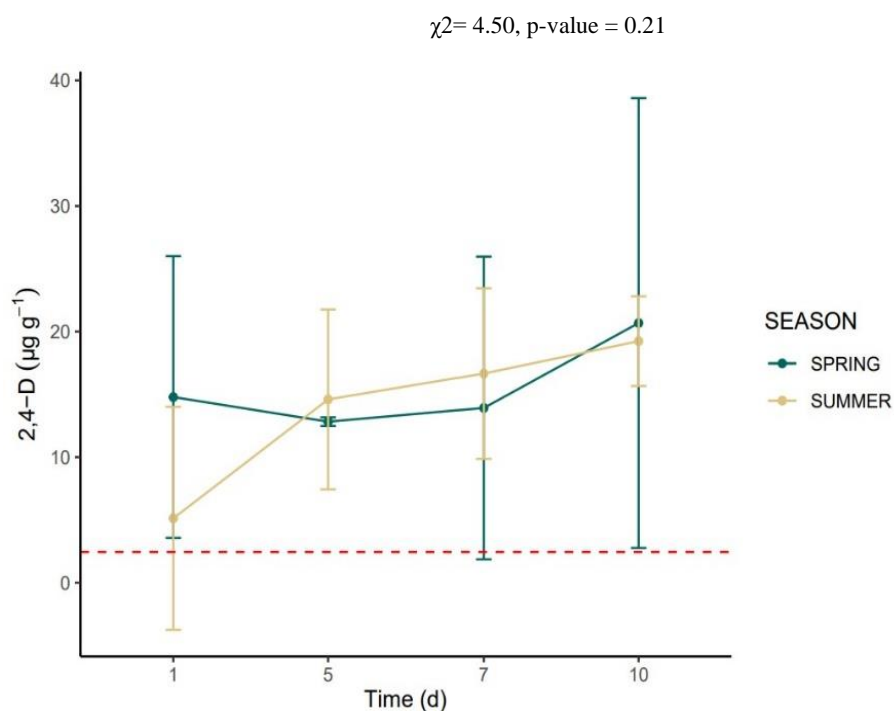


Figure 2. 7 Line plot showing 2,4-D residue levels in leaf tissue collected at the different timepoints and season-simulated conditions (spring and summer). Standard deviation is presented by the error bars from each timepoint where $n=3$. The red dashed line represents the LOQ in leaf tissue, $2.45 \mu\text{g g}^{-1}$. A Kruskal-Wallis test was performed between timepoints and season-simulated conditions. Statistically significant differences were accepted at $p < 0.05$ by Bonferroni correction.

Table 2. 7 Average residual amount found for 2,4-D in leaf tissue samples at spring and summer-simulated conditions and different timepoints.

Season	Day	n	2,4-D ($\mu\text{g g}^{-1}$)
Spring	1	3	14.79 ± 11.22
	5	3	12.82 ± 0.34
	7	3	13.92 ± 12.05
	10	3	20.68 ± 17.91
Summer	1	3	5.13 ± 8.88
	5	3	14.60 ± 7.16
	7	3	16.66 ± 6.79
	10	3	19.24 ± 3.57

herbicide formulation to leach at the varying season-simulated conditions and different autoclaving methods. Overall, the raw average concentration of 2,4-D found in leachate samples (n=18) was $1.71 \pm 0.98 \mu\text{g mL}^{-1}$ (**Figure 2.6A and Table S7**). For season-simulated conditions, higher leachate potential was observed in summer-simulated conditions. However, there was no significant difference of 2,4-D residues in leachate between spring and summer-simulated conditions (p-value = 0.10). Specifically, the raw average residual amount in leachate from spring and summer-simulated samples was $1.32 \pm 0.78 \mu\text{g mL}^{-1}$ and $2.10 \pm 0.88 \mu\text{g mL}^{-1}$, respectively (**Figure 2.6B and Table S7**). Measurements of 2,4-D leachate residues from the different autoclaving methods and season-simulated conditions are shown in **Figure 2.6C**. Non-autoclaved samples in growth chambers simulating spring conditions exhibited less 2,4-D leachate residues than in summer-simulated conditions (**Figure 2.6C and Table S7**). In contrast, there were no differences in the amount of 2,4-D observed in leachate between the simulated seasons in autoclaved samples (**Figure 2.6C and Table S7**). In general, there were no differences in leaching potential between the different autoclaving methods at the varying season-simulated conditions (p-value = 0.16).

Determination of 2,4-D residues in turfgrass leaf tissue. No significant differences were observed in the amount of 2,4-D detected in leaf tissue at the varying season-simulated conditions and timepoints (p-value = 0.21) (**Figure 2.7**). The concentration of 2,4-D in growth chambers simulating spring conditions ranged from $12.82 \pm 0.34 \mu\text{g g}^{-1}$ and $20.68 \pm 17.91 \mu\text{g g}^{-1}$ (**Table 2.5**). Summer-simulated conditions showed 2,4-D concentrations ranging from $5.13 \pm 8.88 \mu\text{g g}^{-1}$ to $19.24 \pm 3.57 \mu\text{g g}^{-1}$ (**Table 2.5**).

Mass balance of 2,4-D at different timepoints. A mass balance was conducted to estimate the amount of 2,4-D loss in the growth chamber study. Approximately 43% and 4% of the

compound was recovered in soil and leaf tissue matrix, respectively, in spring-simulated conditions on day 1 post-application. In the growth chamber simulating summer conditions, approximately 75% and 2% of 2,4-D was recovered in soil and leaf tissue, respectively, on day 1 post-application (**Figure 2.8**). Leachate samples were only collected on day 5. After 5 days of application, there was less recovery of 2,4-D in the soil than on day 1. However, similar amounts of 2,4-D residue were observed in leaf tissue compared to the day 1 post-application.

Interestingly, 2,4-D was detected in leachate samples after 5 days with a recovery ranging from 7% to 13% from both growth chambers. On day 7, a significant loss of 2,4-D was observed in both season-simulation conditions; approximately 1% and 4% of 2,4-D residues were recovered

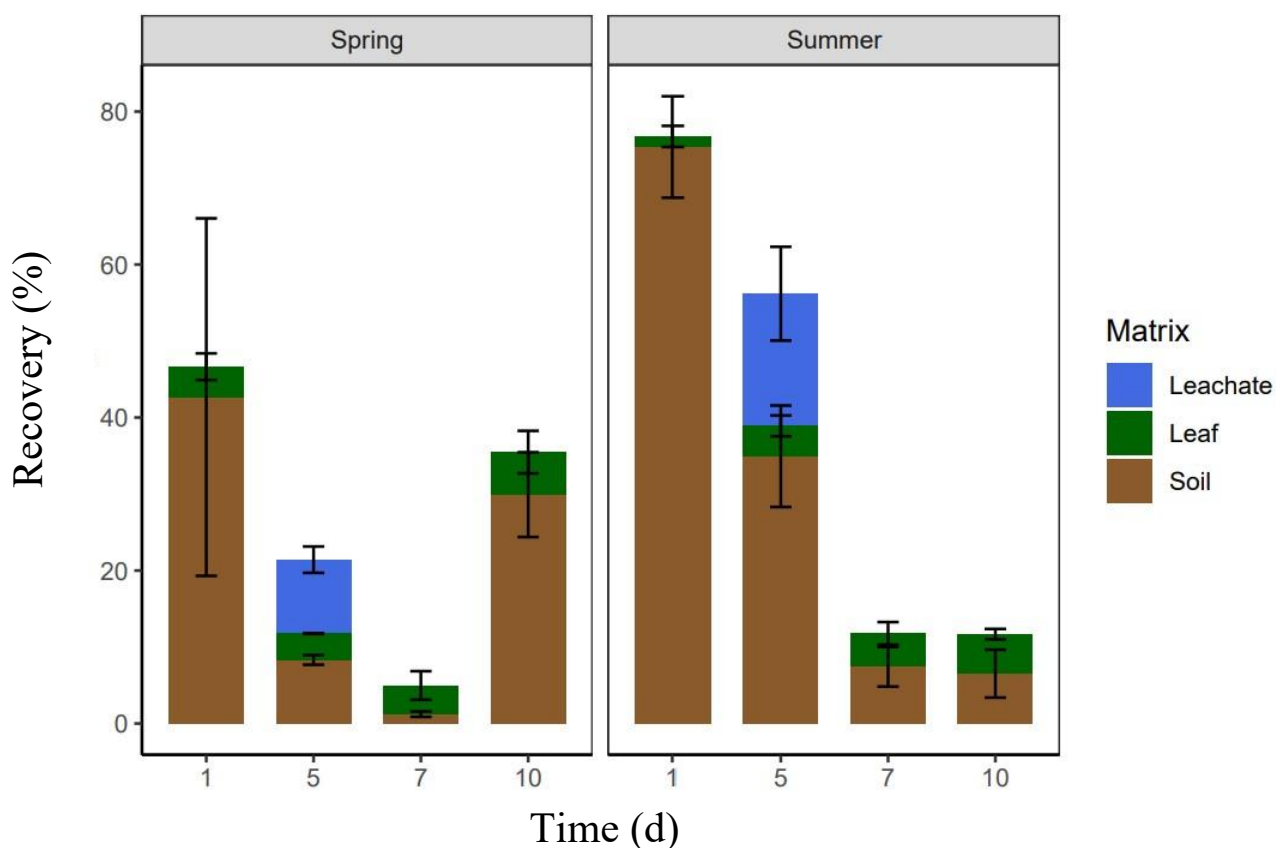


Figure 2. 8 Mass balance for 2,4-D in experimental systems simulating spring or summer seasonal conditions at 1-, 5-, 7-, and 10 – days post application. Recovery percentage of 2,4-D is shown for each day, bottom to top of bars: Soil (brown), leaf (green), and leachate (blue). Leachate samples were only collected at day 5 post application. Errors bars represent the standard deviation where n = 6 for soil samples, n= 6 for leaf, and n = 3 for leachate.

from soil and leaf in spring, respectively, and 7% and 2% in summer conditions. Low recoveries were observed on day 10 compared to 1 and 5 days after application in summer-simulated conditions in both soil and leaf matrices. In contrast, a higher recovery of 2,4-D was observed on day 10 post-application in soil and leaf in spring-simulated conditions.

Discussion

The results of the field growth chamber study suggest that 2,4-D is degraded in less than 10 days in urban soils, resulting in the formation of its major TP, 2,4-DCP. Although we did not observe any significant differences of 2,4-D concentrations between the spring and summer-simulated conditions in soil samples, our results suggest that residues of the analyte were still present in spring-simulated conditions at 10 days after application. Since bacteria primarily degrade 2,4-D in the soil, the longer persistence of 2,4-D in spring-simulated conditions may be due to the limited ability of soil bacteria to degrade 2,4-D in the presence of other carbon sources and slow degrading-activity at colder temperatures.⁵ A previous study conducted by Entry et al. (1995) aligns with this concept, where they found that 2,4-D mineralization and active bacterial biomass were greater in all other seasons except winter, suggesting that microbial communities have a greater capacity to degrade 2,4-D at higher temperatures.³⁴

With respect to the different soil depths assessed in the growth chamber study, the average residual amount of 2,4-D was higher in upper soil layers than in lower soil layers, especially on days 1 and 5 post-application. Factors influencing 2,4-D persistence in upper soil layers may be attributed to the type of soil that was sampled. Previous work has shown that differences in soil type can directly affect how 2,4-D behaves and persists in the environment.^{5,35} For example, 2,4-D's sorption abilities can be directly influenced by available organic matter, where studies have found that sorption of 2,4-D onto soil increases with increasing OM.³⁵⁻³⁸ Since soil samples from

the growth chamber study were collected in a nearby location to where field trials at the O.J. Noer Turfgrass Research station were conducted, we concluded that the type of soil was also that of silt loam texture with an overall 2 to 4% OM, where silt loam soil has been shown to have a positive correlation with OM, according to Hudson (1994).³⁹ Therefore, our results suggest that upper soil layer samples contained higher OM content than lower soil layer samples, thus attributing to 2,4-D's persistence in the initial days of its application. After 5 days of 2,4-D's application, we observed a significant decrease in the amount of 2,4-D residue detected in upper soil layers. As previously mentioned, the degradation of 2,4-D can be performed through abiotic and biotic mechanisms when released to the environment. Although photodecomposition of the herbicide was not measured in this study, it is possible that it may have undergone microbial degradation as photodecomposition, similar to previous work done by Crespín et al. (2001).⁴⁰

Another explanation for the rapid decrease of 2,4-D concentration in upper soil layers and the small amounts of residues detected in the lower soil layer samples may be the leaching process after irrigation. Leaching of 2,4-D to groundwater has been reported in previous studies, mainly due to 2,4-D's weak sorption to soil ($K_{oc} = 45.7 \text{ L kg}^{-1}$).^{25,41} Our study suggests that leaching of 2,4-D occurred in both spring and summer-simulated growth chambers at day 5 post-application. A higher amount of 2,4-D residue in leachate samples was also observed in summer- versus spring-simulated conditions, which can also be explained by 2,4-D's low K_{oc} . It is possible that low microbial activity and OM content at the lower soil depths enhanced the leaching capacity of 2,4-D, as seen in previous research.^{25,36,40}

To assess whether 2,4-D was actively being degraded by soil bacteria or abiotic transformation, a select number of soil samples were autoclaved. We concluded that the objective to autoclave soil samples successfully controlled the growth of soil bacteria that could potentially

degrade 2,4-D. However, it is still possible that colonization of certain bacteria occurred due to post-autoclave colonization. In terms of 2,4-D detection, we did not observe significant differences between autoclaved and non-autoclaved soil samples. However, an interesting result in our findings was the lower amount and variation of 2,4-D detected in autoclaved samples. The process of autoclaving, in addition to inhibiting microbial activity, can also significantly change the soil, altering its physical and chemical properties.⁴² Berns et al. (2008) studied the effect of autoclaving methods on physical changes of the soil and found that autoclaving soils can alter the aggregation state of soil aggregates and change the soil OM structure.⁴³ With this in mind, it is likely that changes in the soil structure after autoclaving promoted 2,4-D's ability to leach quicker than in non-autoclaved samples, thus explaining the lower concentration of 2,4-D in autoclaved soil samples at 1-day post-application. Our results also showed that 2,4-D residues were lower in leachate collected from non-autoclaved samples, mainly in spring-simulated conditions. Considering that intact soil OM was still present in non-autoclaved samples, our findings suggest that 2,4-D may have been present in the soil with high OM content, thus preventing 2,4-D from leaching and actively being degraded by soil bacteria. As for why higher amounts of 2,4-D were observed in leachate collected from non-autoclaved samples in summer-simulated conditions, it is uncertain why these differences exist between the leachate collected from the two season-simulated conditions. However, possible reasons for this difference may be attributed to differences in temperature, soil moisture content, and minor differences in soil type.

2,4-D is a phloem-mobile herbicide, meaning that it can be translocated from the leaves and other tissues to other plant parts.⁶ Although there were no distinct differences in the amount of 2,4-D detected in spring and summer-simulated conditions, our findings exhibited that 2,4-D residues remained stable on the leaf tissue after 10 days post-application. The commercial

formulation of 2,4-D was a 2-EHE (Radar LV4). 2,4-D ester formulations are surface-applied, they are more lipid-soluble and can move through the leaf cuticle more effectively.¹⁴ Although this may explain the steady concentration of 2,4-D in leaf tissue after 10 days post-application, it is unclear whether photodecomposition affected 2,4-D degradation in leaf samples as opposed to soil samples as explained above.

The mass balance conducted for our growth chamber study exhibited higher losses after day 5 post-application. While 2,4-D loss from soil was observed in both season-simulated conditions, higher losses were observed in summer simulation by the end of the study, suggesting that higher seasonal temperatures contributed to increased soil bacterial activity, resulting in the transformation of 2,4-D to 2,4-DCP. However, degradation by photodecomposition and leaching at other time points cannot be ruled due to our findings that 2,4-D was detected in leachate collected at day 5, and considerable losses of 2,4-D were seen within our system.

Lastly, using LC-MS/MS with multiple reaction monitoring and negative electrospray ionization, an SPE and d-SPE method for soil and leaf tissue, respectively, was developed to detect 2,4-D and 2,4-DCP. Previous studies have reported the development of methods for the detection of 2,4-D and 2,4-DCP in various matrices.^{13,31,44,45} Although the extraction and detection method developed and used for this study exhibited less than 50% recovery of 2,4-D when fortified with 20 $\mu\text{g g}^{-1}$ or higher in soil samples, the average amount detected in our actual samples was typically less than 10 $\mu\text{g g}^{-1}$. Therefore, our method proved to be acceptable under these circumstances (**Table 2.4**). Extraction of 2,4-D from leaf samples was also developed and validated, where the recovery ranged from 50% to 195%. In contrast, recoveries of 2,4-DCP in soil ranged from 83% to 95% within the three different fortification levels tested, proving appropriate for our soil

extraction method. In leaf tissue samples, the recovery of 2,4-DCP ranged from 92% to 101% when fortified with 25 $\mu\text{g g}^{-1}$ or higher. Leaf samples fortified with 15 $\mu\text{g g}^{-1}$ were not detected.

Overall, based on the results and assumptions discussed above, our findings suggest that 2,4-D was detected in various matrices including soil, leaf, and leachate; that degradation of 2,4-D resulted in the formation of its major TP in soil, 2,4-DCP, mainly due to bacterial activity; and abiotic transformation may have also influenced 2,4-D breakdown. Indeed, the assumption of abiotic transformation needs to be fully investigated along with biotic transformation in urban soils by analysis in both field and laboratory studies. Focus on developing optimal extraction and analytical methods for detecting 2,4-D, 2,4-DCP, and other 2,4-D TPs is important to better assess the fate and behavior of 2,4-D and other phenoxy herbicides alike. Certainly, providing a broader picture of how 2,4-D moves to other matrix compartments and, in addition, how it is degraded in urban soils will be integral in examining its implications for human exposure.

References

- (1) Milesi, C.; Running, S.; Elvidge, C.; Dietz, J.; Tuttle, B.; Nemani, R. Mapping and Modeling the Biogeochemical Cycling of Turf Grasses in the United States. *Environmental Management* **2005**, *36* (3), 426–438.
- (2) Fulton, W.; Pendall, R.; Harrison, A. Who Sprawls Most? How Growth Patterns Differ Across the U.S. *The Brookings Institution Survey Series* **2001**.
- (3) Charles, J. M.; Cunny, H. C.; Wilson, R. D.; Bus, J. S.; Lawlor, T. E.; Cifone, M. A.; Fellows, M.; Gollapudi, B. Ames Assays and Unscheduled DNA Synthesis Assays on 2,4-Dichlorophenoxyacetic Acid and Its Derivatives. *Mutation Research/Genetic Toxicology and Environmental Mutagenesis* **1999**, *444* (1), 207–216. [https://doi.org/10.1016/S1383-5718\(99\)00074-1](https://doi.org/10.1016/S1383-5718(99)00074-1).
- (4) Aquino, A. J. A.; Tunega, D.; Haberhauer, G.; Gerzabek, M. H.; Lischka, H. Interaction of the 2,4-Dichlorophenoxyacetic Acid Herbicide with Soil Organic Matter Moieties: A Theoretical Study. *European Journal of Soil Science* **2007**, *58* (4), 889–899. <https://doi.org/10.1111/j.1365-2389.2007.00928.x>.
- (5) Islam, F.; Wang, J.; Farooq, M. A.; Khan, M. S. S.; Xu, L.; Zhu, J.; Zhao, M.; Muños, S.; Li, Q. X.; Zhou, W. Potential Impact of the Herbicide 2,4-Dichlorophenoxyacetic Acid on Human and Ecosystems. *Environment International* **2018**, *111*, 332–351. <https://doi.org/10.1016/j.envint.2017.10.020>.
- (6) Song, Y. Insight into the Mode of Action of 2,4-Dichlorophenoxyacetic Acid (2,4-D) as an Herbicide. *Journal Of Integrative Plant Biology* **2014**, *56* (2), 106–113.
- (7) Atwood, D.; Paisley-Jones, C. *Pesticides Industry Sales and Usage 2008-2012 Market Estimates*; U.S. Environmental Protection Agency, 2017.

- (8) Peterson, M.; McMaster, S.; Riechers, D.; Skelton, J.; Stahlman, P. 2,4-D Past, Present, and Future: A Review. *Weed Technology* **2016**, *30* (2), 303–345.
- (9) Qurratu, A.; Reehan, A. A Review of 2,4-Dichlorophenoxyacetic Acid (2,4-D) Derivatives: 2,4-D Dimethylamine Salt and 2,4-D Butyl Ester. **2016**, *11* (19), 10.
- (10) Jeffries, M. D.; Yelverton, F. H.; Ahmed, K. A.; Gannon, T. W. Persistence in and Release of 2,4-D and Azoxystrobin from Turfgrass Clippings. *Journal of Environmental Quality* **2016**, *45* (6), 2030–2037. <https://doi.org/10.2134/jeq2016.03.0081>.
- (11) USEPA. Reregistration Eligibility Decision (RED) for Propiconazole Case No. 3125. July 18, 2006.
- (12) Corke, C. T.; Thompson, F. R. Effects of Some Phenylamide Herbicides and Their Degradation Products on Soil Nitrification. *Can. J. Microbiol.* **1970**, *16* (7), 567–571. <https://doi.org/10.1139/m70-095>.
- (13) Moret, S.; Sánchez, J. M.; Salvadó, V.; Hidalgo, M. The Evaluation of Different Sorbents for the Preconcentration of Phenoxyacetic Acid Herbicides and Their Metabolites from Soils. *Journal of Chromatography A* **2005**, *1099* (1), 55–63. <https://doi.org/10.1016/j.chroma.2005.08.078>.
- (14) Nice, Glenn. *Amine or Ester, Which Is Better?*; Purdue University, Cooperative Extension Service: West Lafayette, IN, 2004.
- (15) Gold, A. J.; Morton, T. G.; Sullivan, W. M.; McClory, J. Leaching of 2,4-D and Dicamba from Home Lawns. *Water Air Soil Pollut* **1988**, *37* (1–2). <https://doi.org/10.1007/BF00226484>.
- (16) Nash, R. G. Comparative Volatilization and Dissipation Rates of Several Pesticides from Soil. *J. Agric. Food Chem.* **1983**, *31* (2), 210–217. <https://doi.org/10.1021/jf00116a007>.

- (17) Microbial degradation and humification of the lawn care pesticide 2,4-dichlorophenoxyacetic acid during the composting of yard trimmings <https://journals.asm.org/doi/epdf/10.1128/aem.61.7.2566-2571.1995> (accessed 2021 -10 -22). <https://doi.org/10.1128/aem.61.7.2566-2571.1995>.
- (18) USEPA. Reregistration Eligibility Decision for 2,4-D https://archive.epa.gov/pesticides/reregistration/web/pdf/24d_red.pdf (accessed 2021 -08 -17).
- (19) Somasundaram, L.; Coats, J. R. Pesticide Transformation Products: Fate and Significance in the Environment. *ACS symposium series (USA)* **1991**, No. 459.
- (20) Coats, J. Pesticide Degradation Mechanisms and Environmental Activation. *ACS Symposium Series* **1991**, 459, 10–30.
- (21) Remucal, C. K. The Role of Indirect Photochemical Degradation in the Environmental Fate of Pesticides: A Review. *Environmental Science: Processes & Impacts* **2014**, 16 (4), 628. <https://doi.org/10.1039/c3em00549f>.
- (22) Nedwell, D. B.; Floodgate, G. D. The Seasonal Selection by Temperature of Heterotrophic Bacteria in an Intertidal Sediment. *Marine Biology* **1971**, 11 (4), 306–310. <https://doi.org/10.1007/BF00352448>.
- (23) Fenner, K.; Canonica, S.; Wackett, L.; Elsner, M. Evaluating Pesticide Degradation in the Environment: Blind Spots and Emerging Opportunities. *Science* **2013**, 341 (6147), 752–758.
- (24) Abate Jote, C. A Review of 2,4-D Environmental Fate, Persistence and Toxicity Effects on Living Organisms. *OMCIJ* **2019**, 9 (1). <https://doi.org/10.19080/OMCIJ.2019.09.555755>.

- (25) Buerge, I. J.; Pavlova, P.; Hanke, I.; Bächli, A.; Poiger, T. Degradation and Sorption of the Herbicides 2,4-D and Quizalofop-P-Ethyl and Their Metabolites in Soils from Railway Tracks. *Environ Sci Eur* **2020**, *32* (1), 150. <https://doi.org/10.1186/s12302-020-00422-6>.
- (26) Smith, A. E. Identification of 2,4-Dichloroanisole and 2,4-Dichlorophenol as Soil Degradation Products of Ring-Labelled [¹⁴C]2,4-D. *Bull. Environ. Contam. Toxicol.* **1985**, *34* (1), 150–157. <https://doi.org/10.1007/BF01609717>.
- (27) Tiedje, J. M.; Duxbury, J. M.; Alexander, M.; Dawson, J. E. 2,4-D Metabolism: Pathway of Degradation of Chlorocatechols by *Arthrobacter* Sp. *J. Agric. Food Chem.* **1969**, *17* (5), 1021–1026. <https://doi.org/10.1021/jf60165a037>.
- (28) Walters, J. *Environmental Fate of 2,4-Dichlorophenoxyacetic Acid*; 2019; p 18.
- (29) Sinclair, C. J.; Boxall, A. B. A. Assessing the Ecotoxicity of Pesticide Transformation Products. *Environ. Sci. Technol.* **2003**, *37* (20), 4617–4625. <https://doi.org/10.1021/es030038m>.
- (30) Average Annual Temperatures by USA State - Current Results <https://www.currentresults.com/Weather/US/average-annual-state-temperatures.php> (accessed 2019 -03 -22).
- (31) Deamarantejr, O.; Brito, N.; Dossantos, T.; Nunes, G.; Ribeiro, M. Determination of 2,4-Dichlorophenoxyacetic Acid and Its Major Transformation Product in Soil Samples by Liquid Chromatographic Analysis. *Talanta* **2003**, *60* (1), 115–121. [https://doi.org/10.1016/S0039-9140\(03\)00113-9](https://doi.org/10.1016/S0039-9140(03)00113-9).
- (32) Bollag, J. M.; Briggs, G. G.; Dawson, J. E.; Alexander, Martin. 2,4-D Metabolism. Enzymic Degradation of Chloropyrocatechols. *J. Agric. Food Chem.* **1968**, *16* (5), 829–833. <https://doi.org/10.1021/jf60159a034>.

- (33) Bollag, J. M.; Helling, C. S.; Alexander, Martin. 2,4-D Metabolism. Enzymic Hydroxylation of Chlorinated Phenols. *J. Agric. Food Chem.* **1968**, *16* (5), 826–828. <https://doi.org/10.1021/jf60159a037>.
- (34) Entry, J. A.; Donnelly, P. K.; Emmingham, W. H. Atrazine and 2,4-D Mineralization in Relation to Microbial Biomass in Soils of Young-, Second-, and Old-Growth Riparian Forests. *Applied Soil Ecology* **1995**, *2* (2), 77–84. [https://doi.org/10.1016/0929-1393\(94\)00046-A](https://doi.org/10.1016/0929-1393(94)00046-A).
- (35) Veeh, R. H.; Inskeep, W. P.; Camper, A. K. Soil Depth and Temperature Effects on Microbial Degradation of 2,4-D. *Journal of Environmental Quality* **1996**, *25* (1), 5–12. <https://doi.org/10.2134/jeq1996.00472425002500010002x>.
- (36) Boivin, A.; Amellal, S.; Schiavon, M.; van Genuchten, M. Th. 2,4-Dichlorophenoxyacetic Acid (2,4-D) Sorption and Degradation Dynamics in Three Agricultural Soils. *Environmental Pollution* **2005**, *138* (1), 92–99. <https://doi.org/10.1016/j.envpol.2005.02.016>.
- (37) Werner, D.; Garratt, J. A.; Pigott, G. Sorption of 2,4-D and Other Phenoxy Herbicides to Soil, Organic Matter, and Minerals. *J Soils Sediments* **2013**, *13* (1), 129–139. <https://doi.org/10.1007/s11368-012-0589-7>.
- (38) Nowak, K. M.; Miltner, A.; Gehre, M.; Schäffer, A.; Kästner, M. Formation and Fate of Bound Residues from Microbial Biomass during 2,4-D Degradation in Soil. *Environ. Sci. Technol.* **2011**, *45* (3), 999–1006. <https://doi.org/10.1021/es103097f>.
- (39) Hudson, B. D. Soil Organic Matter and Available Water Capacity. *Journal of Soil and Water Conservation* **1994**, *49* (2), 189–194.

- (40) Crespín, M. A.; Gallego, M.; Valcárcel, M.; González, J. L. Study of the Degradation of the Herbicides 2,4-D and MCPA at Different Depths in Contaminated Agricultural Soil. *Environ. Sci. Technol.* **2001**, *35* (21), 4265–4270. <https://doi.org/10.1021/es0107226>.
- (41) R. G. Wilson, Jr.; Cheng, H. H. Breakdown and Movement of 2,4-D in the Soil under Field Conditions. *Weed Science* **1976**, *24* (5), 461–466.
- (42) Trevors, J. T. Sterilization and Inhibition of Microbial Activity in Soil. *Journal of Microbiological Methods* **1996**, *26* (1–2), 53–59. [https://doi.org/10.1016/0167-7012\(96\)00843-3](https://doi.org/10.1016/0167-7012(96)00843-3).
- (43) Berns, A. E.; Philipp, H.; Narres, H.-D.; Burauel, P.; Vereecken, H.; Tappe, W. Effect of Gamma-Sterilization and Autoclaving on Soil Organic Matter Structure as Studied by Solid State NMR, UV and Fluorescence Spectroscopy. *European Journal of Soil Science* **2008**, *59* (3), 540–550. <https://doi.org/10.1111/j.1365-2389.2008.01016.x>.
- (44) McManus, S.-L.; Moloney, M.; Richards, K. G.; Coxon, C. E.; Danaher, M. Determination and Occurrence of Phenoxyacetic Acid Herbicides and Their Transformation Products in Groundwater Using Ultra High Performance Liquid Chromatography Coupled to Tandem Mass Spectrometry. *Molecules* **2014**, *19* (12), 20627–20649. <https://doi.org/10.3390/molecules191220627>.
- (45) Koesukwiwat, U.; Sanguankaew, K.; Leepipatpiboon, N. Rapid Determination of Phenoxy Acid Residues in Rice by Modified QuEChERS Extraction and Liquid Chromatography–Tandem Mass Spectrometry. *Analytica Chimica Acta* **2008**, *626* (1), 10–20. <https://doi.org/10.1016/j.aca.2008.07.034>.

Supplementary Materials

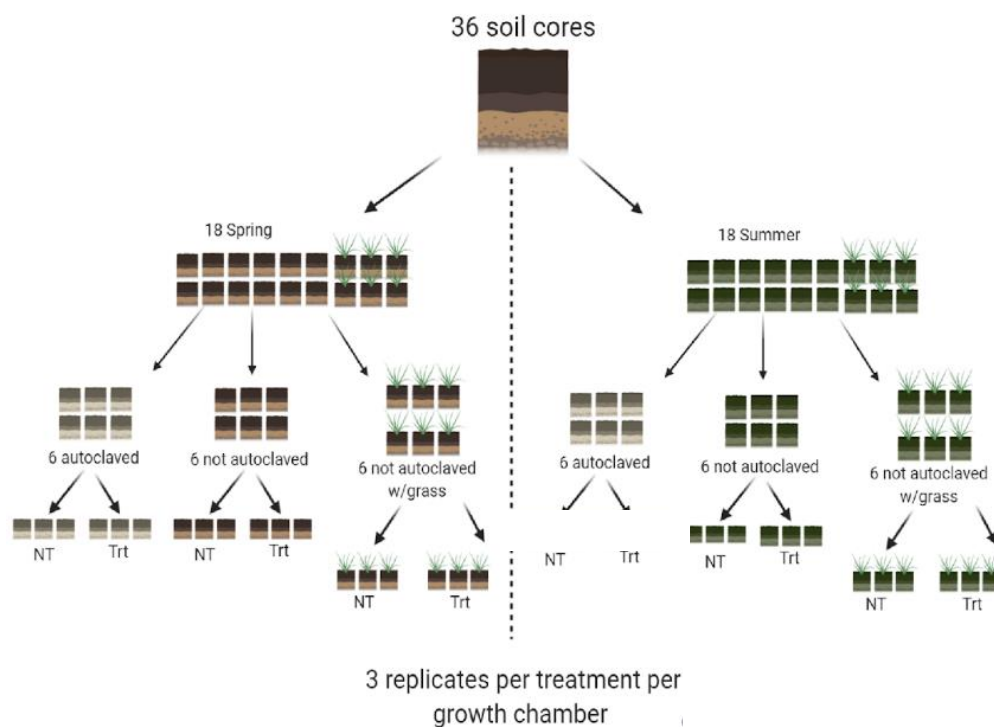


Figure S1. Schematic of the experimental design used for the growth chamber study. Trt = Treated; NT = Non-Treated

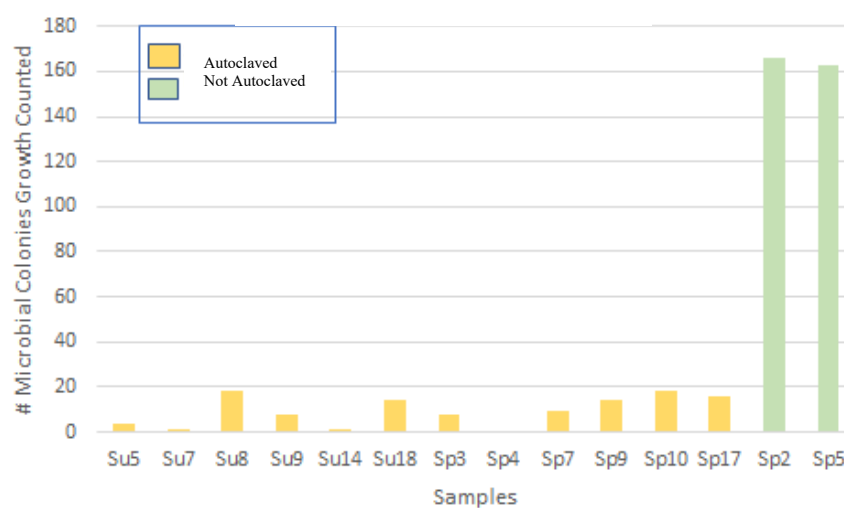


Figure S2. Number of colony-forming units (CFUs)s in autoclaved and non-autoclaved growth chamber soil samples

Table S1. Dataset showing 2,4-D soil residue values and fixed variables implemented in the growth chamber study.

Sample	Replicate	Grass	Autoclaved	Layers	Day	Season	2,4-D ($\mu\text{g g}^{-1}$)	2,4-DCP ($\mu\text{g g}^{-1}$)
S-0001	1	NO_GRASS	NO	UPPER	1	SUMMER	21.77	ND
S-0003	3	GRASS	NO	UPPER	1	SUMMER	17.10	ND
S-0006	1	NO_GRASS	NO	UPPER	1	SUMMER	21.17	ND
S-0007	6	NO_GRASS	YES	UPPER	1	SUMMER	ND	ND
S-0009	6	NO_GRASS	YES	UPPER	1	SUMMER	18.59	ND
S-0010	1	NO_GRASS	NO	UPPER	1	SUMMER	20.54	ND
S-0012	3	GRASS	NO	UPPER	1	SUMMER	7.08	ND
S-0015	3	GRASS	NO	UPPER	1	SUMMER	9.45	ND
S-0018	6	NO_GRASS	YES	UPPER	1	SUMMER	4.34	ND
S-0020	8	GRASS	NO	UPPER	1	SPRING	ND	ND
S-0021	9	NO_GRASS	YES	UPPER	1	SPRING	8.82	ND
S-0022	9	NO_GRASS	YES	UPPER	1	SPRING	10.30	ND
S-0026	12	NO_GRASS	NO	UPPER	1	SPRING	21.64	ND
S-0027	9	NO_GRASS	YES	UPPER	1	SPRING	1.28	ND
S-0031	12	NO_GRASS	NO	UPPER	1	SPRING	21.91	ND
S-0032	12	NO_GRASS	NO	UPPER	1	SPRING	15.34	ND
S-0033	8	GRASS	NO	UPPER	1	SPRING	11.98	ND
S-0034	8	GRASS	NO	UPPER	1	SPRING	7.06	ND
S-0037	1	NO_GRASS	NO	LOWER	1	SUMMER	1.52	ND
S-0039	3	GRASS	NO	LOWER	1	SUMMER	3.14	ND
S-0042	1	NO_GRASS	NO	LOWER	1	SUMMER	< LOQ	ND
S-0043	6	NO_GRASS	YES	LOWER	1	SUMMER	< LOQ	ND
S-0045	6	NO_GRASS	YES	LOWER	1	SUMMER	< LOQ	ND
S-0046	1	NO_GRASS	NO	LOWER	1	SUMMER	1.32	ND
S-0048	3	GRASS	NO	LOWER	1	SUMMER	< LOQ	ND
S-0051	3	GRASS	NO	LOWER	1	SUMMER	ND	ND
S-0054	6	NO_GRASS	YES	LOWER	1	SUMMER	< LOQ	ND
S-0056	8	GRASS	NO	LOWER	1	SPRING	3.59	ND
S-0057	9	NO_GRASS	YES	LOWER	1	SPRING	< LOQ	ND
S-0058	9	NO_GRASS	YES	LOWER	1	SPRING	< LOQ	ND
S-0062	12	NO_GRASS	NO	LOWER	1	SPRING	< LOQ	ND
S-0063	9	NO_GRASS	YES	LOWER	1	SPRING	1.40	ND
S-0067	12	NO_GRASS	NO	LOWER	1	SPRING	< LOQ	ND
S-0068	12	NO_GRASS	NO	LOWER	1	SPRING	1.44	ND
S-0069	8	GRASS	NO	LOWER	1	SPRING	< LOQ	ND
S-0070	8	GRASS	NO	LOWER	1	SPRING	1.24	ND
S-0073	1	NO_GRASS	NO	UPPER	5	SUMMER	2.21	ND
S-0075	3	GRASS	NO	UPPER	5	SUMMER	4.76	ND
S-0078	1	NO_GRASS	NO	UPPER	5	SUMMER	4.56	ND

S-0079	6	NO_GRASS	YES	UPPER	5	SUMMER	ND	ND
S-0081	6	NO_GRASS	YES	UPPER	5	SUMMER	ND	ND
S-0082	1	NO_GRASS	NO	UPPER	5	SUMMER	3.40	ND
S-0084	3	GRASS	NO	UPPER	5	SUMMER	3.75	ND
S-0087	3	GRASS	NO	UPPER	5	SUMMER	7.08	< LOQ
S-0090	6	NO_GRASS	YES	UPPER	5	SUMMER	7.41	ND
S-0091	1	NO_GRASS	NO	LOWER	5	SUMMER	1.82	ND
S-0093	3	GRASS	NO	LOWER	5	SUMMER	< LOQ	ND
S-0096	1	NO_GRASS	NO	LOWER	5	SUMMER	< LOQ	ND
S-0097	6	NO_GRASS	YES	LOWER	5	SUMMER	< LOQ	ND
S-0099	6	NO_GRASS	YES	LOWER	5	SUMMER	< LOQ	ND
S-0100	1	NO_GRASS	NO	LOWER	5	SUMMER	< LOQ	ND
S-0102	3	GRASS	NO	LOWER	5	SUMMER	< LOQ	ND
S-0105	3	GRASS	NO	LOWER	5	SUMMER	< LOQ	ND
S-0108	6	NO_GRASS	YES	LOWER	5	SUMMER	< LOQ	ND
S-0110	8	GRASS	NO	UPPER	5	SPRING	1.05	< LOQ
S-0111	9	NO_GRASS	YES	UPPER	5	SPRING	1.57	ND
S-0112	9	NO_GRASS	YES	UPPER	5	SPRING	1.07	< LOQ
S-0116	12	NO_GRASS	NO	UPPER	5	SPRING	< LOQ	0.12
S-0117	9	NO_GRASS	YES	UPPER	5	SPRING	1.67	ND
S-0121	12	NO_GRASS	NO	UPPER	5	SPRING	1.89	< LOQ
S-0122	12	NO_GRASS	NO	UPPER	5	SPRING	< LOQ	ND
S-0123	8	GRASS	NO	UPPER	5	SPRING	1.33	< LOQ
S-0124	8	GRASS	NO	UPPER	5	SPRING	1.33	< LOQ
S-0128	8	GRASS	NO	LOWER	5	SPRING	< LOQ	ND
S-0129	9	NO_GRASS	YES	LOWER	5	SPRING	< LOQ	ND
S-0130	9	NO_GRASS	YES	LOWER	5	SPRING	< LOQ	< LOQ
S-0134	12	NO_GRASS	NO	LOWER	5	SPRING	< LOQ	< LOQ
S-0135	9	NO_GRASS	YES	LOWER	5	SPRING	< LOQ	< LOQ
S-0139	12	NO_GRASS	NO	LOWER	5	SPRING	< LOQ	< LOQ
S-0140	12	NO_GRASS	NO	LOWER	5	SPRING	< LOQ	< LOQ
S-0141	8	GRASS	NO	LOWER	5	SPRING	< LOQ	< LOQ
S-0142	8	GRASS	NO	LOWER	5	SPRING	< LOQ	< LOQ
S-0145	1	NO_GRASS	NO	UPPER	7	SUMMER	< LOQ	ND
S-0147	3	GRASS	NO	UPPER	7	SUMMER	< LOQ	< LOQ
S-0150	1	NO_GRASS	NO	UPPER	7	SUMMER	< LOQ	< LOQ
S-0151	6	NO_GRASS	YES	UPPER	7	SUMMER	< LOQ	ND
S-0153	6	NO_GRASS	YES	UPPER	7	SUMMER	1.40	< LOQ
S-0154	1	NO_GRASS	NO	UPPER	7	SUMMER	< LOQ	< LOQ
S-0156	3	GRASS	NO	UPPER	7	SUMMER	1.82	ND
S-0159	3	GRASS	NO	UPPER	7	SUMMER	0.99	< LOQ
S-0162	6	NO_GRASS	YES	UPPER	7	SUMMER	1.87	ND
S-0163	1	NO_GRASS	NO	LOWER	7	SUMMER	< LOQ	ND

S-0165	3	GRASS	NO	LOWER	7	SUMMER	< LOQ	< LOQ
S-0168	1	NO_GRASS	NO	LOWER	7	SUMMER	< LOQ	ND
S-0169	6	NO_GRASS	YES	LOWER	7	SUMMER	< LOQ	ND
S-0171	6	NO_GRASS	YES	LOWER	7	SUMMER	< LOQ	< LOQ
S-0172	1	NO_GRASS	NO	LOWER	7	SUMMER	ND	ND
S-0174	3	GRASS	NO	LOWER	7	SUMMER	ND	ND
S-0177	3	GRASS	NO	LOWER	7	SUMMER	ND	< LOQ
S-0180	6	NO_GRASS	YES	LOWER	7	SUMMER	1.04	ND
S-0182	8	GRASS	NO	UPPER	7	SPRING	< LOQ	< LOQ
S-0183	9	NO_GRASS	YES	UPPER	7	SPRING	< LOQ	ND
S-0184	9	NO_GRASS	YES	UPPER	7	SPRING	< LOQ	< LOQ
S-0188	12	NO_GRASS	NO	UPPER	7	SPRING	< LOQ	< LOQ
S-0189	9	NO_GRASS	YES	UPPER	7	SPRING	< LOQ	ND
S-0193	12	NO_GRASS	NO	UPPER	7	SPRING	< LOQ	< LOQ
S-0194	12	NO_GRASS	NO	UPPER	7	SPRING	< LOQ	ND
S-0195	8	GRASS	NO	UPPER	7	SPRING	< LOQ	ND
S-0196	8	GRASS	NO	UPPER	7	SPRING	< LOQ	ND
S-0200	8	GRASS	NO	LOWER	7	SPRING	< LOQ	ND
S-0201	9	NO_GRASS	YES	LOWER	7	SPRING	< LOQ	< LOQ
S-0202	9	NO_GRASS	YES	LOWER	7	SPRING	< LOQ	ND
S-0207	9	NO_GRASS	YES	LOWER	7	SPRING	< LOQ	ND
S-0211	12	NO_GRASS	NO	LOWER	7	SPRING	< LOQ	ND
S-0212	12	NO_GRASS	NO	LOWER	7	SPRING	< LOQ	ND
S-0213	8	GRASS	NO	LOWER	7	SPRING	< LOQ	< LOQ
S-0214	8	GRASS	NO	LOWER	7	SPRING	< LOQ	< LOQ
S-0217	1	NO_GRASS	NO	UPPER	10	SUMMER	< LOQ	< LOQ
S-0219	3	GRASS	NO	UPPER	10	SUMMER	< LOQ	< LOQ
S-0222	1	NO_GRASS	NO	UPPER	10	SUMMER	< LOQ	ND
S-0223	6	NO_GRASS	YES	UPPER	10	SUMMER	< LOQ	ND
S-0225	6	NO_GRASS	YES	UPPER	10	SUMMER	< LOQ	ND
S-0226	1	NO_GRASS	NO	UPPER	10	SUMMER	< LOQ	< LOQ
S-0228	3	GRASS	NO	UPPER	10	SUMMER	1.54	ND
S-0231	3	GRASS	NO	UPPER	10	SUMMER	NA	NA
S-0234	6	NO_GRASS	YES	UPPER	10	SUMMER	2.25	ND
S-0235	1	NO_GRASS	NO	LOWER	10	SUMMER	< LOQ	ND
S-0237	3	GRASS	NO	LOWER	10	SUMMER	< LOQ	ND
S-0240	1	NO_GRASS	NO	LOWER	10	SUMMER	< LOQ	ND
S-0241	6	NO_GRASS	YES	LOWER	10	SUMMER	< LOQ	ND
S-0243	6	NO_GRASS	YES	LOWER	10	SUMMER	< LOQ	ND
S-0244	1	NO_GRASS	NO	LOWER	10	SUMMER	< LOQ	ND
S-0246	3	GRASS	NO	LOWER	10	SUMMER	< LOQ	ND
S-0249	3	GRASS	NO	LOWER	10	SUMMER	10.64	ND
S-0252	6	NO_GRASS	YES	LOWER	10	SUMMER	< LOQ	ND

S-0254	8	GRASS	NO	UPPER	10	SPRING	3.84	ND
S-0255	9	NO_GRASS	YES	UPPER	10	SPRING	2.48	ND
S-0256	9	NO_GRASS	YES	UPPER	10	SPRING	ND	ND
S-0260	12	NO_GRASS	NO	UPPER	10	SPRING	3.12	ND
S-0261	9	NO_GRASS	YES	UPPER	10	SPRING	5.46	ND
S-0265	12	NO_GRASS	NO	UPPER	10	SPRING	ND	ND
S-0266	12	NO_GRASS	NO	UPPER	10	SPRING	< LOQ	< LOQ
S-0267	8	GRASS	NO	UPPER	10	SPRING	3.43	ND
S-0268	8	GRASS	NO	UPPER	10	SPRING	6.08	ND
S-0272	8	GRASS	NO	LOWER	10	SPRING	2.66	ND
S-0273	9	NO_GRASS	YES	LOWER	10	SPRING	< LOQ	ND
S-0274	9	NO_GRASS	YES	LOWER	10	SPRING	2.17	ND
S-0278	12	NO_GRASS	NO	LOWER	10	SPRING	3.62	ND
S-0279	9	NO_GRASS	YES	LOWER	10	SPRING	< LOQ	< LOQ
S-0283	12	NO_GRASS	NO	LOWER	10	SPRING	3.35	ND
S-0284	12	NO_GRASS	NO	LOWER	10	SPRING	5.04	ND
S-0285	8	GRASS	NO	LOWER	10	SPRING	3.66	ND
S-0286	8	GRASS	NO	LOWER	10	SPRING	1.75	< LOQ

Table S2. Average concentrations found for 2,4-D and 2,4-DCP in PV and OJ field soil in May and July season conditions at the varying time points in 2018.

Site	Month	Day	n	Analyte concentration ($\mu\text{g g}^{-1}$ soil)	
				2,4-D	2,4-DCP
PV	May	0	8	3.24 ± 3.31	ND
		7	8	< LOQ	ND
		14	8	< LOQ	ND
		21	8	< LOQ	ND
	July	0	8	2.95 ± 1.87	ND
		7	8	1.51 ± 1.88	9.98 ± 21.25
		14	8	1.68 ± 3.83	3.87 ± 7.53
		21	8	< LOQ	< LOQ
OJ	May	0	8	1.34 ± 2.06	< LOQ
		7	8	< LOQ	< LOQ
		14	8	< LOQ	ND
		21	8	5.61 ± 6.39	ND
	July	0	8	< LOQ	< LOQ
		7	8	< LOQ	< LOQ
		14	8	< LOQ	19.72 ± 17.47
		21	8	< LOQ	15.71 ± 14.71

Experimental conditions consisted of 5 g of soil, followed by the extraction method described in the “soil sample extraction and cleanup” section above. ND = Not Detected; <LOQ = Detected but below the quantification limit.

Table S4. Average concentrations found for 2,4-D and 2,4-DCP in soil at spring and summer-simulated temperatures at the varying time points.

Season	Day	n	Analyte concentration ($\mu\text{g g}^{-1}$ soil)	
			2,4-D	2,4-DCP
Spring	1	18	6.03 ± 7.39	ND
	5	18	0.69 ± 0.64	< LOQ
	7	17	< LOQ	< LOQ
	10	18	2.69 ± 1.85	< LOQ
Summer	1	18	7.15 ± 8.53	ND
	5	18	2.19 ± 2.42	< LOQ
	7	18	< LOQ	< LOQ
	10	18	1.21 ± 2.50	< LOQ

Experimental conditions consisted of 5 g of soil, followed by the extraction method described in the “soil sample extraction and cleanup” section above. ND = Not Detected; <LOQ = Detected but below the quantification limit.

Table S5. Average concentrations found for 2,4-D and 2,4-DCP from autoclaved and non-autoclaved soil samples at the varying time points.

Autoclave Method	Day	n	Analyte concentration ($\mu\text{g g}^{-1}$ soil)	
			2,4-D	2,4-DCP
Autoclaved	1	12	3.93 ± 5.78	ND
	5	12	1.12 ± 2.07	< LOQ
	7	12	< LOQ	< LOQ
	10	12	1.41 ± 1.52	< LOQ
Not Autoclaved	1	24	7.92 ± 8.54	ND
	5	24	1.60 ± 1.84	< LOQ
	7	22	< LOQ	< LOQ
	10	24	2.27 ± 2.57	< LOQ

Experimental conditions consisted of 5 g of soil, followed by the extraction method described in the “soil sample extraction and cleanup” section above. ND = Not Detected; <LOQ = Detected but below the quantification limit.

Table S6. Average concentrations found for 2,4-D and 2,4-DCP from upper and lower soil layers samples at the varying time points.

Layers	Day	n	Analyte concentration ($\mu\text{g g}^{-1}$ soil)	
			2,4-D	2,4-DCP
Upper	1	18	12.13 ± 7.87	ND
	5	18	2.43 ± 2.27	< LOQ
	7	18	< LOQ	< LOQ
	10	18	1.89 ± 1.91	< LOQ
Lower	1	18	1.04 ± 0.97	ND
	5	18	< LOQ	< LOQ
	7	17	< LOQ	< LOQ
	10	18	2.05 ± 2.64	< LOQ

Experimental conditions consisted of 5 g of soil, followed by the extraction method described in the “soil sample extraction and cleanup” section above. ND = Not Detected; <LOQ = Detected but below the quantification limit.

Table S7. Average concentrations found for 2,4-D and 2,4-DCP in leachate samples at day 5 post-application from spring and summer-simulated temperatures samples at the varying autoclaving methods. ND = Not Detected.

Season	Autoclave Method	n	Analyte concentration ($\mu\text{g mL}^{-1}$ soil)	
			2,4-D	2,4-DCP
Spring	Autoclaved	5	1.93 ± 0.84	ND
	Not Autoclaved	12	1.01 ± 0.59	ND
	Autoclaved	6	2.00 ± 0.39	ND
	Not Autoclaved	12	2.15 ± 1.10	ND

Experimental conditions consisted of 5 g of soil, followed by the extraction method described in the “soil sample extraction and cleanup” section above. ND = Not Detected; <LOQ = Detected but below the quantification limit.

Chapter 3. Compositional Shifts in the Bacterial Community at Varying Environmental Conditions and its Impact on 2,4-D Degradation in Urban Soil Landscapes

Abstract

2,4-Dichlorophenoxyacetic acid (2,4-D) is the most used herbicide on urban landscapes in the U.S. Although 2,4-D fate and breakdown have been well documented, interactions with the entire soil microbiome and simultaneous assessments of its transformation products (TPs) in urban soil remain poorly understood. Microorganisms, namely bacteria, are the primary drivers of 2,4-D transformation in the soil. Seasonal environmental variations are key factors that directly influence soil bacterial community structure and function. Our study evaluated the impact of seasonal environmental variation on urban soil bacterial community structure, function, and composition and their influence on 2,4-D degradation in urban landscapes. Alterations of the general soil bacterial community structure was assessed using high-throughput sequencing analysis. Our results suggest that bacterial community composition was distinct at varying seasonal conditions. Field study results showed differences in the bacterial community between field sites, soil depths, and months, with *Proteobacteria* and *Actinobacteria* being highly abundant. Results of the growth chamber study also revealed that bacterial community composition was distinct with a higher abundance of *Proteobacteria* and *Actinobacteria*. Overall bacterial communities differed between season-simulated temperatures, soil depths, sterilization procedures, and treatment applications. Benzoate degradation was the highest predicted pathway in both field sites at upper soil layers as well as in our growth chamber study. Carboxymethylenebutenolidase was the highest predicted enzyme involved in 2,4-D degradation. These findings are essential to understand how varying seasonal factors influence bacterial activity in urban landscapes and emphasizes that seasonal environmental variations shift soil bacterial structure and potential degradation activity in urban landscapes regarding 2,4-D application.

Introduction

According to a U.S. Environmental Protection Agency (EPA) survey, approximately 30 million kg of pesticides were applied to two non-agricultural sectors, referred to as industry/commercial/government and home/garden, in 2012, representing more than 11% of total US pesticide usage.¹ The herbicide 2,4-dichlorophenoxyacetic acid (2,4-D) was the most used active pesticide ingredient in the home and garden sector in 2012, with 3 to 4 million kg used.² 2,4-D is a synthetic auxin herbicide used to control broadleaf weeds in agriculture, aquatic forestry sites, residential lawns, and turfgrass (i.e., Urban landscapes).³ As a mimicker of natural auxin, its mode of action promotes uncontrolled cell division and elongation in plants resulting in abnormal growth and plant death.⁴ The EPA assessed that the half-life of 2,4-D is 6.2 days in aerobic mineral soils. However, this can depend on various factors such as soil type and type of formulation in which it is applied.⁵

Although 2,4-D fate and breakdown have been well documented and studies conducted by the EPA in turf and residential lawns have shown that, when considered as part of an aggregate exposure with food and drinking water, 2,4-D can increase the risk to exposure, its potential adverse impact does not end at the point of application.⁵ 2,4-D herbicide can undergo environmental degradation and may result in transformation products (TPs) that interact with the environment differently than the parent molecule.⁶ Pesticides, in general, undergo various biotic and abiotic mechanisms when released to the environment. The primary abiotic processes through which pesticides are broken down are physical and chemical reactions, such as photodegradation and hydrolysis, oxidation, and reduction reactions.⁷⁻⁹ Biotic interactions are mediated by organisms that include invertebrates, plants, and microorganisms.¹⁰ Moreover, microbial transformation of pesticides can occur via three mechanisms: 1) Co-metabolism, where microbes

cause the incomplete transformation of the pesticide without using it as an energy source thus, requiring another substrate for growth;^{11,12} 2) catabolism, which leads to the complete mineralization of the pesticide;¹³ and 3) detoxification, resulting in the conversion of the pesticide to less harmful metabolites.¹⁴ In soil ecosystems, 2,4-D breakdown is mainly accomplished by a consortium of microorganisms and is influenced by a wide range of environmental factors such as temperature, moisture, cultural management practices, and soil type/conditions (structure, texture, pH, among others).¹⁵

Temperature is one of the most important factors influencing bacterial community structure and function, which may directly or indirectly alter pesticide degradation networks resulting in the formation of TPs.^{10,15,16} For example, alterations in bacterial community structure due to seasonal temperature fluctuations were observed in microbial communities under snow cover in the Rocky Mountains.¹⁷ In another study, alpine soil samples collected during three different seasons also showed differences in the structure and composition of the soil bacterial community.¹⁸ These previous findings suggest that soil microbial communities shift in structure and activity in response to various seasonal conditions. Since microbes are the primary degrader of 2,4-D in the soil, shifts in structure and activity in response to seasonal environmental changes may have significant consequences for how pesticides are transformed.

The degradation of 2,4-D in soils and the catabolic genes and enzymes involved in this process have been extensively studied in the soil bacteria, *Cupriavidus necator JMP134* (formerly known as *Ralstonia eutropha* and *Alcaligenes eutrophus*).¹⁹ *C. necator* harbors the pJP4 plasmid, which contains a gene cluster known as *tfd* (two, four-dichlorophenoxyacetic acid) *ABCDEF*. Within this gene cluster, *tfd* is considered a good reporter for 2,4-D degradation activity.^{19–21} A study using the pure 2,4-D compound was performed to assess the impact of 2,4-D application on

soil bacterial communities.²² The soil bacterial community was significantly altered, and the number of *tfdA* genes increased in response to 2,4-D.²² This previous work, however, focused on the impact of 2,4-D on the genetic structure of bacterial communities rather than the impact of environmentally altered bacteria on 2,4-D metabolism. Another aspect of this study was that it was conducted in a controlled lab setting and did not use a 2,4-D herbicide commercial formulation, which is typically applied in real-life conditions.

Within this context, there is limited knowledge regarding the impact of variable environmental conditions on 2,4-D–bacterial interactions in urban landscapes. Evaluation of soil bacterial communities in response to seasonal temperature changes and their interaction on 2,4-D metabolism is essential to effectively minimize the occurrence of toxic TPs and the potential risk they pose to human and environmental health. This study evaluated the impact of altered turfgrass–associated soil bacterial communities on 2,4-D metabolism by conducting a field study for two consecutive years and a growth chamber study. Specifically, the objective of the field study was to assess how varying seasonal conditions, such as temperature and soil moisture, lead to changes in soil bacterial activities and how potential environment-driven changes in that microbial activity alters 2,4-D metabolism in urban landscapes. We hypothesize that varying seasonal conditions will shift the microbiome structure and function, and in turn, influence the presence of critical 2,4-D degraders. The objectives of the growth chamber study were to (i) isolate environmental factors, such as temperature and photoperiods, to assess potential shifts in the bacterial community and (ii) assess how sterilization methods alter the bacterial community, and how this, in turn, could influence the presence of 2,4-D degraders.

Materials and Methods

Field Study. Field trials were conducted on mature strands of perennial ryegrass (*Lolium perenne*) and Kentucky bluegrass (*Poa pratensis*) at the OJ Noer Turfgrass Research Station (OJ) in Madison, WI, and Pleasant View Golf Course (PV) in Middleton, WI in 2018 and 2019. Soil analysis from each site was performed before conducting our first application for each field trial (See Chapter 2-Table 2.1). Field plots were maintained using standard Wisconsin home lawn practices such as maintaining the grass 2.5 to 3.5 inches tall, applying fertilizer if necessary, and irrigating as needed.²³ All the plants' water needs were provided through supplemental in-ground irrigation based on 75% of the daily evapotranspiration rate. Treatment formulations of 2,4-D and water as a non-treated (NT) control were applied on May 1st and July 1st in 2018 and April 30th and July 3rd in 2019, representing conditions for spring and summer seasons, respectively. 2,4-D was applied to field plots using a nozzle pressure of 40 psi using a CO₂ pressurized boom sprayer with two XR Teejet AI8004 nozzles. Herbicides were agitated by hand and applied at a rate equivalent to 0.35 mL per m² of the commercial 2,4-D product (Radar LV4, Growmark, Bloomington, IL) with an initial concentration of 2.62 mg mL⁻¹. The design consisted of a randomized complete block design with four replications per treatment, where each plot contained an area of 1.39 m². Soil temperature was measured once at each collection day using a digital soil thermometer. Soil moisture content from each plot was measured using a soil moisture meter (Spectrum Technologies, Aurora, IL). Soil cores 2.5 cm in diameter were collected from each plot at 0, 7, 14, and 21 days after treatment application using a stainless-steel piston sampler. Subsamples of leaf, upper soil (top 5 cm), and lower soil (15 to 20 cm depth) were then collected and stored at -80°C until further processing.

Growth Chamber Study. The growth chamber study was conducted in a controlled environment setting at the Plant Pathology Department at UW-Madison. 100 mm diameter soil core samples of 50:50 Perennial ryegrass and Kentucky bluegrass with a depth of 200 mm were collected at the OJ Noer Turfgrass Research Station in Madison, Wisconsin, for a total of 36 samples on July 30th, 2020. Samples were moved to two individual growth chambers for a total of 18 cores per chamber, each simulating one of the average seasonal temperatures and photoperiods listed on (See Chapter 2-Table 2.2) and allowed to acclimate for 14 days.²⁴ A PVC column with a diameter of 101.6 mm and a depth of 203.3 mm was used to hold the collected core samples. The study consisted of a randomized sample design with three replications per treatment per temperature (See Chapter 2, Figure S1).

Treatments of the 2,4-D and NT control were applied after acclimation was achieved after 14 days. 2,4-D was applied to core samples at the same rate as in the field study. Subsamples from each core were collected in the following regions: upper soil (top 5 cm), lower soil (15-20 cm depth), leaf tissue, and leachate. Lysimeters aided in collecting the amount of water flow in the soil. Collection days for 2,4-D and NT samples were at 1-, 5-, 7-, and 10-days post-application, and samples were stored at -80°C until further processing.

Testing Autoclaving Effectiveness in Growth Chamber Core Samples. After acclimation, 6 core samples from each chamber were sterilized twice for 45 min on slow exhaust settings on two consecutive days. Sterilized soil cores were allowed to cool, and 0.1 g of soil was collected from the center of each core to test for the presence of viable bacteria. The soil was diluted in 1 mL of sterilized H₂O, and serial dilutions were then performed and plated in nutrient agar. Plates were incubated at 25°C for two days, and colony-forming units (CFU) were counted after incubation.

Sample Preparation for DNA Isolation. Collected samples from the field study were processed by washing with 20 mL of DI water using a sieve a 50-mL test tube and vortexed for 5 s to remove excess soil. Samples were then sonicated for 7 min using a sonicating water bath and vortexed for 10 s to remove tightly adhered soil and microbial organisms. The soil mixture was poured through a strainer into another 50-mL tube, washed with 30 mL of DI water, and centrifuged for 20 min. After the supernatant was removed, 0.25 g of soil sample was used for DNA extraction.

Samples from the growth chamber study were processed by sieving the soil to remove any leaf residue or rock particles. After sieving, the sample was mixed to ensure a representative collection of soil. 0.25 g of soil sample was then used for DNA extraction.

DNA Isolation, Library Preparation, and Short-Amplicon Sequencing. For upper and lower soil samples from both field and growth chamber studies, 0.25 g soil was used for DNA extraction using a DNeasy PowerLyzer PowerSoil kit (Qiagen Inc., Germantown, MD) following the manufacturer's protocol. An alternative step using phenol:chloroform:isoamyl alcohol, pH 7-8, was implemented in the protocol to increase DNA yield. The nucleic acid concentration was quantified for all extracted DNA samples using a NanoDrop1000 (Thermo Fisher Scientific, Waltham, MA). The following library preparation for amplicon sequencing was conducted according to Cox et al. (2021).²⁵ Briefly, the extracted DNA from field samples was amplified in a 25- μ L reaction mixture comprising 12.5 μ L Kapa HiFi HotStart ReadyMix, 6.5 μ L PCR-grade water, 0.5 μ L of both barcoded forward and reverse primers according to Kozich et al. (2013)²⁶ targeting the v4 region of the 16S rRNA gene, and 5 μ L of the template DNA at 30 ng/ μ L and 15 ng/ μ L for field and growth chamber study samples, respectively. Amplification of the bacterial DNA from the growth chamber study consisted of the same steps mentioned above, using New

England BioLab Q5 HiFi HotStart_Master Mix (Ipswich, MA).

Amplification consisted of the following cycling conditions: 95 °C for 3 min as the initial denaturation step; followed by 25 cycles of 95 °C for 30 s, 55 °C for 30 s, and 72 °C for 30 s; and a final step at 72 °C for 5 min. The amplicons were purified using a ZR-96 Zymoclean™ Gel DNA Recovery kit (Zymo Research, Irvine, CA) and normalized with a Mag-Bind® EquiPure Library Normalization Kit (Omega Bio-Tek Inc, Norcross, GA). The amplicons were then pooled and quantified to 4 nM with a Qubit™ dsDNA HS Assay kit (Thermo Fischer Scientific, Waltham, MA). The final pool was sequenced on Illumina MiSeq with a 2x250bp PE Illumina Reagent Kit v2 (Illumina, Inc., San Diego, CA) in the Biotechnology Center at the University of Wisconsin-Madison.

Amplicon Sequence Processing and Data Analysis. The raw sequencing reads were obtained in fastq format, demultiplexed with default Illumina BaseSpace algorithm, and processed using package “DADA2” in R 3.6.0.²⁷ Quality filtering and denoising of the forward and reverse reads were 230 and 140 bases for the field study, and 200 and 140 bases for the growth chamber study, respectively, according to average quality score. A maximum of 5 and 4 errors was allowed of the forwards and reverse read, respectively, for both field and growth chamber trials. Paired-end reads were then merged, and chimeras were removed. According to the SILVA database (v.138), the resulting de-noised amplicon sequence variants (ASV) were used for taxonomic classification. (ASV and taxonomic tables were then imported to R 3.6.0. ASV tables were rarefied to the minimum number of reads and analyzed using the R packages “phyloseq” and “vegan”. For runs containing negative-control contamination, “Decontam” (version 1.8.0) using the “prevalence” method and a threshold of 0.5 were used to compare the sequences from true positive samples with sequences obtained in the negative controls.²⁸

Differences in the bacterial community composition were assessed using the Bray-Curtis dissimilarity matrix implemented in “vegan” and principal coordinate analysis (PCoA) to visualize dissimilarities among the sample groups using “ggplot2”. The contribution of the environmental factors, temperature, and soil moisture, to the PCoA ordination plots from the field study, was assessed using the R function ‘envfit’ from “vegan”. Permutational multivariate analysis of variance (PERMANOVA) was also conducted to identify the significance of dissimilarities between the groups.

Microbial occurrence networks of PV May, PV July, OJ May, and OJ July field trials conducted in 2018 and 2019 were constructed using Molecular Ecological Network Analysis (MENA) through Random Matrix Theory (RMT)-based methods.²⁹ Networks of NT. Spring, NT Summer, Treated Spring, and Treated Summer conditions were also constructed using MENA. RMT methods serve as a tool to elucidate network interactions in microbial communities and the magnitude of their interactions. The nodes and edge lists were imported into Gephi 0.9.2 to visualize the networks, and ASVs were analyzed at the class level.³⁰ Differential relative abundances were analyzed using Welch’s t-test at a significance level of $\alpha=0.05$ with false-positive detection Storey False Discovery Rate (FDR) using Statistical Analysis of Taxonomic and Functional Profiles (STAMP), version 2.1.3.

Tax4Fun2 was also used to predict pathways performed by soil bacteria in both our field study and growth chamber study and investigate the potential bacterial xenobiotic degradation differences in the Kyoto Encyclopedia of Genes and Genomes (KEGG) reference.³¹ Results were then imported and visualized using SigmaPlot 13.0. Analysis was focused on metabolic functions and pathways associated with xenobiotic degradation abilities, with a particular interest in 2,4-D, derived from the KEGG pathway database.

Results

Field Study

Bacterial communities cluster distinctly between fields sites and soil layers. Average reads obtained from the field study were 20788 ± 1771 per sample. The minimum number of reads was rarefied to 4530. The total number of ASVs detected was 33375, with 98.4% phyla identified and 1.6% unidentified. Bacterial community composition was distinct between OJ and PV field sites at both upper and lower soil layers in 2018 and 2019 (**Figure 3.1A**, see **Supplementary Figure S1**). We implemented the Bray-Curtis distance metric to evaluate multivariate sample distances and visualized it using principal coordinate analysis (PCoA). The PCoA results showed clustering of bacterial communities by layers and sites. Axes 1 and 2 explained 17.7% and 12.3%, respectively, of the variance in the data (**Figure 3.1A**). Upper and lower soil layer bacterial composition was clearly distinguished in each field site as confirmed by PERMANOVA (p-value = 0.001, **Table 3.1**), suggesting apparent differences between soil depth. OJ and PV sites were also distinct (p-value = 0.001, **Table 3.1**), indicating that soil bacterial composition depends on the site and location.

The composition of the bacterial communities in each field site was further compared using differential relative abundance analysis. *Myxococcota*, *Acidobacteriota*, *Proteobacteria*, *Firmicutes*, *Verrucomicrobiota*, and *Bacteroidota* were among the most abundant phyla in the OJ field site, while *Actinobacteriota*, *Nitrospirota*, *Bdellovibrionota*, and *Planctomycetota* were more abundant in PV (**Figure 3.1B**, see **Supplementary Figure S2**). Further, the most abundant phyla were *Proteobacteria* and *Actinobacteria* in OJ and PV field sites, respectively. *Actinobacteria* were most abundant in upper soil layers of the PV field site (**Figure 3.1C**), while *Proteobacteria* were higher in upper soil layers of both PV and OJ field sites (**Figure 3.1D**).

Close inspection revealed that a total of 377 genera from phyla *Proteobacteria* and *Actinobacteria* were observed in both field sites (data not shown). Among these, 17 genera belonging to the class *Alphaproteobacteria* and 11 belonging to *Gammaproteobacteria* demonstrated higher and similar abundance between each field site, where *Hyphomicrobium*, a type of *Alphaproteobacteria*, was most abundant with a mean proportion varying 12 to 14% (**Figure S3A**). In terms of the *Actinobacteria*, 26 genera were found to have a higher abundance in OJ and PV, where *Gaiella* was the most dominant genus identified with a mean proportion varying 30 to 36% (**Figure S3B**).

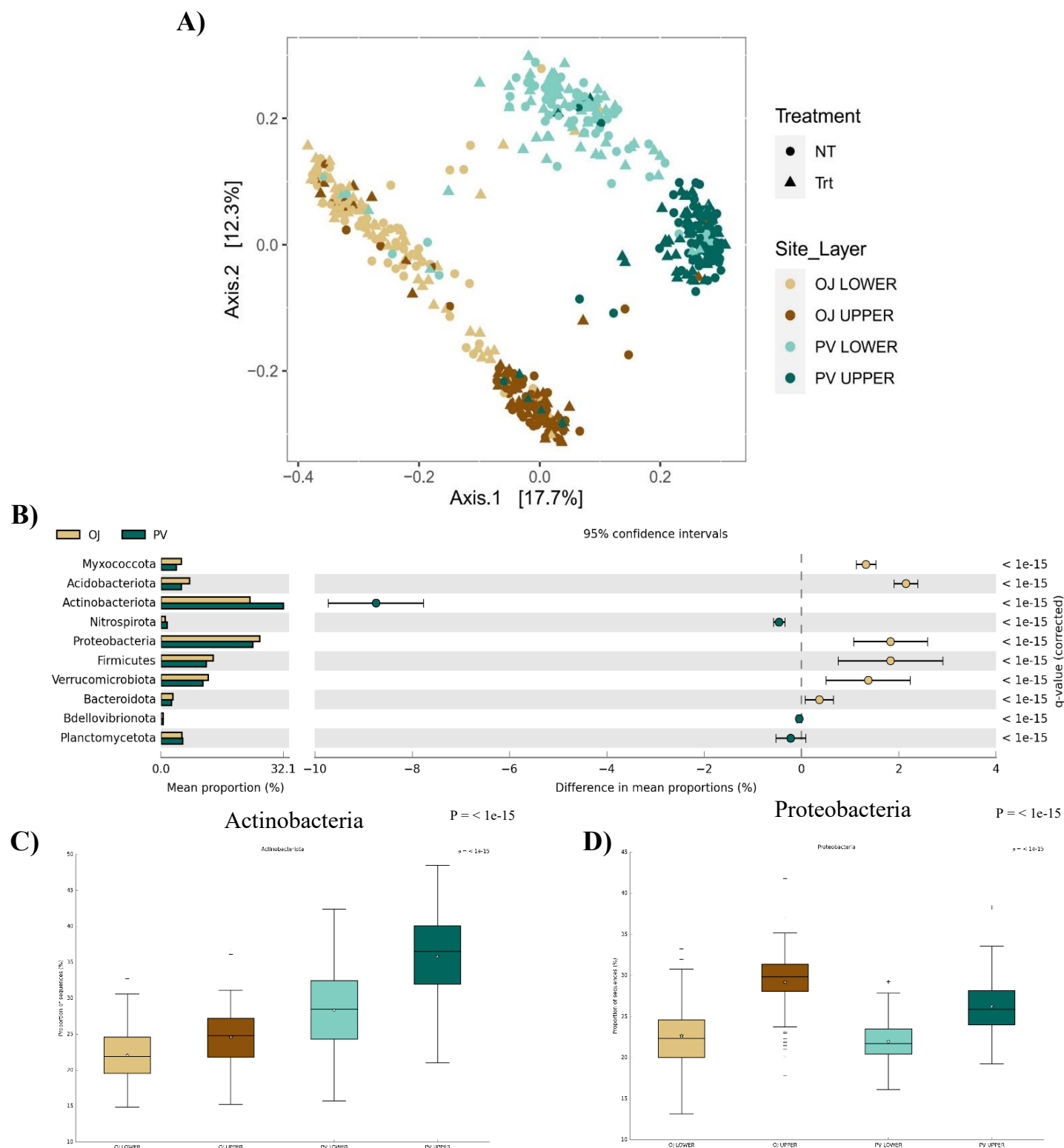


Figure 3. 1 A) Principal coordinates analysis (PCoA) of bacterial communities (16S V4 region) of upper and lower soil layers from OJ and PV field sites collected in 2018 and 2019. The ordination is based on the Bray-Curtis distance metric, with samples clustered by field site and soil layer, and treatments. **B)** Differential relative abundance of bacterial community phyla identified in OJ and PV field sites using Welch's t-test with Storey FDR correction. **C)** Boxplot featuring the differential relative abundance of the phyla Actinobacteria in the different sites and layers using ANOVA with Storey FDR correction. **D)** Boxplot featuring the differential relative abundance of the phyla Proteobacteria in the different sites and layers using ANOVA with Storey FDR correction.

Varying seasonal conditions altered urban soil bacterial community composition. We

assessed the effects of seasonal environmental differences on bacterial community structure in May and July. Soil temperature was measured in the 2018 and 2019 field trials. Average temperatures in both OJ and PV was 18°C in May to 25°C in July 2018. Similarly, the average temperature data collected in 2019 was 15°C in May to 25°C in July (**Figure S4**).

Moisture content was also measured in the individual plots from each field site (**Figure S5**). In May 2018, soil moisture increased significantly between days 7 and 14 with an average of

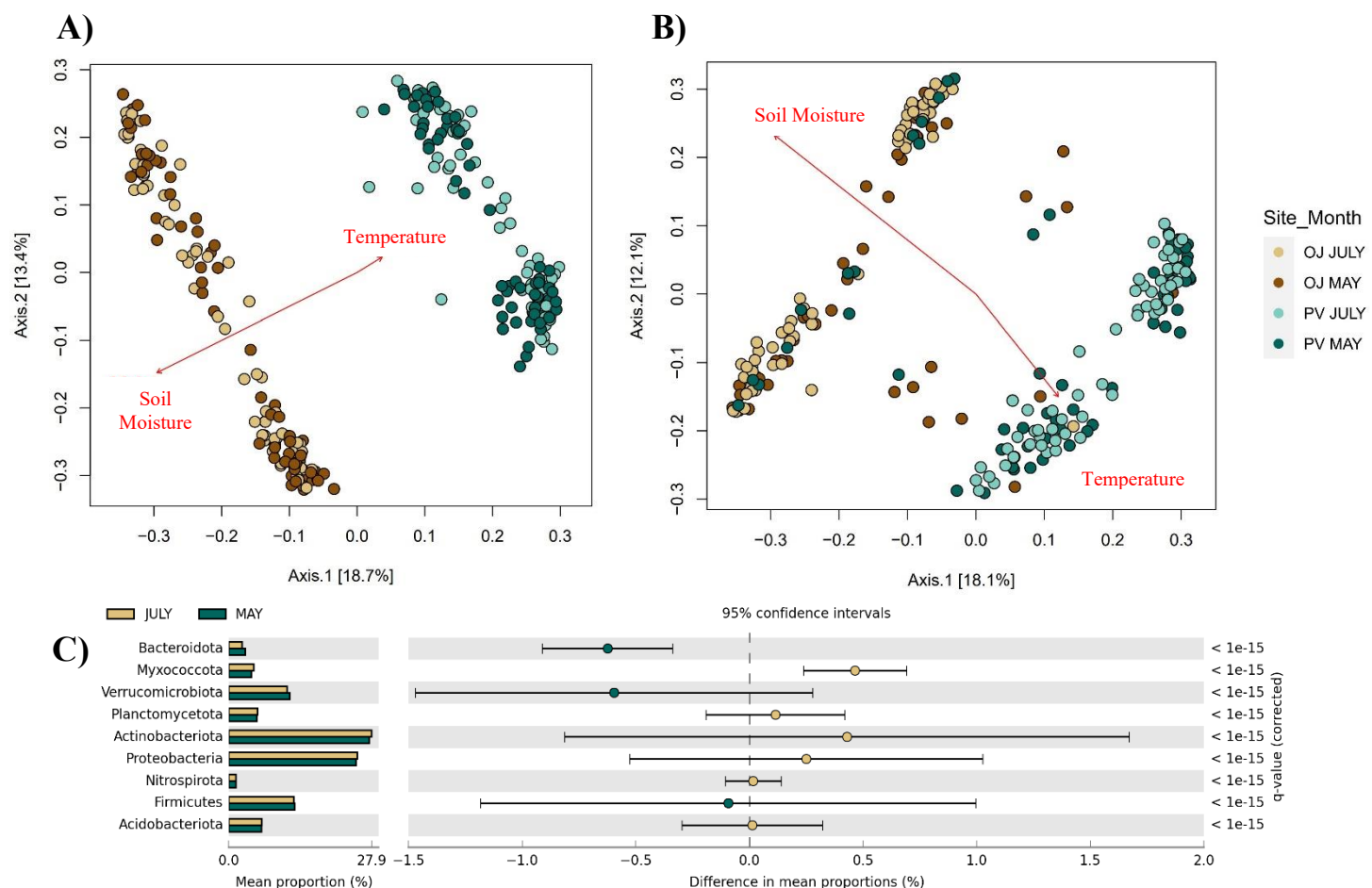


Figure 3. 2 Principal coordinate analysis (PCoA) ordinations of bacterial communities (16S V4 region) derived from A) 2018 and B) 2019 field trials. The PCoA is based on the Bray-Curtis distance metric, with samples clustering by field site (OJ and PV) and month (May and July). OJ July = Yellow; OJ May = Brown; PV July = Light Blue; PV May = Dark Blue. C) Differential relative abundance of bacterial community phyla identified in May and July using Welch's t-test with Storey FDR correction.

50% moisture, followed by a decrease to 30% on day 21. In contrast, moisture content in July 2018 decreased on Day 7, especially in the PV field site with an average measurement of less than 25%, and gradually increased by

Table 3. 1 Comparison of soil bacterial community structure dissimilarity in 2018 and 2019 field trials using paired-PERMANOVA with Bonferroni correction.

Factors	Overall		OJ 2018		PV 2018		OJ 2019		PV 2019	
	R ²	P-value	R ²	P-value	R ²	P-value	R ²	P-value	R ²	P-value
Site	0.128	0.001	—	—	—	—	—	—	—	—
Layer	0.087	0.001	0.127	0.001	0.147	0.001	0.113	0.001	0.129	0.001
Day	0.008	0.030	0.019	0.495	0.015	0.008	0.037	0.036	0.054	0.001
Month	0.004	0.004	0.013	0.027	0.015	0.008	0.011	0.061	0.027	0.001
Year	0.008	0.001	—	—	—	—	—	—	—	—
Treatment	0.002	0.304	0.006	0.480	0.007	0.211	0.006	0.541	0.008	0.118
Site*Layer	0.018	0.001	—	—	—	—	—	—	—	—
Site*Day	0.009	0.002	—	—	—	—	—	—	—	—
Layer*Day	0.012	0.001	0.037	0.007	0.019	0.527	0.068	0.001	0.027	0.222
Site*Month	0.004	0.004	—	—	—	—	—	—	—	—
Layer*Month	0.002	0.051	0.018	0.008	0.008	0.162	0.008	0.201	0.009	0.051
Day*Month	0.005	0.074	0.022	0.261	0.023	0.174	0.015	0.215	0.029	0.001
Site*Year	0.008	0.001	—	—	—	—	—	—	—	—
Layer*Year	0.003	0.023	—	—	—	—	—	—	—	—
Day*Year	0.005	0.166	—	—	—	—	—	—	—	—
Month*Year	0.003	0.015	—	—	—	—	—	—	—	—
Site*Treatment	0.001	0.372	—	—	—	—	—	—	—	—
Layer*Treatment	0.001	0.276	0.007	0.235	0.007	0.337	0.007	0.351	0.006	0.376
Day*Treatment	0.005	0.503	0.018	0.619	0.019	0.500	0.024	0.779	0.026	0.361
Month*Treatment	0.001	0.317	0.006	0.487	0.008	0.203	0.006	0.473	0.006	0.463
Year*Treatment	0.001	0.326	—	—	—	—	—	—	—	—

day 14 in both field sites. May 2019 measurements showed a gradual increase of soil moisture between 35 and 50% in both field sites. Soil moisture measurements in July 2019 decreased from an average of 45% on day 0, to 20 and 30% between day 14 and 37, respectively.

PCoA plots from each site showed few differences between May and July soil bacterial communities in 2018 and 2019 (**Figure 3.2**). In contrast, our PERMANOVA results confirm significant differences between the different months (p-value = 0.004, **Table 3.1**). Further, month effects were also significant across the different sites per year (p-value = 0.027 in OJ 2018; p-value = 0.008 in PV 2018; p-value = 0.061 in OJ 2019; p-value = 0.001 in PV 2019, **Table 3.1**) when each month was analyzed individually (**Table 3.1**), suggesting that bacterial communities differed between the two month's varying seasonal conditions. Sample clustering was based primarily on field site, with each site clustered and then by months. Although the clustering of the bacterial communities did not appear to be well defined between May and July in **Figure 3.2A** and **Figure 3.2B**, a more distinct clustering pattern was observed when PCoA plots were plotted individually for each field site per year (**Figure S6**). Paired-PERMANOVA further showed that the bacterial community structure among site and month interactions was significantly different. OJ May differed from PV May (p=0.006), and PV July (p=0.006); OJ July differed from PV May (p=0.006) and PV July (p=0.006); and PV May differed from PV July (p=0.012) (**Table 3.2**). Notably, the dissimilarities between May and July were higher in the PV site compared to OJ (**Table 3.1**, **Figure S6**). This clustering pattern in the PV site was observed in both 2018 and 2019.

Table 3. 2 Comparison of bacterial community structure dissimilarity in OJ and PV soil from 2018 and 2019 using permutational multivariate analysis of variance (PERMANOVA). The p-values of dispersion test were derived from ANOVA.

Pairs	Overall		2018		2019	
	R ²	P-value	R ²	P-value	R ²	P-value
OJ May vs OJ July	0.0069	0.264	0.013	0.300	0.013	0.330
OJ May vs PV May	0.1230	0.006	0.191	0.006	0.191	0.006
OJ May vs PV July	0.1619	0.006	0.199	0.006	0.199	0.006
OJ July vs PV May	0.1438	0.006	0.200	0.006	0.200	0.006
OJ July vs PV July	0.1824	0.006	0.205	0.006	0.205	0.006
PV May vs PV July	0.0111	0.012	0.017	0.078	0.017	0.066

We found that soil moisture content had an overall vector correlation of 29.8% in 2018 (p-value = 0.049) and 30.9% in 2019 (p-value = 0.004). Temperature, on the other hand, had an overall correlation of 54.9% in 2018 (p-value = 0.001) and 47.0% in 2019 (p-value = 0.001) (**Figure 3.2A and 3.2B**). Therefore, our data showed that soil moisture content and temperature strongly influenced the structure of soil bacterial communities (**Figure 3.2A and 3.2B**).

A co-occurrence network analysis was performed to visualize the plausible bacterial interactions of OJ and PV soil bacteria in May and July (**Figure S7**). The co-occurrence networks showed different patterns among the different field sites and months. Briefly, each node represented an ASV, and node connections (edges) indicate taxa as important shapers of the community structure. PV May (**Figure S7A**) and PV July (**Figure S7B**) co-occurrence networks had an equal number of nodes (nodes = 455). Similarly, OJ May (**Figure S7C**) and OJ July (**Figure S7D**) co-occurrence networks had an equal number of nodes (nodes = 343). There were higher node connections (edges) in PV July versus PV May and in OJ May versus OJ July. There were more *Thermoleophilia*, *Alphaproteobacteria*, *Actinobacteria*, and *Gammaproteobacteria* involved in PV May samples as having potential functional importance than in PV July network. In contrast, more *Thermoleophilia*, *Alphaproteobacteria*, *Actinobacteria*, and *Gammaproteobacteria* were involved in OJ July than in OJ May.

When performing a differential relative abundance analysis of the soil bacterial communities between May and July, we observed that 9 phyla were most abundant. *Bacteroidota*, *Verrucomicrobiota*, and *Firmicutes* were highly abundant in May samples. *Myxococcota*, *Planctomycetota*, *Actinobacteria*, *Proteobacteria*, *Nitrospirota*, and *Acidobacteria* were the most abundant in July samples. Overall, *Proteobacteria* and *Acidobacteria* were the phyla with the highest abundance in both months.

Our PERMANOVA (**Table 3.1**) also showed that day ($P = 0.030$) and year effects ($P = 0.001$) were significant. Overall, site-to-site differences ($R^2 = 0.128$) explained more variation followed by soil layers ($R^2 = 0.089$). Differences in bacterial communities were not observed in 2,4-D-treated versus non-treated samples ($P = 0.304$).

Growth Chamber Study

Bacterial communities are distinct between sterilized and soil layers samples. The average reads obtained from the growth chamber study were 8638 ± 315 per sample. The minimum number of reads was rarefied to 2073 per sample. The total number of ASVs detected was 17067, with 98.88% phyla identified and 1.12% unidentified. Similar to our field study, multivariate sample distances using the Bray-Curtis distance metric were implemented and visualized using PCoA. Axes 1 and 2 explained 11.7% and 10.5%, respectively, of the variance in the data (**Figure 3.3**). Bacterial community composition was significantly distinct between soil layers ($p\text{-value} = 0.001$) as confirmed by the PERMANOVA (**Table 3.3 and Figure 3.3**).

To test our sterilization procedure, sterilized and unsterilized soil was plated with nutrient agar, and CFUs were counted. Unsterilized soil samples contained approximately 160 CFUs, while sterilized samples had less than 20 CFUs (**Figure S8**). Sterilized versus unsterilized samples

were also significantly distinct in overall samples (p-value = 0.001, **Table 3.3**), suggesting that sterilization procedures altered the natural composition of the bacterial community (**Figure 3.3**).

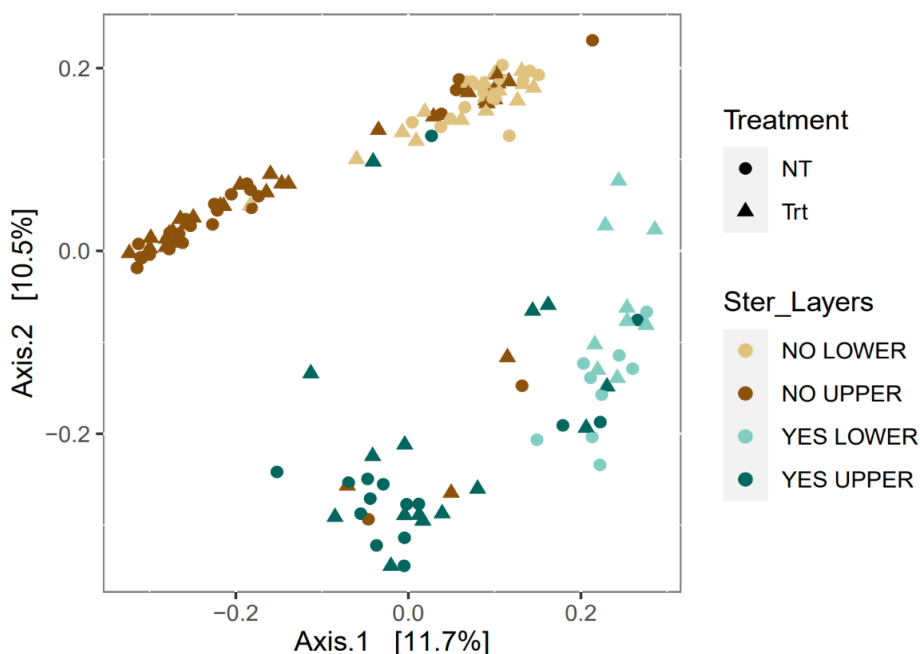


Figure 3. 3 Principal coordinate analysis (PCoA) ordinations of bacterial communities (16S V4 region) of upper and lower soil layers from sterilized (YES) and unsterilized (NO) soil samples. The ordination is based on the Bray-Curtis distance metric, with samples clustered by sterilization and soil layer, and treatments.

Differential relative abundance analysis showed *Firmicutes* as the most abundant phyla in sterilized samples from upper and lower soil layers. *Proteobacteria*, *Planctomycetota*, *Acidobacteria*, *Bacteroidota*, *Myxococcota*, *Verrucomicrobiota*, and *Actinobacteria* were more abundant in unsterilized samples from both upper and lower soil layers (**Figure 3.4A and 3.4B**). The phyla *Verrucomicrobiota*, *Chloroflexi*, *Nitrospirota*, and *Firmicutes*, were more abundant in lower soil layers (**Figure S9**). In contrast, *Bacteroidota*, *Planctomycetota*, *Actinobacteria*, *Myxococcota*, *Proteobacteria*, and *Acidobacteria* were more abundant in upper soil layer samples (**Figure S9**).

Season-simulated temperatures and treatments showed differences in soil bacterial community composition. PcoA axis 1 and 2 explained 11.4% and 8.8%, respectively, of the

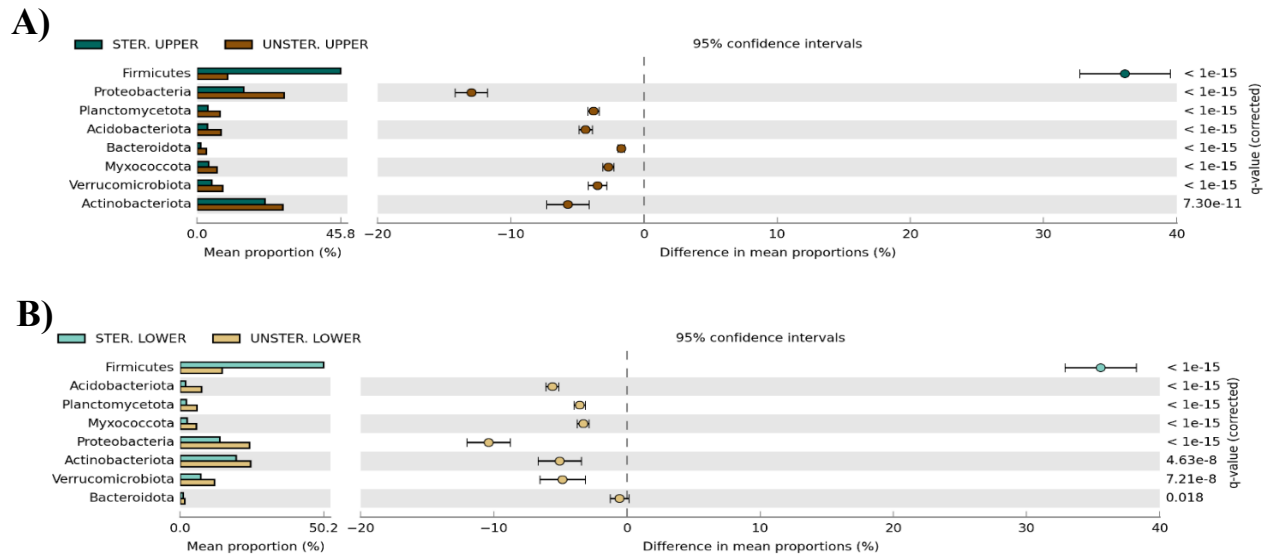


Figure 3. 4 Differential relative abundance of bacterial community phyla identified in sterilized and unsterilized samples from **A)** upper and **B)** lower soil layers using Welch's t-test with Storey FDR correction.

variance in the data (**Figure 3.5A**). The bacterial community of soil samples did not seem to cluster based on the different season-simulated temperatures on PcoA plots using UniFrac distance metrics (**Figure 3.5A**). However, according to PERMANOVA (**Table 3.3**), the season effect (p-value = 0.001) and treatment effect (p-value = 0.001) were significant, suggesting that both season and treatment effects altered the bacterial community composition. According to the overall PERMANOVA, grass (p-value = 0.001), sterilization (p-value = 0.001), day (p-value = 0.021), season (p-value = 0.001), layer (p-value = 0.001), and treatment effects (p-value = 0.001) were significant (**Table 3.3**). Upper and lower soil layer differences ($R^2 = 0.068$) explained more variation followed by sterilization effects ($R^2 = 0.058$). Treatment effects were significant (p-value = 0.001 in spring; p-value = 0.001 in summer). The most different phyla determined by differential relative abundance analysis were *Verrucomicrobiota* and *Firmicutes* for spring-simulated

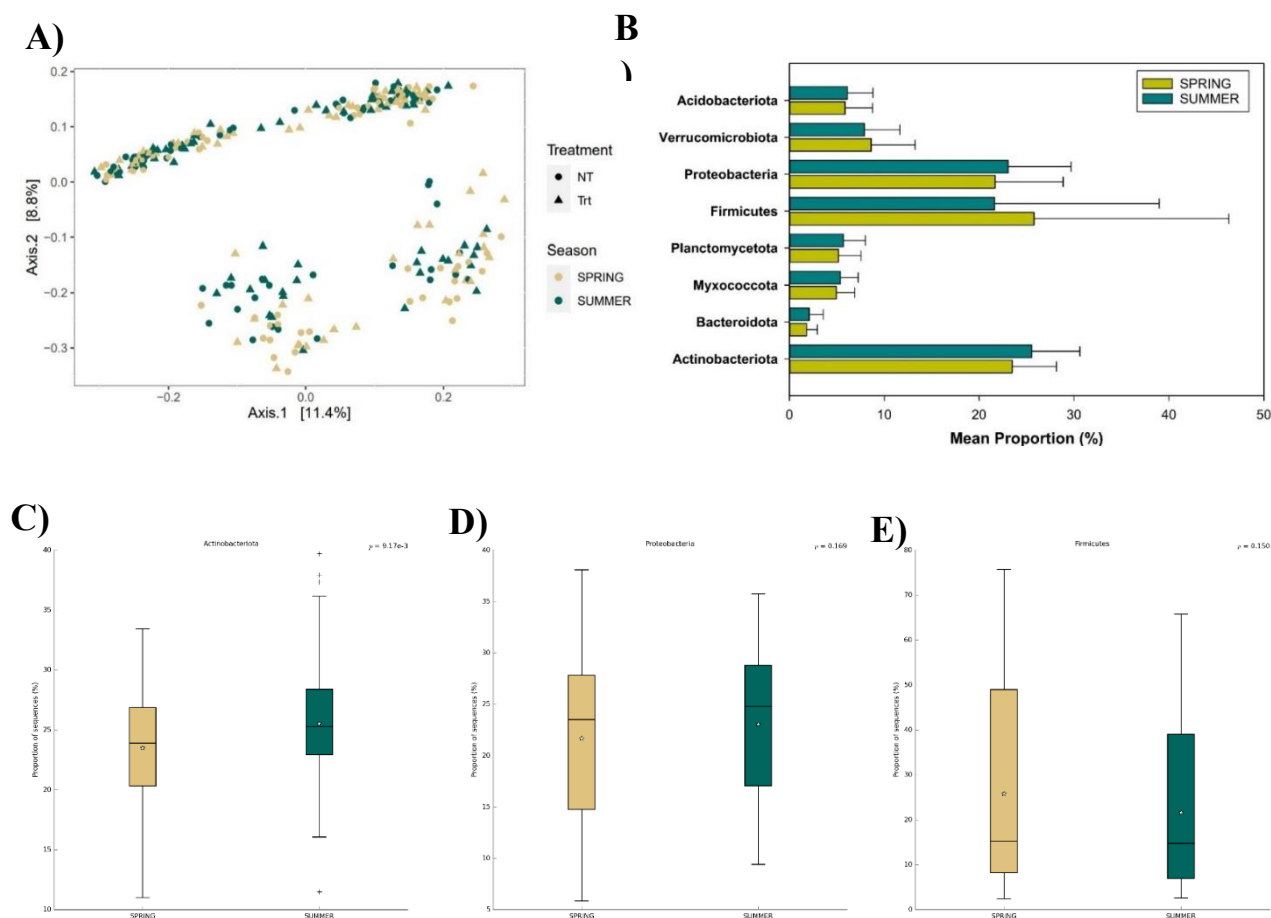


Figure 3. 5 A) Principal coordinate analysis (PCoA) ordinations of bacterial communities (16S V4 region) derived from spring and summer simulated temperatures. The PCoA is based on the Bray-Curtis distance metric, with samples clustering by Season (spring and summer) and Treatment (Trt and NT). **B)** Differential relative abundance of bacterial community phyla identified in spring and summer samples using Welch's t-test with Storey FDR correction. Boxplot featuring the differential relative abundance of the phyla **C)** Actinobacteria, **D)** Proteobacteria, and **E)** Firmicutes temperatures and *Acidobacteriota*, *Proteobacteria*, *Planctomycetota*, *Myxococcota*, *Bacteroidota*, and *Actinobacteriota* for summer-simulated temperatures (**Figure 3.5B**). In general, *Proteobacteria*, *Firmicutes*, and *Actinobacteria* were the most abundant phyla in both spring and summer-simulated temperatures. *Actinobacteriota* was statistically significant in summer versus spring-simulated temperatures conditions (p-value = 0.009) (**Figure 3.5C**). In contrast, no significant differences were observed in *Proteobacteria* (p-value = 0.169) and *Firmicutes* (p-

value= 0.151) between spring and summer-simulated temperatures (**Figure 3.5D** and **Figure 3.5E**).

Table 3. 3 Comparison of bacterial community structure dissimilarity in spring and summer-simulated growth chamber soil samples using permutational multivariate analysis of variance (PERMANOVA). The p-values of the dispersion test were derived from ANOVA.

Factors	Overall		Spring		Summer	
	R ²	P-value	R ²	P-value	R ²	P-value
Grass	0.023	0.001	0.030	0.001	0.025	0.001
Sterilization	0.058	0.001	0.061	0.001	0.065	0.001
Day	0.012	0.021	0.024	0.012	0.021	0.070
Season	0.006	0.001	—	—	—	—
Layers	0.068	0.001	0.073	0.001	0.101	0.001
Treatment	0.004	0.001	0.006	0.001	0.007	0.001
Grass*Day	0.010	0.161	0.019	0.389	0.018	0.243
Sterilization*Day	0.012	0.029	0.021	0.093	0.021	0.068
Grass*Season	0.005	0.001	—	—	—	—
Sterilization*Season	0.005	0.001	—	—	—	—
Day*Season	0.010	0.161	—	—	—	—
Grass*Layers	0.004	0.060	0.008	0.075	0.009	0.032
Sterilization*Layers	0.009	0.001	0.012	0.004	0.014	0.002
Day*Layers	0.006	0.293	0.020	0.213	0.018	0.363
Season*Layers	0.004	0.106	—	—	—	—
Grass*Treatment	0.003	0.001	0.006	0.001	0.006	0.001
Sterilization*Treatment	0.004	0.001	0.010	0.001	0.007	0.001
Day*Treatment	0.009	0.433	0.018	0.491	0.018	0.325
Season*Treatment	0.003	0.001	—	—	—	—
Layers*Treatment	0.004	0.077	0.007	0.132	0.007	0.151

Table 3. 4 Comparison of bacterial community structure dissimilarity in 2-4-D Treated (Trt) and Non-treated (NT) spring and summer-simulated growth chamber soil samples using paired-PERMANOVA with Bonferroni correction.

Pairs	Overall		Treated		Non-treated (NT)	
	R ²	P-value	R ²	P-value	R ²	P-value
SUMMER Trt vs SUMMER NT	0.0073	1.000	—	—	—	—
SUMMER Trt vs SPRING NT	0.0095	0.558	—	—	—	—
SUMMER Trt vs SPRING Trt	0.0085	0.966	0.008	0.151	—	—
SUMMER NT vs SPRING NT	0.0109	0.192	—	—	0.011	0.030
SUMMER NT vs SPRING Trt	0.0107	0.210	—	—	—	—
SPRING NT vs SPRING Trt	0.0064	1.00	—	—	—	—

Further, we observed that the bacterial community structure was not statistically different when performing a paired-PERMANOVA among the various interactions between season-simulated temperatures and treatment (**Table 3.4**). However, when treatments were analyzed separately, summer NT samples differed from spring NT samples (p-value = 0.030) (**Table 3.4**). No differences were observed between summer-treated and spring-treated samples (p-value = 0.151) (**Table 3.4**). In terms of differential abundance, the genera *Polaromonas*, *Rhodoplanes*, *Devosia*, and *966-1*, belonging to the phyla *Proteobacteria* and the genus *Sporacetigenium* belonging to the phyla *Firmicutes*, were more abundant in 2,4-D-treated samples in spring-simulated temperatures. The genera *Methylobacter*, *Ferrovibrio*, *IS-44*, *Microvirga*, *Phenylobacterium*, *Miel-7*, *Tardiphaga*, and *Cupriavidus*; *Sorangium* and *Vulgatibacter*; *Oceanbacillus*, *Clostridium sensu stricto* 3, and *Calditerricola*; *Pir2* lineage; and *ADurb Bin 118* belonging to the phyla *Proteobacteria*, *Myxococcota*, *Firmicutes*, *Planctomycetota*, and *Verrucomicrobiota*, respectively, were differentially more abundant in treated samples at summer-simulated temperatures (**Figure 3.6**).

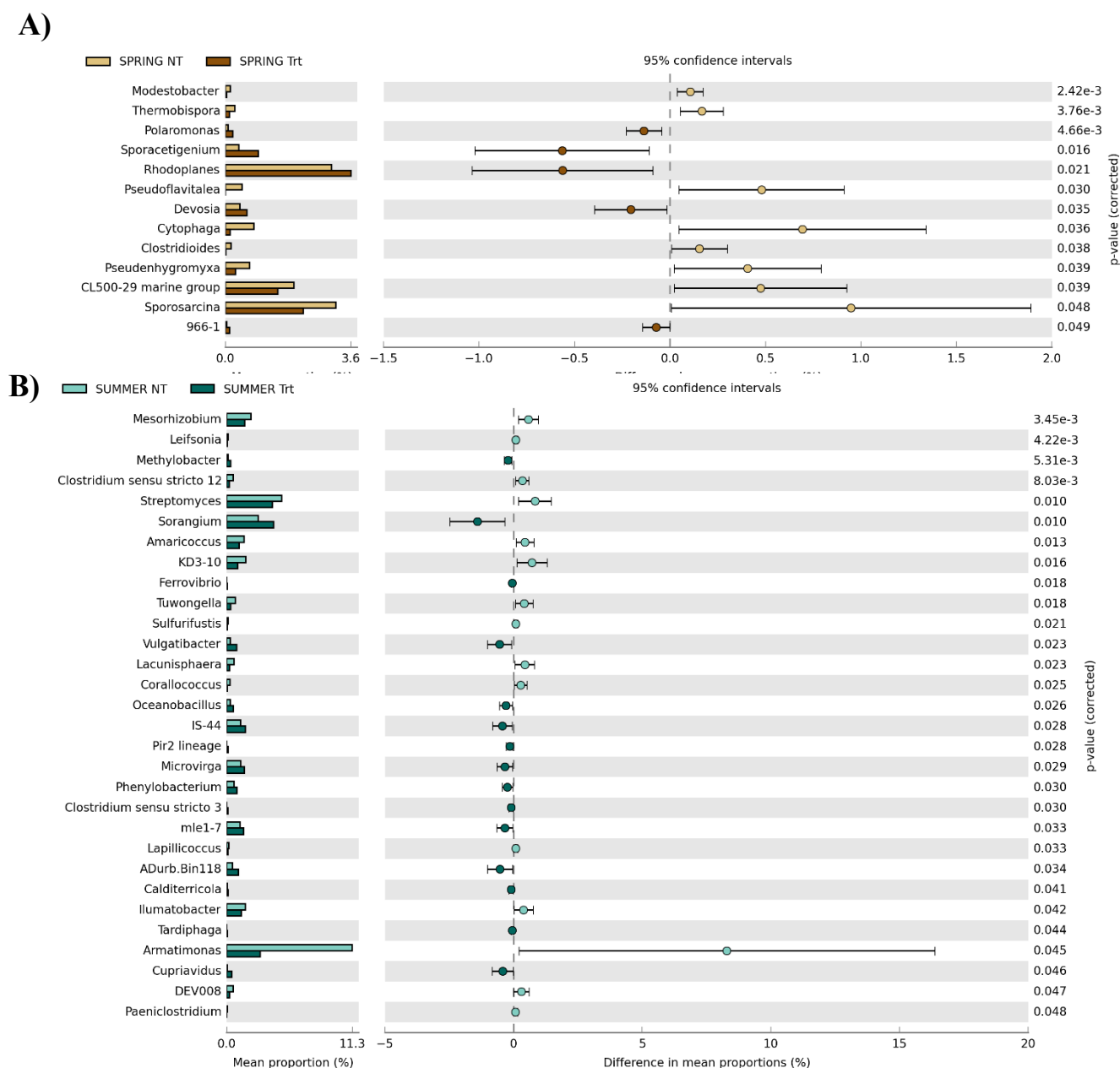


Figure 3. 6 Differential relative abundance of treated (Trt) and non-treated (NT) bacterial microbiome belonging to **A)** Spring and **B)** Summer-simulated temperatures samples at Order level. Welch's t-test was implemented with no correction.

Predicted soil bacterial function reveals important xenobiotic degradation pathways linked to 2,4-D degradation.

Field Study. A total of 21 predicted KEGG pathways relative abundance differences were detected between the upper and lower soil layers (**Figure 3.7**) and the months of May and July

(**Figure 3.8**) in each field site. No significant differences were observed between the different soil layers (**Figure 3.7**) and months (**Figure 3.8**) in each site in terms of the different predicted pathways. Benzoate degradation was, however, the highest predicted xenobiotic degradation pathway at both soil layer depths (**Figure 3.7**) and months (**Figure 3.8**). Styrene, toluene, xylene, chlorocyclohexane and chlorobenzene, fluorobenzoate, bisphenol, benzoate, caprolactam, drug metabolism–cytochrome P450's (CYP450s), metabolism of xenobiotics by CYP450s, and steroid degradation were more abundant in upper soil layer samples (**Figure S10**). In the lower soil layer samples, naphthalene, nitrotoluene, atrazine, ethylbenzene, dioxin, drug metabolism–other enzymes, chloroalkane and chloroalkene, polycyclic aromatic hydrocarbon, furfural, and aminobenzoate degradation were higher than in the upper samples (**Figure S10**).

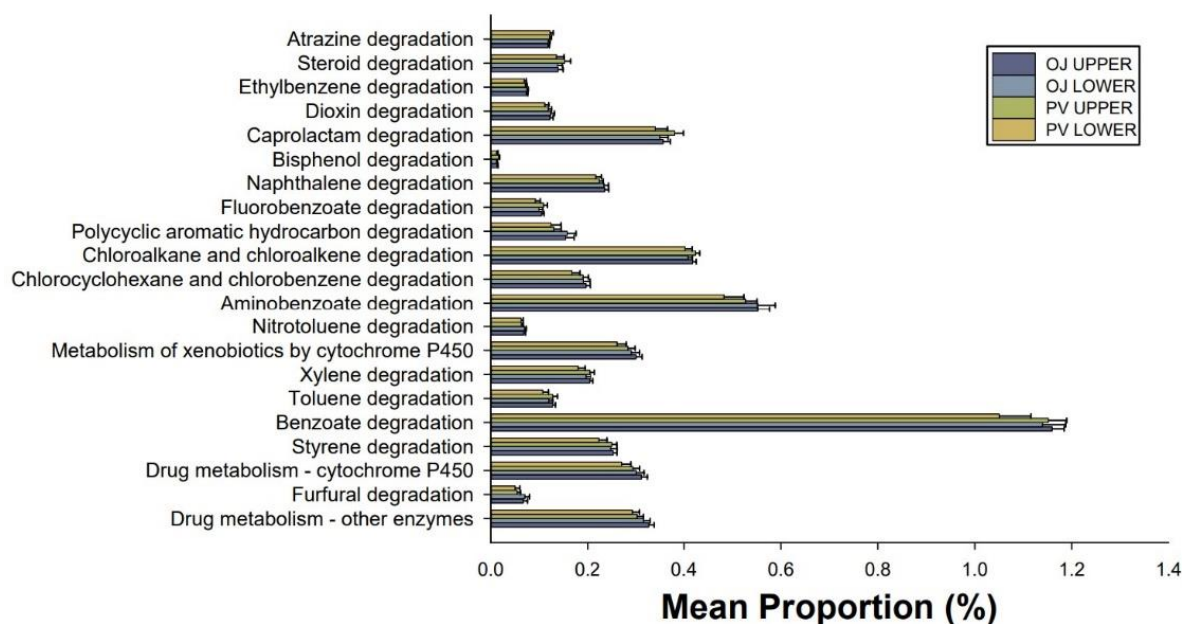


Figure 3. 7. Bar plot of significant differences in predicted xenobiotic degradation pathways of Upper and Lower soil layers from OJ and PV field samples using Tax4Fun2 and Welch's t-test with Storey FDR correction.

For samples collected in 2018, a total of 6 KEGG pathways showed differences between May and July (**Figure S11**). Aminobenzoate, chlorocyclohexane and chlorobenzene, dioxin, nitrotoluene, naphthalene, and benzoate degradation were more abundant in samples collected in July (**Figure S11A**). In contrast, only 1 KEGG pathway showed differences between both months in 2019, where nitrotoluene degradation was predicted to occur in May (**Figure S11B**). A Welch's t-test was used to perform these comparisons with Storey's false discovery rate (FDR) for multiple test correction.

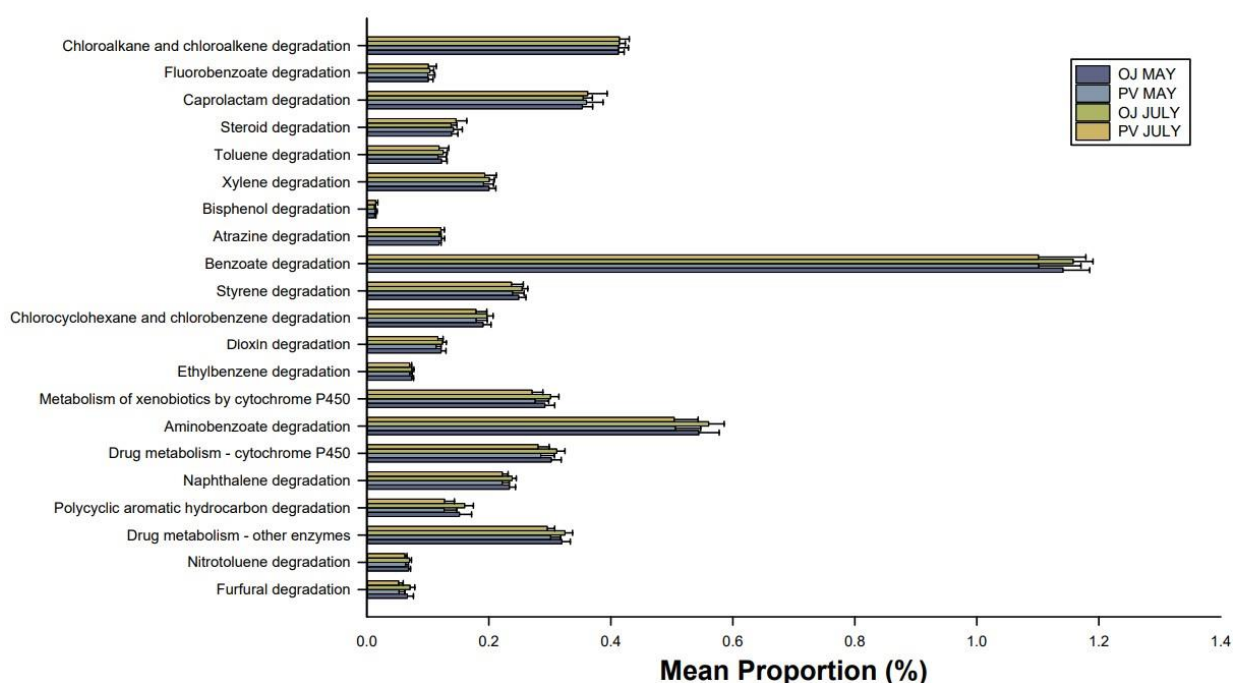


Figure 3. 8 Bar plot of significant differences in predicted xenobiotic degradation pathways of Upper and Lower soil layers from OJ and PV field samples using Tax4Fun2 and Welch's t-test with Storey FDR correction.

Growth Chamber Study. 21 KEGG pathways were predicted between the spring and summer-simulated temperature samples (**Figure 9**). Prediction analysis showed that the benzoate degradation pathway was more abundant in spring and summer-simulated temperature conditions, followed by aminobenzoate, chloroalkane, and chloroalkene degradation. No significant differences in xenobiotic degradation pathways were observed between the different seasonal-simulated temperatures or treatments.

Benzoate degradation was predominant throughout the different sterilization procedures, with a higher predicted occurrence in sterilized samples (**Figure S12**). Xenobiotic degradation pathways predicted to occur in unsterilized samples were toluene, furfural, chlorocyclohexane and chlorobenzene, fluorobenzoate, metabolism of xenobiotics by cytochrome P450's (CYPs), polycyclic aromatic hydrocarbon, aminobenzoate, steroid, drug metabolism induced by CYPs, styrene, and bisphenol degradation (**Figure S12**). Predicted pathways from sterilized samples were chloroalkane and chloroalkene, xylene, ethylbenzene, dioxin, benzoate, naphthalene, atrazine, nitrotoluene, caprolactam, and drug metabolism induced by other enzymes (**Figure S12**).

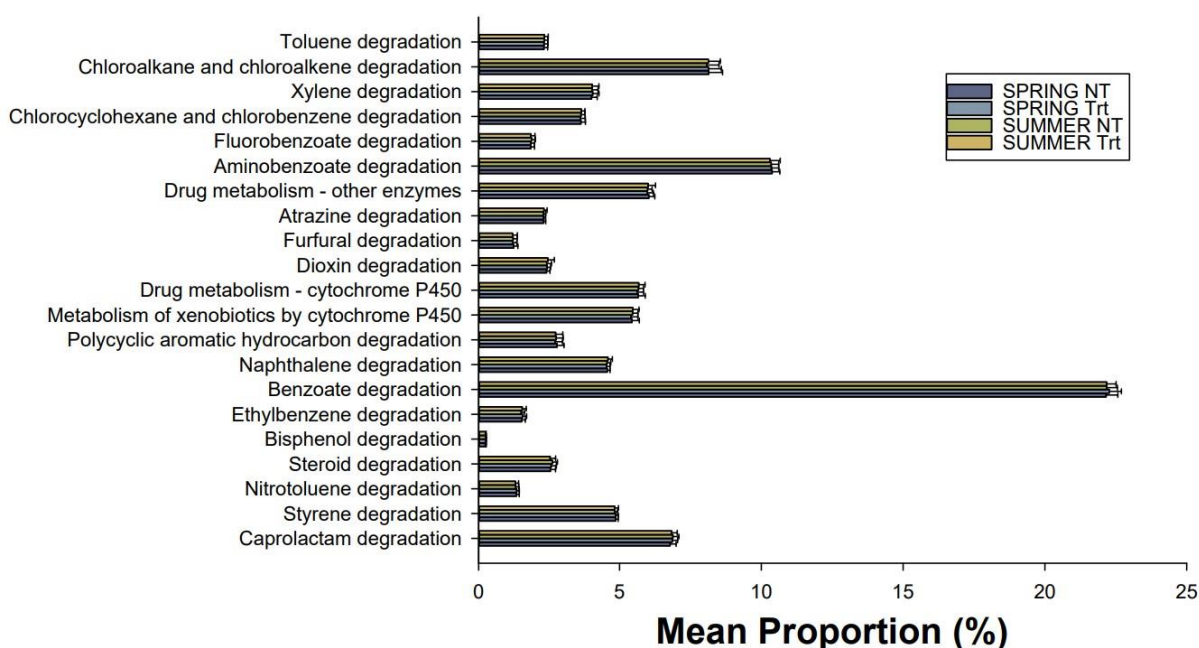


Figure 3. 9 Bar plot of significant differences in predicted xenobiotic degradation pathways of treated (Trt) and Non-treated (NT) samples from spring and summer-simulated temperatures using Tax4Fun2 and Welch's t-test with Storey FDR correction.

21 xenobiotic degradation pathways were predicted to occur in the upper and lower soil layers of the growth chamber study samples. Nitrotoluene, ethylbenzene, atrazine, caprolactam, styrene, benzoate, dioxin, steroid, xylene, aminobenzoate, and furfural degradation pathways were predicted in lower soil layers. Toluene, drug metabolism - CYP450s, fluorobenzoate, metabolism of xenobiotics by CYP450s, chlorocyclohexane and chlorobenzene, drug metabolism - other

enzymes, polycyclic aromatic hydrocarbon, naphthalene, bisphenol, and chloroalkane and chloroalkene degradation pathways were predicted to occur in upper soil layers (**Figure S13**).

Functional Prediction of metabolic enzymes related to 2,4-D degradation in soil.

Tax4Fun was used to predict the functional profiles from our field and growth chamber studies with a particular interest in metabolic enzymes involved in the 2,4-D degradation pathway in soil (**Figure 3.10**).

Field Study. Due to the soil microbiome's ability to degrade contaminants and utilize them as an energy source^{19,32,33}, our analysis was focused on functional metabolic enzymes associated with xenobiotic degradation abilities, with interest in 2,4-D, derived from the KEGG pathway database. We recorded a predicted mean proportion of 0.5% to 0.7% of *TfdA*, 7.4% to 8.6% of *TfdB*, less than 0.0008% of *TfdC*, less than 0.0001% of chloromuconate cycloisomerase (*TfdD*), 15.3% to 16.1% of carboxymethylenebutenolidase (*TfdE*), and 3.0% to 3.2% of maleylacetate reductase (*TfdF*) (**Figure 3.11**). Overall, in both 2018 and 2019, there were no differences in predicted *TfdA* proportion between OJ and PV field sites in May and July (**Figure 3.11**). In contrast, *TfdB* mean proportion was predicted to be higher in OJ versus PV field sites in both years, while the predicted mean proportion of *TfdC* and *TfdD* was negligible in both field sites and months. *TfdE* demonstrated the highest mean proportion. However, no differences in *TfdE* were observed between the field sites and months. *TfdF* mean proportion also did not show any differences between the site and month variables.

Since different gene pathways and soil microbes are involved in 2,4-D degradation, a closer look at other related metabolic enzymes mechanisms showed that the predicted mean proportion of catechol 1,2-dioxygenase (*CatA*), muconate cycloisomerase (*CatB*), and catechol 2,3-dioxygenase (*CatE*) was 5.8% to 6.2%, 3.3% to 4.1%, and 7.0% to 9.8%, respectively. We did not

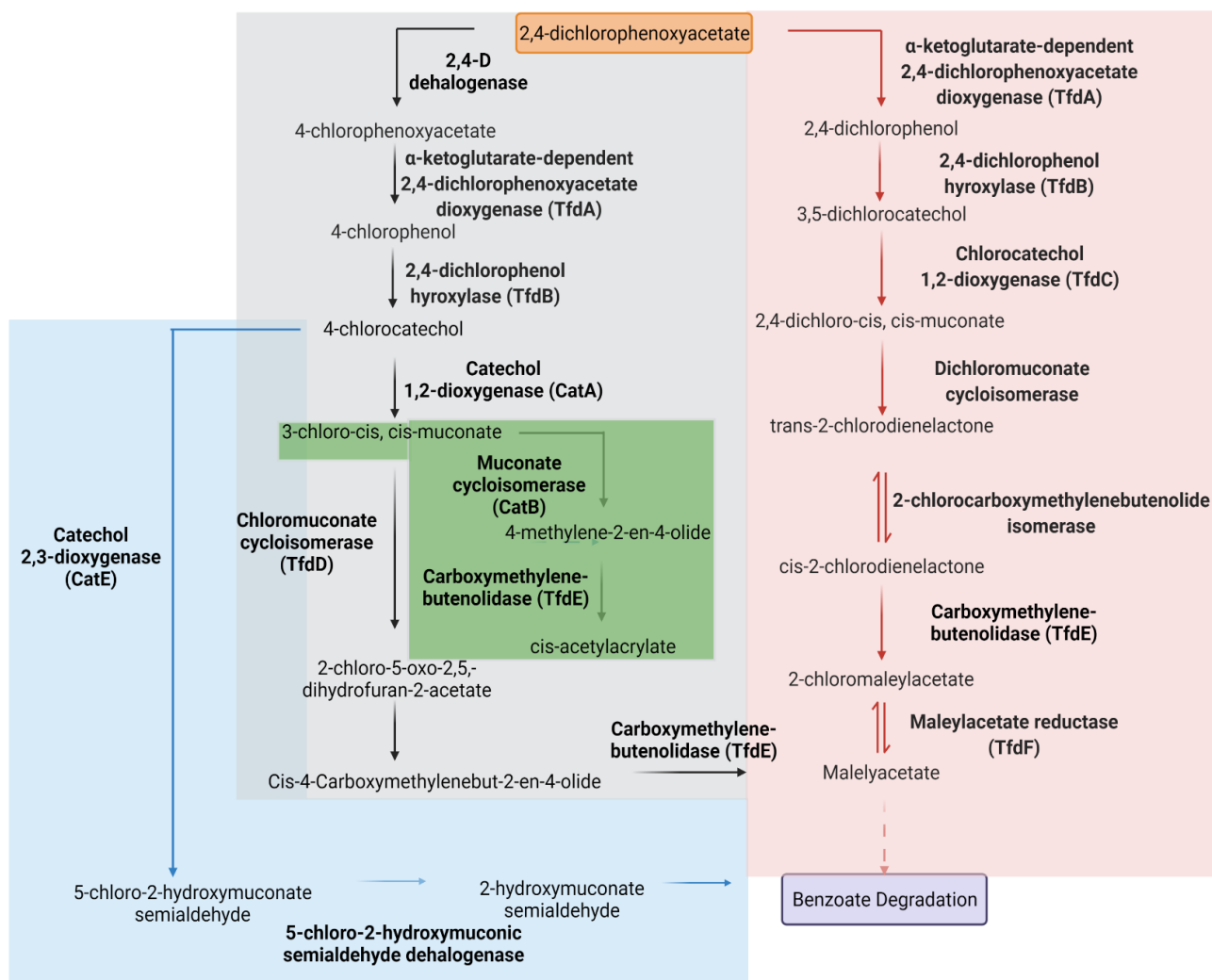


Figure 3. 10 Pathways overviewing the enzymes involved in 2,4-D degradation resulting in benzoate degradation. The enzymes catalyzing the catabolic steps are *TfdA*, α -ketoglutarate dependent 2,4-D dioxygenase enzyme, *TfdB*, 2,4-dichlorophenol hydroxylase, *TfdC*, chlorocatechol 1,2-dioxygenase, *TfdD*, chloromuconate cycloisomerase, *TfdE*, carboxymethelenebutenolidase, and *TfdF*, maleylacetate reductase. Alternative pathways are highlighted in red, grey, green, and blue. Adapted from the chlorocyclohexane and chlorobenzene degradation KEGG pathway.

observe differences in the mean proportion of *CatA* between OJ and PV or the months of May and July. In contrast, *CatB* and *CatE* were higher in OJ versus PV field samples at both 2018 and 2019 trials.

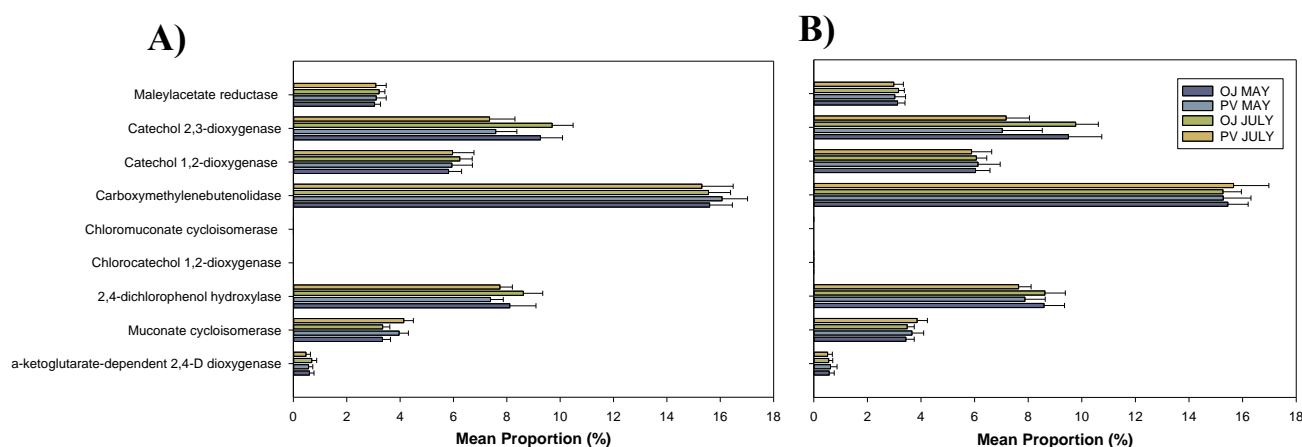


Figure 3. 11 Functional prediction of 9 functions in the KEGG categories involved in bacterial 2,4-D degradation in soil at OJ and PV field sites during the months of May and July in **A)** 2018 and **B)** 2019. Functional prediction was performed with Tax4Fun.

Growth Chamber Study. A predicted mean proportion of 1.3% of *TfdA*, 20.2% to 20.7% of *TfdB*, less than 0.0006% of *TfdC*, 33.5% to 34.5% of *TfdE*, and 6.9% to 7.1% of *TfdF* was recorded in the growth chamber study (**Figure 3.12**). There was no observed predicted mean proportion of *TfdD*. Further, no significant differences were noted in the mean proportion of *TfdA*, *TfdB*, *TfdC*, *TfdE*, and *TdfF* at spring and summer-simulated temperatures and treatments (**Figure 3.12**). *CatA*, *CatB*, and *CatE* genes showed 14.1 to 14.3%, 8.4% to 8.7%, and 13.8% to 14.8%

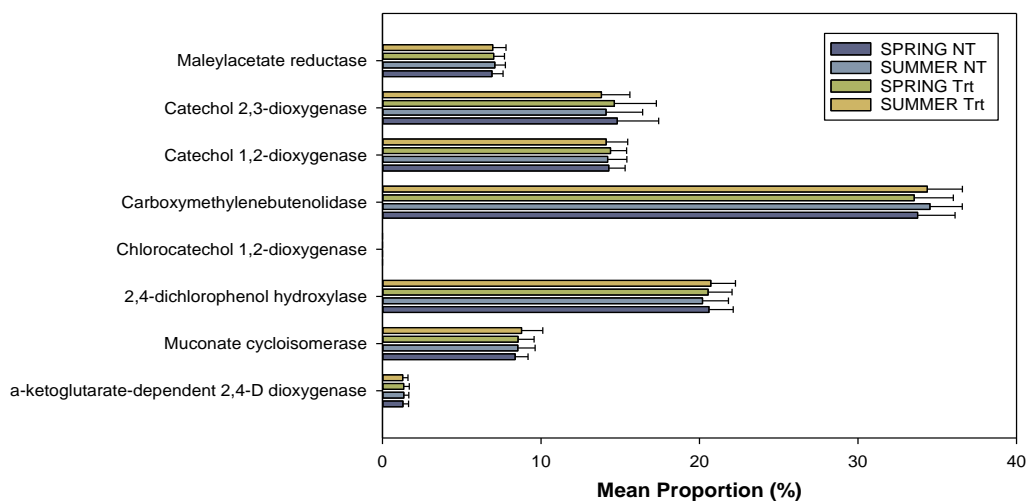


Figure 3. 12 Functional prediction of 8 functions in the KEGG categories involved in bacterial 2,4-D degradation in soil at Spring and Summer-simulated temperatures and treated (Trt) vs non-treated (NT.) applications. Functional prediction was performed with Tax4Fun

predicted mean proportion, respectively. No differences were observed in the mean proportion of *CatA*, *CatB*, and *CatE* at the different simulated temperatures and treatments.

Discussion

Spring vs. Summer Conditions

The two field studies indicate that varying seasonal and environmental conditions, specifically during May and July, altered urban soil bacterial community composition. Our PERMANOVA suggested the bacterial composition and structure were significantly altered by seasonal patterns between both field sites. Additionally, we noticed co-occurrence network shifts between May and July in both field sites, thus supporting our hypothesis that seasonal environmental variations influence the occurrence of bacteria in urban soils. The co-occurrence network analysis in this study may provide new and further supporting details of important bacterial drivers related to 2,4-D biodegradation. Similar to our previous findings, the occurrence network analysis identified *Alphaproteobacteria* and *Actinobacteria* as important key players in shaping the microbiome, which are also known for their ability to degrade pesticide and environmental pollutants, respectively.^{34,35} Soil temperature, when measured at each collection day, significantly correlated with the shifts in the composition of the soil bacterial community, providing additional evidence of the existing rich and diverse bacterial community in urban landscapes and their ability to shift in structure and composition at varying environments. Although our major findings point towards seasonal condition differences (May and July) altering the bacterial community composition, function, and structure, this study adds supporting evidence that soil microbial communities shift in structure and activity in response to a *combination* of various environmental factors from each season, and not just one factor on its own. Further,

measuring both the ambient and soil temperature at each collection day would have likely offered a better insight into the effects of overall temperature at different seasons in the soil microbiome.

Despite the known effect of seasonal temperature changes on the soil microbiome^{17,36–39}, soil moisture content was the strongest environmental factor in structuring the soil bacterial communities. Other studies have also observed dissimilarities of soil microbial communities in response to soil moisture content: Brockett et al. (2012) found that soil moisture was strongly correlated with the functional potential of the soil microbial community in forests⁴⁰; Wardle and Parkinsons (1990) found a reduction of microbial biomass due to drying of soil⁴¹, and Chowdhury et al. (2019) revealed that soil drying altered the structure and function of soil microbial communities and promoted shifts in specific metabolic pathways.⁴²

Spring and summer-simulated temperature effects in the growth chamber study also showed differences between their bacterial community composition. *Proteobacteria* and *Actinobacteria* had the highest abundance between both temperatures. In terms of the interaction between season-simulated temperature and treatment effects, we concluded that this interaction was significant in shaping the bacterial microbiome. Treated soil samples in spring and summer temperatures showed a higher mean proportion of bacteria belonging to the phyla *Proteobacteria*, *Myxococcota*, *Firmicutes*, and *Planctomycetota*. In other studies, soil bacteria belonging to *Proteobacteria* such as *Cupriavidus necator* JMP134^{19,21,43}, *Cupriavidus gilardii*⁴⁴, and *Methylobacterium sp.*⁴⁵ have been isolated from diverse soils and can readily degrade 2,4-D. *Clostridium sensu stricto*, belonging to *Firmicutes*, was one of the most predominant groups in Brazilian soil samples involved in the anaerobic transformation of 2,4-D.⁴⁶ While more research is needed, and although these differentially abundant bacteria were not directly studied for degrading 2,4-D, our findings still provide evidence of 2,4-D degradation occurring in urban soils.

Xenobiotic Degradation Pathways and Metabolic Enzymes Linked to 2,4-D degradation

Benzoate degradation was the highest predicted pathway in July in both field sites at upper soil layers as well as in our growth chamber study. However, no significant differences in benzoate degradation were observed in treated and non-treated samples. Bacteria and genes involved in the degradation of 2,4-D have been widely studied.²¹ In particular, the most extensively studied gene cluster *tfdABCDEF* leads to the complete mineralization of 2,4-D in soil (**Figure 3.10**).^{19,21,47,48} *TfdA* catalyzes the initial step of 2,4-D degradation to form 2,4-dichlorophenol (2,4- DCP) by encoding the α -ketoglutarate dependent 2,4-D dioxygenase enzyme. *TfdB* (2,4-dichlorophenol hydroxylase) transforms 2,4-DCP to 3,5-dichlorocatechol (3,5-DCC), and *tfdC* (chlorocatechol 1,2-dioxygenase) along with the *TfdDEF* –encoded enzymes provide further transformation by metabolizing 3,5-DCC through an intradiol ring cleavage.^{19,21,49} While other pathway mechanisms can occur in the degradation of 2,4-D (**Figure 3.10**), the final reaction leads to benzoate degradation and, ultimately, the TCA cycle. This study also showed that the highest predicted enzyme involved in 2,4-D degradation was *TfdE*. *TfdE* encodes for the enzyme carboxymethylenebutenolidase, which catalyzes the reaction of cis-2-chlorodienelactone to 2-chloromaleylacetate in the *tfdABCDEF* pathway and catalyzes the reaction of 4-methylene-2-en-4-olide to cis-acetylacrylate in an alternative pathway (**Figure 3.10**).

Overall, the findings in this study suggest that the bacterial community structure and diversity were significantly different between OJ and PV field sites in the two consecutive years the study was performed. Differences in the soil bacterial community among the different depths and varying seasonal conditions were also observed in field and growth chamber studies. *Acidobacteria*, *Proteobacteria*, and *Firmicutes* were identified as the most differentially abundant. Although the main focus established in this study was to assess how seasonal shifts influenced the

soil microbiome in urban landscapes, which, in turn, may impact 2,4-D degradation, we also evaluated 2,4-D impacts in treated plots on the bacterial community at the varying seasons. Our results showed that 2,4-D treatment effects were not significant in the field study.

Similarly, our growth chamber study results suggest no differences in bacterial community composition between the two season-simulated temperatures when 2,4-D-treated was applied. In contrast, we did observe that season-simulated temperatures were significantly different in non-treated plots. These results suggest that the intensive management of turfgrass through inputs of pesticides, fertilizers, irrigation, and others, can govern soil bacterial composition and structure and, in cases, overpower environmental factors and conditions. For example, a study conducted by Lupatini et al. (2017) found that organic farming management promoted a richer and more diverse microbiome than conventional farming, i.e., the use of synthetic chemicals for crop and plant management, where lower microbial heterogeneity (diversity) was observed.⁵⁰ Another study by Gabriel et al. (2006) also had similar findings where conventional field systems contained a typical pattern of biotic homogenization.⁵¹ Further, these results align with 2,4-D's recorded short half-life in soil and the role soil microbes may play in adapting and using 2,4-D as a carbon source for energy. In all experiments, we observed a high predicted mean proportion of benzoate degradation and the enzyme carboxymethylenebutenolidase, encoded by the *TfdE* gene. These results propose the complete mineralization of 2,4-D in urban soils and the potential transformation of secondary products that may be more toxic than the parent compound.

Sites, Soil Layers, and Soil Properties

Bacterial community composition was distinct between upper (0-5 cm) and lower (25-30 cm) soil layers. These differences were observed in both field trials conducted in 2018 and 2019 and the growth chamber study. Our results align with previous studies that assessed microbial

community composition at different soil depths.^{52,53} Most importantly, we found that *Actinobacteriota* and *Proteobacteria* played a significant role in the bacterial soil structure in both field and growth chamber studies, especially in shaping the community in upper soil layers. Although *Actinobacteriota* and *Proteobacteria* are common in soil environments^{54–58}, they have shown to be of great importance in improving the bioremediation of pesticides and other contaminants, which is relevant to our study.^{34,35} Our field study also revealed that the genera *Hyphomicrobium* and *Gaiella*, belonging to the phyla *Proteobacteria* and *Acidobacteriota*, respectively, were the most dominant genera identified. *Hyphomicrobium*, belonging to *Alphaproteobacteria*, is known to degrade environmental pollutants ranging from industrial solvents to pesticides.^{59,60} With respect to *Gaiella*, this genus contributes to nutrient cycling, specifically Nitrogen⁶¹, where Bronick and Lal (2005) have shown that soil structure can also affect nutrient availability.⁶² Our soil report analysis for 2018 and 2019 indicates that the soil texture in OJ and PV field samples collected were silt loam and loam soil, respectively. Both of these soil types contain higher nutrient content.⁶³ Therefore, the high relative abundance observed from *Gaiella* may be due to the soil types from each field site. A previous study found that *Gaiellales* was among the most differentially abundant taxa in suburban soils, which contained a soil texture between silt loam and loam soil.⁶⁴

The growth chamber study also aligned with our findings from our field study, where the soil bacterial community composition was distinct at different depths, with *Proteobacteria* and *Actinobacteria* being the most differentially abundant in both upper and lower layers, especially from unsterilized samples.

Sterilization Procedures

We also concluded that sterilized samples were distinct from unsterilized samples. Indeed, our objective to sterilize soil samples successfully controlled the growth of soil bacteria that potentially can degrade 2,4-D. Our results suggest that sterilized soils had a greatly reduced abundance of the families *Proteobacteria*, *Planctomycetota*, *Acidobacteriota*, *Bacteroidota*, *Myxococcota*, *Verrucomicrobiota*, and *Actinobacteriota*, many of which are known to contain 2,4-D degraders. Interestingly, we found a higher differential relative abundance of *Firmicutes* in sterilized upper and lower soil layers. This aligned with findings from previous research where the relative abundance of *Firmicutes* increased, and *Proteobacteria* and *Bacteroidetes* decreased after soil sterilization, respectively.^{65,66} Further, increased abundance after sterilization may also be due to post-sterilization colonization. Overall, these results suggest sterilization procedures can significantly change the soil microbial community composition and structure and effectively inhibit the growth of potential 2,4-D degraders.

Soil microbes are essential indicators of soil quality and have been extensively applied to remediate pesticide-contaminated soils.^{47,67,68} Thus, controlling the ability of soil bacteria capable of degrading 2,4-D through sterilization is essential to assess their role in producing TPs in urban landscapes. Sterilization effects and treatment effects were significant in shaping the soil bacterial microbiome. This result is consistent with our conclusion that sterilization changes the bacterial community, further inhibiting microbes that are adapted to use 2,4-D as an energy source.

2,4-D Treated vs. Non-treated Soils

We did not observe a significant effect of 2,4-D-treated soils on the bacterial community in our field trials in either year. In contrast, the effect of 2,4-D-treated soils on the bacterial community in our growth chamber study was significant likely due to the shortened duration between treatment application and sample collection. The EPA has identified 2,4-D's half-life in

soil to be approximately 6.2 days, depending on environmental factors and soil properties.⁵ Similar to the EPA, other studies have identified that soil microorganisms can degrade 2,4-D in less than 10 days in combination with other processes such as photodegradation and leaching.^{69,70} These previous findings led us to shorten our sampling time for our growth chamber study to better understand the 2,4-D-bacterial interactions and degradation ability in urban soils. We believe the difference in treatment effects between our field and controlled study is likely due to the rapid shorter collection time frame established in the growth chamber study (i.e., collected at day 1 post-application versus day 7 post-application). Degradation of 2,4-D is directly influenced by microbes and is a rapid process in soil environments¹⁹, which reinforced our plan to reduce the sampling time.

To conclude, 2,4-D is commonly applied in urban landscapes, including home lawns and recreational areas, which may further be broken down to other products that may be more toxic than the parent compound.² Because soil microorganisms mainly accomplish 2,4-D degradation, it is essential to understand how varying seasonal factors influence microbial activity. This study emphasizes that seasonal environmental variations shift soil bacterial structure and potential degradation activity in urban landscapes. Our results also state that these differences depend on various factors such as soil depth, soil type, and soil moisture. Furthermore, predicted xenobiotic degradation pathways link the ability of urban soil bacteria to degrade 2,4-D, which ultimately leads to benzoate degradation. Future studies implementing other microbial communities, i.e., bacteria, fungi, archaea, and protozoa, will provide a complete assessment of how these microbes interact at varying seasonal conditions and their role in 2,4-D degradation, as with any other pesticide application. Performing a similar field study where 2,4-D is regularly applied to urban soils will also provide valuable insight into how microbes interact with this pesticide. Lastly,

expanding this study to other commonly applied pesticides is crucial to reduce the non-target impacts of pesticide usage in intensively managed plant systems.

References

- (1) Atwood, D.; Paisley-Jones, C. *Pesticides Industry Sales and Usage 2008-2012 Market Estimates*; US Environmental Protection Agency, **2017**.
- (2) Islam, F.; Wang, J.; Farooq, M. A.; Khan, M. S. S.; Xu, L.; Zhu, J.; Zhao, M.; Muños, S.; Li, Q. X.; Zhou, W. Potential Impact of the Herbicide 2,4-Dichlorophenoxyacetic Acid on Human and Ecosystems. *Environment International* **2018**, *111*, 332–351. <https://doi.org/10.1016/j.envint.2017.10.020>.
- (3) Charles, J. M.; Cunny, H. C.; Wilson, R. D.; Bus, J. S.; Lawlor, T. E.; Cifone, M. A.; Fellows, M.; Gollapudi, B. Ames Assays and Unscheduled DNA Synthesis Assays on 2, 4-Dichlorophenoxyacetic Acid and Its Derivatives. *Mutat Res* **1999**, *444* (1), 207–216. [https://doi.org/10.1016/s1383-5718\(99\)00074-1](https://doi.org/10.1016/s1383-5718(99)00074-1).
- (4) Song, Y. Insight into the Mode of Action of 2,4-Dichlorophenoxyacetic Acid (2,4-D) as an Herbicide: 2,4-D Works as Herbicide. *Journal of Integrative Plant Biology* **2014**, *56* (2), 106–113. <https://doi.org/10.1111/jipb.12131>.
- (5) USEPA. Reregistration Eligibility Decision for 2,4-D https://archive.epa.gov/pesticides/reregistration/web/pdf/24d_red.pdf (accessed 2021 -08 -17).
- (6) Corke, C. T.; Thompson, F. R. Effects of Some Phenylamide Herbicides and Their Degradation Products on Soil Nitrification. *Can. J. Microbiol.* **1970**, *16* (7), 567–571. <https://doi.org/10.1139/m70-095>.
- (7) Somasundaram, L.; Coats, J. R. Pesticide Transformation Products: Fate and Significance in the Environment. *ACS symposium series (USA)* **1991**, No. 459.

- (8) Coats, J. Pesticide Degradation Mechanisms and Environmental Activation. *Acs Symposium Series* **1991**, 459, 10–30.
- (9) Remucal, C. K. The Role of Indirect Photochemical Degradation in the Environmental Fate of Pesticides: A Review. *Environmental Science: Processes & Impacts* **2014**, 16 (4), 628. <https://doi.org/10.1039/c3em00549f>.
- (10) Nedwell, D. B.; Floodgate, G. D. The Seasonal Selection by Temperature of Heterotrophic Bacteria in an Intertidal Sediment. *Marine Biology* **1971**, 11 (4), 306–310. <https://doi.org/10.1007/BF00352448>.
- (11) Singh, R. Microbial Biotransformation: A Process for Chemical Alterations. *JBMOA* **2017**, 4 (2). <https://doi.org/10.15406/jbmoa.2017.04.00085>.
- (12) Horvath, R. S. Microbial Co-Metabolism and the Degradation of Organic Compounds in Nature. *Bacteriol Rev* **1972**, 36 (2), 146–155.
- (13) Huang, X.; He, J.; Yan, X.; Hong, Q.; Chen, K.; He, Q.; Zhang, L.; Liu, X.; Chuang, S.; Li, S.; Jiang, J. Microbial Catabolism of Chemical Herbicides: Microbial Resources, Metabolic Pathways and Catabolic Genes. *Pesticide Biochemistry and Physiology* **2017**, 143, 272–297. <https://doi.org/10.1016/j.pestbp.2016.11.010>.
- (14) Lal, R.; Lal, S.; Shivaji, S.; Pemberton, J. M. Use of Microbes for Detoxification of Pesticides. *Critical Reviews in Biotechnology* **1985**, 3 (1), 1–16. <https://doi.org/10.3109/07388558509150778>.
- (15) Fenner, K.; Canonica, S.; Wackett, L.; Elsner, M. Evaluating Pesticide Degradation in the Environment: Blind Spots and Emerging Opportunities. *Science* **2013**, 341 (6147), 752–758.

- (16) Bollag, J.-M.; Liu, S.-Y. Biological Transformation Processes of Pesticides. *Pesticides in the Soil Environment: Processes, Impacts and Modeling* **1990**, 169–211. <https://doi.org/10.2136/sssabookser2.c6>.
- (17) Lipson, D. A.; Schmidt, S. K. Seasonal Changes in an Alpine Soil Bacterial Community in the Colorado Rocky Mountains. *Applied and Environmental Microbiology* **2004**, 70 (5).
- (18) Monson, R. K.; Burns, S. P.; Williams, M. W.; Delany, A. C.; Weintraub, M.; Lipson, D. A. The Contribution of Beneath-snow Soil Respiration to Total Ecosystem Respiration in a High-elevation, Subalpine Forest. *Global Biogeochemical Cycles* **2006**, 20 (3), n/a–n/a.
- (19) Kitagawa, W.; Kamagata, Y. Diversity of 2,4-Dichlorophenoxyacetic Acid (2,4-D)-Degradative Genes and Degrading Bacteria. In *Biodegradative Bacteria: How Bacteria Degrade, Survive, Adapt, and Evolve*; Springer Japan, 2014; pp 43–57.
- (20) Don, R. H.; Weightman, A. J.; Knackmuss, H. J.; Timmis, K. N. Transposon Mutagenesis and Cloning Analysis of the Pathways for Degradation of 2,4-Dichlorophenoxyacetic Acid and 3-Chlorobenzoate in *Alcaligenes Eutrophus* JMP134(PJP4). *The Journal of Bacteriology* **1985**, 161 (1).
- (21) Kumar, A.; Trefault, N.; Olaniran, A. O. Microbial Degradation of 2,4-Dichlorophenoxyacetic Acid: Insight into the Enzymes and Catabolic Genes Involved, Their Regulation and Biotechnological Implications. *Critical Reviews in Microbiology* **2016**, 42 (2), 194–208.
- (22) Gonod, L. V.; Martin-Laurent, F.; Chenu, C. 2,4-D Impact on Bacterial Communities, and the Activity and Genetic Potential of 2,4-D Degrading Communities in Soil. *FEMS Microbiology Ecology* **2006**, 58 (3), 529–537. <https://doi.org/10.1111/j.1574-6941.2006.00159.x>.

- (23) Lawn Maintenance. 8.
- (24) Average Annual Temperatures by USA State - Current Results
<https://www.currentresults.com/Weather/US/average-annual-state-temperatures.php>
 (accessed 2019 -03 -22).
- (25) Cox, M. S.; Deblois, C. L.; Suen, G. Assessing the Response of Ruminal Bacterial and Fungal Microbiota to Whole-Rumen Contents Exchange in Dairy Cows. *Front Microbiol* **2021**, *12*, 665776. <https://doi.org/10.3389/fmicb.2021.665776>.
- (26) Kozich, J. J.; Westcott, S. L.; Baxter, N. T.; Highlander, S. K.; Schloss, P. D. Development of a Dual-Index Sequencing Strategy and Curation Pipeline for Analyzing Amplicon Sequence Data on the MiSeq Illumina Sequencing Platform. *Appl Environ Microbiol* **2013**, *79* (17), 5112–5120. <https://doi.org/10.1128/AEM.01043-13>.
- (27) Callahan, B. J.; McMurdie, P. J.; Rosen, M. J.; Han, A. W.; Johnson, A. J. A.; Holmes, S. P. DADA2: High Resolution Sample Inference from Illumina Amplicon Data. *Nat Methods* **2016**, *13* (7), 581–583. <https://doi.org/10.1038/nmeth.3869>.
- (28) Davis, N. M.; Proctor, D. M.; Holmes, S. P.; Relman, D. A.; Callahan, B. J. Simple Statistical Identification and Removal of Contaminant Sequences in Marker-Gene and Metagenomics Data. *Microbiome* **2018**, *6* (1), 226. <https://doi.org/10.1186/s40168-018-0605-2>.
- (29) Deng, Y.; Jiang, Y.-H.; Yang, Y.; He, Z.; Luo, F.; Zhou, J. Molecular Ecological Network Analyses. *BMC Bioinformatics* **2012**, *13* (1), 113. <https://doi.org/10.1186/1471-2105-13-113>.
- (30) Bastian, M.; Heymann, S.; Jacomy, M. Gephi: An Open Source Software for Exploring and Manipulating Networks; **2009**. <https://doi.org/10.13140/2.1.1341.1520>.

- (31) Wemheuer, F.; Taylor, J. A.; Daniel, R.; Johnston, E.; Meinicke, P.; Thomas, T.; Wemheuer, B. Tax4Fun2: Prediction of Habitat-Specific Functional Profiles and Functional Redundancy Based on 16S rRNA Gene Sequences. *Environmental Microbiome* **2020**, *15* (1), 11. <https://doi.org/10.1186/s40793-020-00358-7>.
- (32) Zabaloy, M. C.; Gómez, M. A. Isolation and Characterization of Indigenous 2,4-D Herbicide Degrading Bacteria from an Agricultural Soil in Proximity of Sauce Grande River, Argentina. *Ann Microbiol* **2014**, *64* (3), 969–974. <https://doi.org/10.1007/s13213-013-0731-9>.
- (33) Xiao, L.; Jia, H.-F.; Jeong, I.-H.; Ahn, Y.-J.; Zhu, Y.-Z. Isolation and Characterization of 2,4-D Butyl Ester Degrading Acinetobacter Sp. ZX02 from a Chinese Ginger Cultivated Soil. *J Agric Food Chem* **2017**, *65* (34), 7345–7351. <https://doi.org/10.1021/acs.jafc.7b02140>.
- (34) Alvarez, A.; Saez, J. M.; Davila Costa, J. S.; Colin, V. L.; Fuentes, M. S.; Cuozzo, S. A.; Benimeli, C. S.; Polti, M. A.; Amoroso, M. J. Actinobacteria: Current Research and Perspectives for Bioremediation of Pesticides and Heavy Metals. *Chemosphere* **2017**, *166*, 41–62. <https://doi.org/10.1016/j.chemosphere.2016.09.070>.
- (35) Regar, R. K.; Gaur, V. K.; Bajaj, A.; Tambat, S.; Manickam, N. Comparative Microbiome Analysis of Two Different Long-Term Pesticide Contaminated Soils Revealed the Anthropogenic Influence on Functional Potential of Microbial Communities. *Science of The Total Environment* **2019**, *681*, 413–423. <https://doi.org/10.1016/j.scitotenv.2019.05.090>.
- (36) Lipson, D. A.; Schmidt, S. K.; Monson, R. K. Carbon Availability and Temperature Control the Post-Snowmelt Decline in Alpine Soil Microbial Biomass. *Soil Biology and Biochemistry* **2000**, *32* (4), 441–448. [https://doi.org/10.1016/S0038-0717\(99\)00068-1](https://doi.org/10.1016/S0038-0717(99)00068-1).

- (37) Siles, J. A.; Margesin, R. Abundance and Diversity of Bacterial, Archaeal, and Fungal Communities Along an Altitudinal Gradient in Alpine Forest Soils: What Are the Driving Factors? *Microb Ecol* **2016**, *72* (1), 207–220. <https://doi.org/10.1007/s00248-016-0748-2>.
- (38) Adamczyk, M.; Hagedorn, F.; Wipf, S.; Donhauser, J.; Vittoz, P.; Rixen, C.; Frossard, A.; Theurillat, J.-P.; Frey, B. The Soil Microbiome of GLORIA Mountain Summits in the Swiss Alps. *Frontiers in Microbiology* **2019**, *10*, 1080. <https://doi.org/10.3389/fmicb.2019.01080>.
- (39) Islam, W.; Noman, A.; Naveed, H.; Huang, Z.; Chen, H. Y. H. Role of Environmental Factors in Shaping the Soil Microbiome. *Environ Sci Pollut Res* **2020**, *27* (33), 41225–41247. <https://doi.org/10.1007/s11356-020-10471-2>.
- (40) Brockett, B. F. T.; Prescott, C. E.; Grayston, S. J. Soil Moisture Is the Major Factor Influencing Microbial Community Structure and Enzyme Activities across Seven Biogeoclimatic Zones in Western Canada. *Soil Biology and Biochemistry* **2012**, *44* (1), 9–20. <https://doi.org/10.1016/j.soilbio.2011.09.003>.
- (41) Wardle, D. A.; Parkinson, D. Comparison of Physiological Techniques for Estimating the Response of the Soil Microbial Biomass to Soil Moisture. *Soil Biology and Biochemistry* **1990**, *22* (6), 817–823. [https://doi.org/10.1016/0038-0717\(90\)90162-S](https://doi.org/10.1016/0038-0717(90)90162-S).
- (42) Roy Chowdhury, T.; Lee, J.-Y.; Bottos, E. M.; Brislawn, C. J.; White, R. A.; Bramer, L. M.; Brown, J.; Zucker, J. D.; Kim, Y.-M.; Jumpponen, A.; Rice, C. W.; Fansler, S. J.; Metz, T. O.; McCue, L. A.; Callister, S. J.; Song, H.-S.; Jansson, J. K. Metaphenomic Responses of a Native Prairie Soil Microbiome to Moisture Perturbations. *mSystems* *4* (4), e00061-19. <https://doi.org/10.1128/mSystems.00061-19>.
- (43) Don, R. H.; Pemberton, J. M. Properties of Six Pesticide Degradation Plasmids Isolated from *Alcaligenes Paradoxus* and *Alcaligenes Eutrophus*. *J. BACTERIOL.* **1981**, *145*, 6.

- (44) Wu, X.; Wang, W.; Liu, J.; Pan, D.; Tu, X.; Lv, P.; Wang, Y.; Cao, H.; Wang, Y.; Hua, R. Rapid Biodegradation of the Herbicide 2,4-Dichlorophenoxyacetic Acid by *Cupriavidus Gilardii* T-1. *J. Agric. Food Chem.* **2017**, *65* (18), 3711–3720. <https://doi.org/10.1021/acs.jafc.7b00544>.
- (45) Mussy, M. H.; Brucha, G.; Reis, M. G.; Ushimaru, P. I.; Yamashita, M.; Bastos, W. R. Identification of microorganisms resistant to the herbicide 2,4-dichlorophenoxyacetic acid (2,4-D) in soils of Rondonia, Brazil. *Interciencia* **2013**, *38* (5), 353–357.
- (46) Brucha, G.; Aldas-Vargas, A.; Ross, Z.; Peng, P.; Atashgahi, S.; Smidt, H.; Langenhoff, A.; Sutton, N. B. 2,4-Dichlorophenoxyacetic Acid Degradation in Methanogenic Mixed Cultures Obtained from Brazilian Amazonian Soil Samples. *Biodegradation* **2021**, *32* (4), 419–433. <https://doi.org/10.1007/s10532-021-09940-3>.
- (47) Macur, R. E.; Wheeler, J. T.; Burr, M. D.; Inskeep, W. P. Impacts of 2,4-D Application on Soil Microbial Community Structure and on Populations Associated with 2,4-D degradation. *Microbiological Research* **2007**, *162* (1), 37–45. <https://doi.org/10.1016/j.micres.2006.05.007>.
- (48) Don', R. H.; Pemberton, J. M. Genetic and Physical Map of the 2,4-Dichlorophenoxyacetic Acid- Degradative Plasmid PJP4. 3.
- (49) Zharikova, N. V.; Iasakov, T. R.; Zhurenko, E. Yu.; Korobov, V. V.; Markusheva, T. V. Bacterial Genes of 2,4-Dichlorophenoxyacetic Acid Degradation Encoding α -Ketoglutarate-Dependent Dioxygenase Activity. *Biol Bull Rev* **2018**, *8* (2), 155–167. <https://doi.org/10.1134/S2079086418020081>.

- (50) Lupatini, M.; Korthals, G. W.; de Hollander, M.; Janssens, T. K. S.; Kuramae, E. E. Soil Microbiome Is More Heterogeneous in Organic Than in Conventional Farming System. *Frontiers in Microbiology* **2017**, *7*, 2064. <https://doi.org/10.3389/fmicb.2016.02064>.
- (51) Gabriel, D.; Roschewitz, I.; Tschardtke, T.; Thies, C. Beta Diversity at Different Spatial Scales: Plant Communities in Organic and Conventional Agriculture. *Ecological Applications* **2006**, *16* (5), 2011–2021. [https://doi.org/10.1890/1051-0761\(2006\)016\[2011:BDADSS\]2.0.CO;2](https://doi.org/10.1890/1051-0761(2006)016[2011:BDADSS]2.0.CO;2).
- (52) Fierer, N.; Schimel, J. P.; Holden, P. A. Variations in Microbial Community Composition through Two Soil Depth Profiles. *Soil Biology and Biochemistry* **2003**, *35* (1), 167–176. [https://doi.org/10.1016/S0038-0717\(02\)00251-1](https://doi.org/10.1016/S0038-0717(02)00251-1).
- (53) Jiao, S.; Chen, W.; Wang, J.; Du, N.; Li, Q.; Wei, G. Soil Microbiomes with Distinct Assemblies through Vertical Soil Profiles Drive the Cycling of Multiple Nutrients in Reforested Ecosystems. *Microbiome* **2018**, *6* (1), 146. <https://doi.org/10.1186/s40168-018-0526-0>.
- (54) Novello, G.; Gamalero, E.; Bona, E.; Boatti, L.; Mignone, F.; Massa, N.; Cesaro, P.; Lingua, G.; Berta, G. The Rhizosphere Bacterial Microbiota of Vitis Vinifera Cv. Pinot Noir in an Integrated Pest Management Vineyard. *Front. Microbiol.* **2017**, *8*. <https://doi.org/10.3389/fmicb.2017.01528>.
- (55) Opsi, F.; Landa, B.; Zecca, O.; Biddoccu, M.; Barmaz, A.; Cavallo, E. Diversity in Soil Bacterial Communities Structure in Four High-Altitude Vineyards Cultivated Using Different Soil Management Techniques. **2014**, 14297.
- (56) Zarraonaindia, I.; Owens, S. M.; Weisenhorn, P.; West, K.; Hampton-Marcell, J.; Lax, S.; Bokulich, N. A.; Mills, D. A.; Martin, G.; Taghavi, S.; van der Lelie, D.; Gilbert, J. A. The

- Soil Microbiome Influences Grapevine-Associated Microbiota. *mBio* **2015**, 6 (2), e02527-14. <https://doi.org/10.1128/mBio.02527-14>.
- (57) Medo, J.; Maková, J.; Medová, J.; Lipková, N.; Cinkocki, R.; Omelka, R.; Javoreková, S. Changes in Soil Microbial Community and Activity Caused by Application of Dimethachlor and Linuron. *Sci Rep* **2021**, 11, 12786. <https://doi.org/10.1038/s41598-021-91755-6>.
- (58) Zhang, M.-M.; Wang, N.; Hu, Y.-B.; Sun, G.-Y. Changes in Soil Physicochemical Properties and Soil Bacterial Community in Mulberry (*Morus Alba* L.)/Alfalfa (*Medicago Sativa* L.) Intercropping System. *MicrobiologyOpen* **2018**, 7 (2), e00555. <https://doi.org/10.1002/mbo3.555>.
- (59) Kohler-Staub, D.; Frank, S.; Leisinger, T. Dichloromethane as the Sole Carbon Source For *Hyphomicrobium* Sp. Strain DM2 under Denitrification Conditions. *Biodegradation* **1995**, 6 (3), 229–235. <https://doi.org/10.1007/BF00700462>.
- (60) Wang, L.; Wen, Y.; Guo, X.; Wang, G.; Li, S.; Jiang, J. Degradation of Methamidophos by *Hyphomicrobium* Species MAP-1 and the Biochemical Degradation Pathway. *Biodegradation* **2010**, 21 (4), 513–523. <https://doi.org/10.1007/s10532-009-9320-9>.
- (61) Zhang, C.; Tayyab, M.; Abubakar, A. Y.; Yang, Z.; Pang, Z.; Islam, W.; Lin, Z.; Li, S.; Luo, J.; Fan, X.; Fallah, N.; Zhang, H. Bacteria with Different Assemblages in the Soil Profile Drive the Diverse Nutrient Cycles in the Sugarcane Straw Retention Ecosystem. *Diversity* **2019**, 11 (10), 194. <https://doi.org/10.3390/d11100194>.
- (62) Bronick, C. J.; Lal, R. Soil Structure and Management: A Review. *Geoderma* **2005**, 124 (1), 3–22. <https://doi.org/10.1016/j.geoderma.2004.03.005>.
- (63) Importance of soil physical properties <http://safesportsfields.cals.cornell.edu/book/export/html/165> (accessed 2021 -08 -26).

- (64) Wang, H.; Marshall, C. W.; Cheng, M.; Xu, H.; Li, H.; Yang, X.; Zheng, T. Changes in Land Use Driven by Urbanization Impact Nitrogen Cycling and the Microbial Community Composition in Soils. *Sci Rep* **2017**, *7* (1), 44049. <https://doi.org/10.1038/srep44049>.
- (65) Wang, Y.; Xu, Y.; Huang, Q.; Liang, X.; Sun, Y.; Qin, X.; Zhao, L. Effect of Sterilization on Cadmium Immobilization and Bacterial Community in Alkaline Soil Remediated by Mercapto-Palygorskite. *Environmental Pollution* **2021**, *273*, 116446. <https://doi.org/10.1016/j.envpol.2021.116446>.
- (66) Mackie, K. A.; Marhan, S.; Ditterich, F.; Schmidt, H. P.; Kandeler, E. The Effects of Biochar and Compost Amendments on Copper Immobilization and Soil Microorganisms in a Temperate Vineyard. *Agriculture, Ecosystems & Environment* **2015**, *201*, 58–69. <https://doi.org/10.1016/j.agee.2014.12.001>.
- (67) Geetha, M.; Fulekar, M. H. Bioremediation of Pesticides in Surface Soil Treatment Unit Using Microbial Consortia. *African Journal of Environmental Science and Technology* **2008**, *2* (2), 036–045. <https://doi.org/10.4314/ajest.v2i2>.
- (68) Doolotkeldieva, T.; Konurbaeva, M.; Bobusheva, S. Microbial Communities in Pesticide-Contaminated Soils in Kyrgyzstan and Bioremediation Possibilities. *Environ Sci Pollut Res* **2018**, *25* (32), 31848–31862. <https://doi.org/10.1007/s11356-017-0048-5>.
- (69) Boivin, A.; Amellal, S.; Schiavon, M.; van Genuchten, M. Th. 2,4-Dichlorophenoxyacetic Acid (2,4-D) Sorption and Degradation Dynamics in Three Agricultural Soils. *Environmental Pollution* **2005**, *138* (1), 92–99. <https://doi.org/10.1016/j.envpol.2005.02.016>.

- (70) Crespín, M. A.; Gallego, M.; Valcárcel, M.; González, J. L. Study of the Degradation of the Herbicides 2,4-D and MCPA at Different Depths in Contaminated Agricultural Soil. *Environ. Sci. Technol.* **2001**, 35 (21), 4265–4270. <https://doi.org/10.1021/es0107226>.

Supplementary Materials

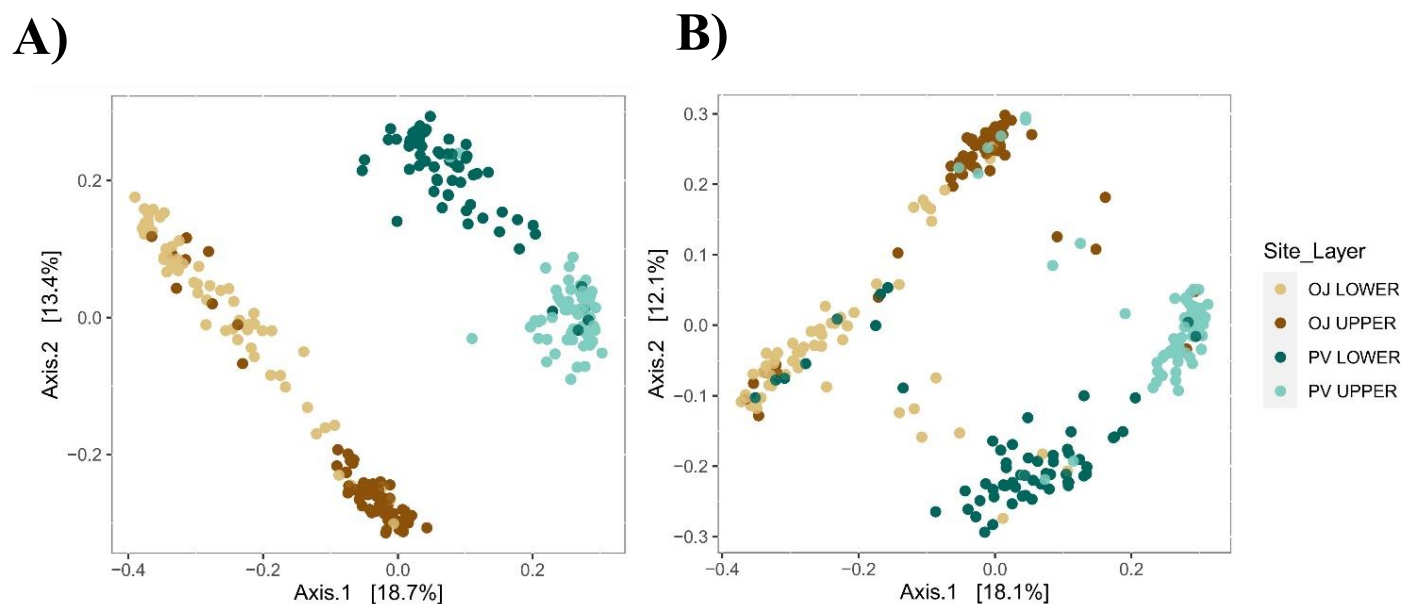


Figure S1. Principal coordinates analysis (PCoA) of bacterial communities (16S V4 region) of upper and lower soil layers from OJ and PV field sites collected in **A)** 2018 and **B)** 2019. The ordination is based on the Bray-Curtis distance metric, with samples clustered by field site and soil layer.

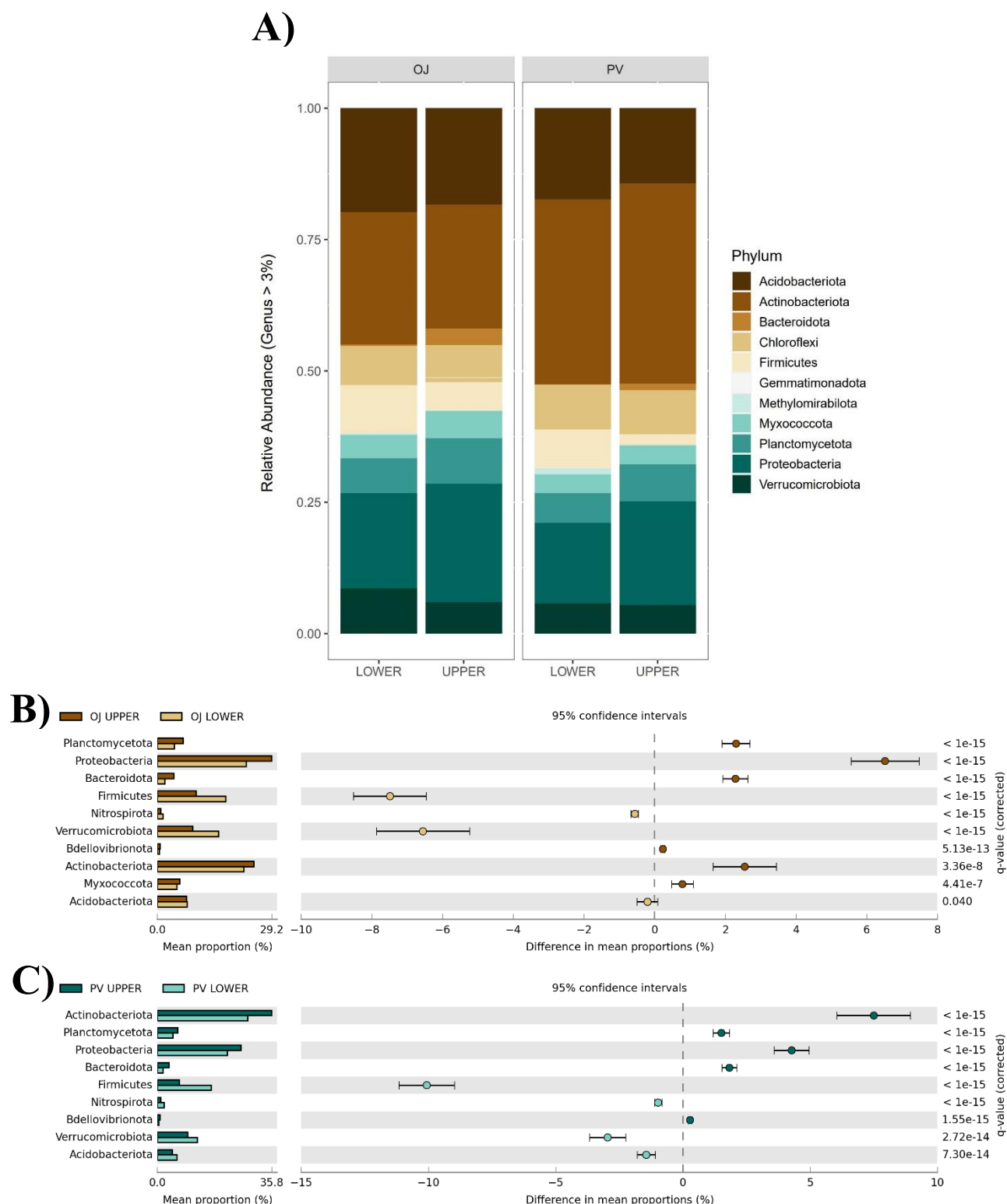


Figure S2. A) Overall average relative abundance of soil bacterial communities of upper and lower soil layers in 2018 and 2019 field trials. Differential relative abundance of **B)** upper and **C)** lower soil layer samples collected in OJ and PV field. Welch's t-test using Storey FDR for multiple test correction.

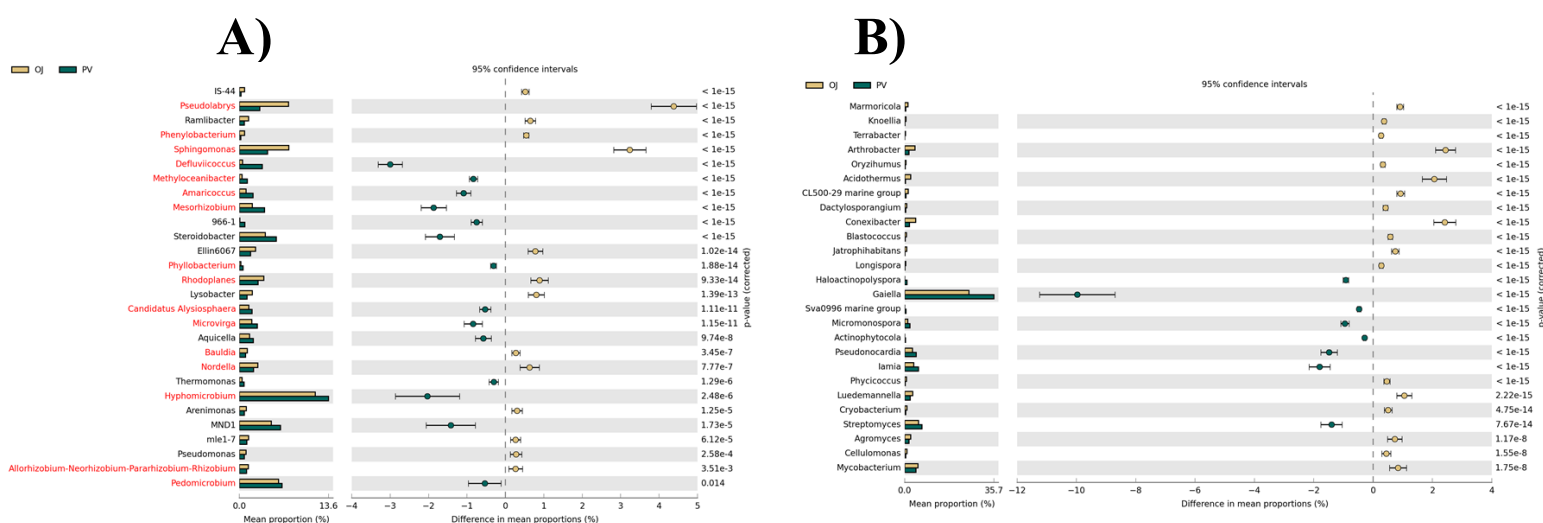


Figure S3. Differential relative abundance of soil bacterial genera belonging to the phyla **A)** Proteobacteria and **B)** Acidobacteria in OJ and PV field sites. Welch's t-test using Storey FDR for multiple test correction. *Genera highlighted in red and black represent Alphaproteobacteria and Gammaproteobacteria, respectively in Figure A.

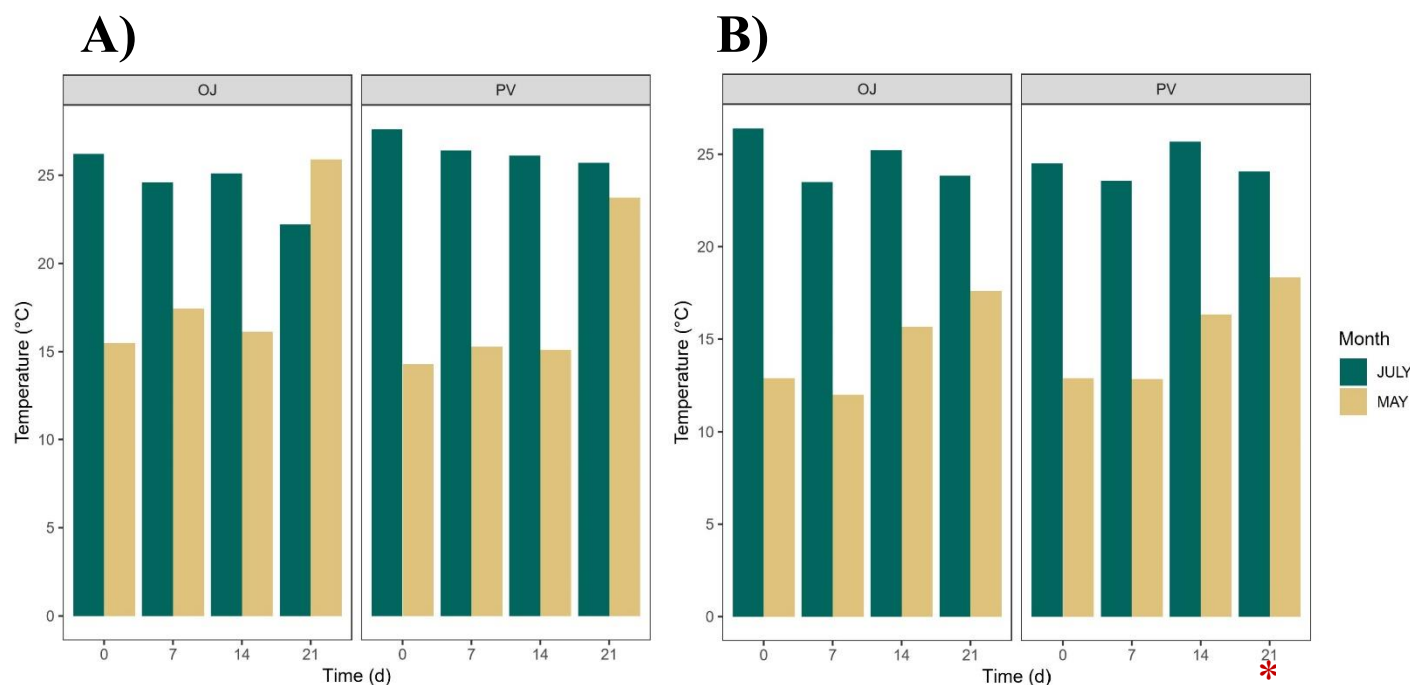


Figure S4. Soil temperature measured on days 0, 7, 14, and 21 post-application at **A)** 2018 and **B)** 2019 field trials. * Soil temperature was measured on Day 37 post-application

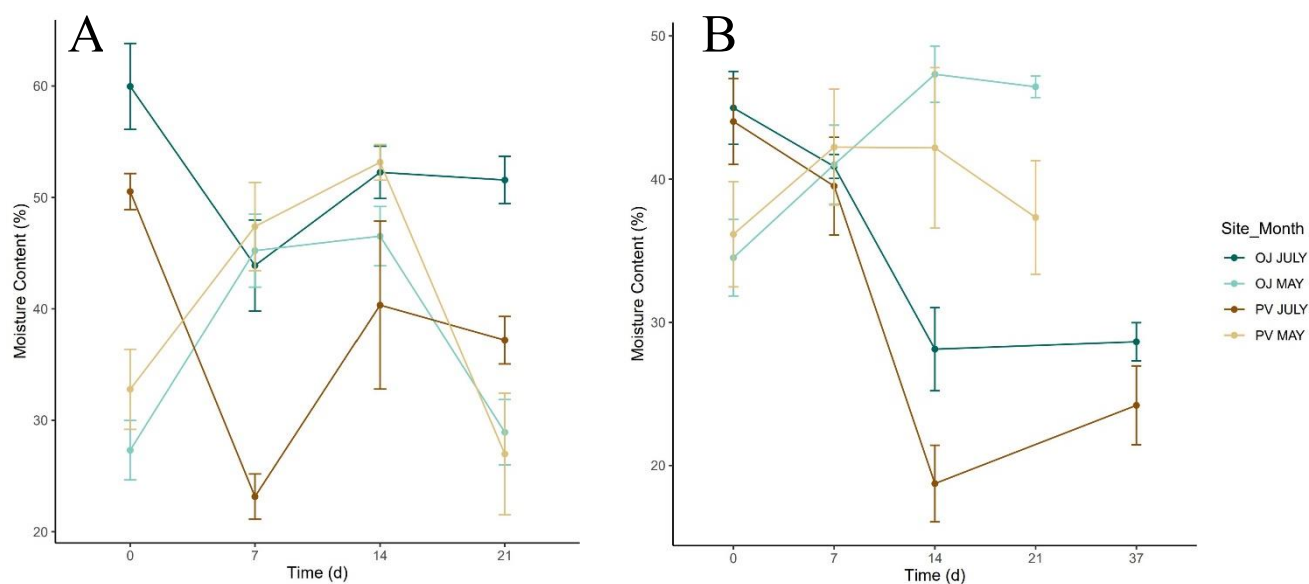


Figure S5. Soil moisture content measured on days 0, 7, 14, and 21 post-application at **A)** 2018 and **B)** 2019 field trials.

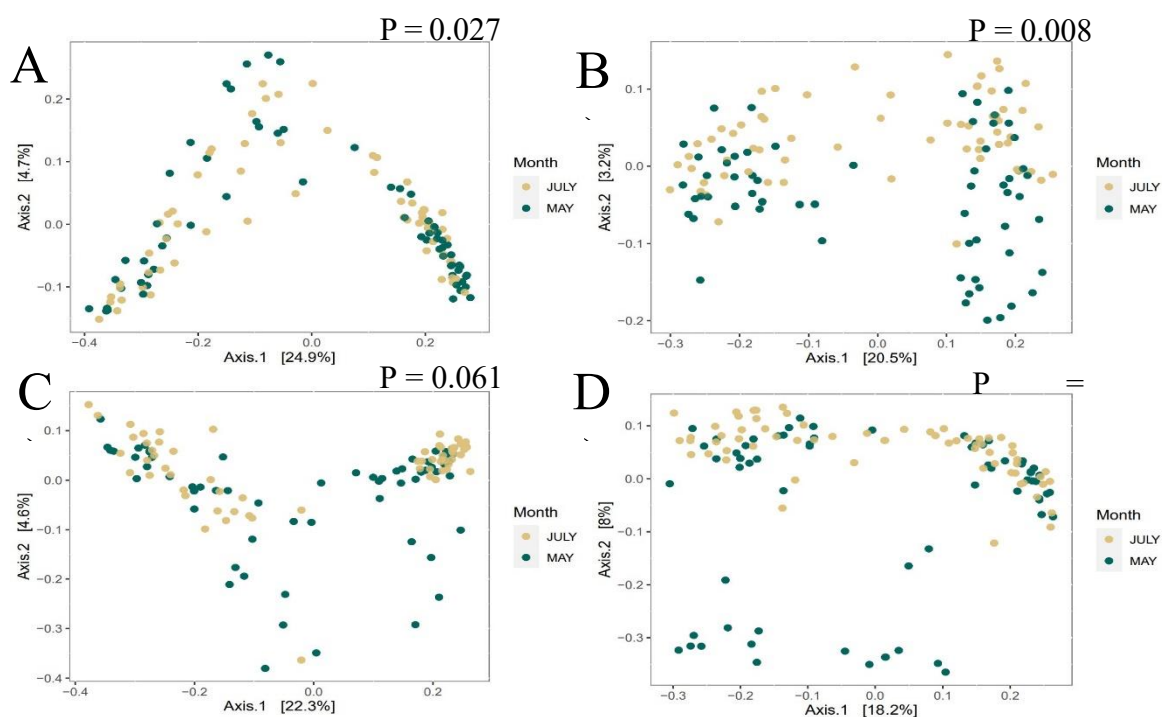


Figure S6. Principal coordinate analysis (PCoA) ordinations of bacterial communities (16S V4 region) derived from **A)** OJ and **B)** PV 2018 and **C)** OJ and **D)** PV 2019 field trials. The PCoA is based on the Bray-Curtis distance metric, with samples clustered by months

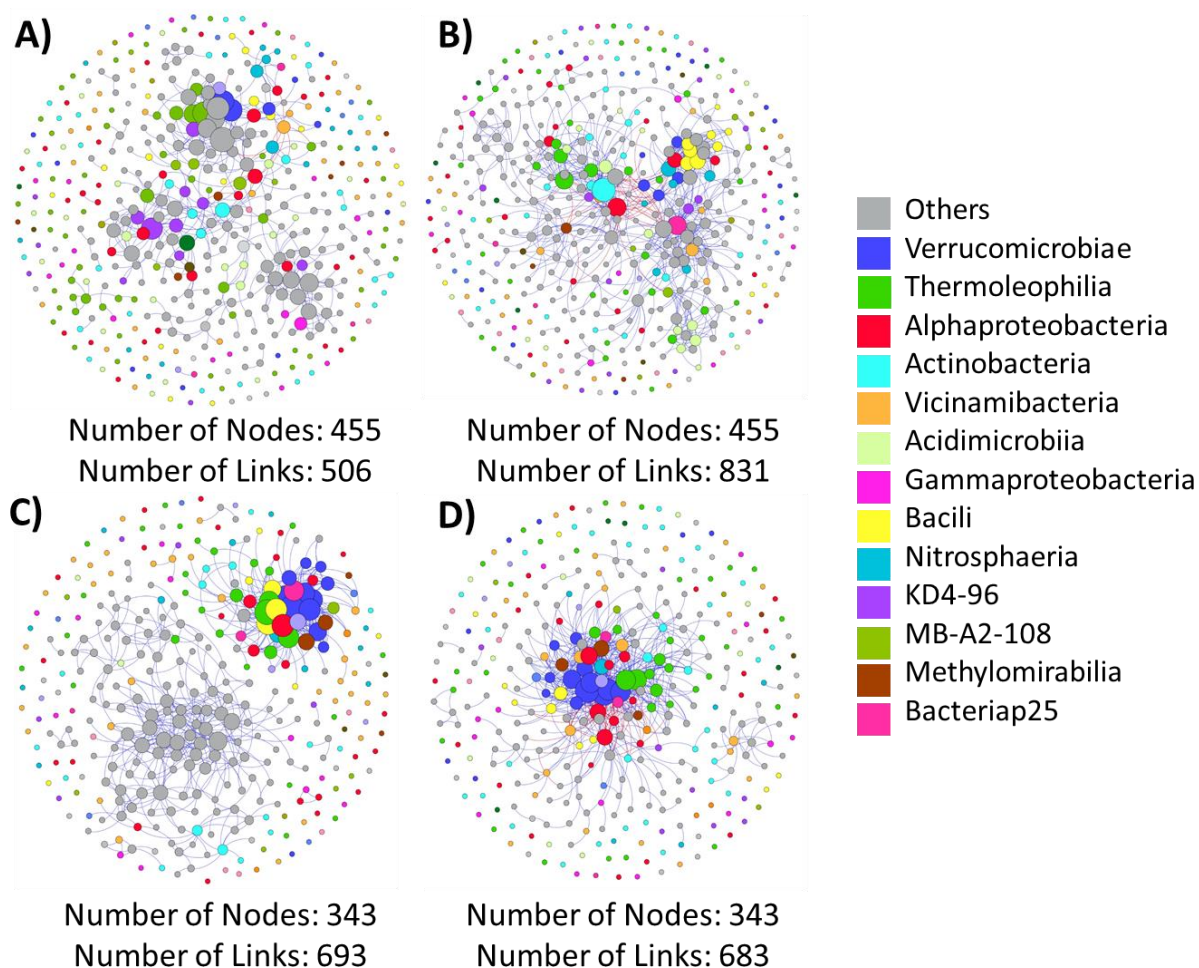


Figure S7. Soil bacterial microbiome co-occurrence networks at phylum level of **A)** PV May, **B)** PV July, **C)** OJ May, and **D)** OJ July samples collected in both 2018 and 2019. Node size was scaled based on in-degree values, blue and red paths represent positive and negative correlation, respectively.

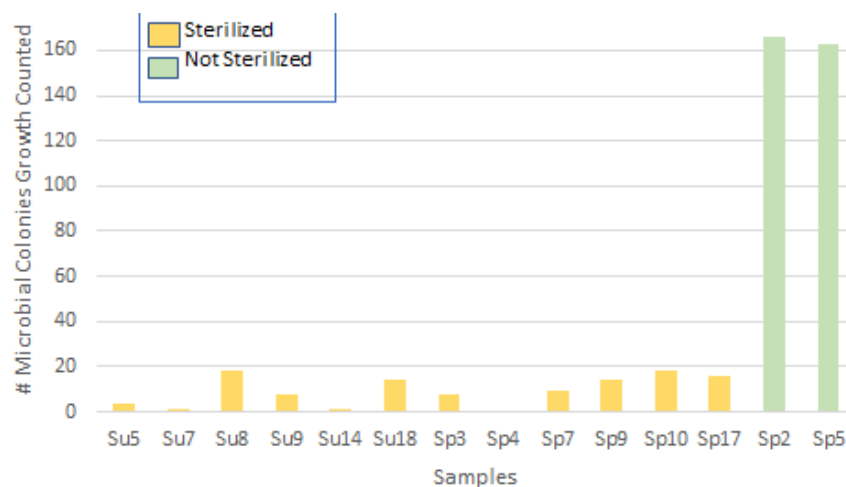


Figure S8. Number of colony-forming units (CFUs) in sterilized and unsterilized growth chamber soil samples

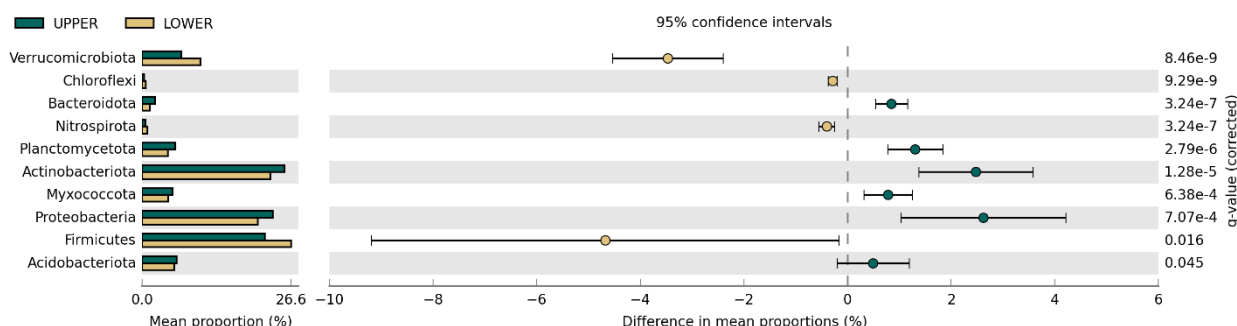


Figure S9. Differential relative abundance analysis of bacterial community phyla identified in the growth chamber study from upper and lower soil layers.

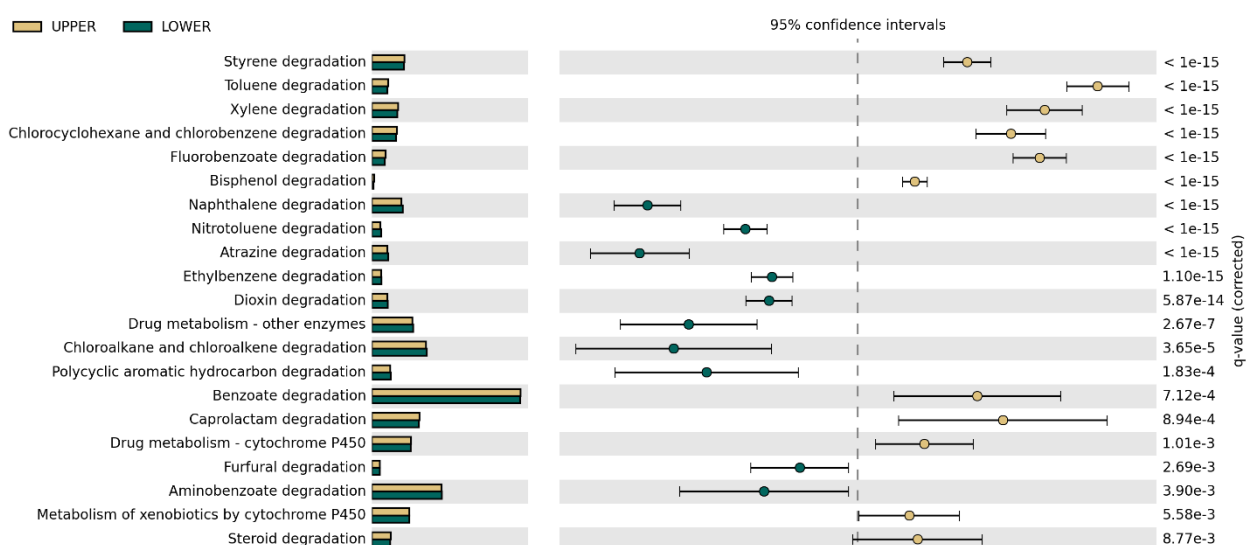


Figure S10. Extended bar plot of significant differences in predicted xenobiotic degradation pathways of Upper and Lower soil field samples using Tax4Fun2 and Welch's t-test with Storey FDR correction.

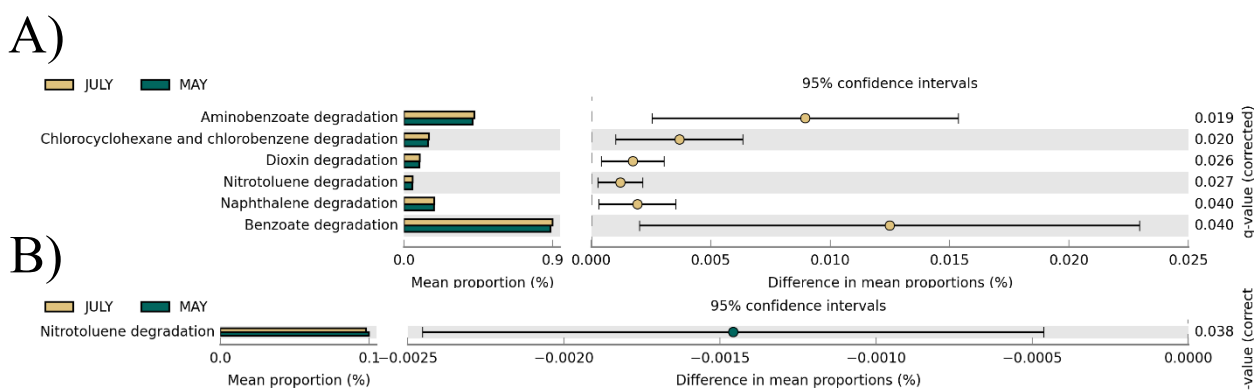


Figure S11. Extended bar plot of significant differences in predicted xenobiotic degradation pathways of A) 2018 and B) 2019 May and July samples using Tax4Fun2 and Welch's t-test with storey FDR correction.

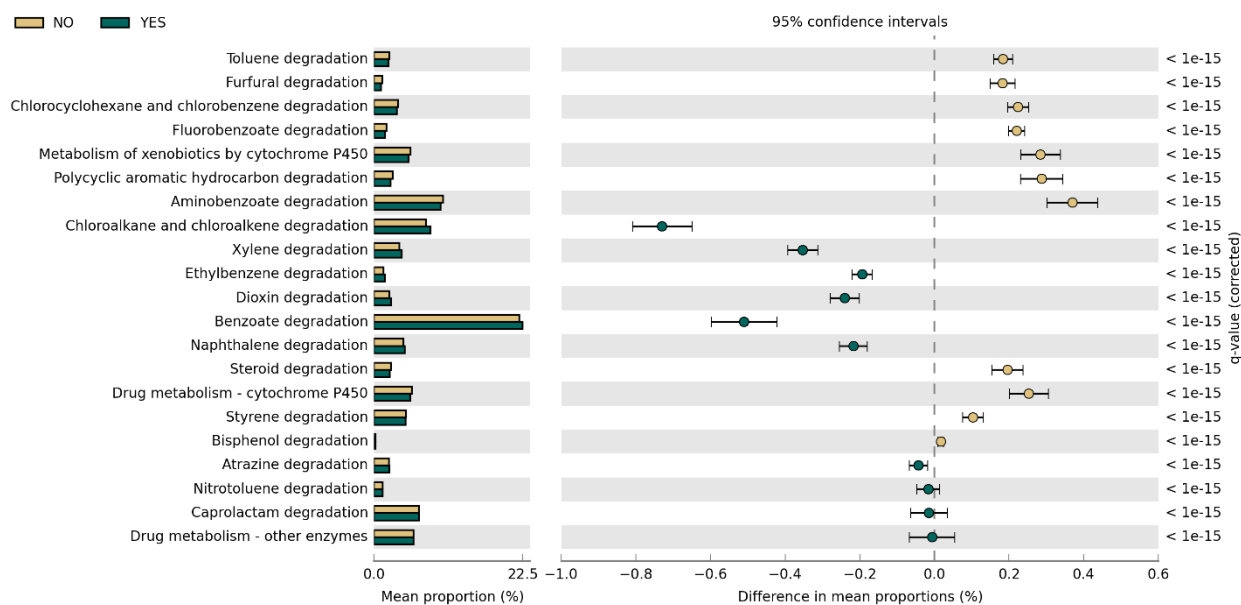


Figure S12. Extended bar plot of significant differences in predicted xenobiotic degradation pathways of sterilized (Yes) and unsterilized (No) samples using Tax4Fun2 and Welch's t-test with Storey FDR correction.

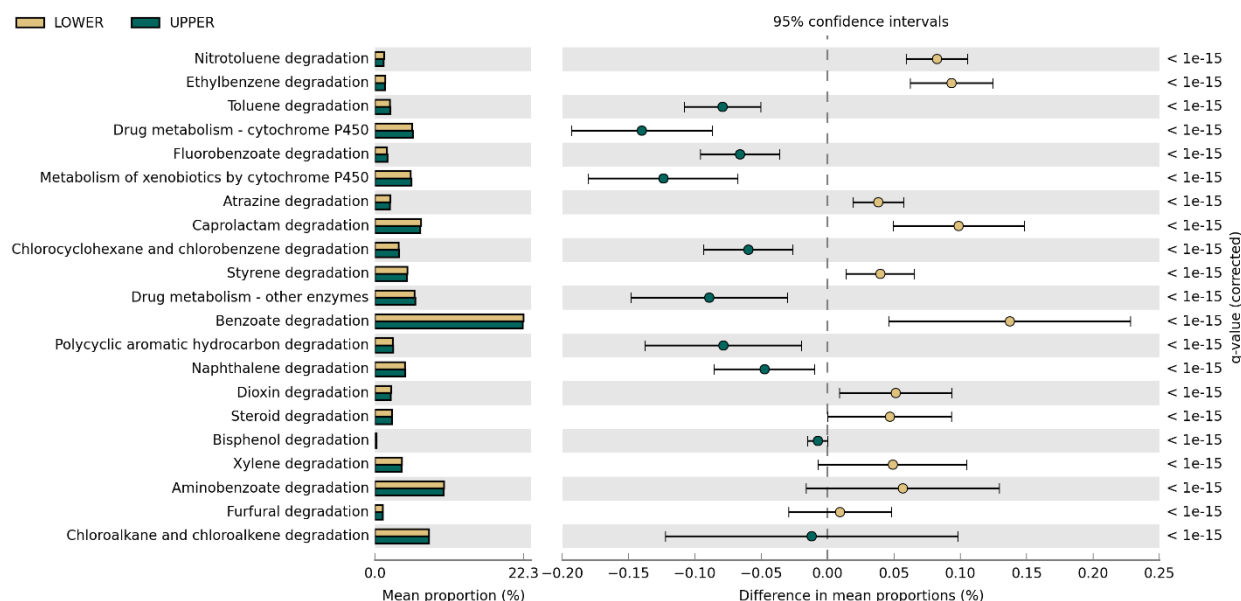


Figure S13. Extended bar plot of significant differences in predicted xenobiotic degradation pathways of growth chamber upper and lower soil layer samples using Tax4Fun2 and Welch's t-test with Storey FDR correction.

Chapter 4. Quantification of the 2,4-D Degrading Gene, *TfdA*, in Urban Soil Bacterial Communities Using qPCR

Abstract

Soil bacteria containing 2,4-dichlorophenoxyacetic acid (2,4-D)-degrading genes have been used as reporters to detect its breakdown activity. Of interest is the *tfdA* gene, which is a good biomarker in detecting 2,4-D degradation. Due to the ability of bacteria to use 2,4-D as an energy source and break it down to subsequent transformation products (TPs), we sought to assess if 2,4-D-degrading activity changed at varying seasonal conditions throughout the season in response to different environmental conditions in urban landscapes. A TaqMan-based qPCR approach was used to detect and quantify the different *tfdA* gene classes (I, II, III) from soil samples obtained in a field trial conducted in two different field sites (PV and OJ) in Madison, WI in 2018 and 2019. A growth chamber study, where temperature and photoperiod were controlled, was also performed. A major finding in this study was that previously published PCR primers targeting the different gene classes resulted in non-specific amplification, leading to false-positive detection in soil samples. Although supporting information of non-specific amplification was found, initial experiments seeking to quantify 2,4-D-degrading activity in the different seasons were also discussed. These results showed that the *tfdA* relative quantity was different among the different seasonal variations, especially for class I and III genes. Initial random forest prediction results also suggested that *Alphaproteobacteria*, *Gammaproteobacteria*, and *Verrucomicrobiae* were important predictors of the class I *tfdA* gene. As for the class III *tfdA* gene, *Actinobacteria*, *Verrucomicrobiae*, and *Gammaproteobacteria* were important predictors. The bacterial taxa identified in the class II *tfdA* prediction model were not important predictors. Altogether, the results suggest that 2,4-D breakdown activity in soil changes at different seasonal conditions, potentially resulting in TP formation in urban landscapes. However, future research to improve

targeting *tfdA* in environmental samples, including those from urban landscapes, is encouraged to obtain a robust representation of 2,4-D-degrading activity and its role in forming TPs.

Introduction

The herbicide 2,4-dichlorophenoxyacetic acid (2,4-D) is a synthetic auxin herbicide used to control broadleaf weeds in residential lawns and turfgrass (i.e., Urban landscapes).¹ Although 2,4-D fate and breakdown have been well documented by the EPA in turf and residential lawns, its potential adverse impact does not end at the point of application.² Transformation products (TPs) might still be detected in soil that interact with the environment differently than 2,4-D.²⁻⁴ The main TP of 2,4-D is 2,4-dichlorophenol (2,4-DCP).⁵ Other 2,4-D TPs include 3,5-dichlorocatechol (3,5-DCC), 4-chlorophenol (4-CP), among others, with varying levels of toxicity.⁶⁻⁸ Of major concern is the application of 2,4-D in urban landscapes at varying seasonal conditions and how this may influence 2,4-D breakdown to its TPs. It is essential to understand the environmental conditions that lead to TP production in soil, especially since bacteria are the primary force of 2,4-D degradation in the soil.

Table 4. 1 *TfdA* gene classes of 2,4-D-degrading bacteria belonging to Group 1 (see Chapter 1, Table 3).

<i>TfdA</i> Class	Description
I	- Located on self-transmissible plasmids
II	- Detected in <i>Betaproteobacteria</i> . - Can be coded in chromosomes. - Amplified only from <i>Burkholderia</i> strains.
III	- 76% identity to class I. - Detected in <i>Betaproteobacteria</i> - Detected in <i>Beta-</i> and <i>Gammaproteobacteria</i> . - 77% identity to class I. - 80% identity to class II.

Specifically, 2,4-D biodegradation has been extensively studied, where bacterial strains have been isolated and shown to degrade and use 2,4-D as its sole carbon source from varying

environments.^{9–15} For example, *Cupriavidus. necator*, *Achromabacter sp.*, and *Flavobacterium peregrinum* bacteria have been shown to oxidize 2,4-D and convert to its main TP, 2,4-dichlorophenol, in a laboratory setting where organisms were grown in mineral salts agar plates with 2,4-D as its carbon source.⁹ Other bacterial strains capable of using 2,4-D as their sole carbon source at high pH values, such as *Delftia acidovorans* P4a, were isolated from concrete samples of a demolished herbicide production plant and enriched with fresh minimal medium containing 2,4-D.^{10,11} Further, it has been demonstrated that *Pseudomonas* (JMP116)¹³ and *Alcaligenes paradoxus* strains¹⁴ contain plasmids that encode for the degradation of 2,4-D. Other isolated strains include members of the *Bradyrhizobium-Agromonas-Nitrobacter* cluster¹² and *Sphingomonas*¹⁵.

Genes have been identified in soil bacteria that serve as reporter genes for detecting or identifying 2,4-D biodegradation.⁹ Specifically, 2,4-D biodegradation has been extensively studied in *Cupriavidus necator* JMP134 (formerly known as *Ralstonia eutropha* and *Alcaligenes eutrophus*).¹⁶ *C. necator* harbors the pJP4 plasmid, which contains a gene cluster known as *tfd* (two, four- dichlorophenoxyacetic acid) ABCDEF. The proposed catabolic pathway can be described in the following steps: (1) 2,4-D is converted to 2,4-DCP by α -ketoglutarate-dependent 2,4-D dioxygenase encoded by *tfdA*; (2) *tfdB* gene encodes for a phenol hydroxylase that metabolizes 2,4-DCP to 3,5-DCC; (3) 3,5-DCC aromatic ring is further cleaved by a pathway encoded by *tfdCDEF* (Figure 4.1).¹⁷ Of special interest within this gene cluster is the *tfdA* gene, which has

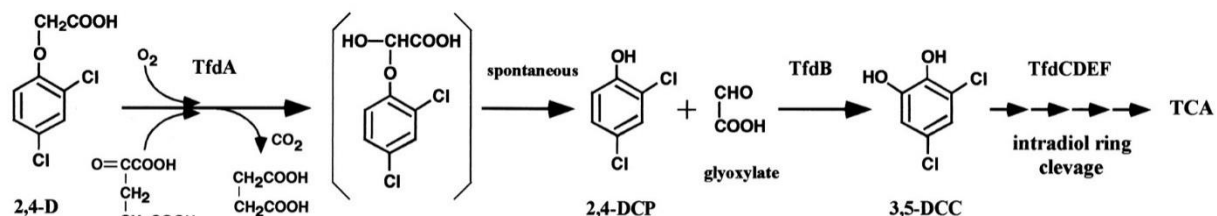


Figure 4. 1 2,4-D degradation pathway encoded by *tfd* genes in *R. eutropha* JMP134. TCA, tricarboxylic acid cycle. Figure obtained from Kitagawa et al. (2002)⁵⁰

been considered a good reporter for 2,4-D degradation activity.¹⁶ Due to its high diversity, bacterial strains containing the *tfdA* gene have been classified into three classes at the genetic level, as shown in **Table 4.1**.^{16–18}

Due to their ability to break down 2,4-D to its TPs, methods to detect and isolate the bacterial strains involved in 2,4-D degradation are of great importance, especially for directly quantifying 2,4-D degrading gene activity in the environment. In order to provide a tool for *tfdA* gene detection and to determine 2,4-D-degrading activity in the soil, primers specific to *tfdA* were initially developed using twenty-five 2,4-D-degrading strains.¹⁹ Because 2,4-D degraders may also have the ability to degrade other phenoxy acids (PA) such as 4-chloro-2-methylphenoxyacetic acid (MCPA) and 2-(4-chloro-2-methylphenoxy)propanoic acid (MCP) using the *tfdABCDEF* gene cluster, Bælum et al. (2006) furthered the development of degenerate primers. These primers specifically targeted the three *tfdA* gene classes.²⁰ As a means to improve the quantitative measure of the *tfdA* gene classes in complex soil samples, Bælum et al. (2009) proceeded in developing a quantitative real-time PCR-based method using a TaqMan-based approach.²¹ To test their qPCR approach, soil microcosms were set up in each study and were spiked with either 2,4-D, MCPA, or MCP to allow specific degraders containing the *tfdA* genes to proliferate.^{20,21} According to their study, the TaqMan-based qPCR method using an 81-bp primer set was developed to target and quantify the three *tfdA* gene classes in environmental samples.²¹ While the TaqMan-based qPCR approach has shown promise in detecting and quantifying *tfdA* in microcosm and enriched media systems, little is known of its ability to successfully quantify the 2,4-D-degrading gene in real-life samples and field studies.

In the present study, our main objective was to determine if 2,4-D degrading activity changes in response to different environmental conditions throughout the season. To achieve our

objective, we (i) assessed 2,4-D-degrading activity in urban soils using the previously developed 81-bp primers and TaqMan-based method to quantify the *tfdA* gene classes in field studies conducted in 2018 and 2019 and a growth chamber study; (ii) identified important bacterial predictors involved with the three *tfdA* gene classes; and (iii) evaluated the specificity of the 81-bp qPCR primer sets in environmental samples.

Materials and Methods

Field Study. Soil cores were sampled at two different depths, upper soil (top 5 cm) and lower soil (15 to 20 cm depth) from the OJ Noer Turfgrass Research Station (OJ) in Madison, WI, and Pleasant View Golf Course (PV) in Middleton, WI. Soil analysis from each site was performed before conducting our first application for each field trial (**See Chapter 2-Table 2.1**). Treatment formulations of 2,4-D and water as a non-treated (NT) control were applied on May 1st and July 1st in 2018 and April 30th and July 3rd in 2019, representing conditions for spring and summer seasons, respectively. 2,4-D formulation was applied to field plots using a nozzle pressure of 40 psi using a CO₂ pressurized boom sprayer with two XR Teejet AI8004 nozzles. The herbicide was agitated by hand and applied at a rate equivalent to 0.35 mL per m² of the commercial 2,4-D product with an initial concentration of 2.62 mg mL⁻¹. A randomized complete block design was created with plots containing an area of 1.39 m² and four replications per treatment. Cores were 2.5 cm in diameter and collected once immediately before product application and then 7, 14, and 21 days after treatment application and kept at -80 °C until further processing.

Growth Chamber Study. 100 mm diameter soil core samples with a depth of 200 mm were collected in the OJ Noer Turfgrass Research Station in Madison, Wisconsin, on July 30th, 2020. Samples were moved to two individual growth chambers, each simulating one of the average seasonal temperatures and photoperiods listed in **Table 4.2** and allowed to acclimate and adapt to

the environmental conditions from each growth chamber for 14 days.²² A PVC column with a diameter of 101.6 mm and a depth of 203.3 mm was used to hold the collected core samples. The study consisted of a completely randomized sample design with three replications per treatment per temperature. Subsamples from each core were collected in the following regions: upper soil (top 5 cm) and lower soil (15-20 cm depth) using a stainless-steel soil core sampler. Collection days were at 1, 5, 7, and 10 days and samples were stored at -80°C until further processing.

Table 4. 2 Temperature and photoperiods simulating spring and summer conditions.

SEASON	GROWTH CHAMBER
SPRING	14h day:10h night 18°C: 6.5°C
SUMMER	15h day: 9h night 28°C:15.5°C

Sample Preparation. Collected samples from the field study were processed by washing with 20 mL of DI water using a sieve on a 50-mL test tube and vortexed for 5 s to remove excess soil and large particles. Samples were then sonicated for 7 min. Using a sonicating water bath and vortexed for 10 s to remove tightly adhered soil and microbial organisms. The soil mixture was poured through a strainer into another 50-mL tube, washed with 30 mL of DI water and centrifuged for 20 min. After the supernatant was removed, 0.25 g of soil sample was used for DNA extraction. Samples from the growth chamber study were processed by sieving the soil to remove any leaf residue or rock particles. After sieving, the sample was mixed to ensure a representative collection of soil. 0.25 g of soil sample was then used for DNA extraction.

Sterilization of Growth Chamber Soil Core Samples. After acclimation, 6 core samples from each chamber were sterilized twice for 45 min on slow exhaust settings on two consecutive days. Sterilized soil cores were allowed to cool, and 0.1 g of soil was collected from the center of

each core to test for the presence of viable bacteria. The soil was diluted in 1 mL of sterilized H₂O, and serial dilutions were then performed and plated in nutrient agar. Plates were incubated at 25°C for two days, and colony-forming units (CFU) were counted after incubation.

DNA Extraction. DNA was extracted from 0.25 g of upper and lower soil samples from field and growth chamber studies using a DNeasy PowerLyzer PowerSoil kit (Qiagen Inc., Germantown, MD) following the manufacturer's protocol. An alternative step using phenol:chloroform:isoamyl alcohol, pH 7-8, was implemented in the protocol to increase DNA yield. Nucleic acid concentration was quantified for all extracted DNA samples using a NanoDrop ND-1000 spectrophotometer (Thermo Fisher Scientific, Waltham, MA).

Bacterial Strains and *TfdA* Reference Genes. *TfdA* class I gene, originally from *R. eutropha*, was provided courtesy of Dr. Jan Roelof van der Meer from the University of Lausanne, Switzerland. The class I gene had been directly ligated into pGEM7-Ampicillin (AMP) vector and transformed into *E. coli* DH5 α competent cells. *TfdA* Class II and Class III genes originated from *Burkholderia* sp. RASC and *Burkholderia cepacia* 2a pIJB1, respectively, were synthesized by Integrated DNA Technologies in a pUCIDT- AMP cloning vector and transformed into *E. coli* AMP-resistant competent cells. Cultures of each class were grown overnight at 37°C on Luria Bertani (LB) medium containing 0.5g L⁻¹ AMP. According to the manufacturer's protocol, DNA plasmid isolations were performed using E.Z.N.A. Plasmid DNA Kit (Omega Bio Tek, Radnor, PA). Plasmid DNA, including *tfdA* class I, II, and III gene fragments, were quantified using a NanoDrop ND-1000 spectrophotometer (ThermoFisher Scientific, Waltham, MA). Plasmids were serially diluted and used as standards for TaqMan® probe-based quantitative real-time PCR as described by (Bælum & Jacobsen, 2009).

Traditional PCR was conducted using the GoTaq® Green Master Mix. Briefly, the 25- μ L reaction mixture contained 100–200 ng of DNA extract, and 1 μ M of the *tfdA*–215 bp primer sets previously designed by Baelum et al. (2009) (**Table 4.3**).²¹ The PCR reaction was performed on an Eppendorf Mastercycler Prothermocycler (Enfield, CT). *TfdA* amplification consisted of the following cycling conditions: 95°C for 3 min as the initial denaturation step, followed by 30 cycles of 95°C for 1 min, 62°C for 1 min, and 72°C for 11 s and a final step at 72°C for 4 min. PCR products were separated using gel electrophoresis on a 1.5% agarose gel in 1X Tris-Acetate-EDTA (TAE) buffer.

Table 4. 3 Primers and probes for qPCR

Oligo name	Target gene	Sequence (5'– 3')	Fragment size (bp)	Annealing Temp. (°C)
<i>tfdA</i> – 215 bp	Class I to III	F: GAG CAC TAC GCR CTG AAY TCC CG R: GTC GCG TGC TCG AGA AG	215	62
<i>tfdA</i> – 81 bp	Class I to III	F: GAG CAC TAC GCR CTG AAY TCC CG R: SAC CGG MGG CAT SGC ATT	81	62
FAM–C I	Class I	56-FAM-TTG CGC TTC-ZEN-CGA ATA GTCGGT GTC-3IABkFQ		62
Cy5–C II	Class II	5Cy5-CGT TGA CTT-TAO-TCA GAA TAC TCT GTG TCG CCA- 3IABRQSp		62
YAK–C III	Class III	5YakYel-TTG ACT TTC-ZEN-AGA ATA GTC CGT ATC GCC AAG- 3IABkFQ		62

Gels were stained with SYBR green dye and visualized under UV light. PCR amplicons were purified and sent for sequencing in the Biotechnology Department at UW-Madison.

Quantitative Real-Time PCR. According to previous work by Baelum et al. (2009),

highly conserved regions that embraced a more diverse region of the *tfdA* genes were chosen.²¹ The iQTM Supermix kit (Bio-Rad Laboratories, Hercules, CA) was used as mastermix, including 0.4 μ M of the *tfdA*–81 bp primer sets and 0.1 μ M of each probe (**Table 4.3**). One-microliter aliquots of DNA template (15–30 ng) were added for a final reaction volume of 25 μ l. The reaction conditions were as follows: 3 min at 95°C for enzyme activation, followed by 35 cycles of 15 s at 95°C and 1 min at 62°C in a Bio-Rad CFX96 Touch Real-Time PCR Detection System. Measurement of fluorescence intensity was performed at the end of the 1 min 62°C step. Quantification was performed in triplicate for each sample. Quantification cycle (C_q) values for the TaqMan assay were defined as the cycle where the measured fluorescence exceeded the calculated baseline threshold line.

Assessing *tfdA* primer specificity. Soil qPCR products from the growth chamber study were randomly selected to evaluate if *tfdA* gene classes were successfully detected and amplified with the primers designed by Baelum et al. (2009).²¹ A cloning reaction was performed using a TOPO[®]-TA cloning kit (Invitrogen, Karlsruhe, Germany). To set up the TOPO[®] reaction, 4 μ l of fresh qPCR product, 1 μ l salt solution and 1 μ l of the pCR^{TM4}-TOPO[®] vector were combined for a final volume of 6 μ l. Two qPCR products were chosen from the growth chamber study, sample #S-0177 and #S-0189, with a relatively low (0.40 to 0.92) and high (1.50 to 4.0) copy number of *tfdA* gene detected, respectively (data not shown). Further, chemical transformation of the pCR^{TM4}-TOPO[®] constructs were performed in One Shot[®] TOP10 and DH5 α competent *E. coli* cells. The cloned plasmids were then subjected to amplification with M13 primers according to the manufacturer's protocol. Product sizes were evaluated using gel electrophoresis (1.5% agarose) with SYBR Safe DNA Gel Stain (Fisher Scientific, Chicago, IL) and purified using a Qiagen PCR Purification Kit (Qiagen, Hilden, Germany). Final products were quantified using a

NanoDrop1000 (Thermo Fisher Scientific, Waltham, MA) and sequenced on 3730XL Genetic Analyzer (ThermoFisher) for Sanger sequencing in the Biotechnology Center at the University of Wisconsin-Madison. Sequences were then assessed for the presence of the *tfdA* gene or *tfdA* gene sequence similarities using the BLASTN program (<http://blast.ncbi.nlm.nih.gov/>).

Data Analysis. For relative quantification, relative copy numbers per ng of DNA for each *tfdA* gene class were calculated using the Bio-Rad CFX Maestro 1.1 software (version 4.1) and mean values were exported to R 3.6.0. For each gene class, the effect of site, sampling day, month, treatment, and layers was assessed using linear regression analysis and analysis of variance (ANOVA) in the field study. Similarly, the effect of sterilization, layers, treatment, sampling day, and season was evaluated to detect each gene class in the growth chamber study. Additionally, pairwise comparisons using Tukey's honest significant difference (HSD) post hoc test was performed using the 'TukeyHSD' function in R to compare the difference between the relative quantity of each class in each time point throughout the different seasons and soil depths. The level of statistical significance was set at $p < 0.05$.

A random forest regression algorithm was implemented to predict key soil bacteria containing *tfdA* gene class I, II, and III in urban soils using the 'randomForest' R package.²³ The model was implemented on 508 and 278 samples for the field and growth chamber study, respectively, using the following parameters: ntree = 500 and default entry of $p/3$, where p is the number of ASVs. Lists of the top taxa involved in *tfdA* gene detection were ranked in increasing order of importance and were implemented in the final model based on percentage increase in mean-squared error (MSE).

Results

Field Study

Relative quantification of the *TfdA* gene classes in urban soil landscapes. Amplification and quantification of each *tfdA* gene class were analyzed at four different time points, ranging from 0 to 21 days after application. The Cq obtained from amplified non-treated samples was used as the control value to account for changes in treated samples.

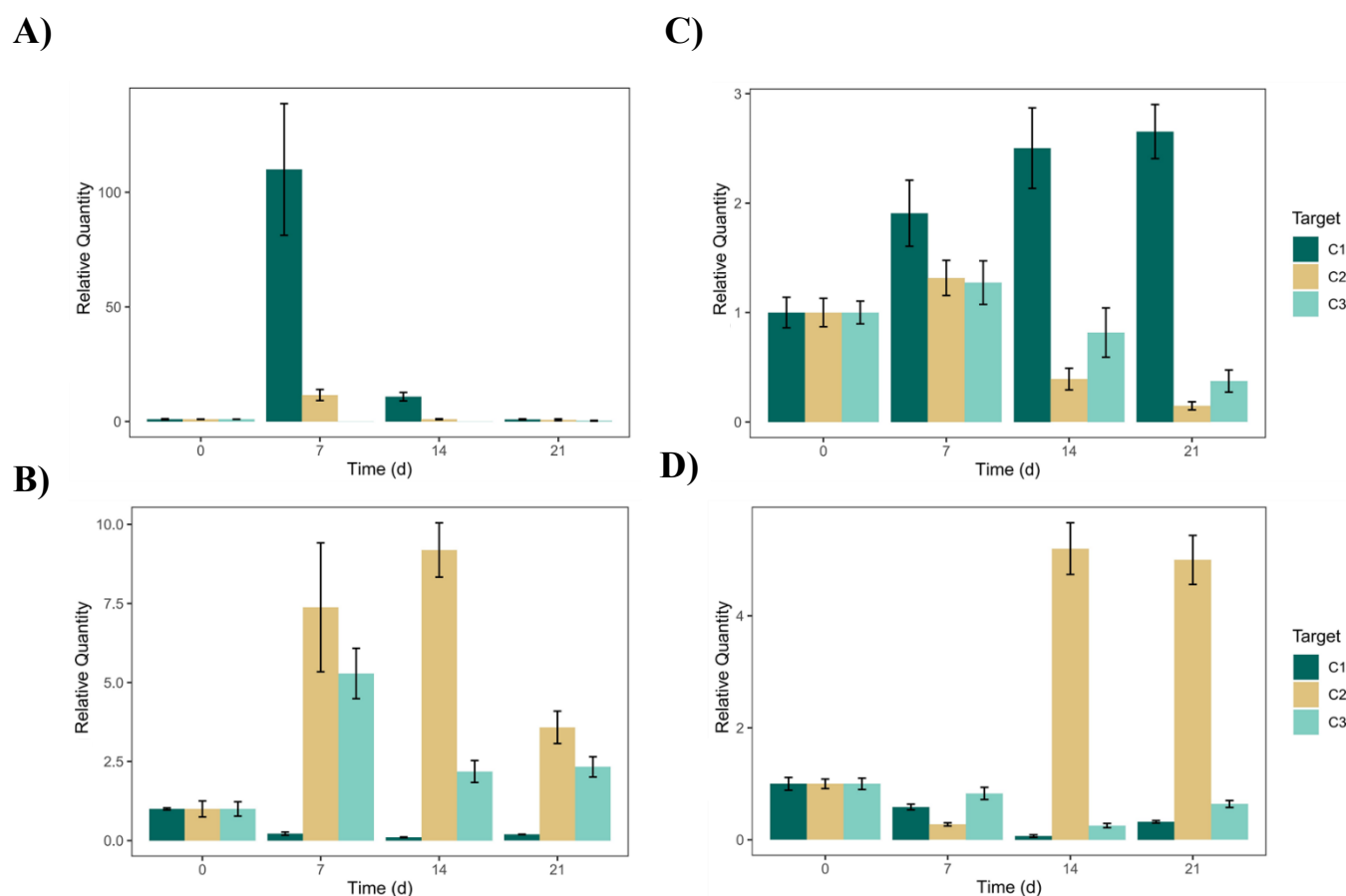


Figure 4. 2 Log relative quantity of *tfdA* classes 1, 2 and 3 at the following field sites and months in 2018: **A)** PV May, **B)** PV July, **C)** OJ May, and **D)** OJ July overall soil samples. Error bars indicate the standard error of the mean.

2018 Field Trial Results. Quantification of the class I gene was detected at PV and OJ field sites in overall (upper and lower) soil samples in May (**Figure 4.2A and 4.2C; Table 4.4**). Further, it is important to note that the relative quantity of class I in PV May (**Figure 4.2A**) was significantly higher at day 7, with over 100 copy numbers, versus PV July (**Figure 4.2B**), OJ May (**Figure 4.2C**), and OJ July (**Figure 4.2D**). The relative quantity of class I in PV May was followed

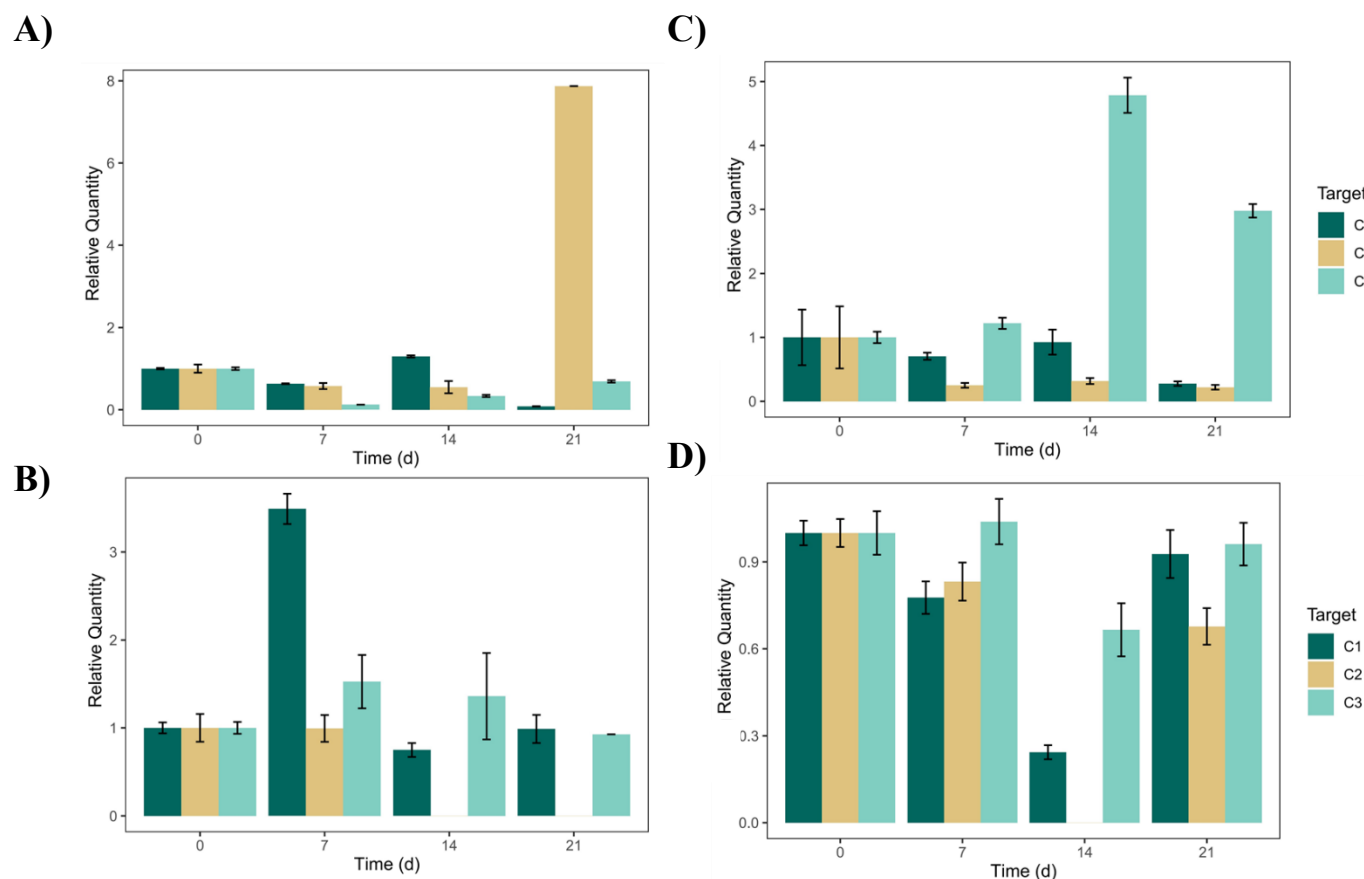


Figure 4.3 Relative quantity of *tfdA* classes 1, 2 and 3 at the following field sites and months in 2019: **A)** PV May, **B)** PV July, **C)** OJ May, and **D)** OJ July. Error bars indicate the standard error of the mean.

by a decrease at days 14 and 21. In OJ May samples, there was a low detection of class I copy numbers, ranging from 1 to 3 (**Figure 4.2C**). Overall, clear differences in copy numbers were observed between the two field sites during May, where class measurements were substantially higher in the PV field site versus OJ (**Figure 4.2A and 4.2C; Table 4.4**). Class II and III copy numbers were lower in both field sites during May. Further, only the month factor revealed a significant effect on the class II gene (**Table 4.4**). In contrast, class I was not detected in either field site during July at either field site (**Figure 4.2B and 4.2D**). Class II detection increased on day 7 post-application in PV July samples, decreasing on day 21 (**Figure 4.2B**). Class III followed a similar trend as class II in PV July samples, where copy number increased on day 7 and gradually

decreased on days 14 and 21 (**Figure 4.2B**). Class III was not detected in OJ July, but class II was detected on days 14 and 21 post-application.

Table 4. 4 Comparison of *tfdA* class I, II, and III quantification in 2018 and 2019 soil field samples using linear regression analysis and analysis of variance (ANOVA). • indicates p-value < 0.1; * indicates p-value < 0.05; ** indicates p-value < 0.01; *** indicates p-value < 0.001; NS=Not Significant.

Factors	Class I	Class II	Class III	Class I	Class II	Class III
Site	***	NS	***	***	NS	***
Layers	NS	NS	***	•	NS	***
Treatment	NS	NS	•	NS	NS	NS
Day	*	NS	**	***	NS	NS
Month	***	***	NS	***	NS	***
Site:Layers	NS	NS	***	NS	NS	***
Site:Treatment	NS	NS	NS	NS	NS	NS
Site:Day	***	NS	***	***	NS	**
Site:Month	***	NS	***	***	NS	***
Layers:Treatment	NS	NS	NS	NS	NS	NS
Layers:Day	NS	NS	NS	NS	NS	NS
Layers:Month	NS	NS	NS	NS	NS	***
Treatment:Day	NS	NS	NS	NS	NS	NS
Treatment:Month	NS	NS	NS	NS	NS	NS
Day:Month	***	NS	***	***	NS	*

2019 Field Trial Results. Site effects were significant in class I and III genes (**Table 4.4**). Specifically, class I and III genes were not detected at PV field sites in May, but class II was quantified at day 21 post-application (**Figure 4.3A**). However, none of the factors exhibited a significant effect on the class II gene (**Table 4.4**). In contrast, class I and II were not detected in OJ, but class III was observed at days 14 and 21 post-application, with a gradual decrease at day 21 (**Figure 4.3C**). Overall, low copy numbers were quantified in both PV and OJ May soil samples. The class I gene was detected on day 7, with an average copy number of 3 during July at PV (**Figure 4.3B**). Class II and III were not detected in PV July (**Figure 4.3B**). There was little to no detection of either *tfdA* gene classes in OJ July field sites (**Figure 4.3D**).

Growth Chamber Study

Table 4. 5 Comparison of *tfdA* class I, II, and III quantification in growth chamber samples using linear regression analysis and analysis of variance (ANOVA). • indicates p-value < 0.1; * indicates p-value < 0.05; ** indicates p-value < 0.01; *** indicates p-value < 0.001; NS=Not Significant.

Factors	Class I	Class II	Class III
Sterilized	•	NS	*
Layers	***	NS	***
Treatment	NS	NS	NS
Day	*	NS	NS
Season	NS	NS	NS
Sterilized*Layers	•	NS	NS
Sterilized*Treatment	•	NS	NS
Sterilized*Day	NS	NS	NS
Sterilized*Season	NS	NS	NS
Layers*Treatment	NS	NS	NS
Layers*Day	*	NS	NS
Layers*Season	NS	NS	NS
Treatment*Day	**	NS	NS
Treatment*Season	NS	NS	•
Day*Season	*	NS	NS

***TfdA* gene class abundance at spring and summer-simulated temperature conditions.** Real-time PCR analysis revealed a low-quantity presence of class I, II, and III *tfdA* genes encoding the 2,4-dichlorophenoxyacetate a-ketoglutarate dioxygenase gene at all time points in treated samples (**Figure 4.4**). However, class I and III genes appeared to have a higher relative quantity (2 to 3 copy numbers) than the class II gene (**Figure 4.4**). Class I gene detection was highest at day 5 post-application in spring-simulated temperatures (**Figure 4.4A**). However, there were no significant differences of the class I gene in spring or summer-simulated temperatures at 1-, 5-, 7-, and 10-days post-application (**Figure 4.4A, Table 4.6**). Little to no detection was observed in class II gene in spring and summer-simulated temperatures (less than 1 copy number). Statistically, there was a significantly relative quantity on day 5 in spring-simulated temperatures versus summer. (**Figure 4.4B, Table 4.6**). Also, a significantly higher copy number was observed on days 7 and 10 post-application (**Figure 4.4B, Table 4.6**). Similar to the class I gene, there were no significant

differences in copy number between the different time points and season-simulated temperatures in the class III gene (**Figure 4.4C, Table 4.6**).

Table 4. 6 Tukey's HSD pairwise comparison of *tfdA* class I, II, and III quantification in growth chamber samples between season-simulated temperatures (spring and summer) and days.

Factors		Class I		Class II		Class III	
Season	Day	Mean	Group	Mean	Group	Mean	Group
SPRING	1	0.64	A	0.18	AB	0.65	A
SUMMER	1	0.61	A	0.14	B	0.53	A
SPRING	5	2.17	A	0.42	A	1.40	A
SUMMER	5	0.94	A	0.00	B	0.84	A
SPRING	7	0.85	A	0.89	C	0.97	A
SUMMER	7	0.85	A	0.89	C	0.65	A
SPRING	10	0.60	A	0.97	C	0.67	A
SUMMER	10	1.20	A	0.81	C	1.34	A

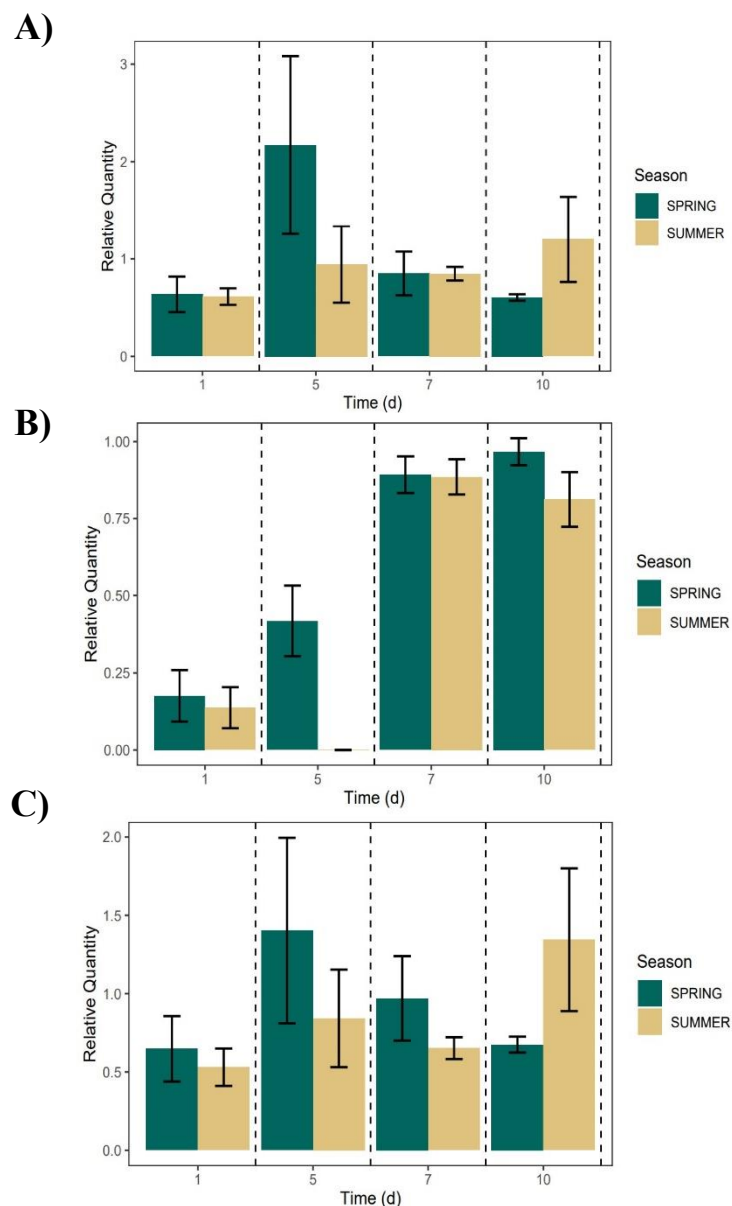


Figure 4. 5 Relative quantity of *tfdA* gene class A) I, B) II, and C) III in urban soil at spring and summer-simulated temperatures in the growth chamber study. Error bars represent the standard error of n=3.

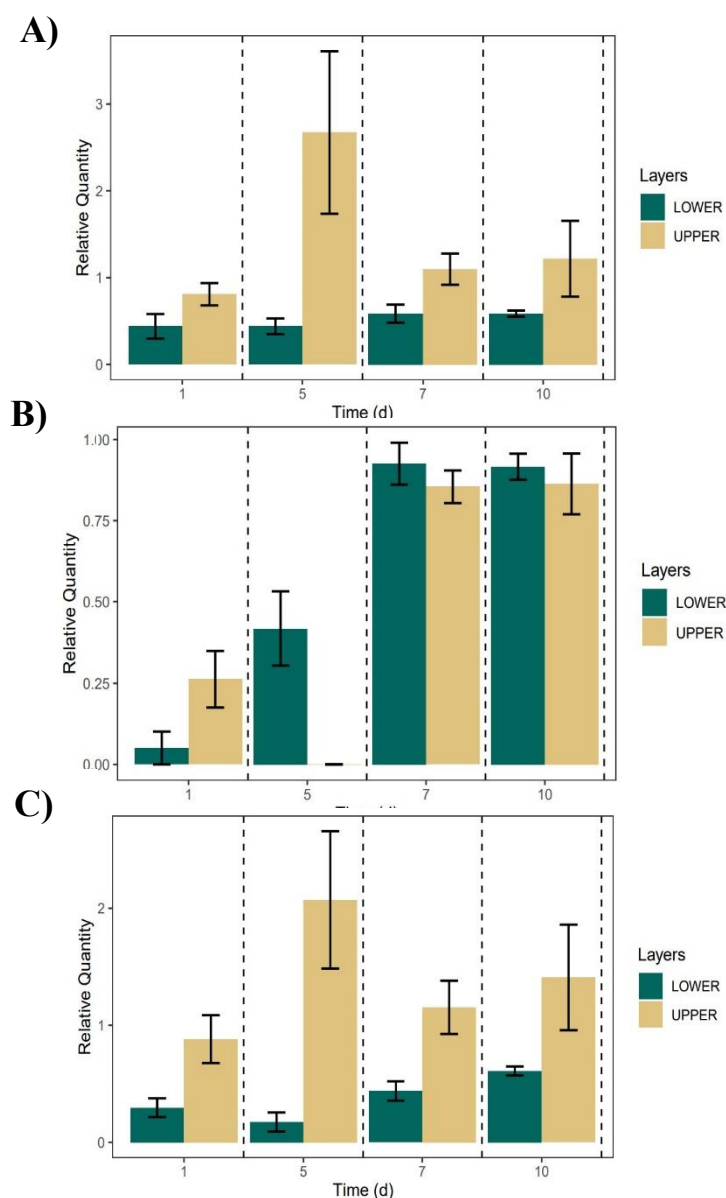


Figure 4. 4 Relative quantity of *tfdA* gene class A) I, B) II, and C) III in urban soil at upper and lower soil layers in the growth chamber study. Error bars represent the standard error of n=3.

Effects of experimental and environmental factors on *tfdA* gene detection. The different factors implemented in the growth chamber study predominantly influenced class I and class III *tfdA* gene relative quantity in 2,4-D-treated samples. Specifically, *tfdA* gene classes were significantly detected in upper soil layers, especially for classes I and III (**Figure 4.5A, Figure**

4.5C, and Table 4.7), where a higher relative quantity was observed on day 5. A small copy number was detected for the class II gene in upper and soil layers (less than 1 copy number). There was a statistically higher relative quantity of the class II gene on day 5 in lower soil layers versus upper soil layers (**Figure 4.5B, Table 4.7**). Also, a significantly higher copy number on days 7 and 10 post-application was observed in both upper and soil layers (**Figure 4.5B, Table 4.7**).

Overall, upper and lower soil layers showed a significant effect on class I and III genes ($P = 0.001$) (**Table 4.5**). The interaction between soil layers and days was also statistically significant for the class I gene ($P = 0.05$) (**Table 4.5**). Sterilization procedures also exhibited an effect on class III gene ($P = 0.05$), but not in class I or II class I gene ($P = 0.05$) but not in class II or III (**Table 4.5**). Although treatment effects were not significant in either gene class, treatment and day interactions exhibited an effect on the class I gene, suggesting that treatment impacted *tfdA* relative quantity (**Table 4.5**).

Table 4. 7 Tukey's HSD pairwise comparison of *tfdA* class I, II, and III quantification in growth chamber samples between soil layers (upper and lower) and days.

Factors		Class I		Class II		Class III	
Layers	Day	Mean	Group	Mean	Group	Mean	Group
UPPER	1	0.81	A	0.26	AB	0.88	AB
LOWER	1	0.44	A	0.05	A	0.30	B
UPPER	5	2.67	B	0.00	A	2.07	A
LOWER	5	0.44	A	0.42	B	0.17	B
UPPER	7	1.10	AB	0.85	C	1.15	AB
LOWER	7	0.58	A	0.93	C	0.44	B
UPPER	10	1.22	AB	0.86	C	1.41	AB
LOWER	10	0.59	A	0.92	C	0.61	B

Important bacterial predictors of *tfdA* gene classes I, II, and III in urban soils.

We used a random forest algorithm analysis to predict key bacteria potentially containing the *tfdA* gene detected in urban soils. We predicted important soil bacterial taxa with each *tfdA* gene classes (I, II, and III) in overall samples at phylum and class level for this model.

Field Study. The model explained 7.54% of the variance of the *tfdA* gene abundance when using these taxa as predictors. With respect to the class I gene, the model featured 12 bacterial classes (**Figure 4.6A**). *Alphaproteobacteria* (*Proteobacteria*), *MB-A2-108* (*Actinobacteria*), *Verrucomicrobiae* (*Verrucomicrobiota*), *Actinobacteria* (*Actinobacteriota*), and *Planctomycetes* (*Firmicutes*) were the top five predictors for *tfdA* class I gene (**Figure 4.6A**). The model explained -3.81% of the variance predicting the *tfdA* gene abundance when using these taxa as predictors for class II. This model featured 13 bacterial classes,

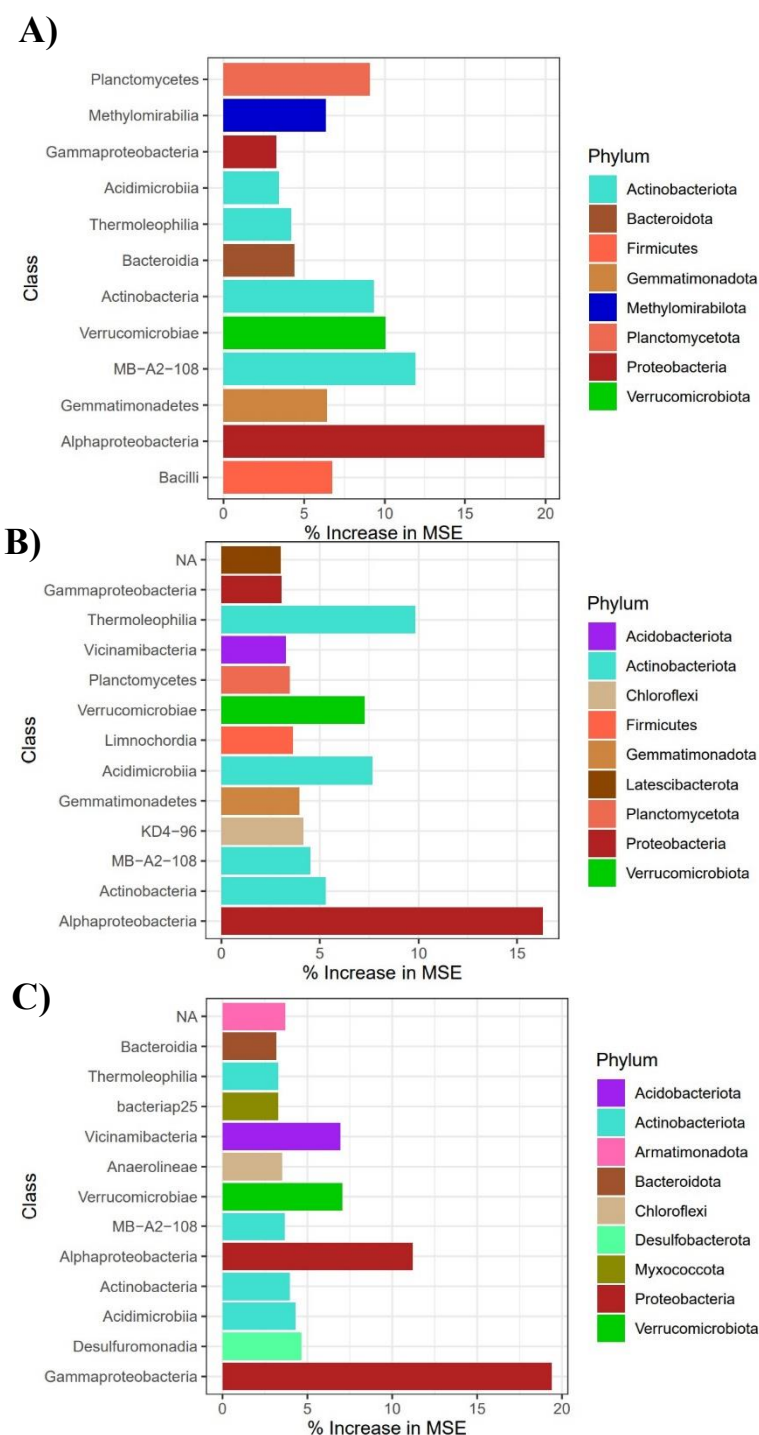


Figure 4. 6 Bacteria classified by random forest algorithms as most important predictors in **A)** class I, **B)** class II, and **C)** class III *tfdA* gene in urban soil samples (n=508) collected from 2018 and 2019 field trials.

one of which was not classified (**Figure 4.6B**). Similar to the class I model, the top five predictors for *tfdA* class II were *Alphaproteobacteria*, *Thermoleophilia* (*Actinobacteriota*), *Acidimicrobiia* (*Actinobacteriota*), *Verrucomicrobiae*, and *Actinobacteria* (**Figure 4.6B**). The class III model

explained 32.98% of the variance predicting the *tfdA* gene abundance when using these taxa as predictors and featured 13 bacterial taxa (**Figure**

4.6C). *Gammaproteobacteria* (*Proteobacteria*) was an important predictor for the *tfdA* class III gene, followed by *Alphaproteobacteria*, which exhibited higher importance in class I and II models. *Verrucomicrobiae*

(*Verrucomicrobiota*) and *Vicinamibacteria* (*Acidobacteriota*) were also among the top predictors in the class III model (**Figure 4.6C**).

Growth Chamber Study. The class I model explained 15.7% of the variance predicting the *tfdA* gene abundance (**Figure 4.7A**). Overall, 16 bacterial classes displayed high importance in

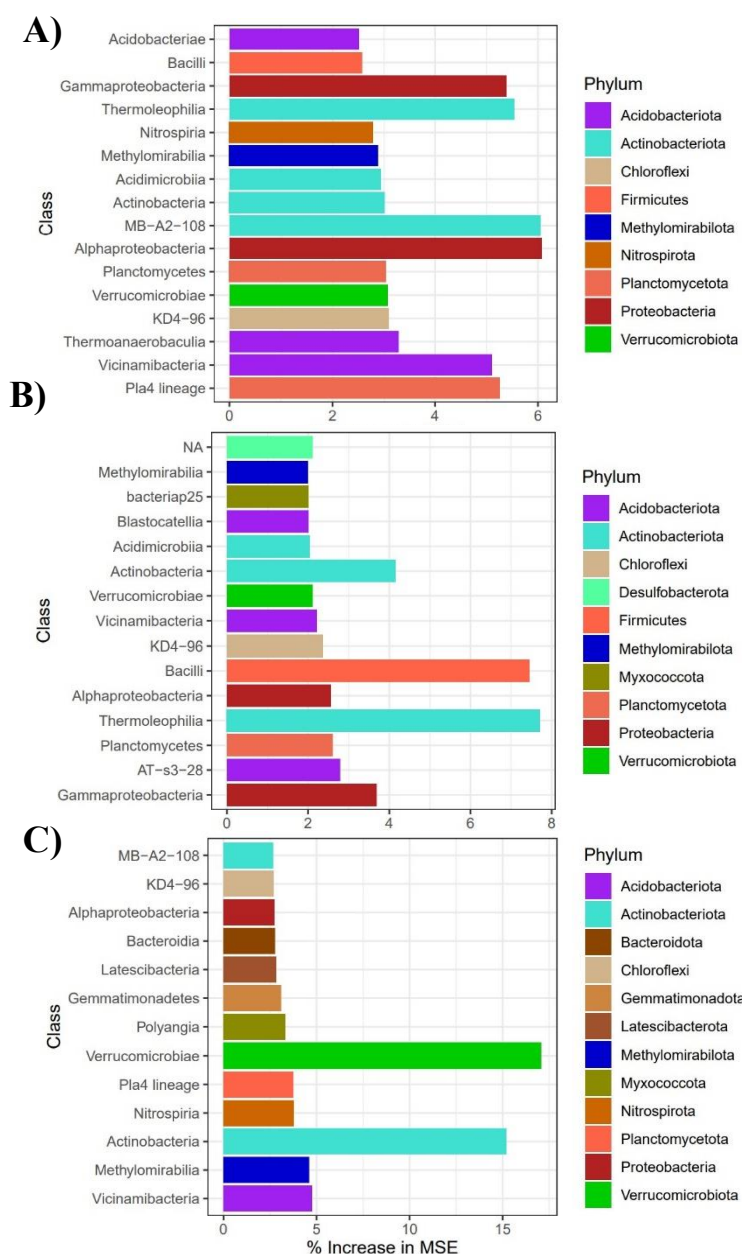


Figure 4. 7 Key bacteria classified by random forest algorithms as most important predictors in **A)** class I, **B)** class II, and **C)** class III *tfdA* gene in urban soil samples (n=278) collected from the growth chamber

the class I model (**Figure 4.7A**). Of those 16 classes, *Alphaproteobacteria* and *Gammaproteobacteria* were among the top important bacterial classes, having a higher increase in MSE for the class I *tfdA* gene model (**Figure 4.7A**). Following *Proteobacteria*, another important bacterial phylum was *Actinobacteria*, where the classes *Thermoleophilia* and *MB-A2-108* also had a higher percentage increase in MSE. *Vicinamibacteria* and *Pla4lineage (Firmicutes)* also exhibited high importance in the class I model (**Figure 4.7A**). The class II model explained - 2.68 % of the variance predicting the *tfdA* gene abundance and did not show a high percentage increase in MSE compared to class I (**Figure 4.7B**). However, our analysis showed *Thermoleophilia*, *Bacilli (Firmicutes)*, *Actinobacteria*, and *Gammaproteobacteria* to be key for predicting *tfdA* class II out of 15 bacterial classes (one unidentified) (**Figure 4.7B**). 13 bacterial classes were featured in the *tfdA* class III model. However, only two– *Verrucomicrobiae* and *Actinobacteria*– presented the highest percentage increase in MSE (**Figure 4.7C**). The model for class III explained 12.98% of the variance predicting the *tfdA* gene abundance when using these taxa as predictors (**Figure 4.7C**).

Positive or false positive detection? – Assessing *tfdA* primer specificity and validity of our qPCR results.

Confirming the presence of *tfdA* reference genes used as standards for qPCR. Initially, we wanted to confirm the presence of *tfdA* reference genes classes in plasmids used as the standards for qPCR. *TfdA* class I, II, and III amplification products using traditional PCR and primers developed by Bælum et al. (2009) (**Table 4.3**) generated single bands of ~200 bp size when run on gel electrophoresis (**Figure S1**).²¹ To ultimately confirm the identity of our *tfdA* standards, identification of nucleotide similarities, based on the *tfdA* gene sequences of the three 2,4-D degrading classes, was performed using the BLASTN program (<http://blast.ncbi.nlm.nih.gov/>). Reference sequences retrieved from GenBank to confirm each *tfdA* class were: Class I, *R.*

eutropha JMP134 *pJP4* ([AY365053.1](#)); Class II, *B. tropica* strain RASC*tfdA* ([EU827441.1](#)); class III, *B. cepacia* 2a *pIJB1* ([JX847411.1](#)) (data not shown).

Testing specificity of previously published primer sets in *tfdA* reference genes. Singleplex (**Figure S2**), duplex (**Figure S3**) and multiplex (**Figure S4**) qPCR reactions were performed to test the specificity of the 81-bp primer sets and probes for each gene class. Undiluted (1X), 1:100, and 1:10⁴ dilutions were prepared for each gene class. Overall, there were no significant changes in C_q values between singleplex and multiplex reactions (**Figure S4**).

Determining primer specificity in qPCR amplified soil DNA from growth chamber study. We compared the relative quantification of the three *tfdA* gene classes from our initial field trial and growth chamber qPCR results. Field trials conducted in 2018 (**Figure 4.2**) and 2019 (**Figure 4.3**) exhibited notable variation in the relative quantity of *tfdA* gene classes. For example, the class I gene had a relative quantity of approximately 100 copy numbers in PV May 2018 field trials (**Figure 4.2A**) while less than 10 copy numbers were quantified in OJ May 2018 (**Figure 4.2B**), PV July 2018 (**Figure 4.2B**), and OJ July 2018 (**Figure 4.2D**). Similar results were observed for 2019 field trials, where less than 8 copy numbers were quantified in each field site and month (**Figure 3**). Also, our growth chamber study revealed variations in the relative quantity where quantification was less than 3 copy numbers for class I gene (**Figure 4.4A**), less than 1 copy number for the class II gene (**Figure 4.4B**) and less than 2 copy numbers of the class III gene (**Figure 4.4C**). Less than 3 copy numbers of all *tfdA* gene classes were quantified in the different soil depths from the growth chamber study (**Figure 4.5**). Due to this variation in amplification, we hypothesized that the previously designed 215-bp and 81-bp primers resulted in significant non-target amplification.

To test our hypothesis, we first randomly selected a qPCR product from the 2,4-D treated

group in the growth chamber study and ran it on a 1.5% agarose gel. As a qualitative result, the reference *tfdA* gene standard exhibited successful amplification at a band size lower than 100 bp, consistent with our desired product size (81-bp) (**Figure 4.8**). In contrast, our soil qPCR product presented several bands at different sizes, suggesting non-specific amplification.

To further assess whether non-specific amplification using the 81-bp *tfdA* gene primers was occurring, we performed a cloning reaction, and chemical transformation on two fresh soil qPCR products from upper and lower soil treated samples collected from the growth chamber study. Amplicons from the high (upper soil layer sample collected at day 7 from spring-simulated temperature conditions, sample #S-0189) and low (lower soil layer sample collected at day 7 from summer-simulated temperature conditions, sample #S-0177) quality samples showed three distinct band sizes as confirmed via agarose gel electrophoresis, indicating that pCR^{TM4}-TOPO[®] vector was successfully cloned and transformed into *E. coli* competent cells (**Figure S5**).

DNA plasmids were subsequently extracted and amplified using M13 primers, revealing varying band sizes (**Figure S6**). Amplified plasmids from sample S-S showed a band size at approximately 400 bp (**Figure S6**). In contrast, samples S-T, S-U, and S-V displayed a 200 to 300 bp band size. Lastly, sample S-W presented a band size larger than 500 bp (**Figure S6**). As a final means to evaluate our primer target specificity, samples were submitted for Sanger sequencing in the Biotechnology Center at the

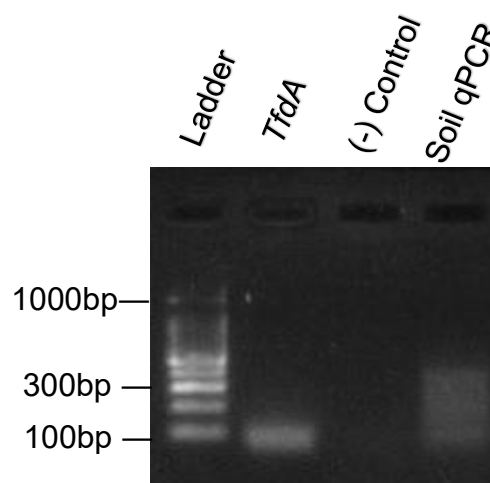


Figure 4. 9 Electrophoresis gel of a qPCR amplification product of *tfdA* class I in soil sample collected from the growth chamber study.

University of Wisconsin-Madison. Sequence alignments and similarities were performed with the

tfdA Class I, II, and III reference sequences using the BLASTN program (<http://blast.ncbi.nlm.nih.gov/>). The percent identity of the samples for the class I, II, and III genes averaged at 94.17%, 92.91%, and 92.91%, respectively (**Table S1**). E-values were also representative of similarity between the aligned sequences, with values as low as 1×10^{-7} in sample S-V, 1×10^{-6} in sample S-T, and 1×10^{-7} in sample S-T, for class I, II, and III reference genes, respectively (**Table S1**). Although percent identities and e-values indicate that sample sequences were similar to the *tfdA* reference genes, it is important to note that the query length from all the samples showed lower than 20% alignment with the reference genes, meaning that more than 80% of the samples compared to the reference sequences had different organization and length; only 6 to 18%, 5 to 17%, and 5 to 17%, for class I, II, and III, respectively was calculated as the percent query coverage (**Table S1**). Additionally, sequences producing significant alignments when performing a general BLAST did not exhibit any *similarities in tfdA gene class I, II, or III*.

Discussion

The *tfdA* 2,4-D-degrading gene classes exhibited high variability in detection and quantification in urban soils at both field sites and growth chamber study. We hypothesized that the variability and quantification in our samples were due to non-target amplification in our qPCR approach. Since the 1990s, detection assays have been developed and optimized to quantify *tfdA* genes in soil samples.^{19,20,24,25} Specifically, Bælum et al. (2009) designed a multiplex qPCR assay to target the three *tfdA* gene classes, which we implemented in our study, and consisted in the use of an 81-bp degenerate primer set targeting a highly specific region of the gene and probes to quantify the different classes.²¹ Other studies have also utilized the same primer sets to quantify *tfdA* in sediment and icesheet samples.^{26,27} So far, the studies that have tested these primers and studied PA herbicide degradation pathways involve their experiments in spiked environmental

samples with the pure active PA herbicide.^{20,21,26,28,29} However, the use of this assay raised uncertainty in our detection and quantification results. Although random forest analysis predicted bacterial classes known to degrade 2,4-D and other PA, our specificity results suggest that the 81-bp primers used in the TaqMan-based approach resulted in non-target amplification. These findings were established using only two soil samples from the growth chamber study and provide limited evidence for non-specific amplification. However, the cloning and chemical transformation of plasmids and the consistent sequencing results obtained in this study support the hypothesis that the 81-bp primers result in significant non-target amplification in environmental samples. qPCR methods to effectively quantify genes in environmental samples requires developing and optimizing primers with robust specificity to the targeted genes of interest. Future steps to improve *tfdA* specificity involve designing primer sets that should be tested for a wider range of environmental samples, including those treated with commercialized PA herbicides in real-world conditions. Implementing primers designed for other genes that are part of the *tfd* pathway such as *tfdB* (encodes for 2,4-dichlorophenol hydroxylase and converts 2,4-dichlorophenol to 3,5-dichlorocatechol) and *tfdC* (encodes for chlorocatechol 1,2-dioxygenase and promotes the degradation of 3,5-dichlorocatechol) will also aid in elucidating the regulation of the *tfd* pathway in soil bacteria and determining key bacterial players in using 2,4-D as a carbon source in soil as described in previous studies.^{30,31}

We sought to discuss our overall qPCR results without disregarding our findings that non-specific amplification occurred in the two environmental samples tested. Although supporting information of non-specific amplification is present, we believe that quantifying the *tfdA* gene may continue to have important implications for 2,4-D-degrading activity in urban soils at varying seasonal conditions. In our initial experiments, a trend in 2018 was observed where the class I and

class II *tfdA* genes were more abundant in PV and OJ field sites, respectively, in May and July. In contrast, we did not observe the same trend in 2019 samples in either field site or month. These differences in *tfdA* relative quantity carefully suggest that 2,4-D degrading activity changes over a year and aligns with our findings from Chapter 3 that varying seasonal conditions and factors can shift soil bacterial structure and, in turn, influence the 2,4-D degrading activity.

No differences were observed between the 2,4-D-treated and NT samples in terms of the *tfdA* gene quantity. The apparent lack of effect of 2,4-D in *tfdA* detection could be attributed to the rate the herbicide was applied in the field. The US Environmental Protection Agency (EPA) allows 2,4-D application rates to turf and residential lawns at 1.5 pounds acid equivalent per acre per application (lb acre^{-1}).³² We used a commercialized product of 2,4-D and applied it using a spray nozzle on our field plots and soil cores of our growth chamber experiments and at a lower rate ($0.45 \text{ lb acre}^{-1}$) than what the EPA recommends. Also, in contrast to our study, previous research had added pure active 2,4-D to media at a concentration of 3 mM to isolate and identify 2,4-D-degrading isolates.^{19,33} Other studies that evaluated PA degradation quantified the *tfdA* gene using previously set up microcosms where the active ingredient MCPA or 2,4-D were applied at concentrations of 2.3 mg kg^{-1} and 5 mg kg^{-1} per soil.^{20,34} Most important differences to note were that these studies, although applied 2,4-D at different concentrations, were conducted in a controlled laboratory setting using the pure active ingredient and not a commercialized product. Adjuvants are usually found as part of the herbicide formulation that help increase herbicide efficacy when applied.³⁵ A study conducted using the commercial herbicide mesotrione (Callisto[®]) suggested that adjuvants have potential side-effects on microbial populations and may also affect pesticide bioavailability for microorganisms that can use pesticides as an energy source.³⁶ To our knowledge, no studies

have yet determined the effects of adjuvants in 2,4-D commercial products on the general microbial community.

In the growth chamber study, significantly higher *tfdA* quantification was observed in upper soil layers. This result aligns with our observation that the bacterial community composition differs between the two soil depths (see Chapter 3), suggesting that soil bacteria from upper soil layers may have contributed to 2,4-D degradation pathways. Another family of 2,4-D-degrading genes is *cadRABKC*, which was initially discovered two decades after the *tfd* gene system from an organism present in a non-2,4-D-contaminated site.^{16,17} Like *tfdA*, the *cadA* gene is responsible for catalyzing the transformation of 2,4-D to 2,4-DCP. This gene system has been widely found in the genera *Bradyrhizobium*, *Sphingomonas*, and possibly others.³ Although the *cadA* gene has bolstered our knowledge of 2,4-D biodegradation research, all bacteria that harbor *cad* genes are not necessarily capable of degrading 2,4-D,¹⁶ explaining why we chose the *tfdA* gene to serve as a marker for 2,4-D biodegradation.

Additional reasons for the variability in detection and no statistically observed treatment effect may also be due to rapid 2,4-D degradation, where *tfdA* levels had decreased, and the pathway proceeded with subsequent degradation of its TP, 2,4-DCP. The soil bacterial community in our tested urban field sites may have also lacked the *tfdA* gene or were not adapted to degrade 2,4-D, which further explains our findings. To our knowledge, 2,4-D has never been applied in the field sites used in our study.

Bacteria involved in class I and class III *tfdA* gene models were considered important predictors of each class. This finding was in agreement with Batioğlu-Pazarbaşı et al. (2012), where they found that *tfdA* class I and class III genes only appeared in samples able to mineralize 2,4-D.²⁶ Our random forest analysis predicted that the class I *tfdA* gene was mainly found in

Alphaproteobacteria, *Gammaproteobacteria*, and *Verrucomicrobiae*. *Actinobacteria*, *Verrucomicrobiae*, and *Gammaproteobacteria* were found to be important predictors of the class III *tfdA* gene. Although *Actinobacteriota* and *Proteobacteria* are common in soil environments^{37–41}, they have shown great importance in degrading pesticides and other contaminants.^{42,43} It is, for this reason, assessing how varying seasonal conditions impact soil bacterial activity is important to improve our understanding of the mechanisms that govern pesticide-bacterial interactions and aid in reducing non-target impacts of pesticide usage.

References

- (1) Charles, J. M.; Cunny, H. C.; Wilson, R. D.; Bus, J. S.; Lawlor, T. E.; Cifone, M. A.; Fellows, M.; Gollapudi, B. Ames Assays and Unscheduled DNA Synthesis Assays on 2, 4-Dichlorophenoxyacetic Acid and Its Derivatives. *Mutat Res* **1999**, *444* (1), 207–216. [https://doi.org/10.1016/s1383-5718\(99\)00074-1](https://doi.org/10.1016/s1383-5718(99)00074-1).
- (2) USEPA. Reregistration Eligibility Decision for 2,4-D https://archive.epa.gov/pesticides/reregistration/web/pdf/24d_red.pdf (accessed 2021 -08 -17).
- (3) Kumar, A.; Trefault, N.; Olaniran, A. O. Microbial Degradation of 2,4-Dichlorophenoxyacetic Acid: Insight into the Enzymes and Catabolic Genes Involved, Their Regulation and Biotechnological Implications. *Critical Reviews in Microbiology* **2016**, *42* (2), 194–208.
- (4) Corke, C. T.; Thompson, F. R. Effects of Some Phenylamide Herbicides and Their Degradation Products on Soil Nitrification. *Can. J. Microbiol.* **1970**, *16* (7), 567–571. <https://doi.org/10.1139/m70-095>.
- (5) Abate Jote, C. A Review of 2,4-D Environmental Fate, Persistence and Toxicity Effects on Living Organisms. *OMCIJ* **2019**, *9* (1). <https://doi.org/10.19080/OMCIJ.2019.09.555755>.
- (6) Duchnowicz, P.; Koter, M.; Duda, W. Damage of Erythrocyte by Phenoxyacetic Herbicides and Their Metabolites. *Pesticide Biochemistry and Physiology* **2002**, *74* (1), 1–7. [https://doi.org/10.1016/S0048-3575\(02\)00139-6](https://doi.org/10.1016/S0048-3575(02)00139-6).
- (7) Bukowska, B. Effects of 2,4-D and Its Metabolite 2,4-Dichlorophenol on Antioxidant Enzymes and Level of Glutathione in Human Erythrocytes. *Comparative Biochemistry and Physiology Part C: Toxicology & Pharmacology* **2003**, *135* (4), 435–441. [https://doi.org/10.1016/S1532-0456\(03\)00151-0](https://doi.org/10.1016/S1532-0456(03)00151-0).

- (8) Ma, Y.; Han, J.; Guo, Y.; Lam, P. K. S.; Wu, R. S. S.; Giesy, J. P.; Zhang, X.; Zhou, B. Disruption of Endocrine Function in in Vitro H295R Cell-Based and in in Vivo Assay in Zebrafish by 2,4-Dichlorophenol. *Aquatic Toxicology* **2012**, *106–107*, 173–181. <https://doi.org/10.1016/j.aquatox.2011.11.006>.
- (9) Steenson, T. I.; Walker, N. The Pathway of Breakdown of 2:4-Dichloro- and 4-Chloro-2-Methyl-Phenoxyacetic Acid by Bacteria. *Journal of general microbiology* **1957**, *16* (1).
- (10) Hoffmann, D.; Müller, R. H.; Kiesel, B.; Babel, W. Isolation and Characterization of an Alkaliphilic Bacterium Capable of Growing on 2,4-Dichlorophenoxyacetic Acid and 4-Chloro-2-Methylphenoxyacetic Acid: 2,4-D and MCPA Degrading Bacterium. *Acta Biotechnologica* **1996**, *16* (2–3), 121–131. <https://doi.org/10.1002/abio.370160205>.
- (11) Hoffmann, D. A Transposon Encoding the Complete 2,4-Dichlorophenoxyacetic Acid Degradation Pathway in the Alkalitolerant Strain Delftia Acidovorans P4a. *Microbiology* **2003**, *149* (9), 2545–2556. <https://doi.org/10.1099/mic.0.26260-0>.
- (12) Itoh, K.; Kanda, R.; Momoda, Y.; Sumita, Y.; Kamagata, Y.; Suyama, K.; Yamamoto, H. Presence of 2, 4-D-Catabolizing Bacteria in a Japanese Arable Soil That Belong to BANA(Bradyrhizobium-Agromonas-Nitrobacter-Afipia)Cluster in α -Proteobacteria. *Microbes and Environments* **2000**, *15* (2), 113–117. <https://doi.org/10.1264/jsme2.2000.113>.
- (13) Pemberton, J. M.; Fisher, P. R. 2,4-D Plasmids and Persistence. *Nature* **1977**, *268* (5622), 732–733. <https://doi.org/10.1038/268732a0>.
- (14) Fisher, P. R.; Appleton, J.; Pemberton, J. M. Isolation and Characterization of the Pesticide-Degrading Plasmid PJP1 from Alcaligenes Paradoxus. *Journal of Bacteriology* **1978**, *135* (3), 798–804. <https://doi.org/10.1128/jb.135.3.798-804.1978>.

- (15) McGowan, C.; Fulthorpe, R.; Wright, A.; Tiedje, J. M. Evidence for Interspecies Gene Transfer in the Evolution of 2,4-Dichlorophenoxyacetic Acid Degraders. *Appl Environ Microbiol* **1998**, *64* (10), 4089–4092. <https://doi.org/10.1128/AEM.64.10.4089-4092.1998>.
- (16) Kitagawa, W.; Kamagata, Y. Diversity of 2,4-Dichlorophenoxyacetic Acid (2,4-D)-Degradative Genes and Degrading Bacteria. In *Biodegradative Bacteria: How Bacteria Degrade, Survive, Adapt, and Evolve*; Springer Japan, 2014; pp 43–57.
- (17) Kitagawa, W.; Takami, S.; Miyauchi, K.; Masai, E.; Kamagata, Y.; Tiedje, J. M.; Fukuda, M. Novel 2,4-Dichlorophenoxyacetic Acid Degradation Genes from Oligotrophic Bradyrhizobium Sp. Strain HW13 Isolated from a Pristine Environment. *Journal of Bacteriology* **2002**, *184* (2), 509–518. <https://doi.org/10.1128/JB.184.2.509-518.2002>.
- (18) Zharikova, N. V.; Iasakov, T. R.; Zhurenko, E. Yu.; Korobov, V. V.; Markusheva, T. V. Bacterial Genes of 2,4-Dichlorophenoxyacetic Acid Degradation Encoding α -Ketoglutarate-Dependent Dioxygenase Activity. *Biol Bull Rev* **2018**, *8* (2), 155–167. <https://doi.org/10.1134/S2079086418020081>.
- (19) Vallaey, T.; Fulthorpe, R. R.; Wright, A. M.; Soulas, G. The Metabolic Pathway of 2,4-Dichlorophenoxyacetic Acid Degradation Involves Different Families of TfdA and TfdB Genes According to PCR-RFLP Analysis. *FEMS Microbiology Ecology* **1996**, *20* (3), 163–172. <https://doi.org/10.1111/j.1574-6941.1996.tb00315.x>.
- (20) Bælum, J.; Henriksen, T.; Hansen, H. C. B.; Jacobsen, C. S. Degradation of 4-Chloro-2-Methylphenoxyacetic Acid in Top- and Subsoil Is Quantitatively Linked to the Class III TfdA Gene. *Appl Environ Microbiol* **2006**, *72* (2), 1476–1486. <https://doi.org/10.1128/AEM.72.2.1476-1486.2006>.

- (21) Bælum, J.; Jacobsen, C. S. TaqMan Probe-Based Real-Time PCR Assay for Detection and Discrimination of Class I, II, and III TfdA Genes in Soils Treated with Phenoxy Acid Herbicides. *Appl Environ Microbiol* **2009**, 75 (9), 2969–2972. <https://doi.org/10.1128/AEM.02051-08>.
- (22) Average Annual Temperatures by USA State - Current Results <https://www.currentresults.com/Weather/US/average-annual-state-temperatures.php> (accessed 2019 -03 -22).
- (23) Liaw, A.; Wiener, M. Classification and Regression by RandomForest. *R News* **2002**, 2 (3), 18–22.
- (24) Nicolaisen, M. H.; Baelum, J.; Jacobsen, C. S.; Sørensen, J. Transcription Dynamics of the Functional TfdA Gene during MCPA Herbicide Degradation by *Cupriavidus Necator* AEO106 (PRO101) in Agricultural Soil. *Environ Microbiol* **2008**, 10 (3), 571–579. <https://doi.org/10.1111/j.1462-2920.2007.01476.x>.
- (25) Streber, W. R.; Timmis, K. N.; Zenk, M. H. Analysis, Cloning, and High-Level Expression of 2,4-Dichlorophenoxyacetate Monooxygenase Gene TfdA of *Alcaligenes Eutrophus* JMP134. *J Bacteriol* **1987**, 169 (7), 2950–2955.
- (26) Batioğlu-Pazarbaşı, M.; Bælum, J.; Johnsen, A. R.; Sørensen, S. R.; Albrechtsen, H.-J.; Aamand, J. Centimetre-Scale Vertical Variability of Phenoxy Acid Herbicide Mineralization Potential in Aquifer Sediment Relates to the Abundance of TfdA Genes. *FEMS Microbiology Ecology* **2012**, 80 (2), 331–341. <https://doi.org/10.1111/j.1574-6941.2012.01300.x>.
- (27) Microbial Degradation of 2,4-Dichlorophenoxyacetic Acid on the Greenland Ice Sheet <https://journals.asm.org/doi/epub/10.1128/AEM.00400-12> (accessed 2021 -09 -21). <https://doi.org/10.1128/AEM.00400-12>.

- (28) Baelum, J.; Nicolaisen, M. H.; Holben, W. E.; Strobel, B. W.; Sørensen, J.; Jacobsen, C. S. Direct Analysis of TfdA Gene Expression by Indigenous Bacteria in Phenoxo Acid Amended Agricultural Soil. *ISME J* **2008**, 2 (6), 677–687. <https://doi.org/10.1038/ismej.2008.21>.
- (29) Gonod, L. V.; Martin-Laurent, F.; Chenu, C. 2,4-D Impact on Bacterial Communities, and the Activity and Genetic Potential of 2,4-D Degrading Communities in Soil. *FEMS Microbiology Ecology* **2006**, 58 (3), 529–537. <https://doi.org/10.1111/j.1574-6941.2006.00159.x>.
- (30) Hoffmann, D.; Kleinsteuber, S.; Müller, R. H.; Babel, W. Development and Application of PCR Primers for the Detection of Thetfd Genes InDelftia Acidovorans P4a Involved in the Degradation of 2,4-D. *Acta Biotechnologica* **2001**, 21 (4), 321–331. [https://doi.org/10.1002/1521-3846\(200111\)21:4<321::AID-ABIO321>3.0.CO;2-I](https://doi.org/10.1002/1521-3846(200111)21:4<321::AID-ABIO321>3.0.CO;2-I).
- (31) Lillis, L.; Clipson, N.; Doyle, E. Quantification of Catechol Dioxygenase Gene Expression in Soil during Degradation of 2,4-Dichlorophenol. *FEMS Microbiol Ecol* **2010**, 73 (2), 363–369. <https://doi.org/10.1111/j.1574-6941.2010.00906.x>.
- (32) USEPA. Pesticides - Fact Sheet for 2,4-D https://www3.epa.gov/pesticides/chem_search/reg_actions/reregistration/fs_PC-030001_30-Jun-05.pdf (accessed 2021 -08 -17).
- (33) Vallaeys, T. Isolement d'une Communaute, Microbienne Degradant l'acide 2,4-Dichlorophenoxyacetique a Partir d'un Sol de Dijon., Universite Lille I. France, 1992.
- (34) Zabaloy, M. C.; Gómez, M. A. Isolation and Characterization of Indigenous 2,4-D Herbicide Degrading Bacteria from an Agricultural Soil in Proximity of Sauce Grande River, Argentina. *Ann Microbiol* **2014**, 64 (3), 969–974. <https://doi.org/10.1007/s13213-013-0731-9>.
- (35) Jordan, T. Adjuvant Use with Herbicides: Factors to Consider <https://www.extension.purdue.edu/extmedia/ws/ws-7.html> (accessed 2021 -10 -08).

- (36) Crouzet, O.; Batisson, I.; Besse-Hoggan, P.; Bonnemoy, F.; Bardot, C.; Poly, F.; Bohatier, J.; Mallet, C. Response of Soil Microbial Communities to the Herbicide Mesotrione: A Dose-Effect Microcosm Approach. *Soil Biology and Biochemistry* **2010**, *42* (2), 193–202. <https://doi.org/10.1016/j.soilbio.2009.10.016>.
- (37) Novello, G.; Gamalero, E.; Bona, E.; Boatti, L.; Mignone, F.; Massa, N.; Cesaro, P.; Lingua, G.; Berta, G. The Rhizosphere Bacterial Microbiota of Vitis Vinifera Cv. Pinot Noir in an Integrated Pest Management Vineyard. *Front. Microbiol.* **2017**, *8*. <https://doi.org/10.3389/fmicb.2017.01528>.
- (38) Opsi, F.; Landa, B.; Zecca, O.; Biddoccu, M.; Barmaz, A.; Cavallo, E. Diversity in Soil Bacterial Communities Structure in Four High-Altitude Vineyards Cultivated Using Different Soil Management Techniques. **2014**, 14297.
- (39) Zarraonaindia, I.; Owens, S. M.; Weisenhorn, P.; West, K.; Hampton-Marcell, J.; Lax, S.; Bokulich, N. A.; Mills, D. A.; Martin, G.; Taghavi, S.; van der Lelie, D.; Gilbert, J. A. The Soil Microbiome Influences Grapevine-Associated Microbiota. *mBio*, **2015**, *6* (2), e02527-14. <https://doi.org/10.1128/mBio.02527-14>.
- (40) Medo, J.; Maková, J.; Medová, J.; Lipková, N.; Cinkocki, R.; Omelka, R.; Javoreková, S. Changes in Soil Microbial Community and Activity Caused by Application of Dimethachlor and Linuron. *Sci Rep* **2021**, *11*, 12786. <https://doi.org/10.1038/s41598-021-91755-6>.
- (41) Zhang, M.-M.; Wang, N.; Hu, Y.-B.; Sun, G.-Y. Changes in Soil Physicochemical Properties and Soil Bacterial Community in Mulberry (Morus Alba L.)/Alfalfa (Medicago Sativa L.) Intercropping System. *MicrobiologyOpen* **2018**, *7* (2), e00555. <https://doi.org/10.1002/mbo3.555>.

- (42) Alvarez, A.; Saez, J. M.; Davila Costa, J. S.; Colin, V. L.; Fuentes, M. S.; Cuozzo, S. A.; Benimeli, C. S.; Polti, M. A.; Amoroso, M. J. Actinobacteria: Current Research and Perspectives for Bioremediation of Pesticides and Heavy Metals. *Chemosphere* **2017**, *166*, 41–62. <https://doi.org/10.1016/j.chemosphere.2016.09.070>.
- (43) Regar, R. K.; Gaur, V. K.; Bajaj, A.; Tambat, S.; Manickam, N. Comparative Microbiome Analysis of Two Different Long-Term Pesticide Contaminated Soils Revealed the Anthropogenic Influence on Functional Potential of Microbial Communities. *Science of The Total Environment* **2019**, *681*, 413–423. <https://doi.org/10.1016/j.scitotenv.2019.05.090>.

Supplementary Materials

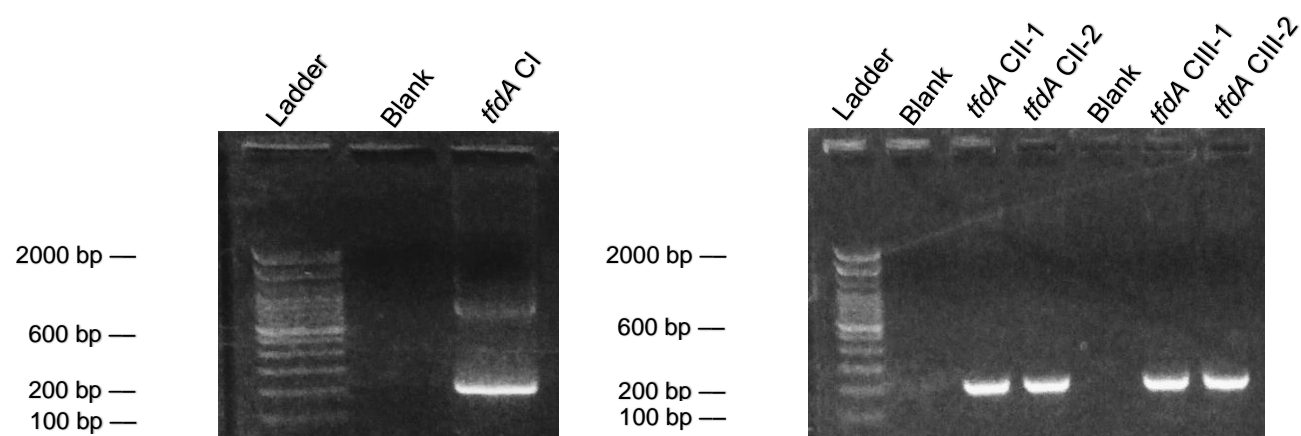


Figure S1. Electrophoresis gel of *tfdA* classes I, II, and III PCR products.

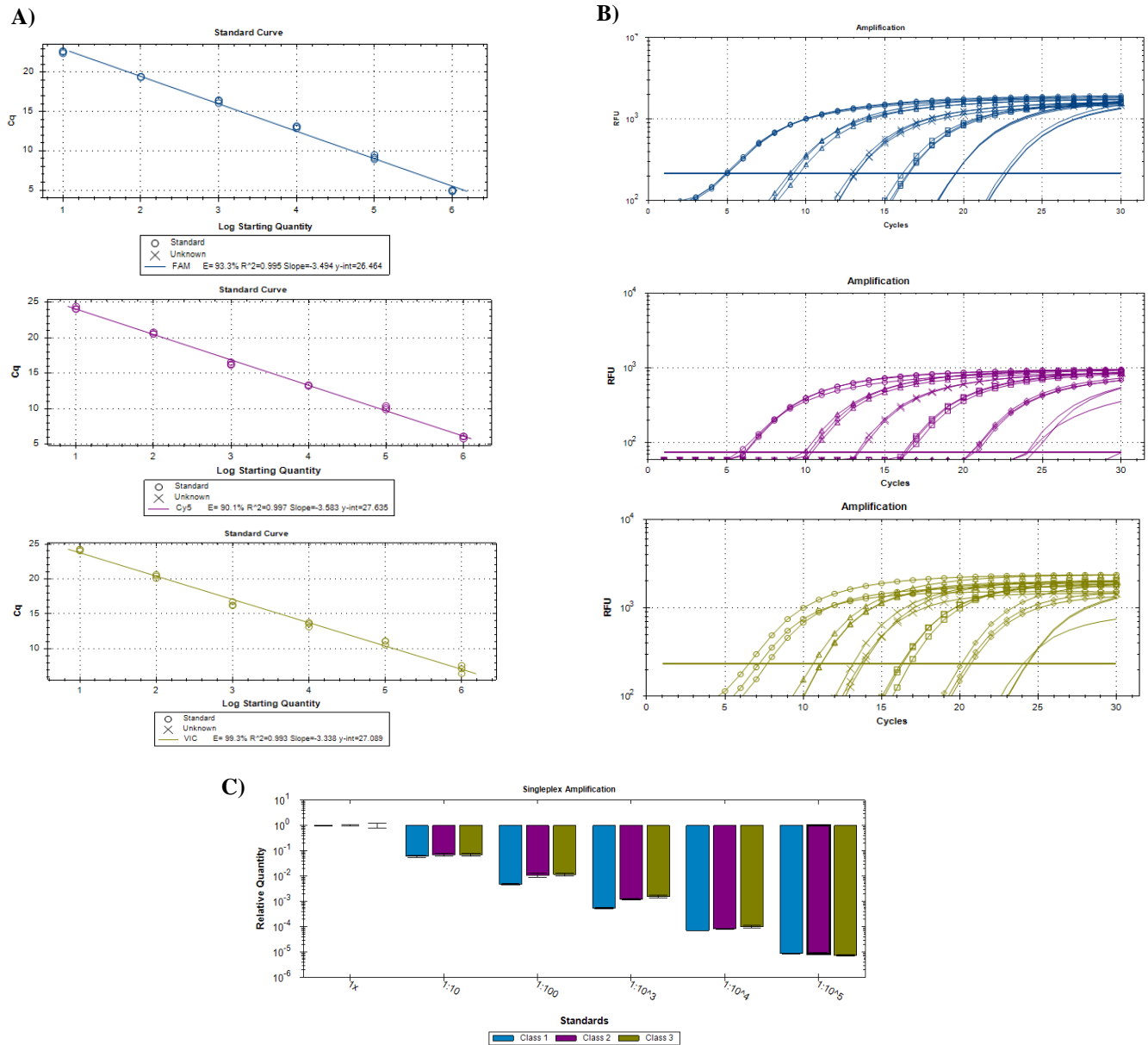


Figure S2. Amplification and standard curves of *tfdA* classes I-III qPCR. **A)** Standard curve generated by plotting the C_q values versus the tenfold serial dilutions of each of the three classes of the *tfdA* gene. **B)** Amplification of tenfold dilutions ranging from 10^6 to 10 copies of each *tfdA* gene class. Reactions were amplified in triplicate along with no-template controls. **C)** Side-by-side comparison of qPCR amplification of classes I, II, and III.

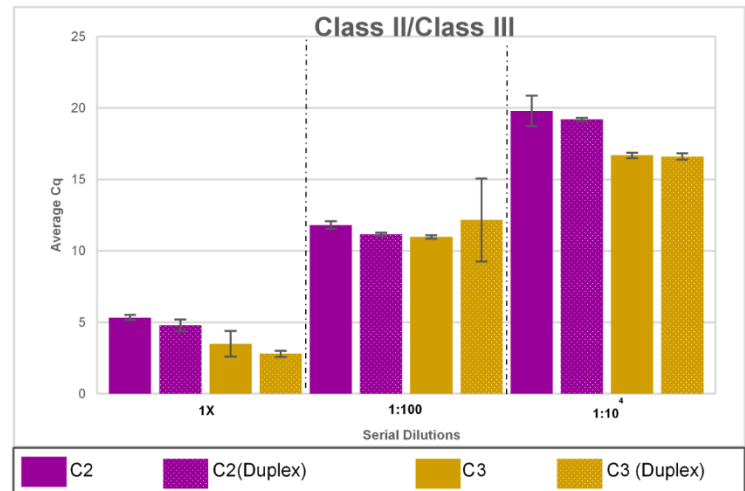
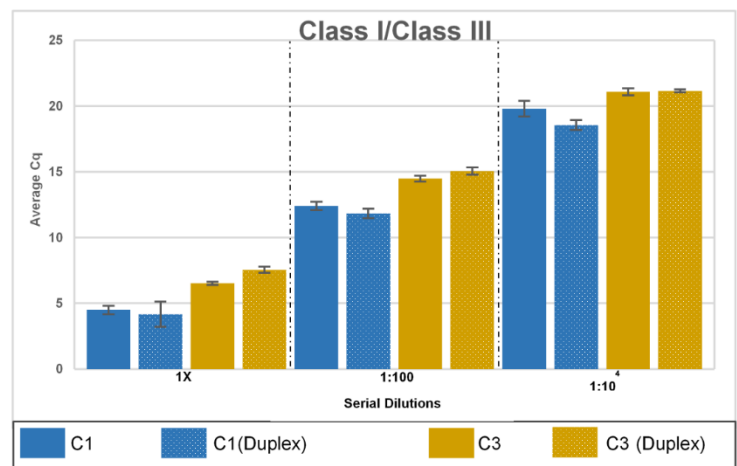
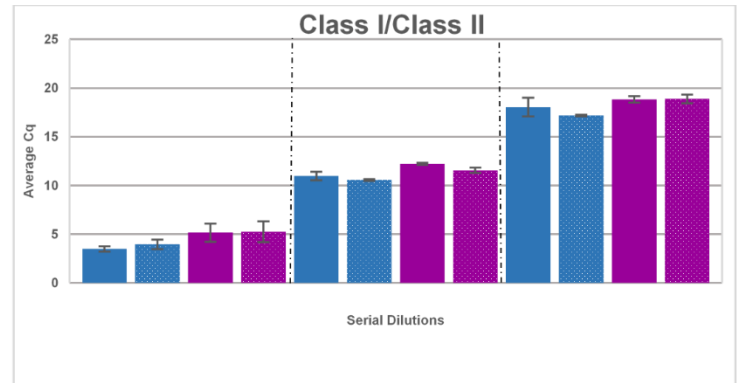
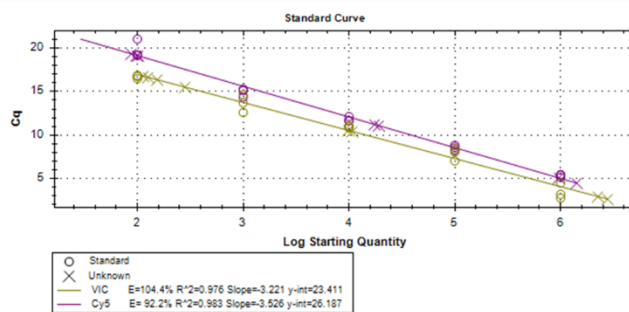
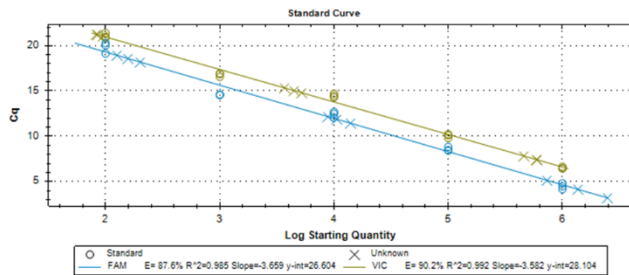
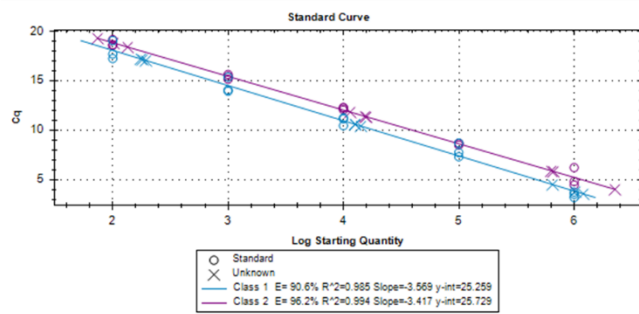


Figure S3. *qPCR duplex reaction assay validation of the three *tfdA* class genes. A) Standard curves of Class I/Class II, Class I/Class III, and Class II/Class III duplex reactions. B) Comparison of average Ct values between 1X, 1:100, and 1:10⁴ duplex and singleplex reactions. Note that for each assay, there were no significantly observed changes in singleplex and duplex reactions between each gene class.*

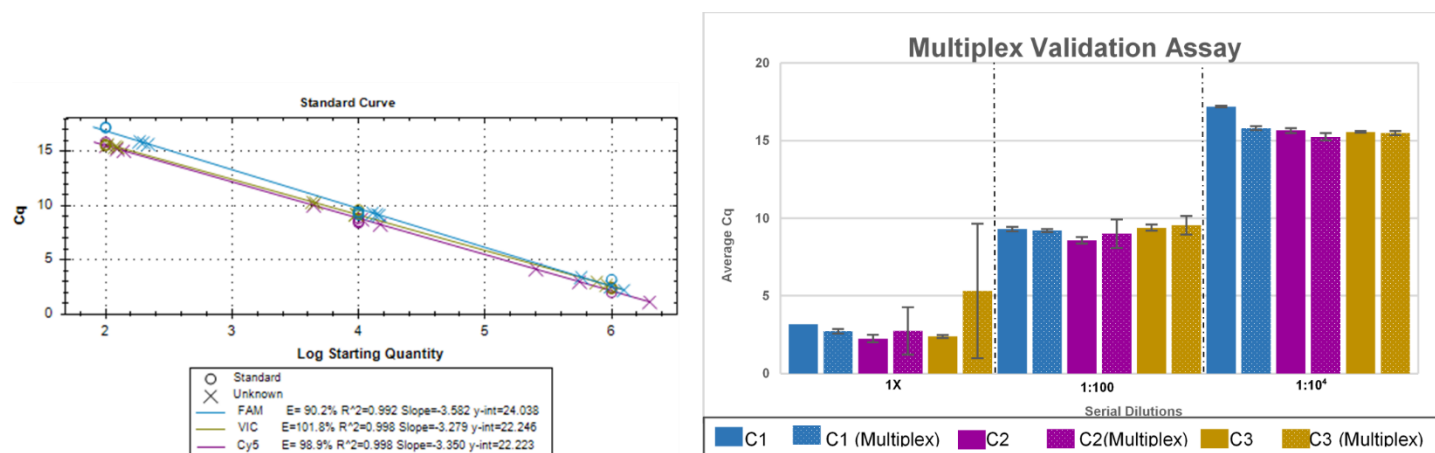


Figure S4. qPCR multiplex reaction assay validation of the three *tfdA* class genes. **A)** Standard curves of Class I/Class II/Class III multiplex reactions. **B)** Comparison of average Cq values between 1X, 1:100, and 1:10⁴ singleplex and multiplex reactions.

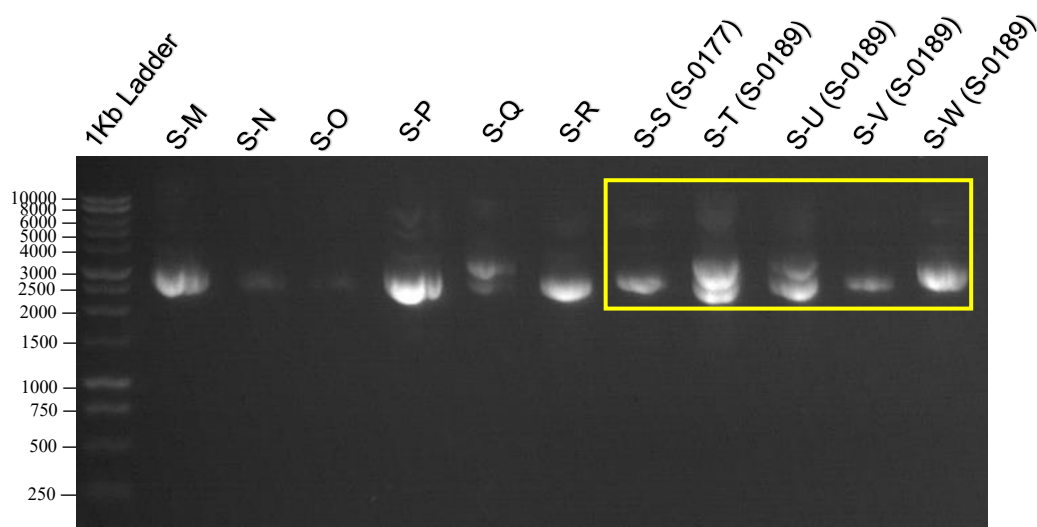


Figure S5. Electrophoresis gel of isolated and amplified plasmids using M13 primers. Bands highlighted within yellow box indicate soil samples from the growth chamber study.

Reference Gene	Sample		Max Score	Total Score	Query Cover (%)	E-value	Identity (%)
R. eutropha (Class I)	S-S	(S-	38.3	71.1	10	6.00E-06	95.65
	0177)						
	S-T	(S-	35.6	70.2	18	1.00E-05	91.67
	0189)						
	S-U	(S-	32.8	32.8	7	1.00E-04	95.00
B. tropica (Class II)	0189)						
	S-V	(S-	42.8	80.1	15	1.00E-07	92.86
	0189)						
	S-W	(S-	38.3	71.1	6	1.00E-05	95.65
	0189)						
B. tropica (Class II)	S-S	(S-	33.7	85.9	12	7.00E-05	91.30
	0177)						
	S-T	(S-	40.1	69.3	17	1.00E-06	95.83
	0189)						
	S-U	(S-	27.4	27.4	6	6.00E-03	94.12
D. acidovorans (Class III)	0189)						
	S-V	(S-	37.4	37.4	8	4.00E-06	92.00
	0189)						
	S-W	(S-	33.7	61.2	5	1.00E-04	91.30
	0189)						
D. acidovorans (Class III)	S-S	(S-	33.7	85.9	12	7.00E-05	91.30
	0177)						
	S-T	(S-	40.1	69.3	17	1.00E-06	95.83
	0189)						
	S-U	(S-	27.4	27.4	6	6.00E-03	94.12
D. acidovorans (Class III)	0189)						
	S-V	(S-	37.4	37.4	8	4.00E-04	92.00
	0189)						
	S-W	(S-	33.7	61.2	5	1.00E-04	91.30
	0189)						

Table S1. NCBI BLAST hits for top pairwise alignments between tfdA classes I, II, and III genes and sequenced plasmids.

Chapter 5. Assessment of Temperature and Time Following Application as Predictors of Propiconazole Translocation in *Agrostis stolonifera*

This chapter has been adapted from the manuscript that is under revision in J. Agric. Sci. Technol.: “Assessment of Temperature and Time Following Application as Predictors of Propiconazole Translocation in *Agrostis stolonifera*.” The manuscript was authored by Amarilys E. González Vázquez, Kurt R. Hockemeyer, Megan McConville, Christina K. Remucal, Paul L. Koch.

Abstract

Propiconazole is a xylem-mobile fungicide used to suppress psychrophilic fungi on amenity turfgrass in temperate climates during the winter. The ability of turfgrass plants to translocate propiconazole during cold temperatures is unclear, with important implications for adequate fungal suppression and potential environmental contamination. We assessed the impact of temperature and time following application on the amount of propiconazole translocated into individual turfgrass plants and created a linear mixed-effects (LME) model to predict propiconazole uptake. Propiconazole was applied near the base of individual creeping bentgrass plants grown in controlled environment chambers at four different temperatures (22°C, 14°C, 10°C, 1°C). Propiconazole quantification was performed on individual 1-cm leaf segments using liquid chromatography-tandem mass spectrometry and assessed 24, 48, and 72 hours (h) following application. Propiconazole concentrations were consistently highest in the lowest leaf segment (0 to 1 cm above the soil surface) regardless of temperature or time following application. Peak propiconazole concentrations were observed between 24 and 48 h after application. Using the LME model, leaf segment correlated most strongly with higher propiconazole concentration, followed by time after application and temperature. Our results indicate that propiconazole translocation in amenity turfgrass is primarily limited to the lowest segment of the plant regardless of temperature or time following the application. These findings provide important information for the effective use of xylem-mobile fungicides to treat low-temperature turfgrass diseases.

Keywords: Propiconazole, turfgrass, plant uptake, translocation, temperature, fungicides

Introduction

Snow molds such as Typhula blight (*Typhula incarnata* and *Typhula ishikariensis*) and Microdochium patch (*Microdochium nivale*) are the primary low-temperature diseases of amenity turfgrass around the world.^{1,2} Control of snow molds in turfgrass is traditionally obtained with one or two fungicide applications in the fall shortly before snow cover, and in many cases, a mixture of fungicide active ingredients is required to obtain adequate disease control.^{3,4} The appropriate timing of these fungicide applications is essential for disease control and has been the source of considerable debate in recent years. Some turfgrass managers choose to apply fungicides well in advance of snowfall while the plant is still growing, potentially resulting in rapid fungicide degradation before snow cover and leaving the grass susceptible to snow mold development over the winter.⁵ Others attempt to avoid fungicide degradation by applying fungicide immediately before snow cover arrives, though it is unclear whether the fungicides are absorbed and translocated within the plant at colder temperatures.³ Timing the application in late fall may also lead to an increased risk for environmental contamination if the fungicides are applied to frozen soils, limiting plant uptake and resulting in runoff to non-target areas.⁶

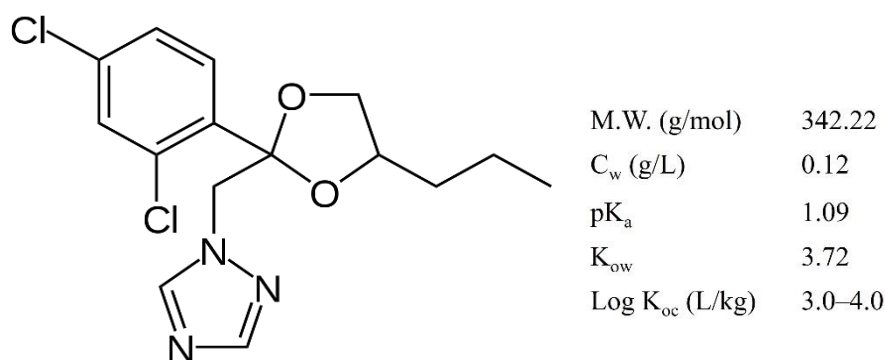


Figure 5. 1 Chemical structure and physicochemical properties of propiconazole. M.W. = Molecular weight; C_w = Water solubility; pK_a = Acid dissociation constant; K_{ow} = n-octanol-water partition coefficient; K_{oc} = organic carbon to water partition coefficient; soil adsorption coefficient.

The most common fungicides used to suppress snow mold pathogens are triazoles or C-14 demethylation inhibitors (DMI).⁷ DMI fungicides inhibit oxidative sterol α -demethylation in the ergosterol biosynthesis pathway in fungal cells.⁸ Once ergosterol inhibition occurs, membrane function becomes disrupted, and fungal growth stops.⁸ Propiconazole (1-[(2-(2,4-dichlorophenyl)-4-propyl-1,3-dioxolan-2-yl) methyl]-1H-1,2,4-triazole) is a common DMI used for plant disease management in numerous agricultural and horticultural crops and is widely used for snow mold control on golf course turfgrass (**Figure 5.1**).⁷ Propiconazole is an acropetal penetrant that infiltrates the outer plant cuticle and translocates apoplastically into the xylem.⁷ Once inside the xylem, the fungicide moves along a water potential gradient upwards in the plant toward leaf tips and margins (**Figure 5.2**).⁷ Propiconazole is classified as persistent, potentially toxic, and a possible human carcinogen by the US Environmental Protection Agency.⁹ With an acid dissociation constant (pK_a) of 1.09, water solubility of 0.12 g L^{-1} , and an organic carbon to water partition coefficient ($\log K_{oc}$) of approximately 3 to 4 L kg^{-1} , propiconazole is primarily

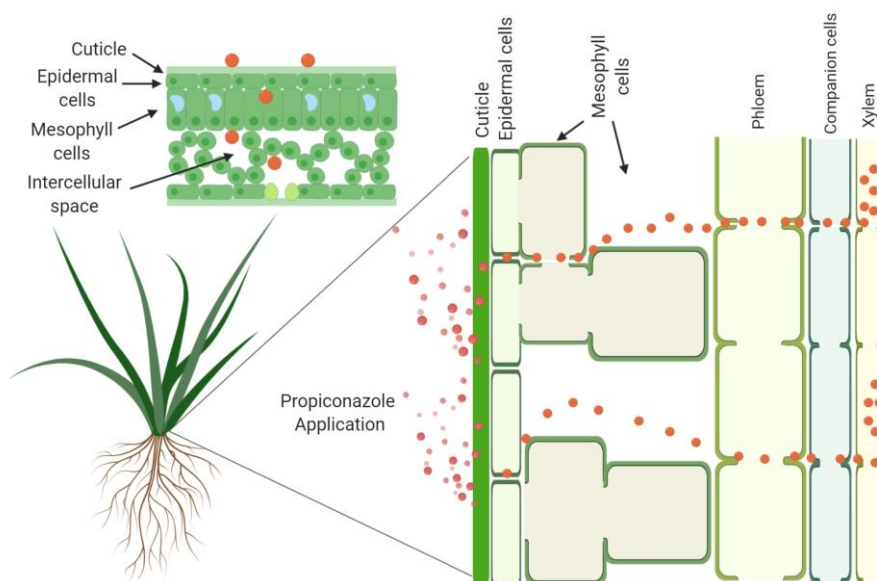


Figure 5. 2 Diagram depicting apoplastic translocation of propiconazole. Acropetal penetrants diffuse through the cuticle, travel to the vasculature tissue, and enter the xylem, where they are transported upward to leaf tips. Red dots represent the propiconazole molecule. Created with BioRender.com

deprotonated at circumneutral pH, is slightly soluble, has a high affinity for soil, and is likely to accumulate in soils, resulting in the potential risk of environmental contamination.⁸⁻¹⁰ Propiconazole in the soil is predominantly biodegraded with little influence of photolysis and hydrolysis and has a half-life between 40 and 70 days.⁸ The half-life of propiconazole in soil can change dramatically with temperature (i.e., from ~109 days at 18°C to ~450 days at 5°C).¹¹

Although pesticide fate processes such as uptake (defined here as the process by which pesticides are absorbed by plants through leaves and roots) and translocation (the movement within the plant from the site of application to distant tissues) can be inferred from their physicochemical properties, temperature also influences the rate and amount of pesticide uptake and translocation in plants.^{12,13} Previous studies observed that the rate of uptake of organic chemicals in the cuticular membranes of plants increased by one order of magnitude with increasing temperature from 17°C to 34°C.¹⁴ In contrast, another study observed that uptake of the pesticides simazine, diuron, and ethirimol in barley was not affected by temperature changes from 1°C to 20°C, except for 2,4-D, where uptake increased at warmer temperatures.¹⁵ Additional research demonstrated that the translocation of 2,4-D in maize was largely unaffected by temperatures at 17/9°C and 22/14°C (day/night).¹⁶ While the results from these studies on herbicides provide valuable information on temperature effects on pesticide translocation in plants, there is limited information on the behavior of fungicides when applied to turfgrass at colder temperatures. However, it has been shown that temperature variation in plants such as wheat and barley, can disrupt membrane proteins involved in translocation, impeding uptake of azoxystrobin and ethirimol fungicides, respectively, and movement within the plant.^{15,17}

Most research on pesticide uptake and translocation in plants has been conducted at temperatures between 15 and 30°C in food grains, fruits, and vegetables. Notable exceptions

include studies on herbicides such as 2,4-D, dicamba, MCPA, and dichlorprop that have examined their application and effect on injury to winter wheat at temperatures less than 0°C.¹⁸ There is little research on the topic of fungicide uptake in either cold temperatures or amenity turfgrasses, leaving a critical knowledge gap regarding this common use of fungicides. With this in mind, we hope to obtain a better understanding of how turfgrass plants absorb and translocate propiconazole in cold environments and use that understanding to create a model to predict the impact of temperature on the uptake and translocation of similar chemicals.

The primary objectives of this study were to (1) assess the duration and distance of propiconazole upward mobility into turfgrass leaves in conditions that reflect a late fall and early winter environment and (2) develop a simple plant uptake model specific to DMI fungicides that takes into consideration leaf height, time after application, and temperature. We hypothesized that distance of upward propiconazole mobility would decrease, and the duration of uptake would increase in response to colder temperatures. An improved initial understanding of propiconazole uptake at colder temperatures will provide important use information for turfgrass managers for which there is currently no information, and also drive future research that will address fungicide usage in cold environments and the potential for non-target environmental impacts.

Materials and Methods

Chemicals and Reagents. Propiconazole and its internal standard 2,2,3,3,3-propyl-D5 (d5) were purchased from Fisher Scientific Co. (Hanover Park, IL) and Crescent Chemical Co., Inc. (Islandia, NY), respectively. The formulated commercial product containing propiconazole (Banner MAXX) was purchased from Syngenta Crop Protection (Greensboro, NC). Acetonitrile (ACN) and formic acid were used as high-performance liquid chromatography (HPLC)-grade solvents and obtained from Fisher Scientific Co. Ultrapure water was also obtained using a Milli-

Q water purification system maintained at 18.2 M Ω cm. Anhydrous sodium acetate (CH₃COONa) and lysing matrix D 2-mL tubes were acquired from Fisher Scientific Co. and MP Biomedicals (Santa Ana, CA), respectively. Dispersive solid-phase extraction (d-SPE) 2-mL tubes containing primary secondary amines (PSA), graphitized carbon black (GCB), and magnesium sulfate (MgSO₄) were obtained from Agilent Technologies, Inc. (Folsom, CA).

Preparation of Standard Solution. A 1 $\mu\text{g mL}^{-1}$ stock solution was prepared in 100% ACN for both propiconazole and d5 and stored at -20°C until further use. Standard solutions of each analyte were then prepared from the initial stock solution at the concentrations of 1, 5, 10, 25, 50, and 100 ng mL⁻¹ using ACN and H₂O at a ratio of 80:20 (v/v) through serial dilution.

Plant Preparation. Seventy-two 50-mL polypropylene tubes of 115 mm length and 30 mm diameter (Falcon®, Radnor, PA) were filled with an artificial growth medium consisting of a 1:1 ratio of Turface MVP (Buffalo Grove, IL) and Sungro propagation mix horticulture soil (Agawam, MA). The artificial growth medium had an average (n=3) total organic carbon content (TOC) of 3.62%. A single seed of creeping bentgrass (*Agrostis stolonifera* 'Pennncross') was planted in the center of each tube and maintained at a 3-cm cutting height under optimal growth conditions (14 h photoperiod, 21°C day temperature, 13°C nighttime temperature) for eight weeks until the plants matured. Each treatment was conducted on individual plants due to the destructive nature of the sampling.

Treatments and Experimental Design. Following maturation, 18 individual plants were placed in one of four controlled environment chambers to mimic four different dates during the fall in Madison, WI, USA, including the average temperature and photoperiod.¹⁹ Specifically, chambers were set at either 22°C with a 12-h photoperiod, 14°C with an 11-h photoperiod, 10°C with a 10-h photoperiod, or 1°C with a 9-h photoperiod representing Sept 10, Oct 24, Nov 12, and

Dec 23, respectively. Plants were placed in each growth chamber and allowed to acclimate for two weeks before treatments were applied.

Propiconazole or water was applied near the base of each plant following the two weeks of acclimation. Care was taken to apply the propiconazole solution to the soil immediately adjacent to the plant and not the plant itself to allow for accurate measurement of uptake from the base to upper leaf segments. For propiconazole-treated plants, 1 mL of Banner MAXX solution at a concentration of 1,624 μg propiconazole per mL of water was applied, which is a concentration equal to what would be applied in a field environment for control of psychrophilic fungi. For water-treated controls, 1 mL of Milli-Q water was applied in the same manner as the propiconazole treatment. The plants were immediately returned to their respective growth chambers and cut at the soil surface 24, 48, or 72 h after application using sterile scissors. To quantify how much propiconazole had been translocated to different plant heights, each plant was immediately cut into three segments (0 to 1 cm above the soil surface, 1 to 2 cm, and 2 to 3 cm) using a sterile razorblade. Leaf blades were weighed before extraction, individually placed in 2-mL microcentrifuge tubes, and frozen at -80°C until further processing. The entire study was repeated twice with three replicates per treatment per time point.

Sample Preparation. Each 1-cm sample of creeping bentgrass was transferred to an individual lysing matrix D tube, and 25 μL of the internal standard propiconazole d5 ($1 \mu\text{g mL}^{-1}$) was applied directly to the leaf material (final concentration of 25 ng mL^{-1}). The d5 was left to adhere to the leaf material for 5 min, and then 975 μL of ACN:H₂O (80:20, v/v) was added for a final volume of 1 mL. Samples were macerated using an MP Biomedicals FastPrep-24 benchtop homogenizer at 6 m s^{-1} for 40 s and then centrifuged at 5,000 rpm for 5 min. Following centrifugation, 50 mg of MgSO₄ and 15 mg of anhydrous sodium acetate were added to remove

excess water from the sample. Samples were again centrifuged at 5,000 rpm for 5 min to separate solid and liquid portions, and the entire liquid portion from the top was removed via pipette and transferred to a 2-mL d-SPE tube, shaken vigorously by hand for one min, and centrifuged a third time at 5,000 rpm for 5 min. All liquid was transferred to a 2-mL amber glass sample vial (Fisher Scientific Co.) for liquid chromatography-tandem mass spectrometry (LC-MS/MS) analysis.

LC-MS/MS Quantification and Analysis. Quantitative analysis of propiconazole and d5 was performed on an Agilent 1260 HPLC coupled to a 6460 Triple Quadrupole MS and supported by a Peak NM32LA Nitrogen Generator. Standard solutions of propiconazole and propiconazole d5 were prepared at concentrations of 1, 5, 10, 25, 50, and 100 ng mL⁻¹ to evaluate method accuracy. Chemical separation was achieved using an Agilent Poroshell 120 EC-C18 column (3.0 mm x 50 mm, 2.7 µm particle size). An isocratic gradient using 40% solvent A (10:90 v:v ACN:H₂O and 0.1% formic acid) and 60% solvent B (100% ACN) was used. The mobile phase flow rate was 0.25 mL min⁻¹, and the column temperature was set at 30°C. The injection volume was 5 µL for all standards and sample extracts. Mass spectrometry analysis used positive electrospray ionization (ESI) with the following source parameters: capillary voltage of 3,500 V, nebulizer pressure of 45 psi, gas flow of 7 L min⁻¹, gas temperature of 300°C, sheath gas flow of 10 L min⁻¹, and sheath gas temperature of 350°C. Detection was acquired using multiple reaction monitoring (MRM detection) with a dwell time of 200 ms. Ion transitions 342.1/158.9 *m/z* for propiconazole and 347.1/159 *m/z* for d5 were quantified using Agilent's MassHunter Workstation software. Initial sample aliquots with concentrations above the range of calibration were diluted 1:10 or 1:100 and re-analyzed. Given the known concentration of d5 applied, a conversion factor (CF) for each raw value was calculated by dividing the acquired concentration of the internal standard over the expected concentration, according to **eq 1**:

$$CF = \frac{C_{d5 \text{ acquired}} (ng \text{ mL}^{-1})}{C_{d5 \text{ expected}} (ng \text{ mL}^{-1})} \quad (1)$$

The amount of active ingredient measured on the LC-MS/MS in each sample (C_x) in $ng \text{ mL}^{-1}$ was then multiplied to the CF to obtain the corrected propiconazole concentration (CC_x) as shown in **eq 2**:

$$CC_x (ng \text{ mL}^{-1}) = CF * C_x \quad (2)$$

Before converting the raw data, the 1-cm leaf samples were weighed (approximately 0.0023g) to account for the mass per volume ratio during extraction. With this information, **eq 3** was used to transform the raw data to $\mu g \text{ g}^{-1}$ of leaf tissue sampled before statistical analysis:

$$CC_x * \left(\frac{1 \mu g}{1000 ng} \right) * \left(\frac{1 mL}{0.0023 g} \right) * (Dil. Factor) = CC_x (\mu g \text{ g}^{-1}) \quad (3)$$

LC-MS/MS Method Validation. Recovery experiments were performed to verify the effectiveness of the propiconazole extraction method. Four replicates of both leaf and pure solution were analyzed following the addition of 25 ng mL^{-1} propiconazole and 25 ng mL^{-1} propiconazole d5. Standard curves demonstrated optimal linearity ($R^2 > 0.994$) for each compound (data not shown). Pesticide extraction and matrix effects showed average recoveries of 106.27% (n=4) for propiconazole and 99.86% (n=4) for propiconazole d5. The limits of detection (LOD) and quantification (LOQ) of propiconazole were calculated from the signal-to-noise ratio corresponding to 3 and 10 times the noise level, respectively. The LOD and LOQ were 1.36 and 4.12 ng mL^{-1} , respectively.

Data Processing and Statistical Analysis. A linear mixed-effects (LME) model using the *lme4* package in R software, version 3.6.2, was used to predict and evaluate the effect of temperature, time, and leaf segment on propiconazole uptake. Before utilizing the model, normality of residuals and homogeneity of variance were tested using the Shapiro-Wilk test and

Levene's test, respectively. Since these conditions were not met, the propiconazole uptake data from each run was log transformed using the *BestNormalize* package. Outliers from the log-transformed data were then identified using the Interquartile Range (IQR) method in R and excluded from the analysis.

Temperature, time, and leaf segment were incorporated as fixed effects, including their interaction, into the LME model for both runs. Considering that leaf segments from the same leaf blade sample were not independent, intercepts for samples were classified as random effects. To test the significance of our random effects, we compared our LME with a linear regression model that excluded the random effect, using a log-likelihood ratio (LL) test and the Akaike Information Criterion (AIC) via ANOVA (R function: ANOVA), where lower AIC and higher LL ratio scores indicated the best fit model (**Table S1**). Based on the fit statistics, random effects were not significant in Run 1 (p-value = 0.12) or in Run 2 (p-value = 0.08). Despite the random effects not being statistically significant, AIC and LL values were still lower and higher, respectively, when using the LME model and was, ultimately, the model chosen to complete our analysis.

Pairwise differences of estimated marginal means (EMMs) for the fixed factors were computed using the *emmeans* package to compare the difference between uptake of propiconazole in the leaf segments throughout the varying temperatures and time. The role of EMMs was to estimate each fixed factor's marginal means used on the LME model. This estimation allowed equal weight to each data point, thus providing a predicted value leaning towards normality. The level of statistical significance was set at $p < 0.05$.

The performance of the LME analysis was also assessed to develop a fungicide uptake prediction model. The total model, which included all fixed effects, and univariate models that included one variable at a time, were generated. This assessment was done to determine the

proportion of fungicide uptake variation explained by the fixed effects conjunctively and individually. Predictive power was calculated as the proportion of explained variance (R^2) using the *MuMIN* package in R.

Results

Table 5. 1 Average raw uptake amount of propiconazole ($\mu\text{g g}^{-1}$) from leaf segments at varying time points per temperature per run^a

Run	Time (hpi)	Temperature (°C)	<i>Average Residual Amount ($\mu\text{g g}^{-1}$) per Leaf Segment (cm)</i>					
			0-1		1-2		2-3	
			Mean	SE	Mean	SE	Mean	SE
1	24	1	101.28	34.26	0.00	0.00	0.00	0.00
		10	221.75	76.53	8.91	3.50	4.18	2.21
		14	138.51	98.36	9.94	5.34	4.21	2.34
		22	89.47	25.29	14.09	13.07	18.21	17.20
	48	1	260.87	41.67	3.99	1.62	1.28	0.82
		10	77.66	34.03	8.30	1.12	3.10	0.34
		14	35.83	16.77	3.08	1.48	1.74	0.62
		22	38.93	10.55	4.11	1.02	3.35	1.64
	72	1	421.24	421.24	1.29	0.54	0.23	0.11
		10	547.97 ^b	350.94	13.72	4.99	2.66	1.33
		14	0.00	0.00	2.57	1.29	3.16	1.94
		22	303.39	145.93	3.17	2.63	1.78	1.45
2	24	1	76.49	27.65	0.00	0.00	0.79	0.79
		10	81.63	63.05	0.58	0.26	2.61	2.45
		14	127.13	11.45	19.95	10.05	0.12	0.09
		22	64.66	28.62	7.47	6.81	0.00	0.00
	48	1	144.69	9.58	0.96	0.36	0.32	0.20
		10	55.68	39.77	0.31	0.20	1.04	0.77
		14	182.58 ^b	12.19	2.24	1.28	8.61	7.78
		22	77.72	65.25	1.03	0.40	1.08	0.67
	72	1	25.40	25.22	0.00	0.00	0.35	0.35
		10	12.83	1.99	0.71	0.71	0.57	0.57
		14	12.98	12.98	0.02	0.02	0.00	0.00
		22	101.11	81.43	0.11	0.11	0.00	0.00

^aThe data presented are the mean value \pm the standard error (SE), n= 3; ^bHighest uptake of propiconazole in both runs; ^chpi=hours post-application.

Propiconazole Concentration in Leaf Segments. The highest concentration of propiconazole across all temperatures and time points was detected in the 0 to 1 cm leaf segment, averaging $547.97 \pm 350.94 \mu\text{g g}^{-1}$ and $182.58 \pm 12.19 \mu\text{g g}^{-1}$ in runs 1 and 2, respectively (**Table**

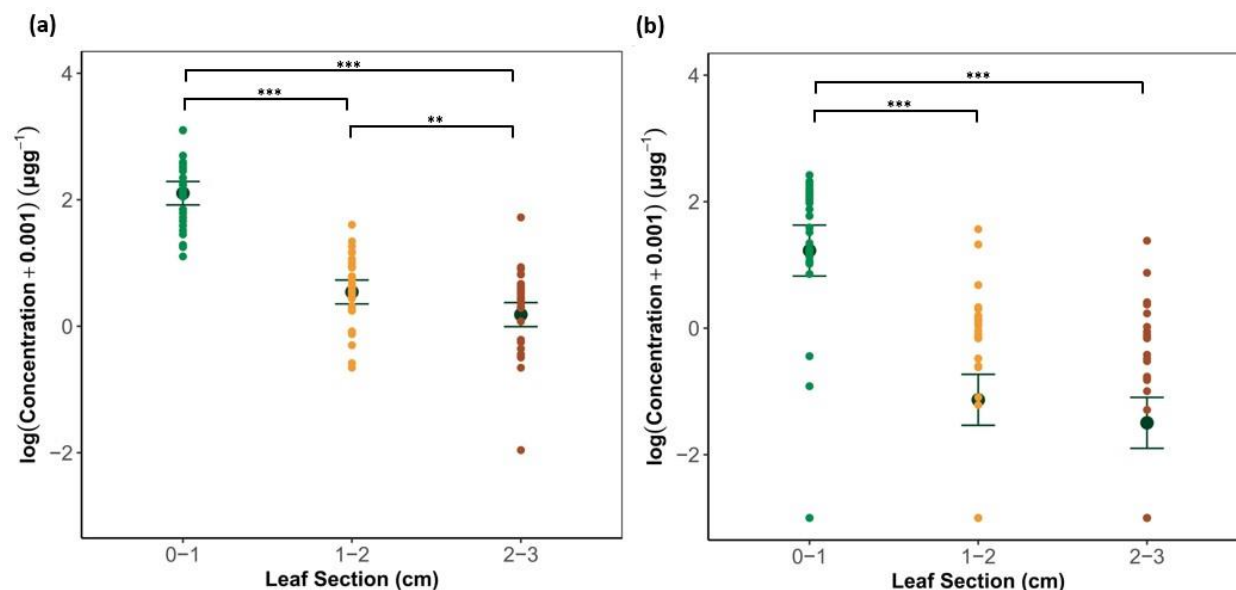


Figure 5.3 Log-transformed propiconazole concentrations detected in 0-1 (green), 1-2 (yellow), and 2-3 cm (red) leaf blade segments (n=3) for **(a)** Run 1 and **(b)** Run 2. Results are presented as the raw normalized values. An estimated marginal means \pm 1 SE was implemented for pairwise comparison and statistical analysis of the significance between each leaf segment, presented by the black dots. Double asterisks (**) indicate $p \leq 0.01$; and triple asterisks (***) indicate $p \leq 0.001$.

5.1). Overall, the raw average residual amount of propiconazole ranged from $0.21 \pm 0.18 \mu\text{g g}^{-1}$ to $318.15 \pm 135.57 \mu\text{g g}^{-1}$ over the time points and $0.32 \pm 0.19 \mu\text{g g}^{-1}$ to $282.46 \pm 125.25 \mu\text{g g}^{-1}$ at the different temperatures among all leaf segment samples in both runs (**Table S2**). Translocation of propiconazole in the 1-2 cm and 2-3 cm leaf segments was significantly lower than the 0-1 cm leaf segment (**Figure 5.3**). Minor differences in propiconazole concentration between the 1-2 and 2-3 cm leaf segments were observed in Run 1 but not Run 2. We also conducted a mass balance calculation to estimate the average concentration of propiconazole found in the leaf samples compared to the total amount of propiconazole applied. The total amount of propiconazole applied to the base of each plant was $1,624 \mu\text{g}$, and the total amount detected in all the leaf segments combined was less than $0.18 \pm 0.003\%$ and $0.04 \pm 0.001\%$ in runs 1 and 2, respectively. The

highest average percent recovery was found in the 0-1 cm leaf segment at 0.026% and 0.011% for runs 1 and 2, respectively (**Figure S1**).

Time After Application and Temperature Impacts on Propiconazole Uptake.

Propiconazole concentration was highest at 48 h post-application in Run 2, but no impact of time was observed in Run 1 (**Figure 5.4a**). Also, we noticed a significant decline in concentration at 72 h in Run 2 (**Figures 5.4b and 5.5b**).

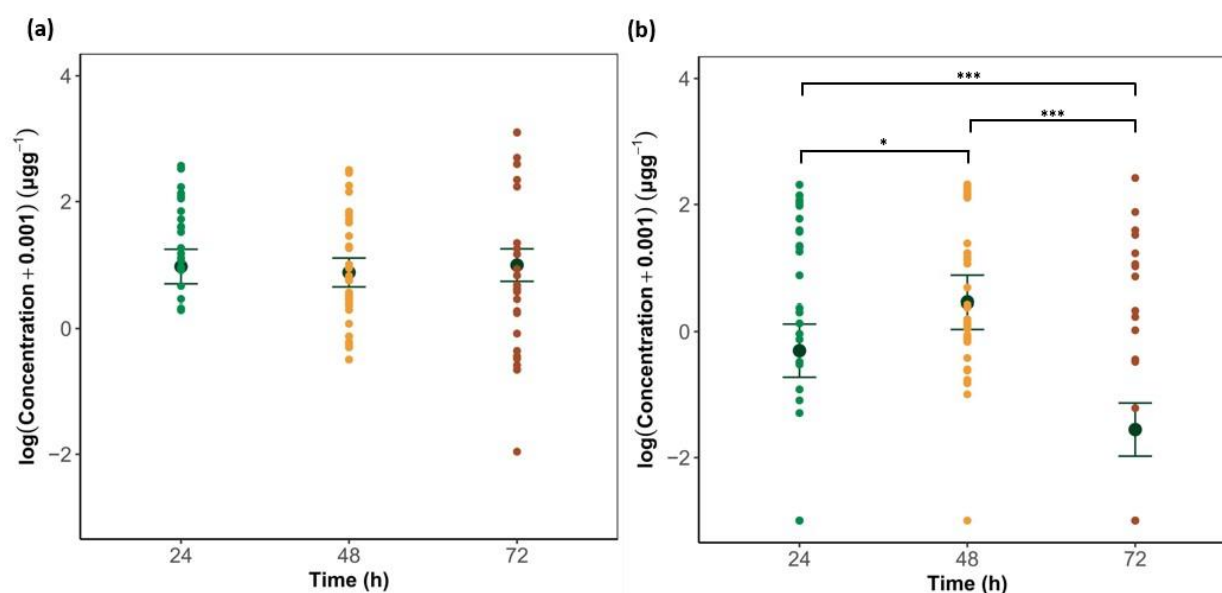


Figure 5. 4 Log-transformed propiconazole concentrations detected in samples (n=3) at 24 (green), 48 (yellow), and 72-hpi (red) for **(a)** Run 1 and **(b)** Run 2. Results are presented as the raw normalized values. An estimated marginal means ± 1 SE was implemented for pairwise comparison and statistical analysis of the significance between each timepoint, presented by the black dots. A single asterisk (*) indicates $p \leq 0.05$; and triple asterisks (***) indicate $p \leq 0.001$.

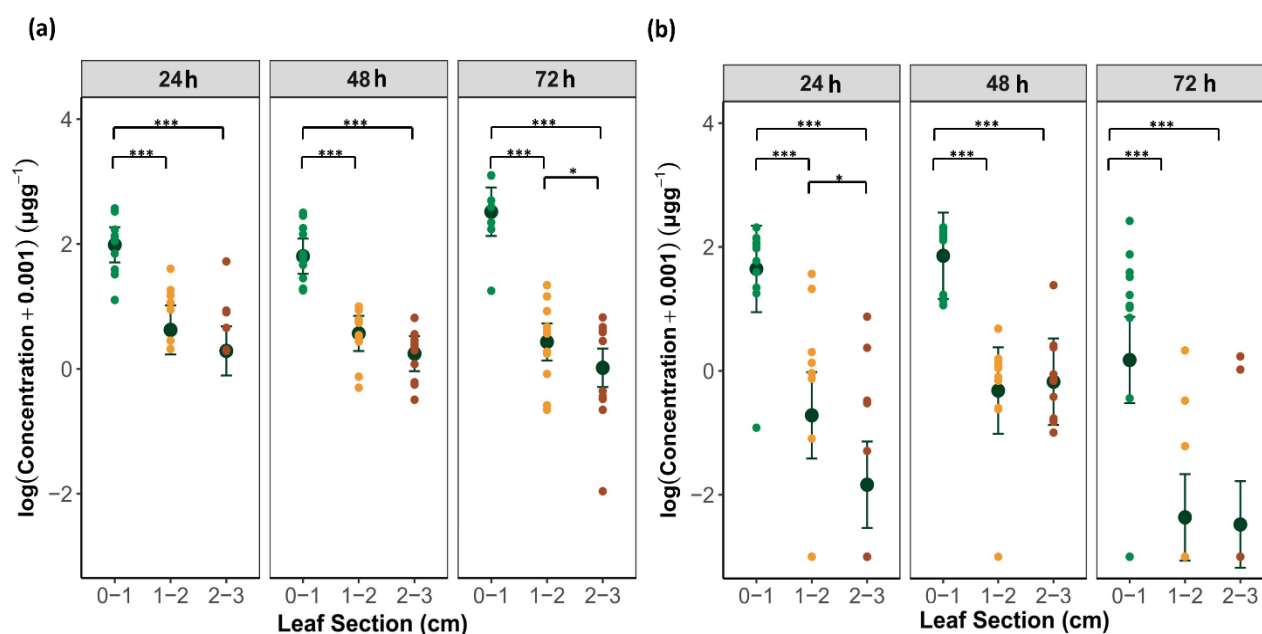


Figure 5.5 Log-transformed propiconazole concentration detected in 0-1 (green), 1-2 (yellow), and 2-3 cm (red) leaf blade segments at 24, 48, and 72-hpi for (a) Run 1 and (b) Run 2. Results are presented as the raw normalized values. An estimated marginal means ± 1 SE was implemented for pairwise comparison and statistical analysis of the significance between each leaf segment at each timepoint, presented by the black dots. A single asterisk (*) indicates $p \leq 0.05$; and triple asterisks (***) indicate $p \leq 0.001$.

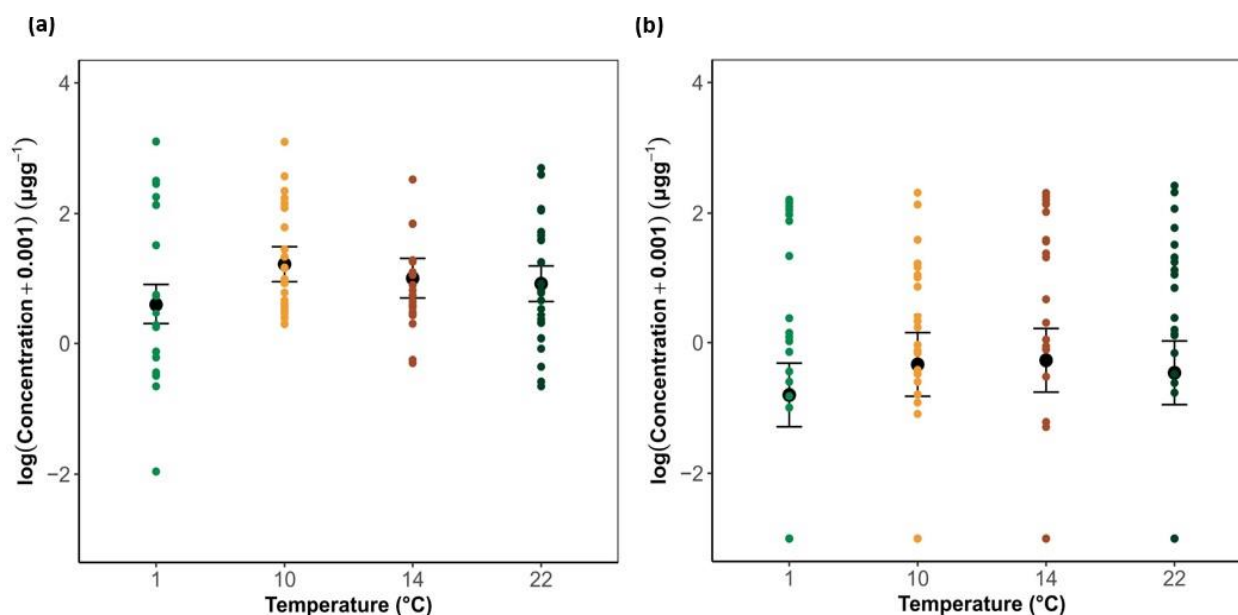


Figure 5.5 Log-transformed propiconazole concentration detected at temperatures 1 (green), 10 (yellow), 14 (red), and 22 °C (dark green) in (a) Run 1 and (b) Run 2. Results are presented as the raw normalized values. An estimated marginal means ± 1 SE was implemented for pairwise comparison and statistical analysis of the significance between each temperature, presented by the black dots.

Overall, there was no impact of temperature on propiconazole uptake (**Figure 5.6**). However, when looking more specifically at leaf segments within each run, we observed propiconazole concentrations in Run 1 increased in the 1-2 and 2-3 cm leaf segment at 10 and 22°C compared to 1°C (**Figure 5.7**).

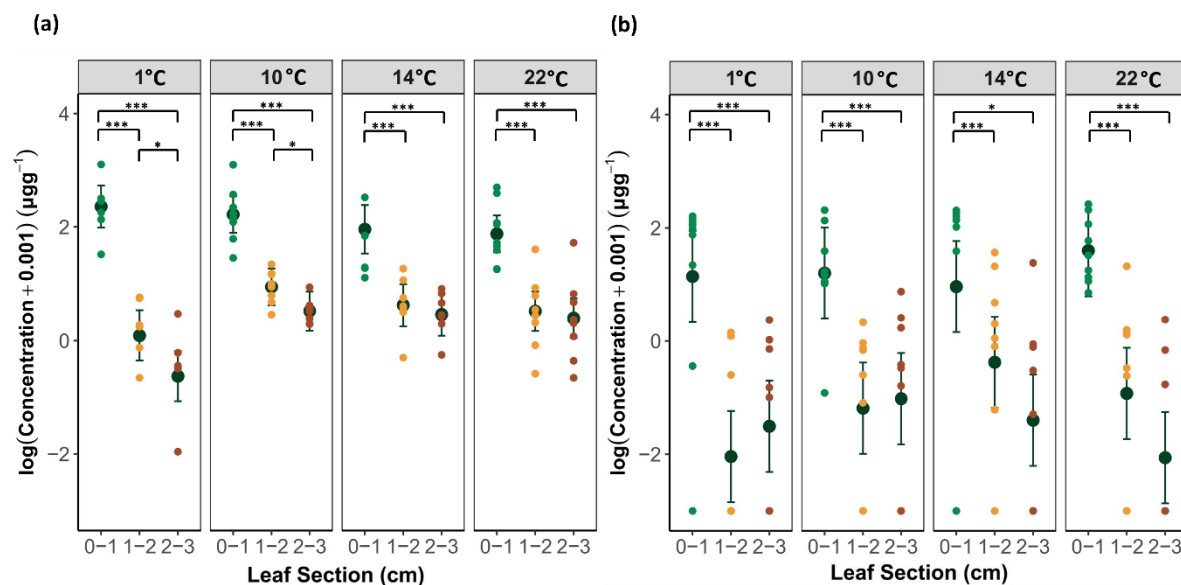


Figure 5. 6 Log-transformed propiconazole concentration detected in 0-1 (green), 1-2 (yellow), and 2-3 cm (red) leaf blade segments at 1, 10, 14, and 22°C for (a) Run 1 and (b) Run 2. Results are presented as the raw normalized values. An estimated marginal means \pm 1 SE was implemented for pairwise comparison and statistical analysis of the significance between each leaf segment at each temperature, presented by the black dots. A single asterisk (*) indicates $p \leq 0.05$; and triple asterisks (***) indicate $p \leq 0.001$.

Linear Mixed Effects of Propiconazole Uptake. An LME model analysis was used to evaluate the effect of temperature, time, leaf segment, and their interactions on propiconazole uptake. Coefficient estimates (B), confidence intervals (CI), p-values (P), and degrees of freedom (df) for each predictor and their interactions are provided in **Table S3**. Time (Run 1: B = 0.01, P = 0.249; Run 2: B = -0.04, p-value= 0.084; **Figure 5.4**), temperature (Run 1: B = -0.05, P = 0.136; Run 2: B = -0.04, P = 0.341; **Figure 5.6**), and their interactions (Run 1: B = -0.00, P = 0.986; Run 2: B = -0.00, P = 0.869) suggest that both individual and interactive effects did not influence

propiconazole translocation. In Run 1, time and its interaction with leaf segment ($B = -0.01$, $P = 0.016$) significantly influenced propiconazole uptake (**Figure 5.5a**). In contrast to Run 1, we did not observe an effect of the interaction between time and leaf segment ($B = 0.01$, $P = 0.301$) on uptake in Run 2 (**Figure 5.5b**). Leaf segment (Run 1: $B = -0.75$, $P = 0.002$; Run 2: $B = -1.51$, $P = 0.003$) influenced uptake in both runs as shown in **Figure 5.3**. Further, we observed a significant influence on propiconazole uptake between temperature and its interaction with leaf segment in Run 1 ($B = 0.03$, $P = 0.007$) but not in Run 2 ($B = -0.02$, $P = 0.291$) (**Figure 5.7**).

Development of a Fungicide Uptake Prediction Model. The LME analysis was further used to generate a model to predict propiconazole uptake. Temperature, time, and leaf segment were used as the explanatory variables. A random effect was based on the overall leaf blade sample to account for the variability of each leaf segment. The predictive power (r^2) of the total LME model was 0.714 and 0.52 when random effects were included and 0.638 and 0.399 when random effects were excluded from Runs 1 and 2, respectively (**Table S3, Figure 5.8**). Univariate models showed considerable variation in predictive power between fungicide uptake and explanatory variables from both runs, especially with the leaf segment variable. Leaf segment significantly

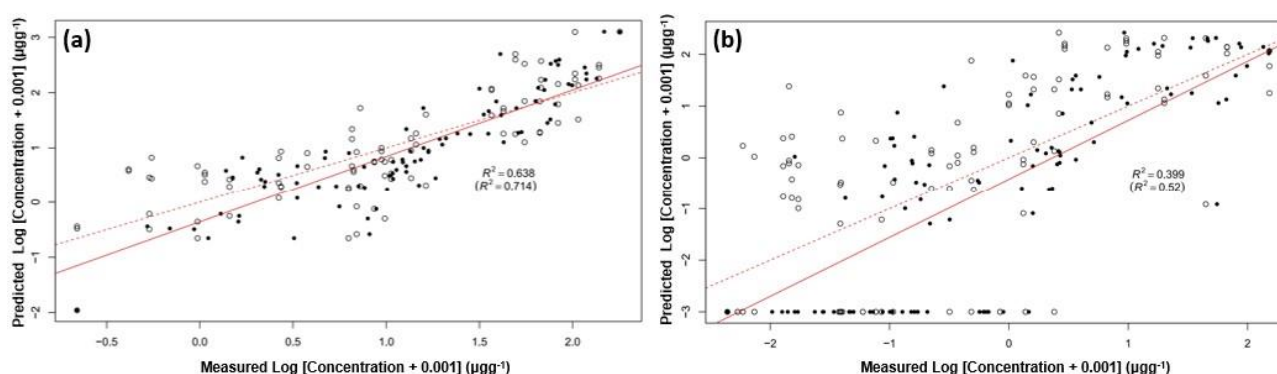


Figure 5. 7 Correlation between measured and predicted log transformed propiconazole uptake in (a) Run 1 and (b) Run 2. Predictive power of linear mixed effect models including temperature, time, and leaf segment as the explanatory variables. All panels show dots for predicted versus measured values of propiconazole uptake, with black dots including and open dots excluding random effects. Red solid lines and dotted lines depict the model fits when random effects are included (R^2 value in parentheses) and excluded (upper R^2 value), respectively.

increased the predictive power of the model, which was retained after excluding the random effects (Run 1: from $r^2 = 0.665$ to $r^2 = 0.570$; Run 2: from $r^2 = 0.502$ to $r^2 = 0.327$) (**Figures 5.9a and 5.9b**). In contrast, uptake did not exhibit a strong association with time post- application. Uptake was associated equally with time in Run 1 ($r^2 = 0.061$) and Run 2 ($r^2 = 0.069$) when random effects were included and excluded (**Figures 5.9c and 5.9d**). Temperature was the weakest predictor of fungicide uptake with an r^2 of 0.001 and 0.026 for Runs 1 and 2, respectively. Yet, excluding the random effects continued to show that r^2 decreased markedly in both runs (Run 1: $r^2 = 0.001$ and Run 2: $r^2 = 0.004$; random effects excluded). Overall, models with leaf segment or temperature as

the explanatory variables showed that predictive power decreased significantly when random effects were excluded from the model (**Figure 5.9**).

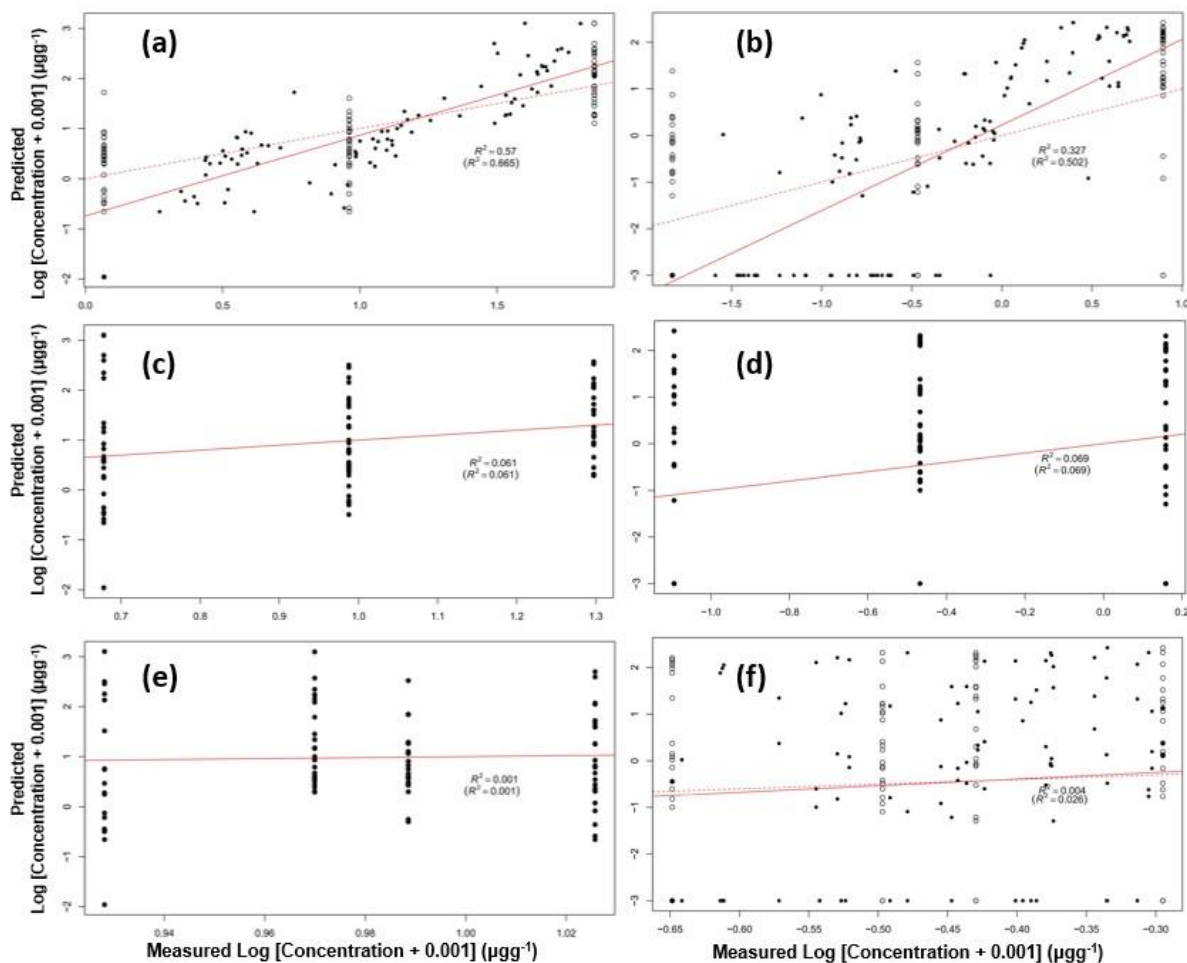


Figure 5. 8 Correlation between measured and predicted log transformed propiconazole uptake in Run 1 (**a**, **c**, **e**) and Run 2 (**b**, **d**, **f**). Predictive power of linear mixed effect models of the individual explanatory variables, (**a**) and (**b**) leaf segment, (**c**) and (**d**) time, and (**e**) and (**f**) temperature. All panels show dots for predicted versus measured values of propiconazole uptake, with black dots including and open dots excluding random effects. Red solid lines and dotted lines depict the model fits when random effects are included (R^2 value in parenthesis) and excluded (upper R^2 value), respectively.

Discussion

The results from our research clearly indicate that leaf segment was the most influential factor in determining propiconazole concentration (**Figure 5.3**, **Table S3**). Propiconazole concentrations were highest in the 0-1 cm leaf segment regardless of temperature or time after

application (**Figures 5.5 and 5.7**). While it is unclear why there was a negligible upward movement of propiconazole in our study (**Figure S1**), past research and resources addressing fungicide uptake can offer potential perspective.⁷ As an acropetal penetrant fungicide, propiconazole is subject to a water potential gradient where it moves from the base of the plant toward the apex as it diffuses through the cuticle and enters the xylem.⁷ However, the base of the turfgrass plant is typically surrounded by a mix of leaf, stem, and soil material that is high in organic matter and may tightly sorb fungicides. Our results (**Figures 5.3 and 5.5**) are consistent with that of a previous study that found propiconazole concentrations were negligible in Kentucky bluegrass leaf residues seven days after application but high in the thatch layer found near the base of the plant that is rich in organic matter.²⁰ Studies performed in rice-paddy soil also showed that propiconazole remained sorbed where organic matter was the highest.²¹ According to the mobility classification system developed by the Food and Agriculture Organization (FAO), the predicted $\log K_{oc}$ of propiconazole, 3-4 L kg⁻¹, suggests that this compound is moderately sorptive in soil, which may explain the limitation of translocation into the turfgrass plant.^{7,22,23}

Previous research has found that fungicide uptake is influenced by temperature and several other environmental factors,²⁴ so we hypothesized that propiconazole uptake in our study would decrease at lower temperatures due to decreased acropetal translocation rates. However, our results showed little influence of temperature on propiconazole uptake (**Figure 5.6**). In general, there were no apparent effects of temperature among the varying leaf segments, especially in the second run of the study. In terms of temperature, Namiki et al.²⁵ found that pesticide uptake via the roots, with the exception of tolclofos-methyl, increased significantly with increasing temperature between 15°C and 25°C in spinach leaves. However, the varying results presented among different studies demonstrate that other key factors (physicochemical properties, soil moisture, pH, organic carbon

content) involved in determining the fate and behavior of pesticides should also be considered. Examples of these key factors are shown in Shone and Wood,¹⁵ where physical sorption and pH played a significant role in retaining pesticides in the roots. Our findings support these previous studies and indicate that a complex mixture of environmental factors, soil properties, and pesticide characteristics determine pesticide uptake rather than a single factor such as temperature.^{15,17,25}

The LME models we created that excluded random effects performed poorly in predicting propiconazole uptake. The inclusion of random effects suggests that the variation between samples allows us to improve our ability to describe how the explanatory variables are related to fungicide uptake. When explanatory variables were assessed separately, leaf segment was the strongest predictor in uptake when random effects were included in our analysis, followed by time after application and temperature (**Figure 5.9**). Time after application and temperature did not show meaningful predictive power in either of our runs when evaluated individually. Similar to the LME analysis, our results demonstrate the high variability in temperature effects between both runs. While various models have been developed to predict the uptake and translocation of organic chemicals in crop plants,^{17,26–28} a consensus has not been reached to determine a universal model that may be applied to a wide range of pesticides with different physicochemical properties. The partition-limited model^{17,29} is mainly applied in the passive uptake of chemicals from soil or water to plants and assumed that equilibrium between the chemical in the external water and the chemical in the plant has been reached. Another predictive tool that has been developed involves the use of the type of plant species, pesticide mobility within soil, plant transpiration stream, and plant growth, among other parameters to assess plant uptake.²⁶ Other studies have focused solely on creating simple qualitative models to predict foliar uptake.³⁰ The fungicide uptake prediction model presented here was developed using the established LME analysis and applied in our study

with special interest in determining the effectiveness of leaf segment, time, and temperature as predictors of propiconazole uptake. Although certain limitations in the accurate determination of fungicide uptake in turfgrass arise in our model, it may still be implemented as a prediction tool that would improve our understanding of the uptake and translocation of commonly applied fungicides in turfgrass that have similar modes of action and physicochemical properties as propiconazole (i.e., azoxystrobin, fluoxastrobin, and tebuconazole).⁷ However, further research in the field and with additional fungicides is required to confirm our findings and validate our pesticide uptake prediction model under field conditions.

Another interesting observation in our study was the low amount of propiconazole found in the leaves compared to the initial amount added. Only 0.18% and 0.04% of applied propiconazole was detected in the entire plant in Run 1 and 2, respectively. While sorption to soil may limit the mobility of propiconazole under our experimental conditions, other factors may contribute to limited uptake by turfgrass. One potential explanation for the lack of propiconazole uptake into the plant is the soil moisture content in the growing medium. Roy et al.³¹ found that propiconazole sorbed more strongly to soil organic matter when soil moisture was low (26.1% volumetric water content), which limited uptake through the plant roots. Although soil moisture and soil water content were not measured in our study, it is possible that water deficiency at points during the study led to reduced propiconazole uptake beyond the lower segment of the plant. Another explanation for the lack of uptake may be the physiological growth process of the turfgrass plant. New turfgrass leaves emerge from the center of the plant near the top, leaving the oldest leaves in the outermost and lowest region.⁷ In our study, we deposited propiconazole adjacent to the base of the plant near the oldest leaves, which would likely result in accumulation near the base of the plant and may have limited translocation to the newly emerging leaves near the top.

Because each plant was maintained at a 3-cm height and maintained as one single stem for ten weeks, this process may have also inadvertently removed older leaves that had retained the pesticide. Finally, the lack of propiconazole uptake may be attributable to limited root development needed to absorb the fungicide. Propiconazole is an acropetal penetrant and relies on a well-developed root system for efficient absorption.⁷ A mature and dense root system would increase the absorption of propiconazole, and it is possible that the 10-wk age of our plants was not sufficient to promote root growth that would effectively absorb the fungicide.^{32,33}

Although the trends with respect to leaf section and time were similar across the duplicate runs, there was a large difference in the overall amount of propiconazole detected in the plants between runs 1 and 2. We can determine no obvious reasons for these differences as the methods used were identical in both runs. However, possible reasons for this difference include pesticide application procedure, preparation of the artificial growth medium, and maintenance of the leaf samples. In other words, it is possible that leaf samples in the second run were exposed to a lower concentration of propiconazole, which would, in part, also explain the differences in the average raw uptake presented in **Table 5.1**. The differences in Runs 1 and 2 further highlight the need for independent replicates in complex environmental systems.

These research results have important implications for the effective use of fungicides to treat diseases predominant in cold environments and their potential non-target environmental impact. The apparent lack of significant mobility above the bottom cm of the plant, regardless of temperature, suggests that turfgrass managers need to focus on good product coverage rather than rely on redistribution of the fungicide through uptake and translocation to achieve acceptable disease control. Good product coverage can be achieved through the selection of proper nozzles, water volume, sprayer speed, and several other factors.⁷ Only approximately 0.1% of the applied

fungicide was absorbed into the plant in our study, meaning that 99.9% was available for non-target contamination. This is similar to pesticide mass balance calculations in other research on pesticide fate but still indicates the need to further study the non-target fate of fungicides and other pesticides applied in cold environments.³⁴ Application methods that increase pesticide absorption and retention into or on the plant in cold environments would not only improve the level of plant disease control but also lessen the amount of pesticide available for potential non-target impacts.

This study indicates that propiconazole does not significantly translocate upwards beyond the bottom 1 cm of a turfgrass plant, regardless of temperature or the time following application. Future research on plant uptake of fungicides should implement controls for environmental variables such as soil moisture and soil organic carbon content, significantly influencing the degree of pesticide uptake. Replicating this work in a hydroponic system would greatly reduce the variability of the growing media and more precisely allow for the uptake and measurement of propiconazole from the water into the plant leaves. Implementing other parameters in our prediction model, such as the fungicide's physicochemical properties, root-soil transfer rate, plant type and growth, may also provide a more accurate understanding of how fungicides are absorbed and translocated in varying environmental conditions, with a particular interest in managing low-temperature diseases in turfgrass landscapes.

Abbreviations Used

DMI, demethylation inhibitor; d-SPE, dispersive solid-phase extraction; ACN, acetonitrile; LC-MS/MS, liquid chromatography-tandem mass spectrometry; ESI, electrospray ionization; CF, conversion factor; C_x , amount of active ingredient measured; CC_x , corrected concentration; LME, linear mixed-effects; LL, log-likelihood; AIC, Akaike information criterion.

References

- (1) Hsiang, T.; Liao, A.; Benedetto, D. Sensitivity of *Sclerotinia Homoeocarpa* to Demethylation-Inhibiting Fungicides in Ontario, Canada, after a Decade of Use. *Plant Pathology* **2007**, *56* (3), 500–507.
- (2) Mann, R. L.; Newell, A. J. A Survey to Determine the Incidence and Severity of Pests and Diseases on Golf Course Putting Greens in England, Ireland, Scotland, and Wales. *A survey to determine the incidence and severity of pests and diseases on golf course putting greens in England, Ireland, Scotland, and Wales*. **2005**, *10*, 224–229.
- (3) Hsiang, T.; Matsumoto, N.; Millett, S. M. Biology and Management of *Typhula* Snow Molds of Turfgrass. *Plant Disease* **1999**, *83* (9), 788–798.
- (4) Dahl, A., S. Snowmold of Turf Grasses as Caused by *Fusarium Nivale*. *Phytopath* **1934**, *24* (3), 197–214.
- (5) Koch, P. L.; Stier, J. C.; Kerns, J. P. Snow Cover Has Variable Effects on Persistence of Fungicides and Their Suppression of *Microdochium* Patch on Amenity Turfgrass. *Plant Pathology* **2015**, *64* (6), 1417–1428.
- (6) Leslie, A. R. *Handbook of Integrated Pest Management for Turf and Ornamentals*; Taylor & Francis, 1994.
- (7) Latin, R. *A Practical Guide to Turfgrass Fungicides*; Mycology; The American Phytopathological Society, 2017.
- (8) Tomlin, Clive. *The Pesticide Manual: A World Compendium: Incorporating the Agrochemicals Handbook*; British Crop Protection Council ; Royal Society of Chemistry, Information Sciences: Farnham, Surrey; Cambridge, 1994.

- (9) USEPA. Reregistration Eligibility Decision (RED) for Propiconazole Case No. 3125. July 18, 2006.
- (10) Ulrich, N.; Endo, S.; Brown, T. N.; Watanabe, N.; Bronner, G.; Abraham, M. H.; Goss, K.-U. UFZ - LSER Database Available from <http://www.ufz.de/lserd> (accessed Feb 10, 2021).
- (11) Bromilow, R. H.; Evans, A. A.; Nicholls, P. H. Factors Affecting Degradation Rates of Five Triazole Fungicides in Two Soil Types: 2. Field Studies. *Pesticide Science* **1999**, 55 (12), 1135–1142.
- (12) Matthiesen, R. L.; Ahmad, A. A.; Robertson, A. E. Temperature Affects Aggressiveness and Fungicide Sensitivity of Four *Pythium* Spp. That Cause Soybean and Corn Damping Off in Iowa. *Plant Disease* **2015**, 100 (3), 583–591.
- (13) Whittle, C. M. Translocation and Temperature. *Annals of Botany* **1964**, 28 (110), 339–344.
- (14) Baur, P.; Schönherr, J. Temperature Dependence of the Diffusion of Organic Compounds across Plant Cuticles. *Chemosphere* **1995**, 30 (7), 1331–1340.
- (15) Shone, M. G. T.; Wood, A. V. A Comparison of the Uptake and Translocation of Some Organic Herbicides and a Systemic Fungicide by Barley: I. Absorption in Relation to Physico-Chemical Properties. *Journal of Experimental Botany* **1974**, 25 (85), 390–400.
- (16) Gauvrit, C.; Gaillardon, P. Effect of Low Temperatures on 2,4-D Behaviour in Maize Plants. *Weed Research* **1991**, 31 (3U)SE, 135–142.
- (17) Ju, C.; Zhang, H.; Yao, S.; Dong, S.; Cao, D.; Wang, F.; Fang, H.; Yu, Y. Uptake, Translocation, and Subcellular Distribution of Azoxystrobin in Wheat Plant (*Triticum Aestivum* L.). *J. Agric. Food Chem.* **2019**, 67 (24), 6691–6699.

- (18) Robinson, M. A.; Letarte, J.; Cowbrough, M. J.; Sikkema, P. H.; Tardif, F. J. Winter Wheat (*Triticum Aestivum* L.) Response to Herbicides as Affected by Application Timing and Temperature. *Can. J. Plant Sci.* **2015**, 95 (2), 325–333.
- (19) NOAA Online Weather Data - Madison Dane Co, WI Daily Data for a Month <https://w2.weather.gov/climate/xmacis.php?wfo=mkx> (accessed Mar 3, 2020).
- (20) Schumann, G.L.; Clark, J.M.; Doherty, J.J.; Clarke, B.B. Application of DMI Fungicides to Turfgrass with Three Delivery Systems. In *Fate and Management of Turfgrass Chemicals*; American Chemical Society: Washington, DC; Vol. 743, pp 150–163.
- (21) Kim, I. S.; Beaudette, L. A.; Shim, J. H.; Trevors, J. T.; Suh, Y. T. Environmental Fate of the Triazole Fungicide Propiconazole in a Rice-Paddy-Soil Lysimeter. *Plant and Soil* **2002**, 239 (2), 321–331.
- (22) US EPA, O. Guidance for Reporting on the Environmental Fate and Transport of the Stressors of Concern in Problem Formulations <https://www.epa.gov/pesticide-science-and-assessing-pesticide-risks/guidance-reporting-environmental-fate-and-transport> (accessed Mar 5, 2021).
- (23) Assessing soil contamination A reference manual <http://www.fao.org/3/X2570E/X2570E06.htm> (accessed Mar 5, 2021).
- (24) Wauchope, R. D.; Yeh, S.; Linders, J. B. H. J.; Kloskowski, R.; Tanaka, K.; Rubin, B.; Katayama, A.; Kördel, W.; Gerstl, Z.; Lane, M.; Unsworth, J. B. Pesticide Soil Sorption Parameters: Theory, Measurement, Uses, Limitations and Reliability. *Pest Management Science* **2002**, 58 (5), 419–445.
- (25) Namiki, S.; Otani, T.; Motoki, Y.; Seike, N. The Influence of Brassica Rapa Var. Perviridis Growth Conditions on the Uptake and Translocation of Pesticides. *J Pestic Sci* **2018**, 43 (4), 248–254.

- (26) Hwang, J.-I.; Lee, S.-E.; Kim, J.-E. Comparison of Theoretical and Experimental Values for Plant Uptake of Pesticide from Soil. *PLoS One* **2017**, *12* (2).
- (27) Briggs, G. G.; Bromilow, R. H.; Evans, A. A. Relationships between Lipophilicity and Root Uptake and Translocation of Non-Ionised Chemicals by Barley. *Pesticide Science* **1982**, *13* (5), 495–504.
- (28) Trapp, Stefan.; Matthies, Michael. Generic One-Compartment Model for Uptake of Organic Chemicals by Foliar Vegetation. *Environ. Sci. Technol.* **1995**, *29* (9), 2333–2338.
- (29) Chiou, C. T.; Sheng, G.; Manes, M. A Partition-Limited Model for the Plant Uptake of Organic Contaminants from Soil and Water. *Environ. Sci. Technol.* **2001**, No. 35, 1437–1444.
- (30) Stock, D.; Holloway, P. J.; Grayson, B. T.; Whitehouse, P. Development of a Predictive Uptake Model to Rationalise Selection of Polyoxyethylene Surfactant Adjuvants for Foliage-Applied Agrochemicals. *Pesticide Science* **1993**, *37* (3), 233–245.
- (31) Roy, C.; Gaillardon, P.; Montfort, F. The Effect of Soil Moisture Content on the Sorption of Five Sterol Biosynthesis Inhibiting Fungicides as a Function of Their Physicochemical Properties. *Pest Management Science* **2000**, *56* (9), 795–803.
- (32) Wherley, B. G.; Sinclair, T. R.; Dukes, M. D.; Schreffler, A. K. Nitrogen and Cutting Height Influence Root Development during Warm-Season Turfgrass Sod Establishment. *Agronomy Journal* **2011**, *103* (6), 1629–1634.
- (33) Boeker, P. Root Development of Selected Turf Grass Species and Cultivars. In *Proceedings of the Second International Turfgrass Research Conference*; John Wiley & Sons, Ltd, 1974; pp 55–61.
- (34) Carriger, JohnF.; Rand, GaryM.; Gardinali, PieroR.; Perry, WilliamB.; Tompkins, MichaelS.; Fernandez, AdolfoM. Pesticides of Potential Ecological Concern in Sediment

from South Florida Canals: An Ecological Risk Prioritization for Aquatic Arthropods. *Soil & Sediment Contamination* **2006**, *15* (1), 21–45.

Supplementary Materials

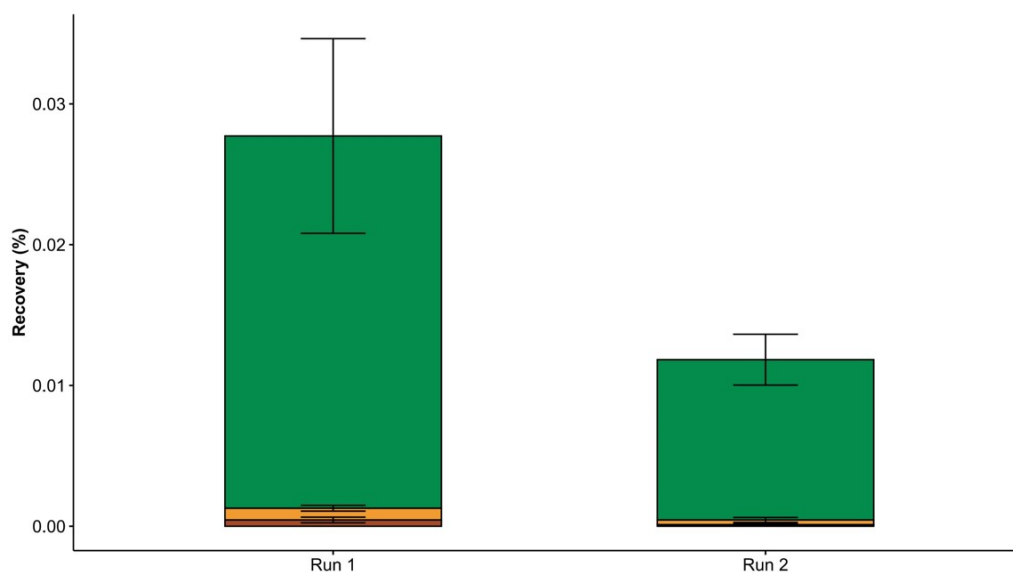


Figure S1. Mass balance for propiconazole in Run 1 and Run 2 after leaf sample collection. Fraction recoveries shown for each leaf segment, top to bottom of bars: 0-1 cm (green), 1-2 cm (orange), and 2-3 cm (red). Negligible amounts of propiconazole were detected in leaf segments compared to the initial amount, $1624 \mu\text{g mL}^{-1}$, added. Error bars represent $1 \pm \text{SE}$ ($n = 36$).

Table S1. Fit statistics for model selection between ordinary linear regression and Linear-Mixed Effects analysis.

Model	Run 1			Run 2		
	AIC ^a	LL ^b	Pr (>Chisq) ^c	AIC ^a	LL ^b	Pr (>Chisq) ^c
Linear	169.28	-76.64		407.83	-195.92	
Linear Mixed Effect	168.81	-75.41	0.1162	406.78	-194.39	0.0808

^aAIC = Akaike's information criterion; ^bLL = Log-likelihood; ^cA Chi-square test was implemented to determine the best fit model and significance of random effects.

Table S2. Overall raw uptake amount of propiconazole ($\mu\text{g g}^{-1}$) from leaf segment at varying time points and temperature per run^a

<i>Average Residual Amount ($\mu\text{g g}^{-1}$) per Leaf Segment (cm)</i>							
Run		0-1		1-2		2-3	
1	Time (hpi) ^b	Mean	SE	Mean	SE	Mean	S.E.
	24	137.76	32.12	8.24	3.47	6.65	4.27
	48	103.32	30.43	4.87	0.83	2.37	0.50
	72	318.15 ^c	135.57	5.19	1.95	1.96	0.68
	Temperature (°C)						
	1	261.13	131.01	1.76	0.77	0.51	0.31
	10	282.46 ^d	125.25	10.31	1.98	3.32	0.78
	14	58.11	35.50	5.19	2.03	3.04	0.96
	22	143.93	58.99	7.13	4.24	7.78	5.65
2	Time (hpi) ^b	Mean	SE	Mean	SE	Mean	S.E.
	24	87.48	17.60	7.00	3.55	0.88	0.63
	48	115.17	22.62	1.14	0.37	2.76	1.96
	72	38.08	21.47	0.21 ^e	0.18	0.23	0.16
	Temperature (°C)						
	1	82.20	20.56	0.32 ^f	0.19	0.49	0.27
	10	50.05	23.75	0.54	0.23	1.41	0.82
	14	107.56	25.70	7.40	4.30	2.91	2.66
	22	81.16	31.69	2.87	2.28	0.36	0.26

^a The data presented are the mean value \pm the standard error (S.E.), n= 3; ^bhpi=hours post application; ^c Highest uptake at the varying time points among both runs; ^d Highest uptake at the varying temperatures among both runs; ^e Lowest uptake at the varying time points among both runs; ^f Lowest uptake at the varying temperatures among both runs.

Chapter 6. Concluding Remarks and Future Directions

This dissertation's research provides insights into how varying seasonal environmental conditions alter soil bacterial activity, resulting in the degradation of 2,4-D and formation of its major transformation product (TP), 2,4-DCP, in urban landscapes. This dissertation provides further information on the fate and behavior of 2,4-D in urban landscapes, its potential to interact with soil bacteria, and how external environmental factors influence soil bacterial response in urban landscapes. Overall, this dissertation provides one of the building blocks for further research in the field, in bridging analytical chemical analysis with microbial ecology while integrating external environmental factors, and ultimately, help in reducing the non-target impacts of pesticide usage in home lawns and recreational areas. The key findings and future directions are summarized in the following text:

1. *2,4-D is actively being degraded in urban soils and transformed into 2,4-DCP.* 2,4-D was the most used herbicide in home lawns and gardens in 2009 and 2012.¹ Due to its frequent use in urban landscapes, it is important to better understand its adverse impacts on non-target organisms, especially its ability to undergo environmental degradation and transform into products that may behave differently.^{2,3} Additionally, because 2,4-D is commonly applied at varying seasonal conditions in urban landscapes, it is important to evaluate pesticide TP formation in these areas. Through two field trials conducted in 2018 and 2019 in two different field sites and a growth chamber study, I found that 2,4-D is degraded and transformed to 2,4-DCP in urban soils, where 2,4-DCP was also detected. Through my findings from the growth chamber study, I concluded that 2,4-D has the capacity to leach to groundwater, however, 2,4-DCP was not detected in leachate samples. While also a stable amount of 2,4-D residue was detected in leaf tissue, transformation to 2,4-DCP was

not detected. Chapter 2 suggests that 2,4-D was detected in soil, leaf, and leachate; that degradation of 2,4-D resulted in the formation of its major TP, 2,4-DCP, in urban soils through biotic transformation; and abiotic transformation may have also influenced 2,4-D breakdown but was not the main route of degradation. However, to obtain a more complete picture of the occurrence of 2,4-D in urban landscapes, abiotic transformation should be investigated along with biotic transformation. Overall, the findings from the field and growth chamber study in Chapter 2 supports our hypothesis that 2,4-D breakdown is influenced by seasonal variations and can result in the formation of 2,4-DCP in urban landscapes, mainly via bacteria degradation. This adds further support that 2,4-D along with 2,4-DCP could present increased risk to non-target organisms in urban areas such as home lawns.

2. *Soil bacterial community is distinct at varying seasonal conditions in urban landscapes.*

Temperature is one of the most important factors influencing bacterial community structure and function, which may directly or indirectly alter pesticide degradation networks resulting in the formation of TPs.⁴⁻⁶ Previous research suggests that soil microbial communities shift in structure and activity in response to various seasonal conditions.^{7,8} In Chapter 3, I assessed how varying seasonal conditions, such as temperature and soil moisture, lead to changes in soil bacterial activities and how potential environment-driven changes in that activity altered 2,4-D metabolism in urban landscapes. Using high-throughput sequencing analysis, I found that the soil bacterial community composition was distinct at varying seasonal conditions in the field and growth chamber study. Through various prediction analyses, I also found that xenobiotic degradation pathways such as benzoate degradation pathways was linked to 2,4-D degradation, specifically, form the well

well-known *tfdABCDEF* pathway discussed in Chapter 4. Overall, results from Chapter 3 tied with Chapter 2 suggest that bacteria shifted at varying seasonal conditions and were mainly involved in the degradation of 2,4-D in urban soils. Future research to expand on 2,4-D biodegradation in soil involves the assessment of other microbial communities, i.e., bacteria, fungi, archaea, and protozoa, to provide a complete assessment of how these microbes interact at varying seasonal conditions and their role in 2,4-D degradation.

3. *Previously published primers targeting the 2,4-D-degrading gene, tfdA, elicits non-specific amplification in soil samples.* The *tfdA* gene has been considered a good reporter for 2,4-D degradation activity.⁹ Bælum et al. (2009) developed a quantitative real-time PCR-based method using a TaqMan-based approach to quantify the three *tfdA* gene classes.¹⁰ In Chapter 4, I found that the three *tfdA* gene classes exhibited high variability in detection and quantification in urban soils at both field sites and growth chamber study. From these results, I hypothesized that the variability and quantification in our soil samples were due to non-target amplification in the qPCR approach established by Bælum et al. (2009). Using samples from the growth chamber study and sequencing techniques, I found that non-specific amplification was, indeed, occurring. Overall, Chapter 4 suggests the need to improve targeting the *tfdA* gene classes in environmental samples by developing and optimizing primers with robust specificity to the targeted genes of interest. Future steps to improve *tfdA* specificity involve designing primer sets that should be tested for a wider range of environmental samples in real-world conditions.
4. *Propiconazole translocation in amenity turfgrass is limited to the lowest segment of the plant regardless of temperature or time following the application.* The control of snow molds in turfgrass is traditionally obtained with one or two fungicide applications in the

fall shortly before snow cover, and in many cases, a mixture of fungicide active ingredients is required to obtain adequate disease control.^{11,12} The appropriate timing of propiconazole applications is essential for disease control and has been the source of considerable debate. Chapter 5 introduces a side study that I conducted to assess the duration and distance of propiconazole upward mobility into turfgrass leaves and develop a plant uptake model specific to DMI fungicides. The main finding from this study suggests that propiconazole does not significantly translocate upwards beyond the bottom 1 cm of a turfgrass plant, regardless of temperature or the time following application. Further, the fungicide uptake prediction model presented in Chapter 5 was developed with special interest in determining the effectiveness of leaf segment, time, and temperature as predictors of propiconazole uptake. Future studies implementing additional parameters may provide a more accurate understanding of how fungicides are absorbed and translocated in varying environmental conditions, with a particular interest in managing low-temperature diseases in turfgrass landscapes.

References

- (1) Atwood, D.; Paisley-Jones, C. Pesticides Industry Sales and Usage 2008-2012 Market Estimates; U.S. Environmental Protection Agency, **2017**.
- (2) USEPA. Reregistration Eligibility Decision (RED) for Propiconazole Case No. 3125. July 18, 2006.
- (3) Corke, C. T.; Thompson, F. R. Effects of Some Phenylamide Herbicides and Their Degradation Products on Soil Nitrification. *Can. J. Microbiol.* **1970**, 16 (7), 567–571. <https://doi.org/10.1139/m70-095>.
- (4) Nedwell, D. B.; Floodgate, G. D. The Seasonal Selection by Temperature of Heterotrophic Bacteria in an Intertidal Sediment. *Marine Biology* **1971**, 11 (4), 306–310. <https://doi.org/10.1007/BF00352448>.
- (5) Fenner, K.; Canonica, S.; Wackett, L.; Elsner, M. Evaluating Pesticide Degradation in the Environment: Blind Spots and Emerging Opportunities. *Science* **2013**, 341 (6147), 752–758.
- (6) Bollag, J.-M.; Liu, S.-Y. Biological Transformation Processes of Pesticides. *Pesticides in the Soil Environment: Processes, Impacts and Modeling* **1990**, sssabookseries (pesticidesinthe), 169–211. <https://doi.org/10.2136/sssabookser2.c6>.
- (7) Lipson, D. A.; Schmidt, S. K. Seasonal Changes in an Alpine Soil Bacterial Community in the Colorado Rocky Mountains. *Applied and Environmental Microbiology* **2004**, 70 (5).
- (8) Monson, R. K.; Burns, S. P.; Williams, M. W.; Delany, A. C.; Weintraub, M.; Lipson, D. A. The Contribution of Beneath-snow Soil Respiration to Total Ecosystem Respiration in a High-elevation, Subalpine Forest. *Global Biogeochemical Cycles* **2006**, 20 (3), n/a–n/a.

- (9) Kitagawa, W.; Kamagata, Y. Diversity of 2,4-Dichlorophenoxyacetic Acid (2,4-D)-Degradative Genes and Degrading Bacteria. In *Biodegradative Bacteria: How Bacteria Degrade, Survive, Adapt, and Evolve*; Springer Japan, 2014; pp 43–57.
- (10) Bælum, J.; Jacobsen, C. S. TaqMan Probe-Based Real-Time PCR Assay for Detection and Discrimination of Class I, II, and III TfdA Genes in Soils Treated with Phenoxy Acid Herbicides. *Appl Environ Microbiol* **2009**, 75 (9), 2969–2972.
<https://doi.org/10.1128/AEM.02051-08>.
- (11) Hsiang, T.; Matsumoto, N.; Millett, S. M. Biology and Management of Typhula Snow Molds of Turfgrass. *Plant Disease* **1999**, 83 (9), 788–798.
<https://doi.org/10.1094/PDIS.1999.83.9.788>.
- (12) Dahl, A., S. Snowmold of Turf Grasses as Caused by *Fusarium Nivale*. *Phytopath* **1934**, 24 (3), 197–214.